

7710 FILE COPY

HSD-TR-90-025

AD-A225 104



SEISMIC RESPONSE OF SONIC BOOM-COUPLED RAYLEIGH WAVES

Mark R. Legg
Jerold M. Haber

BBN Systems and Technologies Corporation
21120 Vanowen Street
Canoga Park, CA 91303

June 1990

DTIC
ELECTE
AUG 07 1990
S E D

Final Report for Period June 1989 - June 1990

Approved for public release; distribution is unlimited.

Noise and Sonic Boom Impact Technology
Human Systems Division
Air Force Systems Command
Brooks Air Force Base, TX 78235-5000

90 00 00 054

NOTICE

When Government drawings, specifications, or other data are used for any purpose other than in connection with a definitely Government-related procurement, the United States Government incurs no responsibility nor any obligation whatsoever. The fact that the Government may have formulated or in any way supplied the said drawings, specifications, or other data, is not to be regarded by implication, or otherwise as in any manner construed, as licensing the holder, or any other person or corporation; or conveying any rights or permission to manufacture, use, or sell any patented invention that may in any way be related thereto.

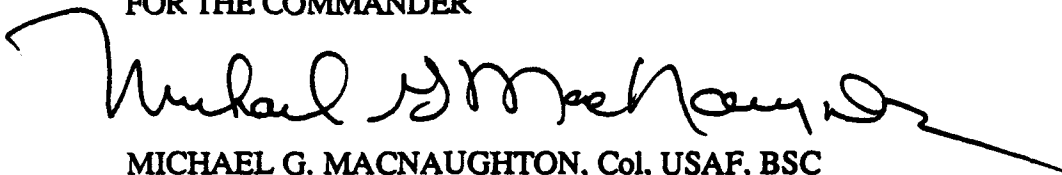
This report has been reviewed and is releasable to the National Technical Information Service (NTIS), where it will be available to the general public, including foreign nationals.

This report has been reviewed and is approved for publication.



PRESTON S. HALL
Deputy NSBIT Program Manager

FOR THE COMMANDER



MICHAEL G. MACNAUGHTON, Col, USAF, BSC
Program Director
Human Systems

Please do not request copies of this report from the Human Systems Division. Copies may be obtained from DTIC. Address your request for additional copies to:

Defense Technical Information Center
Cameron Station
Alexandria VA 22304-6145

If your address has changed, if you wish to be removed from our mailing list, or if your organization no longer employs the addressee, please notify HSD/XART, Brooks AFB TX 78235-5000 to help us maintain a current mailing list.

Copies of this report should not be returned unless return is required by security considerations, contractual obligations, or notice on a specific document.

UNCLASSIFIED
SECURITY CLASSIFICATION OF THIS PAGE

REPORT DOCUMENTATION PAGE				Form Approved OMB No. 0704-0188	
1a. REPORT SECURITY CLASSIFICATION Unclassified			1b. RESTRICTIVE MARKINGS		
2a. SECURITY CLASSIFICATION AUTHORITY			3. DISTRIBUTION/AVAILABILITY OF REPORT Approved for public release; distribution is unlimited		
2b. DECLASSIFICATION/DOWNGRADING SCHEDULE					
4. PERFORMING ORGANIZATION REPORT NUMBER(S) Report 7316, NSBIT Task Order 0018			5. MONITORING ORGANIZATION REPORT NUMBER(S) HSD-TR-90-25		
6a. NAME OF PERFORMING ORGANIZATION BBN Systems and Technologies Corporation /ACTA, Inc.		6b. OFFICE SYMBOL (If applicable) HSD/YAH (NSBIT)		7a. NAME OF MONITORING ORGANIZATION HSD/YAH (NSBIT)	
6c. ADDRESS (City, State, and ZIP Code) 21120 Vanowen Street, Canoga Park, CA 91303		7b. ADDRESS (City, State, and ZIP Code) Wright-Patterson AFB OH 45433-6573			
8a. NAME OF FUNDING/SPONSORING ORGANIZATION Noise and Sonic Boom Impact Technology		8b. OFFICE SYMBOL (If applicable) HSD/YAH (NSBIT)		9. PROCUREMENT INSTRUMENT IDENTIFICATION NUMBER F33615-86-C-0530	
8c. ADDRESS (City, State, and ZIP Code) Wright-Patterson AFB OH 45433-6573		10. SOURCE OF FUNDING NUMBERS			
		PROGRAM ELEMENT NO 63723F		PROJECT NO. 3037	
				TASK NO 02	
				WORK UNIT ACCESSION NO. 02	
11. TITLE (Include Security Classification) (U) Seismic Response of Sonic Boom-Coupled Rayleigh Waves					
12. PERSONAL AUTHOR(S) Egg, Mark R. and Haber, Jerold M.					
13a. TYPE OF REPORT Final		13b. TIME COVERED FROM 89/11/6 to 90/5/6		14. DATE OF REPORT (Year, Month, Day) 1990 June 28	
15. PAGE COUNT 246					
16. SUPPLEMENTARY NOTATION					
17. COSATI CODES			18. SUBJECT TERMS (Continue on reverse if necessary and identify by block number) Sonic boom, Rayleigh waves, seismic energy, propagation, unconventional and conventional structures, structural damage, geologic profile, SOA, MOA		
FIELD	GROUP	SUB-GROUP			
24	02, 07				
19. ABSTRACT (Continue on reverse if necessary and identify by block number) <p>Whenever sonic booms strike the ground a certain amount of energy is transferred to the ground which propagates as seismic waves. Under most conditions, the energy transfer is very inefficient, and the seismic wave energy is dissipated over a relatively short distance. If, however, a supersonic aircraft flew in a manner so that the sonic boom carpet velocity matched the propagation velocity of seismic surface waves (Rayleigh waves), the magnitude of the seismic waves would be amplified. For special soil (ground) characteristics, the energy transfer into the ground becomes more efficient. The seismic energy can propagate with little dissipation, allowing the magnitude of the ground vibrations to build up to damaging levels. If the vibration characteristics of the ground match those of a structure, the potential for structural damage may be significant.</p> <p>Three types of conditions are necessary for sonic boom-coupled Rayleigh waves to pose a</p>					
20. DISTRIBUTION/AVAILABILITY OF ABSTRACT <input checked="" type="checkbox"/> UNCLASSIFIED/UNLIMITED <input type="checkbox"/> SAME AS RPT. <input type="checkbox"/> DTIC USERS			21. ABSTRACT SECURITY CLASSIFICATION Unclassified		
22a. NAME OF RESPONSIBLE INDIVIDUAL Robert Kull, Major, USAF			22b. TELEPHONE (Include Area Code) (513) 255-3376		22c. OFFICE SYMBOL HSD/YAH (NSBIT)

Unclassified

19. (continued) threat. The overflown geologic (soil) profile must be characterized by a low velocity layer over a higher velocity layer. An aircraft must fly a steady maneuver for which the sonic boom carpet speed varies by no more than approximately $\pm 10\%$ over a distance of several wave lengths. The structures in the region must have natural frequencies matching those of the Rayleigh waves and the amplitude and duration of the waves must be great enough to cause damage.

Numerous near-surface geologic conditions and soil profiles of the appropriate character exist near supersonic operating areas. This study presents a method to evaluate and classify these conditions based on existing geologic and soil survey maps. A significant portion of supersonic flight satisfies the second condition. The primary maneuvers that fail to satisfy this condition are portions of maneuvers close to time points resulting in a focus at ground level. Structural elements of conventional low-rise construction and other unconventional structures have natural response frequencies that fall within the range of the resonant Rayleigh waves. Therefore, although of low probability, a potential threat of damage to structures from such conditions near supersonic operating areas exists. This study recommends a field test program to quantify the magnitude of the effect and a mapping program to delineate affected regions.

Unclassified

TABLE OF CONTENTS

	FOREWORD	xi
	ACKNOWLEDGMENTS	xiii
	EXECUTIVE SUMMARY	xv
1.0	INTRODUCTION	1
	1.1 Objective	1
	1.2 Background	1
	1.3 Literature Review	3
	1.3.1 Environmental Impact Assessment Documents	3
	1.3.2 Litigation and Claims	5
	1.3.3 Open Scientific Literature	6
	1.3.4 Conclusions of Literature Survey	16
2.0	DEFINITION OF SOIL TYPES AND SEISMIC PROPAGATION CONDITIONS	19
	2.1 Introduction	19
	2.2 Geological Setting	25
	2.2.1 Climate and Relief	25
	2.2.2 Depositional Environment	28
	2.2.3 Source Rocks	31
	2.2.4 Age and Geological History--Weathering and Formation of Soils	31
	2.2.5 Depth of Burial--Compaction and Induration	32
	2.2.6 Biological Activity	33
	2.3 Properties of the Soil Profile	33
	2.3.1 Mineralogy	33
	2.3.2 Grain Size and Shape	34
	2.3.3 Porosity and Pore Fluid	34
	2.3.4 Saturation and Moisture Content	35
	2.4 Representative Soil and Geologic Profiles	36
	2.4.1 Near-Surface Waveguide	39
	2.5 Rayleigh Wave Dispersion Curves	40
	2.6 Amplitudes of Resonant Sonic Boom-Coupled Rayleigh Waves	62
	2.7 Conclusions--Geologic Conditions Conducive to Rayleigh Wave Resonance	63
3.0	RANGE OF SONIC BOOM FOOTPRINT CHARACTERISTICS	67
	3.1 Characteristics of the Sonic Boom Footprint	68
	3.2 Supersonic Maneuvers	75
	3.2.1 Straight, Level, Non-accelerating Flight	75
	3.2.2 Straight, Level, Accelerating Flight	76

TABLE OF CONTENTS (continued)

	3.2.3 Diving Acceleration	84
	3.2.4 Constant Speed Turns	89
	3.3 Summary	91
4.0	RESONANT CHARACTERISTICS OF TYPICAL STRUCTURES	93
	4.1 Introduction	93
	4.2 Conventional Structures	95
	4.3 Unconventional Structures	99
	4.4 Human Tolerance	104
	4.5 Summary	108
5.0	CONCLUSIONS AND RECOMMENDATIONS	109
	5.1 Summary of Major Conclusions	111
	5.2 Recommendations	113
	APPENDIX A - ANNOTATED BIBLIOGRAPHY	115
	APPENDIX B - SOILS AND GEOLOGIC INFORMATION	129
	APPENDIX C - GLOSSARY OF SOILS AND GEOLOGICAL TERMS	179
	APPENDIX D - SEISMIC MODELS FOR COMPUTATION OF RAYLEIGH WAVE DISPERSION CURVES	191
	REFERENCES	241

Accession For	
NTIS CDA&I	<input checked="" type="checkbox"/>
NTIS TAB	<input type="checkbox"/>
Unannounced	<input type="checkbox"/>
Justification	
By	
Distribution/	
Availability Codes	
Avail and/or	
Special	
A-1	

LIST OF FIGURES

Figure 1-1:	Typical Surface Wave Dispersion Curves.	8
Figure 1-2:	Phase Velocity and Group Velocity of Dispersive Surface Waves.	8
Figure 1-3:	Normal Mode Propagation in a Wave Guide.	11
Figure 2-1:	Sonic Boom-Coupled Rayleigh Wave Resonance Condition.	20
Figure 2-2:	Development of Rayleigh Wave Characteristics.	23
Figure 2-3:	Map Showing Location of Supersonic Operating Areas (SOAs) and the Major Geologic Provinces in the Western United States.	27
Figure 2-4:	Theoretical Rayleigh Wave Dispersion Curves and Observed Seismic Wave Frequency Versus Aircraft Velocity for the Dry Lake Area at Edwards AFB.	42
Figure 2-5:	Rayleigh Wave Phase Velocity Dispersion Curves for the Simple Clay Lake Bed Model.	45
Figure 2-6:	Rayleigh Wave Dispersion Curves for Phase Velocity (V) and Group Velocity (U) for the Simple 10-m Thick Clay Lake Bed Model Shown in the Inset.	46
Figure 2-7:	Rayleigh Wave Phase Velocity Dispersion Curves for a Simple 100-m Thick Clay Lake Bed Model.	49
Figure 2-8:	Rayleigh Wave Phase Velocity Dispersion Curves for the Simple 1-m Thick Clay Lake Bed Model.	50
Figure 2-9:	Rayleigh Wave Phase Velocity Dispersion Curves for the Mojave Desert Crustal Structure Shown in the Inset (after Hadley, 1978).	51
Figure 2-10:	Rayleigh Wave Phase Velocity Dispersion Curves for the Mojave Desert Near-Surface Geological Structure Shown in the Inset (after Hadley, 1978).	52
Figure 2-11:	Rayleigh Wave Phase Velocity Dispersion Curves for the Mojave Desert Near-Surface Geological Structure Shown in the Inset (after Hadley, 1978).	55
Figure 2-12:	Rayleigh Wave Phase Velocity Dispersion Curves for the Near-Surface Geologic Structure Shown in the Inset (after Sabatier et al., 1986b).	56
Figure 2-13:	Rayleigh Wave Phase Velocity Dispersion Curves for the Near-Surface Geologic Structure Shown in the Inset (after Sabatier and Raspel, 1988).	57
Figure 2-14:	Rayleigh Wave Phase Velocity Dispersion Curves for the Near-Surface Geologic Structure Shown in the Inset (after Sabatier et al., 1986a).	58
Figure 2-15:	Rayleigh Wave Phase Velocity Dispersion Curves for the Near-Surface Geologic Structure Shown in the Inset (after Fumal and Tinsley, 1985).	59
Figure 2-16:	Rayleigh Wave Phase Velocity Dispersion Curves for the Near-Surface Waveguide Structure Shown in the Inset (modified from Hays et al., 1978).	60

LIST OF FIGURES (continued)

Figure 2-17:	Rayleigh Wave Phase Velocity Dispersion Curves for the Near-Surface Waveguide Structure Shown in the Inset (modified from Hays et al., 1978).	61
Figure 3-1:	Selected Sonic Boom Waveforms.	69
Figure 3-2:	Measured Sonic-Boom Pressure Signatures at Several Points Along the Ground Track of Airplane A in Steady-Level Flight.	70
Figure 3-3:	Trace Speed as a Function of Speed and Altitude for Constant Speed, Constant Altitude, Level Flight.	75
Figure 3-4:	Peak Overpressure as a Function of Speed and Altitude for a Fighter (F-15) Flying at a Constant Speed and a Constant Altitude.	77
Figure 3-5:	Peak Overpressure as a Function of Speed and Altitude for a Fighter-Bomber (FB-111) Flying at a Constant Speed and a Constant Altitude.	78
Figure 3-6:	Sonic Boom Signature Durations as a Function of Speed and Altitude for a Fighter (F-15) Flying at a Constant Speed and Altitude.	78
Figure 3-7:	Sonic Boom Signature Durations as a Function of Speed and Altitude for a Fighter-Bomber (FB-111) Flying at a Constant Speed and Altitude.	79
Figure 3-8:	Trace Speed as a Function of Distance Along the Flight Track for Level Accelerated Flight at an Altitude of 10,000 Feet MSL ($\dot{M}=0.01$ per sec).	79
Figure 3-9:	Detail of Trace Speed versus Distance (Altitude=10,000 Feet MSL, $\dot{M}=0.01$ per sec).	81
Figure 3-10:	Trace Speed as a Function of Distance Along the Flight Track for Level Accelerated Flight at an Altitude of 10,000 Feet MSL ($\dot{M}=0.015$ per sec).	81
Figure 3-11:	Trace Speed as a Function of Distance Along the Flight Track for Level Accelerated Flight at an Altitude of 45,000 Feet MSL ($\dot{M}=0.01$ per sec).	82
Figure 3-12:	Trace Speed as a Function of Distance Along the Flight Track for Level Accelerated Flight at an Altitude of 45,000 Feet MSL ($\dot{M}=0.015$ per sec).	82
Figure 3-13:	Relationship Between Focus Location and Trace Speed Plots.	83
Figure 3-14:	F-15 Level Acceleration at 10,000 Feet (Plotkin, 1985).	84
Figure 3-15:	F-15 Level Acceleration at 45,000 Feet (Plotkin, 1985).	85
Figure 3-16:	Trace Speed as a Function of Distance Along the Flight Track for an Accelerated Dive from 15,000 Feet at a Dive Angle of 45 Degrees ($\dot{M}=0.01$ per sec).	86
Figure 3-17:	Trace Speed as a Function of Distance Along the Flight Track for an Accelerated Dive from 35,000 Feet at a Dive Angle of 45 Degrees ($\dot{M}=0.01$ per sec).	87

LIST OF FIGURES (continued)

Figure 3-18:	F-4 30 Degree Dive from 15,000 Feet (Plotkin, 1985).	88
Figure 3-19:	F-4 30 Degree Dive from 30,000 Feet (Plotkin, 1985).	88
Figure 3-20:	F-15 10 Degree Dive from 15,000 Feet (Plotkin, 1985).	89
Figure 3-21:	F-15 Level Turn at 10,000 Feet (Plotkin, 1985).	90
Figure 4-1:	Putting Vibrations in Perspective (Amick, 1988).	94
Figure 4-2:	Particle Velocities Resulting in Damage (Siskind et al., 1980).	97
Figure 4-3:	Probability Damage Analysis Summary (Siskind et al., 1980).	98
Figure 4-4:	Safe Levels of Blasting Vibration for Houses Using a Combination of Velocity and Displacement (Siskind et al., 1980).	98
Figure 4-5:	Vibration Criteria for Sensitive Equipment (Unger, 1985).	103
Figure 4-6:	Human Tolerance Standards for RMS Vibrations Exceeding 1-Minute Duration (Siskind et al., 1980).	104
Figure 4-7:	Human Response to Transient Vibration Velocities of Various Durations (Siskind et al., 1980).	105
Figure 4-8:	Tentative Relationship Between Annoyance and Number of Exposures to Blast Vibration Levels (Fidell et al., 1983).	106
Figure 4-9:	Alternative Relationship of Annoyance and Number of Exposures to Blast Vibration Levels (Fidell et al., 1983).	107
Figure B-1:	Map Showing Location of Eglin AFB and Santa Rosa County, Florida.	140
Figure B-2:	Map Showing Location of Gandy and Nellis SOAs and the Meadow Valley Area.	143
Figure B-3:	Map Showing Location of Reserve MOA and Catron County, New Mexico.	158
Figure B-4:	Map Showing Location of Valentine SOA and Jeff Davis County, Texas.	167
Figure B-5:	Map Showing Location of White Sands Missile Range in New Mexico.	174

LIST OF TABLES

Table 2-1:	Typical Elastic Parameters for Surficial Deposits.	21
Table 2-2:	List of Supersonic Operating Areas.	22
Table 2-3:	Depositional Environments.	29
Table 2-4:	Representative Seismic Velocity Models.	38
Table 3-1:	Maneuvers Simulated with PCBOOM.	72
Table 4-1:	Damage Levels from Blasting.	99
Table 4-2:	Safe Vibration Levels (Esteves, 1978).	101
Table B-1:	Points-of-Contact: Soils Conservation Service.	129
Table B-2:	List of Published Soil Surveys Near SOAs.	130
Table B-3:	Geologic References for Supersonic Operating Areas.	131

FOREWORD

This report was prepared by ACTA, Incorporated as subcontractor to BBN Systems and Technologies in fulfillment of Task Order 0018, under the Noise and Sonic Boom Impact Technology (NSBIT) Program, Contract No. F33615-86-C-0530.

The NSBIT Program is conducted by the United States Air Force, Air Force Systems Command, under the direction of Major Robert Kull, Jr., Program Manager. The NSBIT Technical Manager is Mr. Scott Hall. The BBN effort is directed by Mr. B. Andrew Kugler, Program Manager.

ACKNOWLEDGMENTS

The authors would like to express their grateful appreciation to Dr. James Battis of the Air Force Geophysical Laboratory, Dr. Tony Embleton of the NRC in Ottawa, Canada, Dr. William Galloway as consultant to BBN, Mr. Gary Muckel of the Soils Conservation Service, and Mr. Mark Barber, for their assistance in finding many of the important references that were reviewed in this study. The support of Dr. Gordon Stewart, seismologist and president of Pacific Geophysics, Inc., who prepared the Rayleigh wave phase velocity dispersion curves for this study is gratefully acknowledged. The authors also appreciate the assistance of the regional Soil Conservation Service offices for providing the soils studies.

EXECUTIVE SUMMARY

At present, the impact of U.S. Air Force supersonic operations on structures is evaluated based on the assumption that the only potential threat is direct sonic boom damage. While this is normally the primary source of damage, as early as the 1960s suggestions were made that, under the proper conditions, seismic waves induced by sonic boom might present an additional significant threat. Three sets of conditions must combine to generate this potential threat. These conditions involve the following factors:

- the characteristics of the local soil and surficial geology;
- the characteristics of the sonic boom and sonic boom carpet; and
- the characteristics of the structures at risk.

Analysis of these characteristics in Supersonic Operating Areas (SOAs) has identified the types of conditions of greatest concern for seismic waves to be a significant contributor to damages. A field test has been outlined to assess the significance of this hazard.

Whenever sonic booms strike the ground, a certain amount of energy is transferred to the ground which propagates as seismic waves. Normally, the energy transfer is inefficient. Moreover, whatever energy is imparted to the ground normally dissipates in a relatively short distance. It was suggested that if a supersonic aircraft flies in a manner so that the sonic boom carpet velocity matches the propagation velocity of a seismic surface wave (Rayleigh wave) over a sufficient distance, the Rayleigh wave amplitude increases as a result. Given sufficient amplitude and duration of the wave train generated, at a frequency matching the resonant frequency of a structure, the damage potential of the seismic waves might be important.

This study investigated the feasibility of such a damage mechanism. A literature review was performed to assess pertinent public concerns, relevant expert testimony in sonic boom litigation cases, and pertinent theoretical and experimental work in the open scientific literature. Members of the public have expressed concerns regarding potential sonic boom damage to a variety of unconventional structures and various kinds of sensitive equipment. These concerns provided a

guideline to choosing structures whose responses needed to be considered. Discussions with key individuals in various U.S. Air Force (USAF) commands failed to disclose any pertinent litigation. Although disappointing, it was not particularly surprising given the highly technical nature of the air-coupled Rayleigh wave damage theory. On the other hand, review of the open scientific literature provided important insights into the problem.

The following is a summary of some of the pertinent findings in the literature. The coupling between the acoustic and seismic waves may be stronger than would be expected based upon a simple comparison of the acoustic impedance of the air and soil, particularly in porous soils. A thin, low-velocity layer of soil on top of a thick high-velocity layer acts as a waveguide. The waves which develop in the low-velocity layer are characterized by a single frequency dependent on the thickness of the layer and its seismic velocity. This type of soil/geological structure has been responsible for the development of strong reverberations from earthquakes. A similar phenomenon is observed in exploration seismology. Typical soils that have a low seismic velocity include soft porous soils, clay lake beds, and bay mud deposits.

Based on these insights, specific soil or geologic conditions that may lead to resonant sonic boom-coupled Rayleigh waves were identified, using a four-step process. Consideration of geological processes allowed characterization of the environment where low-velocity soils may occur so that these areas could be identified within the SOAs. Surficial geological conditions representative of SOAs were identified by examining maps of soils and surficial geology and soils studies obtained from the U.S. Geological Survey, state geological offices, and the Soils Conservation Service. These characterizations of the geological soils conditions in SOAs were used in conjunction with soil borings and seismic refraction profiles described in the scientific literature for locations near SOAs to develop realistic shallow geologic (soil) profiles. For each of these profiles, a theoretical calculation was made of the Rayleigh wave phase velocities as a function of frequency. This theoretical analysis allowed identification of the sonic boom carpet velocities required for effective seismic coupling for that particular profile. It also provided a basis for estimating the duration of the resonance and amplitude of vibration that might result.

The seismic waves generated by resonant coupling with the sonic boom will affect a very limited geographical area. They are most likely to pose a threat within the region of strong resonant

coupling. Outside of this region, the amplitude of these waves will diminish rapidly with distance. Under the most favorable conditions (waveguide), the maximum amplitude will decrease at a rate approximately proportional to the distance traveled.

Earlier studies indicated that, in order for coupled Rayleigh waves to develop significant amplitudes, the sonic boom carpet speed must not deviate by more than about ± 10 percent over a distance of several wavelengths. A theoretical examination of sonic boom carpet speeds associated with a variety of maneuvers (level constant speed flight, accelerated level flight, accelerated climbs and dives, and constant speed turns) demonstrated that this condition can be met for a large variety of steady maneuvers. The condition failed to be satisfied in the vicinity of the types of focuses that real maneuvers generate.

Most of the structures that may be exposed to sonic boom-coupled Rayleigh waves have natural frequencies between 1 and 10 Hz, although there is a significant group of structures that have resonant frequencies in the range of 10 to 40 Hz. A variety of estimates has been proposed for damage thresholds for vibration. For plaster walls and wallboard, the damage threshold may be as low as a displacement of 0.03 in and a peak particle velocity of 0.2 in per second for frequencies as low as 1 Hz. For sensitive archeological or historical structures, under the most adverse conditions, peak particle velocities of half this magnitude may be of concern. Based on the limited empirical data that have been accumulated, it is estimated that peak particle velocities in excess of these thresholds may be generated under the most adverse conditions.

A field test program is recommended in order to quantify the amplitude of the vibration levels that may be generated. This program would involve a number of low altitude supersonic flights over an array of geophones placed in a geological structure conducive to producing resonant Rayleigh waves, such as near the Bonneville salt flats. This type of test would either a) demonstrate conclusively that, under the most adverse conditions, sonic boom-induced resonant Rayleigh waves do not pose a threat, or b) provide a quantitative indication of the magnitude of the threat.

SEISMIC RESPONSE OF SONIC BOOM-COUPLED RAYLEIGH WAVES

1.0 INTRODUCTION

1.1 Objective

Public law 96-588, the National Environmental Policy Act (NEPA) of 1969, requires the United States Air Force (USAF) and the U.S. Navy to conduct environmental assessments of its flight activities. NEPA and other regulations apply not only to flight operations near air bases, but also to operations in about 350 Military Operating Areas (MOAs) and Restricted Areas (RAs), and along about 400 Military Training Routes (MTRs), encompassing roughly a half million square miles of domestic airspace. Compliance with the statutory and regulatory environmental requirements is not a simple task for the USAF. An assessment of the potential consequences of these operations and a response to public concerns about possible consequences generates significant technical and practical challenges.

This study addresses these needs by investigating the conditions under which potentially damaging ground vibrations may be generated by sonic booms. At present the impact of USAF supersonic operations on structures is evaluated based on the assumption that the only potential threat is direct sonic boom damage. While this is normally the primary source of damage, as early as the 1960s suggestions were made that, under the proper conditions, seismic waves induced by sonic booms might pose an additional significant threat. The objective of this study is to investigate the generation of ground vibrations due to sonic booms, and to characterize the conditions under which seismic waves may contribute to the sonic boom structural damage threat. This report documents the first phase of this study.

1.2 Background

The literature regarding structural damage caused by sonic boom was reviewed under an earlier study funded by the Noise and Sonic Boom Impact Technology (NSBIT) program (Haber et al., 1989). Seismic waves generated by sonic booms were observed by several investigators (Baron et al., 1966; Goforth and McDonald, 1968; McDonald and Goforth, 1969; Espinosa et al., 1968; Cook

and Goforth, 1970; Bradley and Stevens, 1973; Grover, 1973; Weber, 1972). These studies found that the amplitude of the seismic motions was small and insufficient to damage structures. Peak ground vibrations observed from overpressures of 3.5 psf were less than 1% of a strict damage threshold established by the Bureau of Mines (Goforth and McDonald, 1968).

Theoretical studies showed that the greatest ground motion and structure acceleration response would occur under the resonant condition, that is, when the velocity of the sonic boom pressure wave is equal to the velocity of the Rayleigh waves in the ground (Press and Ewing, 1951a; Goforth and McDonald, 1968; Baron et al., 1966). The resonant peak of the ground response is very narrow. If the velocity of the sonic boom shock wave deviates more than 10% from the Rayleigh wave speed, the ground coupling is greatly reduced. Few cases of the actual resonant conditions, where the ground motions may be amplified by the sonic boom-Rayleigh wave coupling, have been reported (Espinosa et al., 1968; Goforth and McDonald, 1968).

Investigations reviewed during this study concluded that significant structure response to the sonic boom-coupled Rayleigh waves is unlikely due to the very specific conditions required to produce the resonant condition; i.e., the aircraft must be traveling with a velocity equal to the Rayleigh wave velocity in the ground for a significant distance.

The present study extended this work with a literature review addressing three primary sources of information: a) USAF Environmental Impact Assessment documents, b) litigation and claims, and c) open scientific literature. The literature review was performed to assess pertinent public concerns, possible relevant expert testimony in sonic boom litigation cases, and pertinent theoretical and experimental work to identify specific conditions for which sonic boom-coupled Rayleigh waves could reach a damaging level.

The literature review indicated that three types of conditions were necessary in order for sonic boom-coupled Rayleigh wave resonance to pose a significant threat to structures, structural elements, or sensitive equipment. These conditions are characteristics of the surficial geology (soil), supersonic aircraft maneuvers, and properties of the structures at risk. The balance of this section presents the results of the literature review. Section 2 presents the results of an evaluation of the soil types and near-surface geologic structure conducive to the development of sonic boom-coupled Rayleigh wave

resonance. Section 3 develops the characteristics of the sonic boom environment generated by tactical supersonic training operations and the types of maneuvers which may permit development of sonic boom-coupled seismic waves. Section 4 reviews the resonant characteristics of typical structures and provides an indication of the vibration levels corresponding to the threshold of damage. Section 5 summarizes the study findings and presents recommendations for further research to provide the USAF the necessary guidelines to be able to evaluate and manage the damage potential of air-coupled seismic waves.

1.3 Literature Review

The literature search addressed three primary sources of information, each of which is presented in the following material.

1.3.1 Environmental Impact Assessment Documents

A review of USAF Environmental Impact Assessment documents and public comments was conducted to establish the pertinent public concern surrounding this issue. Environmental Impact Statements for the Valentine and Reserve MOAs were reviewed in detail to determine concern relevant to the sonic boom-coupled surface waves. Results of this analysis are presented under three categories: (1) concerns specifically related to seismic effects of sonic boom; (2) concerns indirectly related to seismic effects; and (3) other concerns that may relate to the seismic response associated with sonic booms.

The entire issue of seismic effects of sonic booms generated only a limited public response. Most of the public concern specifically related to the seismic effects of sonic booms was directed toward the possible damage to archaeological or historical sites by the sonic boom and related shaking. No specific mention of the sonic boom-coupled surface wave phenomenon was found. Nevertheless, the pertinent concern is whether the sonic boom or seismic waves induced by the boom can damage archaeological or historical sites. Air Force Geophysical Laboratories (AFGL, Batts, 1983) performed a study addressing the possibility of sonic boom damage to Indian petroglyphs in support of the Valentine MOA environmental assessment. The study concluded that the damage potential was insignificant. Public comments suggested that the study done by AFGL was too limited

in scope because its conclusions were based upon observations of only a few sonic booms with small overpressures.

The AFGL study evaluation of the potential sonic boom damage to Indian petroglyphs convincingly demonstrates that the chance of sonic boom damage to those particular structures is insignificant. Nevertheless, care must be used in extrapolating these results to other types of structures located in different geologic settings.

Another concern related to the seismic effects of sonic boom is the potential for damage to water wells and water storage tanks, which are critical facilities in the arid climate. The public comments expressed concern about the damage potential of the sonic boom propagating through the air into the well. Also, there is concern about the generation of rockfalls or landslides by the sonic boom in the mountainous areas. Lastly, a suggestion was made to install seismographs in the supersonic operating area to monitor the sonic boom effects; this was considered unfeasible by the Air Force, but could provide data needed for evaluating the sonic boom-coupled surface wave phenomenon.

Public concerns that are indirectly related to the sonic boom-induced surface wave phenomenon are associated with particular types of structures that may be damaged by the sonic boom and possible coupled Rayleigh waves. In addition to the archaeological sites (mainly rock shelters, cliff dwellings, petroglyphs and other ruins), particular concern was expressed regarding the vulnerability of adobe buildings, the typical construction in these remote areas. This concern was enhanced because most adobe buildings would be considered substandard or not "up-to-code." Nevertheless, such buildings are the standard in the region, have survived many decades, and are still habitable. Because of inherent weaknesses in such construction, or because of the age of such structures, they may be particularly susceptible to damage from the sonic booms or seismic effects. Other unconventional structures that were mentioned include mobile homes, house trailers or campers that are set up in camping parks located in the MOAs and the radio telescope (Very Large Array or VLA) located near the Reserve MOA.

Lastly, other concerns that may be related to the sonic boom-coupled Rayleigh wave effects mostly involve the potential for focused booms or superboms. This concern is relevant to this

project in determining the types of maneuvers and resultant sonic boom wave character that may be responsible for air-coupled Rayleigh waves. The amplitude, durations, carpet trace speed, and lateral extent of such focused booms must be known to evaluate the seismic potential of supersonic operations.

1.3.2 Litigation and Claims

A top-level review of litigation and claims history was conducted to identify specific cases where damage was considered to have been caused by the seismic waves generated by the sonic boom coupling. No relevant litigation or claims were found. The following table lists the principal agencies and points-of-contact made in this search.

Points of Contact

TAC	Alton Chavis
TAC (Legal Staff)	Carolyn Davis
SAC (JAG)	Dan Jarlanski
SAC (Public Affairs)	Alan Dockery
Air Staff General Counsel	Doug Hedy
Air Staff Claims and Litigations	Paul Cormier
Headquarters USAF (LEEVX)	Herb Dean
Justice Department	Dorothy Burakreis
Air Force Systems Command (AFSC)	Ed Keppel

In no instance were the contacts familiar with any instance involving seismic effects or Raleigh waves. When the concern about Rayleigh waves and resonance was described, one source cited a claim involving an F-15 overflight of St. Louis at 41,000 ft, wherein the claimant asserted that a 14 ft masonry column was damaged by sympathetic resonance. The Air Force estimated the loading at 1.3 psf. The claim was denied. No expert testimony was offered. Another contact thought that a recent incident involving a hush house was attributable to resonant seismic waves. The USAF investigating committee established that acoustic and not seismic vibration was the cause.

Based upon the above contacts, it was established that there is no pertinent litigation.

1.3.3 Open Scientific Literature

Review of the scientific literature related to the occurrence of sonic boom-coupled Rayleigh waves is necessary to define the problem. The theory of air-coupled surface waves has existed for several decades (Lamb, 1932; Press and Ewing, 1951a and b; Press and Oliver, 1955; Ewing et al., 1957); the observation of the simultaneous arrival of a tidal disturbance with the airborne pressure wave associated with the eruption of Krakatoa in 1883 stimulated some of this research (Press and Ewing, 1951a). Additional, more detailed research, including experimental observations, was triggered by the development of the supersonic transport and concern for possible damage resulting from the associated sonic booms. Haber et al. (1989) reports the result of a review of major papers relevant to the sonic boom-coupled surface waves. Additional literature search and review of relevant material in other related aspects of seismology, including earthquake strong ground motion and exploration seismology, provides important information regarding the near surface resonance phenomena that could result in damaging ground shaking.

1.3.3.1 Air-Coupled Rayleigh Waves

Seismologists have known of the air-coupled Rayleigh wave phenomenon for almost half a century. Lamb (1932) derived the theoretical formulation for surface waves generated by propagation of an acoustic pressure pulse over an elastic medium. Following this approach, other seismologists (Press and Ewing, 1951a and b; Ewing and Oliver, 1955) studied the phenomena of air-coupled surface waves generated by air shots in seismic prospecting and of air-coupled flexural waves generated in ice and laboratory models. Other studies were concerned with the propagation of air-coupled surface waves generated by blasts or infrasound, such as those associated with mining activities, warfare, rocket launches, or engine tests (Crowley and Ossing, 1969; Donn et al., 1971; Sabatier and Raspel, 1988). Several good seismology textbooks, including Ewing et al. (1957), Brekhovskikh (1960), Bullen (1960), and Aki and Richards (1980), discuss the theory behind air-coupled surface waves.

A fundamental characteristic of air-coupled surface waves, predicted by theory and confirmed by experimental work, is their harmonic nature. Air-coupled surface waves are monochromatic; most of their energy is concentrated at one particular frequency. Rayleigh waves, such as those generated

by earthquakes or explosions, are often "dispersive" because of the layered geologic structure at the earth's surface. This dispersion means that surface wave energy of different frequencies travels with different velocities (Figure 1-1); with time, an original pulse-shaped waveform spreads out into a long train of sinusoidal waves with varying frequencies (Figure 1-2). For the air-coupled surface waves, the phase velocity--the velocity of wave crest propagation--must be equal to the sound velocity in the air above. This requirement ensures constructive interference between the incident air wave (sonic boom) with the Rayleigh wave traveling along the earth's surface. Because each discrete frequency is associated with one particular phase velocity of a dispersive seismic wave (for a given mode or harmonic), air-coupled surface waves propagate with only one frequency for each mode. Typically, only the fundamental mode is excited, although higher modes are sometimes observed (Espinosa et al., 1968; Goforth and McDonald, 1968).

Another effect of dispersion is to increase the duration of shaking; this is caused by the difference between the group velocity and the phase velocity. The group velocity is the velocity that the wave energy propagates (Figure 1-2). The group velocity may be greater than or less than the phase velocity in a dispersive medium. For typical geological materials, the group velocity is lower than the phase velocity (Figure 1-1). Because the group velocity is lower than the phase velocity, the seismic energy follows the arrival of the acoustic wave, that is, the ground starts vibrating with the arrival of the sonic boom shock and continues reverberating for a time thereafter. Because the sonic boom continues to generate coupled Rayleigh waves along the ground surface, whose energy propagates at the group velocity, the vibrations from the earlier ground coupling reaches a given observation point at some time after the arrival of the acoustic wave where the group velocity is lower than the carpet trace speed. Where the group velocity is higher, precursory seismic wave energy may arrive shortly before the acoustic wave. In general, however, because the surface waves are coupled to the sonic boom, affected structures will be shaking at the same time that the airborne acoustic pressure pulses arrive. Hence, the two effects: seismic shaking and acoustic wave overpressure may combine to produce a greater effect than if they arrived separately.

Sonic boom-coupled surface waves propagate with a phase velocity equivalent to the carpet trace speed of the sonic boom footprint. Because most rocks have high seismic velocities relative to most aircraft and sonic boom velocities, only low-velocity, near-surface soil layers are important

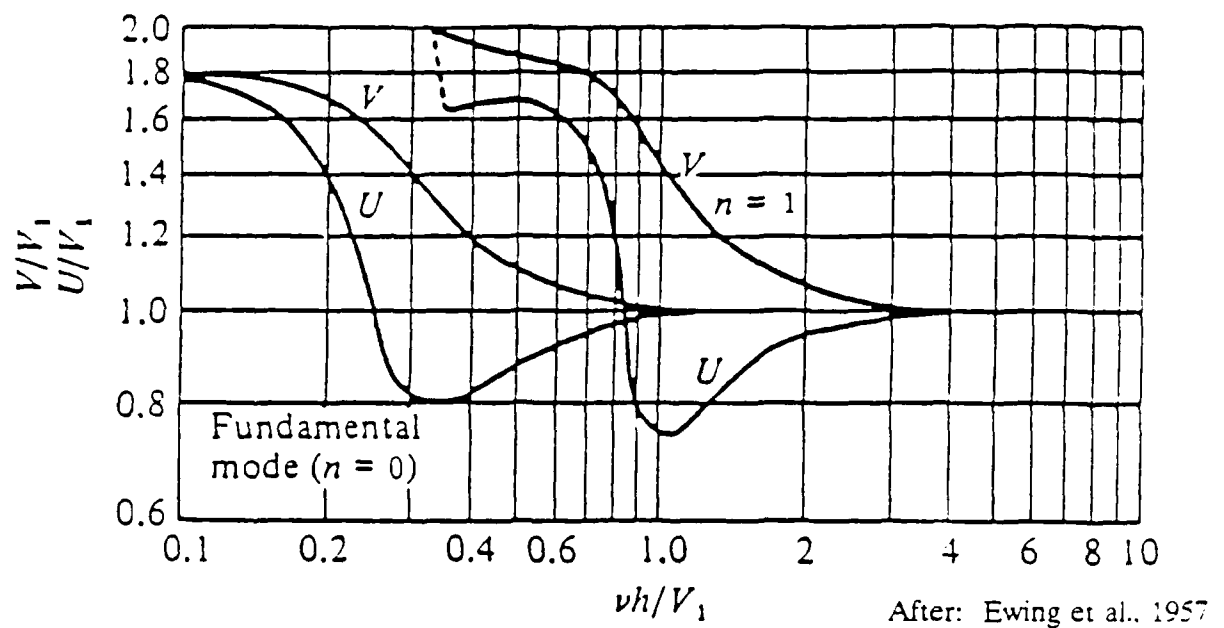


Figure 1-1. Typical Surface Wave Dispersion Curves (Ewing et al., 1957). Typical surface wave dispersion curves showing the phase velocity (V) and group velocity (U) versus frequency (ν) for the fundamental ($n=0$) and first higher ($n=1$) modes, where V_1 is the seismic velocity and h is the thickness of the waveguide.

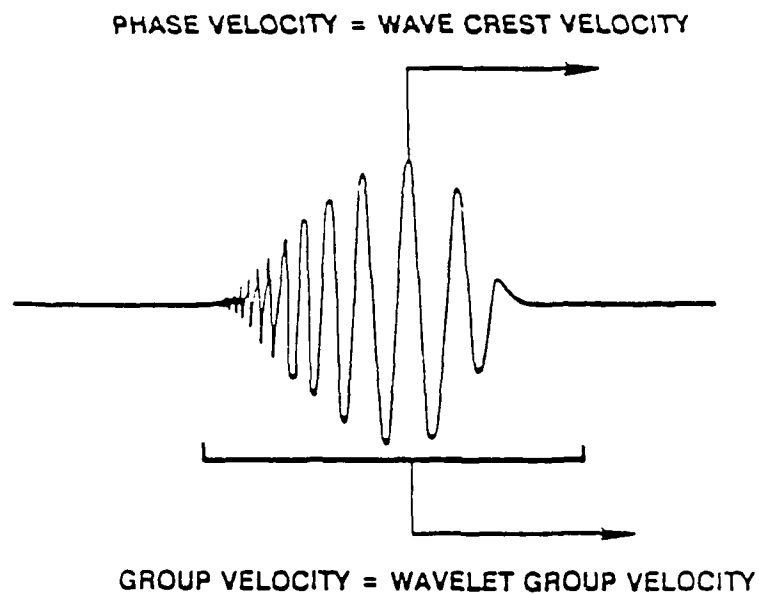


Figure 1-2. Phase Velocity and Group Velocity of Dispersive Surface Waves. The phase velocity is the velocity of propagation of the wave crests. The group velocity is the velocity of propagation of the wave energy packet (group of wavelets).

in determining the characteristics of sonic boom-coupled Rayleigh waves. Studies of the coupling mechanism find greater coupling of the acoustic wave with the seismic wave than that predicted solely by the acoustic impedance mismatch at the air-soil interface (Sabatier et al., 1986a and b). The increased coupling occurs by the strong dissipation of an acoustic wave within the pore fluid of the soil that transmits the seismic wave energy into the solid matrix of the porous surface layer. The ground surface is not a uniform solid, but is a composite of solid soil grains surrounded by fluid filled pore space. Within this soil layer composite, three types of acoustic waves can propagate: (1) an acoustic pressure wave in the pore fluid; (2) a compressional wave in the solid soil grains; and (3) a shear wave in the solid soil grains. The sonic boom shock wave is readily coupled to the pore fluid generating the pore fluid wave. Because the pore fluid wave must travel an extremely sinuous and indirect path between the soil grains, its velocity of propagation is very slow. Furthermore, this acoustic pore fluid wave is strongly dissipated by drag on the solid soil grains. This strong dissipation couples the pore fluid wave motion directly into the solid soil grains as both compressional and shear waves. The shear waves are usually better coupled because their propagation velocity is slower, and more comparable to the velocity of the sonic boom shock. A more porous, air-filled surface layer results in better coupling.

The area of the surface required for the coupling was found to be very small (about 1 m²; Sabatier et al., 1986b). These observations suggest that strong coupling of sonic booms with seismic surface waves is a local phenomenon--surficial geologic or soil conditions are most important in determining the coupling effect. This result is consistent with the measurements of seismic waves generated by sonic booms that showed the seismogram character to be more closely related to the geologic condition than to the sonic boom acoustic wave character (Goforth and McDonald, 1968).

For this study, sonic boom-coupled seismic waves with frequencies in the range typical of the natural response of structures are most significant. A preliminary evaluation of the natural response frequencies of typical structures that might be affected by sonic booms, low-rise and light conventional structures have natural frequencies of about 1 to 10 Hz.

Rayleigh waves of the 1 to 10 Hz frequency band are generally limited to very shallow, low-velocity soil layers with thicknesses less than about 100 m. Porous surficial soils studied by Sabatier et al. (1986a and b) regarding the coupling mechanism had thicknesses of about 1 to 5 m. Low

velocity layers are often referred to as "waveguides" (Figure 1-3) because the wave energy is "trapped" within the low velocity layer by multiple reflections from the higher velocity layer below and the low density air above. Because of interference between the multiple-reflected waves, only a particular set of discrete frequency waves can propagate within the waveguide without strong dissipation. These discrete frequency waves are called the "normal modes" of the waveguide. A simple method of estimating the natural response frequencies of the normal modes excited in a waveguide follows (following Sheriff and Geldart, 1982; and Sabatier et al., 1986a).

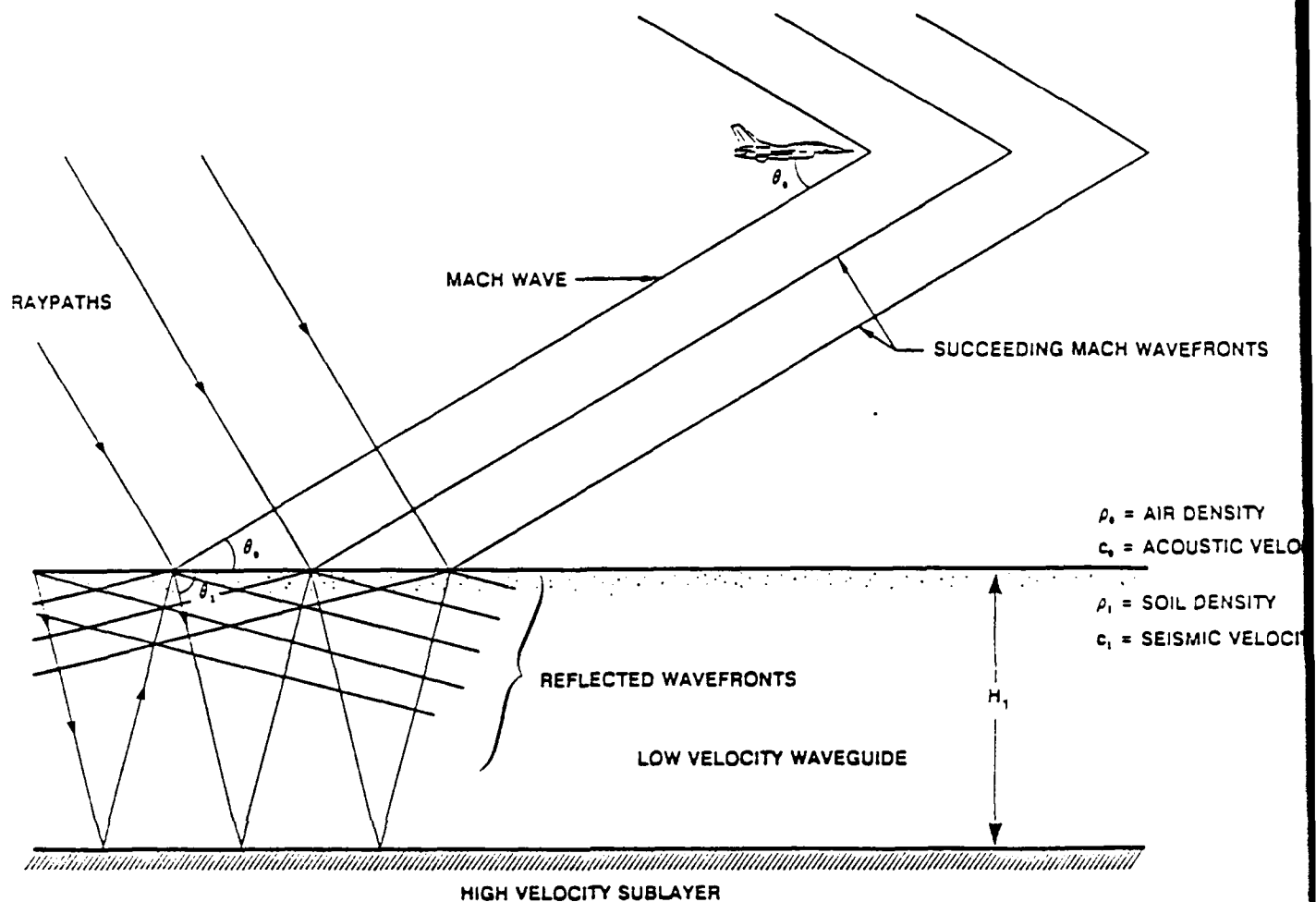


Figure 1-3. Normal Mode Propagation in a Waveguide. Successive arrivals of the sonic boom "Mach wave" at the earth's surface result in refraction of this wave into the low velocity waveguide. The refracted waves become trapped in the low velocity waveguide and continue to reverberate, by bouncing back and forth between the boundaries of the waveguide. This reverberation is enhanced by constructive interference when the wave that travels from the top of the waveguide down and back to the next reflection at the top of the waveguide arrives "in-phase" with the wave refracted by the succeeding Mach wave intersection at that point. This constructive interference occurs only for a number of discrete frequencies, called normal modes, associated with the thickness and seismic velocity of the waveguide. The mode number, integer value which varies from $n = 0, 1, 2, \dots$, is related to the number of wavelengths which can fit along the raypath within the waveguide between successive reflections. The fundamental mode ($n = 0$) is associated with $\frac{1}{4}$ wavelength between the top and bottom of the wavelength. It is only $\frac{1}{4}$ wavelength because there is a phase reversal of 180° (π or $\frac{1}{2}$ wavelength) at the upper (free) surface.

For a single surface layer waveguide, the response frequencies of the normal modes are defined by:

$$f_n = \left(\frac{2n + 1}{4H} \right) \cdot \left[\frac{c}{[1 - (c/c_0)^2 \sin^2 \phi_0]^{\frac{1}{2}}} \right] \quad \text{for } n = 0, 1, 2, \dots \quad (1 - 1)$$

where H is the thickness of the waveguide (low-velocity soil layer), c is the seismic velocity (either compressional wave or shear wave) within the waveguide, c_0 is the acoustic velocity in the air, and ϕ_0 is the angle of incidence of the acoustic ray in the air (measured with respect to the vertical). The surface wave modes can be described as the result of the complex constructive interference pattern of multiple-reflecting body waves (compressional or shear waves) within the waveguide. The angle that these rays make with the horizontal boundaries of the waveguide must be beyond the critical angle, i.e., the angle for total internal reflection at the lower boundary. Therefore, the seismic velocity of the half-space (or lower layers that bound the waveguide) must be high enough to insure total reflectivity within the waveguide for trapping the seismic energy. Other waves with steeper reflection angles may exist, but these, called "leaky modes," dissipate more rapidly because some energy is transmitted into the high seismic velocity sublayer and leaks out of the waveguide.

For sonic boom coupling, a rough estimate of the natural frequencies that may be excited in the waveguide can be made as follows. Snell's Law states:

$$\frac{\cos \theta_0}{c_0} = \frac{\cos \theta_1}{c_1} = \text{Constant} \quad (1 - 2)$$

where θ_0 and θ_1 are the emergence angles (measured with respect to the horizontal) of the rays within the air and waveguide ($\sin \phi = \cos \theta$), and c_0 and c_1 are the velocities of the two media. For constant, level supersonic flight in a homogenous (unstratified) atmosphere, the relationship between the Mach speed M of the aircraft and the Mach angle θ_0 , which is equal to the angle of emergence of the sonic boom at a flat, horizontal ground surface, is given by:

$$\sin \theta_0 = \left[1 - (1/M)^2 \right]^{1/2} \quad (1 - 3)$$

Combining this equation with the earlier relationship for the normal mode frequencies allows us to express the normal mode frequencies as a function of aircraft speed as follows:

$$f_n = \left(\frac{2n + 1}{4H} \right) \cdot \left[\frac{1}{c^2} - \frac{1}{c_0^2} \left(\frac{1}{M^2} \right) \right]^{-1/2} \quad (1 - 4)$$

The real atmosphere is stratified, of course, and will cause refraction of the Mach wave (sonic boom) as it propagates to the ground. Nevertheless, the above equation provides first order estimates of the natural frequencies of interest. The effects of atmospheric refraction can be easily considered by modifying the $\sin \theta_0$ term, or by defining a Mach number based upon the acoustic velocity at the ground level.

Examination of this equation reveals the following general conclusions: (a) as M increases, θ_0 decreases, (b) the raypath of the sonic boom intersects the ground at a steeper angle, and (c) f_n decreases. There is a low frequency cutoff value (for infinite Mach number) determined by the following relation:

$$f_n = (2n + 1) \cdot \left(\frac{c}{4H} \right) \quad (1 - 5)$$

Further examination of the above equations shows that thicker layers and lower velocity waveguides have lower natural frequencies. For a nominal thickness of 25 m and a waveguide seismic velocity of 100 m/sec, the fundamental mode of the trapped wave is about 1 Hz. In the earth, most low-velocity, near-surface waveguides are likely to have somewhat higher average seismic velocities. Very low-velocity porous soil layers would be relatively thin (<10 m) because compaction at greater depths would rapidly decrease the porosity and increase the seismic velocity. Dry soils would tend to have lower seismic velocities because of the very low acoustic velocity of the air in the pore space.

Increased moisture content would tend to increase the compressional wave velocity, while the shear wave velocity would stay very low because fluids have zero shear modulus. The effects of moisture content can be quite dramatic (Attenborough et al., 1986).

1.3.3.2 Earthquake Strong-Ground Motion

Recent observations of strong shaking during earthquakes show the destructive potential of resonant site conditions. In particular, resonant soil vibrations in Mexico City were responsible for almost total destruction of modern buildings in specific parts of the city. Such destructive ground motions are most unlikely for sonic boom-induced surface waves, yet the specific soil and shallow geologic structure responsible for the resonant conditions are relevant to the determination of potential resonant conditions for sonic boom-coupled Rayleigh waves. Important differences between earthquake-induced and sonic boom-coupled Rayleigh waves include: 1) earthquakes are within the earth and, therefore, the seismic waves are very well-coupled to the ground, whereas sonic booms are in the atmosphere and, in general, are weakly coupled to the ground; 2) phase velocities of earthquake waves are much higher than those of the air-coupled (sonic boom) surface waves and, therefore, may couple over a much broader bandwidth of Rayleigh wave energy; and 3) seismic energy released during earthquakes is many orders-of-magnitude greater than that of a sonic boom. Notwithstanding these differences, the important effects of local site conditions during earthquake shaking are relevant to the possible Rayleigh wave resonance associated with sonic boom-coupled seismic energy.

Studies of the recent destructive earthquake in Mexico City showed that surface wave resonance in low seismic velocity, clay lake bed deposits was responsible for most of the destruction to buildings (Anderson et al., 1986). Even though much of Mexico City is built upon the ancient lake bed, the major destruction was confined to parts of this basin that were near the edge, where the clay layer was about 25-m to 45-m thick. The high water content and low rigidity of the clay deposits are associated with very low shear wave velocities (<100 m/sec) that allowed the incident body wave (P- and S-waves) from the distant earthquake to become trapped in this near-surface waveguide and amplified into strong, harmonic surface waves (Bard et al., 1988; Celebi et al., 1987; Lermo et al., 1988; Romo et al., 1988; Rukos et al., 1988; Sanchez-Sesma et al., 1988; Seed et al., 1988; Singh et al., 1988). The natural frequency of this surface wave resonance was essentially the same as the

natural frequency of the 9-18 story buildings in this area (0.2 to 0.5 Hz) resulting in almost total destruction of such structures. In addition to the strong amplification, the duration of the strong shaking was increased several fold because of both the near-surface effects and the underlying deep sedimentary basin geologic structure.

A major conclusion of these studies is that local variations in the near-surface seismic velocity structure are very significant--strong shaking at sites separated by only a few hundred meters showed substantial variation in amplitude, duration, and character. This conclusion is consistent with the previously stated conclusions regarding the air-coupled Rayleigh wave phenomenon. Another important observation from the earthquake studies is that local surface waves generated near the edge of the basin propagate toward the region of thickening, low-velocity layer thickness and produce longer duration of shaking in the thicker areas. Because these locally-generated surface waves have very low group velocity (velocity at which the energy propagates), they dissipate rapidly with distance, and so the strong shaking effects are confined to the edges of the basin.

1.3.3.3 Exploration Seismology

Exploration seismologists are very familiar with the ringing of near-surface layers in some areas, which is considered a serious coherent noise problem that makes acquisition of good subsurface reflection data very difficult. Most of this coherent noise is called "ground roll," and is, in fact, the Rayleigh wave (sometimes called pseudo-Rayleigh wave) energy trapped in the near-surface, low-velocity layer. Recognition that some of this ground roll propagates at the same velocity as the sound speed in the air led seismologists to study the theoretical aspects of the air-coupled Rayleigh wave phenomenon (Press and Ewing, 1951b; Press and Oliver, 1955). Modern land-based exploration seismology often uses buried dynamite shots to avoid strong air-coupled ground roll in some difficult data areas. Most of the literature discussed in the air-coupled Rayleigh wave section (1.3.3.1) of this report is related to the exploration seismology problem. The use of geophone spreads, with several geophones, spaced out over a substantial distance and with numerous controlled source locations and shot times, allowed the experimental confirmation of the air-coupled surface wave theory. The near-surface, low-velocity waveguide is known as the weathering layer in exploration seismology.

1.3.4 Conclusions of Literature Survey

Review of Air Force environmental assessment documents showed few public concerns directly related to the coupled Rayleigh wave phenomenon. Indirectly related concerns focused upon specific structural types that may be damaged, including archaeological sites, historical structures, old adobe buildings, water wells and storage tanks, house trailers, and radio telescopes. In addition, much concern was expressed regarding the possibility of focused booms or superbooms. All of these issues are considered in this report.

A top-level review of litigation and claims history found no pertinent litigation or claims regarding the sonic boom-coupled Rayleigh wave phenomenon.

Review of the open scientific literature provides a better understanding of the phenomenon of air-coupled surface waves. Several decades of research in the seismological community have focused on the air-coupled surface wave problem with regard to the low frequency "ground roll" that causes unwanted interference in seismic exploration. This research demonstrates that the resonant condition for sonic boom coupling to Rayleigh waves requires a low-velocity surficial layer or waveguide. The strongest resonant coupling occurs when a low-velocity layer overlies a more competent (compacted soil or hard rock), high-velocity layer, forming a waveguide in which the seismic energy can be trapped and propagate with little attenuation.

Air-coupled surface waves are highly monochromatic in character, consisting of relatively long, sinusoidal trains of oscillations at one particular frequency. Typically, only the fundamental mode is excited, but higher modes (with higher frequency content) are observed. The frequencies of the normal modes within the waveguide are directly related to the seismic velocity and aircraft speed. The normal mode frequency is inversely proportional to the thickness of the waveguide.

Resonant coupling of the sonic boom with the Rayleigh waves occurs when the carpet trace speed of the sonic boom matches the Rayleigh wave phase velocity of the ground below. Wave propagation within a waveguide is dispersive, with many different frequencies each associated with a particular phase velocity; therefore, in general, at least one particular frequency will be associated with the sonic boom carpet trace speed. If the near-surface geology has relatively high Rayleigh wave

phase velocities, then only special maneuvers, such as the climbing or diving maneuvers that increase the carpet trace speed to high values, would cause the resonant condition.

Other studies of the air-coupled surface waves found that the mechanism for greater coupling is the dissipation of a low-velocity pore fluid wave in the upper soil layer. High-porosity, low-velocity soils would be associated with the greatest potential for strong sonic boom-coupled Rayleigh wave resonance. Lower porosity or increased moisture content tend to increase the seismic velocities and, therefore, diminish the possibility of the Rayleigh wave resonance phenomenon. The resonant coupling phenomenon was found to be a very local phenomenon; changing the near surface soil conditions over a small area ($<1 \text{ m}^2$) results in local enhancement or diminution of the coupling mechanism.

For the sonic boom-coupled surface waves to be potentially damaging, the resonant Rayleigh wave frequencies must be similar to that of structures in the area affected. Review of natural periods of structures that may be affected by the sonic boom-coupled surface waves shows that houses and other low-rise construction have natural response frequencies (1 to 10 Hz) comparable to Rayleigh wave frequencies of shallow, thin (1 to 100 m), low-velocity (10 to 500 m/sec) soil layers. Because the surface waves are coupled to the sonic boom, affected structures will be shaken by the seismic waves at the same time the airborne acoustic pressure pulses strike. Therefore, the combined effect of these two loadings should be considered.

Earthquake strong-motion studies find that strong resonant interaction between the incident body waves (P- and S-waves) with low-velocity near-surface layers, such as the clay lake bed deposits in Mexico City, caused extreme shaking. Almost total destruction occurred to buildings with natural response frequencies that matched those of the resonant surface waves. These studies found that the greatest amplification occurred near the edges of the sedimentary basins, where strong, local, low-velocity surface waves were generated. Again, the strong resonance condition proved to be a very local effect.

2.0 DEFINITION OF SOIL TYPES AND SEISMIC PROPAGATION CONDITIONS

2.1 Introduction

Experimental observations of seismic waves induced by sonic boom showed that the character of the ground motion is more closely related to the local soil and surficial geology than to the character of the N-wave that induces the ground motion (Goforth and McDonald, 1968). Some of the experimental seismograms showed prolonged ringing lasting for a few minutes after the passage of the N-wave. The monochromatic nature of the ringing is highly suggestive of Rayleigh waves trapped in a shallow, low-velocity soil waveguide. An important part of this project is to identify specific soil or geologic conditions that may lead to resonant sonic boom-coupled Rayleigh waves.

Because there are an infinite variety of shallow soil and geologic profiles that may be encountered in the real world, the scope of this effort was narrowed to representative profiles most likely to be associated with the resonant condition. The resonant condition occurs when the carpet trace speed of the sonic boom ground intersection exactly matches the local Rayleigh wave phase velocity (Figure 2-1). Because the carpet trace speed of the sonic boom, similar to the aircraft ground speed (roughly 300 to 850 m/sec for Mach 1.0-2.5), is very low compared to typical seismic velocities in geologic materials (Table 2-1), only those near-surface deposits that have very low Rayleigh wave phase velocities are susceptible to the resonant condition. Such materials might include loosely consolidated soils, loess, and playa lake deposits. This study focuses on identifying surficial deposits present in or near Supersonic Operating Areas (SOAs; Table 2-2, Figure 2-3) that may have Rayleigh wave phase velocities comparable to the aircraft speeds. Consideration of the geological setting (Figure 2-2) allows characterization of the general depositional environment where such low velocity soils may occur so that these areas may be identified within the SOAs.

In order to define surficial geologic conditions representative of regions where the SOAs are located, maps of soils and surficial geology were obtained from the U.S. Geological Survey, state geological offices, and the Soils Conservation Service. Lists of points-of-contact for soils and other geologic information, and reference lists of published soils and geologic maps in the vicinity of the SOAs are included in Appendix B. Because many SOAs are located in remote back country areas, soils studies for several specific areas containing SOAs are unavailable. Soils studies for adjacent

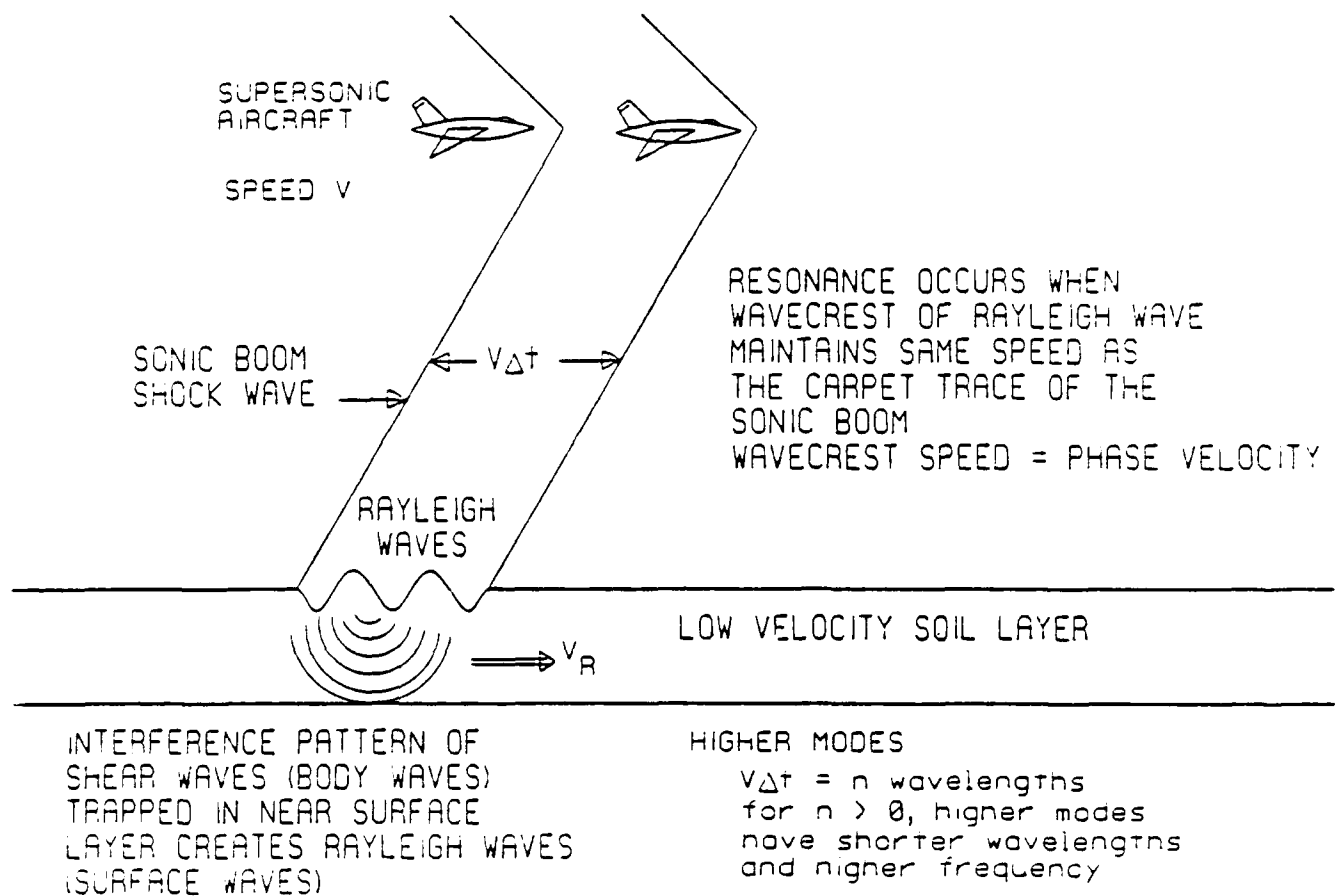


Figure 2-1. Sonic Boom-Coupled Rayleigh Wave Resonance Condition.

Table 2-1. Typical Elastic Parameters for Surficial Deposits.

Material	Specific Gravity	Compressional Velocity (m/sec)	Shear Velocity (m/sec)
WATER	1.0	1500	0.0
CLAY	1.2 - 1.5	1100 - 2500	150 - 625
SAND	1.4 - 2.0	600 - 1800	270 - 500
MUDSTONE	2.0 - 2.6	900 - 1000	300
SHALE	2.0 - 2.7	2150 - 2800	650 - 2250
SANDSTONE	2.0 - 2.7	1100 - 4300	600 - 2250
LIMESTONE	2.2 - 2.8	1700 - 6100	2800 - 3100
ROCK SALT	1.9 - 2.2	4100 - 4600	2370 - 2650
ANHYDRITE	2.8 - 3.0	4100 - 7600	2370 - 4390
BASALT	2.4 - 3.1	5425 - 6400	2700 - 3200
GRANITE	2.5 - 2.8	5000 - 5900	2800 - 3100

SOURCE: Sydney P. Clark, (ed.), 1966, Handbook of Physical Constants, rev. ed., *Geological Society of America Memoir 97*.

Table 2-2. List of Supersonic Operating Areas.

	ARIZONA
<i>Gladden (Luke AFB)</i>	Maricopa, La Paz, Yavapai, and Yuma Counties, Arizona.
<i>Luke Ranges (Luke AFB)</i>	Pima and Yuma Counties, Arizona
<i>Sells (Luke AFB)</i>	Pima County, Arizona
	CALIFORNIA
<i>Bullion Mountain (George AFB)</i>	San Bernardino County, California
<i>Edwards (Edwards AFB)</i>	Kern, Los Angeles, and San Bernardino Counties, California
<i>Panamint Valley (George AFB)</i>	Inyo County, California
	FLORIDA
<i>Eglin (Eglin AFB)</i>	Inland and Offshore Operating Areas
	NEVADA
<i>Nellis (Nellis AFB)</i>	Clark, Lincoln, and Nye Counties, Nevada
	NEW MEXICO
<i>White Sands (Holloman AFB)</i>	
<i>Reserve (Holloman AFB)</i>	Catron, Cibola, and Socorro Counties, New Mexico
	TEXAS
<i>Valentine (Holloman AFB)</i>	Brewster, Culberson, Hudspeth, Jeff Davis, Presidio, Reeves Counties, Texas
	UTAH/NEVADA
<i>Gandy (Hill AFB)</i>	Elko County, Nevada
	Juab and Tooele Counties, Utah
	UTAH
<i>Utah TTR (Hill AFB)</i>	Tooele and Juab Counties, Utah

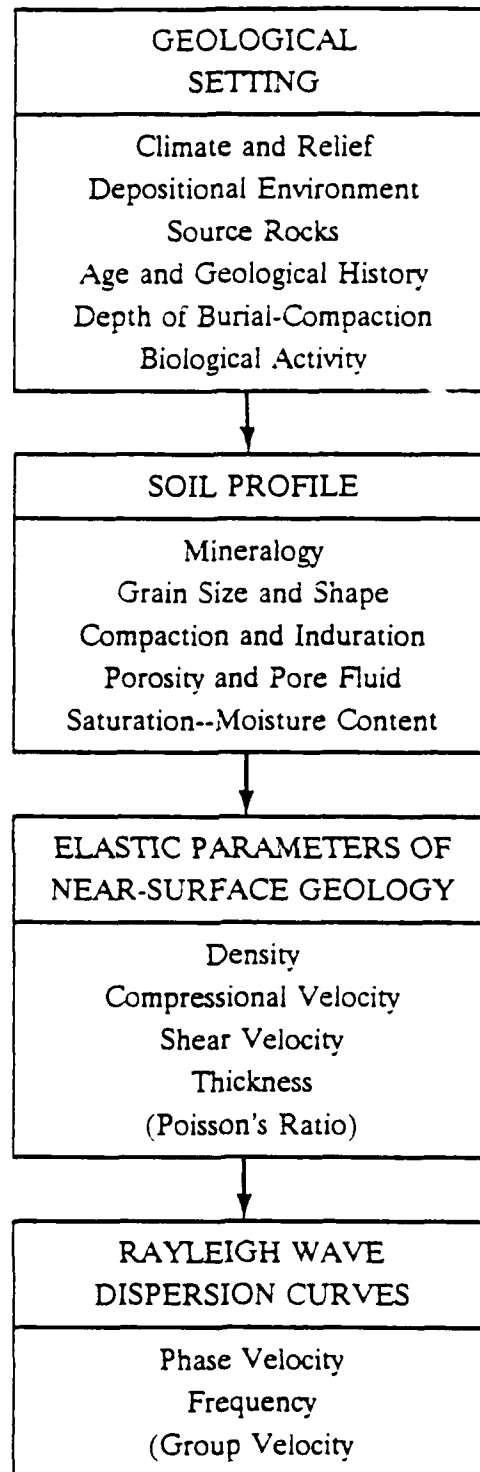


Figure 2-2. Development of Rayleigh Wave Characteristics.

areas and regional geologic maps, however, provide data adequate to characterize the near-surface geologic conditions for developing the seismic velocity profiles representative of all areas.

Detailed mapping of the soils and near-surface deposits in SOAs that may be susceptible to the resonant condition would require a more substantial data collection effort than is possible in this preliminary investigation. Nevertheless, broad areas of general depositional environments likely to include such areas have been mapped in some of the SOAs on the existing geologic and soils studies maps. These studies also describe the local climate and other factors related to the seasonal moisture content of the soils.

Realistic shallow geologic profiles (soil profiles) for the computation of the Rayleigh wave dispersion curves (phase velocity versus frequency) are obtained from a combination of soil borings and seismic refraction profiles described in the scientific literature for locations near actual SOAs. In addition, for the underlying bedrock and deeper earth's crust, seismic velocity structure determined by earthquake seismologists is included (Langston and Helmberger, 1974; Hadley, 1978; Priestley and Brune, 1978; Boore and Fletcher, 1982). Although the high seismic velocities associated with the bedrock structure are unlikely to experience the sonic boom resonant condition (Goforth and McDonald, 1968; Espinosa et al., 1968), computation of Rayleigh wave phase velocities for realistic earth structures including these deeper geologic layers is important for bracketing the full range of phase velocities that may be encountered in the SOAs. Additional shallow geologic seismic velocity profiles are obtained from actual measured profiles used for earthquake microzonation studies in the tectonically active parts of the western United States. For example, in the Los Angeles (Antelope Valley; Fumal and Tinsley, 1985) and Salt Lake City (Hays et al., 1978) areas, seismic velocities of the near-surface soils have been measured in order to predict zones where strong amplification of earthquake ground shaking may occur. Such areas, characterized by low shear velocity sediments, may also be susceptible to the sonic boom-Rayleigh wave resonance condition.

Rayleigh wave phase velocity curves calculated by Dr. Gordon Stewart, seismologist, for the representative seismic velocity profiles are presented and their significance to the sonic boom-Rayleigh wave resonance phenomenon are discussed. Most of these curves were determined for low-velocity surficial soil conditions with thicknesses that are likely to have sonic boom-coupled Rayleigh wave resonance at frequencies between 1 and 10 Hz. These frequencies represent the natural resonant frequencies of structures most likely to be affected by the sonic boom-coupled seismic waves

(Section 3). Special near-surface geological conditions, such as a low velocity waveguide, are found to be most susceptible to the Rayleigh wave resonance condition. Crude estimates of the ground motion that may be experienced under such conditions are estimated and compared with damage criteria. Lastly, a glossary of soils and geologic terminology is included in Appendix C.

2.2 Geological Setting

Figure 2-2 outlines the general approach to determination of the near-surface seismic velocity profiles for computing the representative Rayleigh wave phase velocity curves. First, parameters of the geological setting relevant to determination of the near-surface conditions must be considered. Relevant parameters include climate and relief, depositional environment, source rocks, age and geological history of the deposits, depth of burial of sediments, and biological activity. Consideration of these parameters allows us to classify soil profiles and near-surface geological conditions for development of the representative profiles for calculation of the Rayleigh wave phase velocities. This classification will aid in defining areas where conditions conducive to the Rayleigh wave resonance condition may be found. Following sections will describe the key factors and methods used to develop the seismic parameters for the soil profiles.

2.2.1 Climate and Relief

In order to define the soil types and seismic propagation conditions that may be encountered in SOAs, it is necessary to review the geological setting of the region. Except for the MOAs in Florida, and off the east coast, where supersonic operations occur over the sea, most SOAs of concern to this study are located in parts of the western United States (Figure 2-3). Geologists call this region the "Cordillera" of western North America. As defined by Holmes (1965), the Cordillera is "a broad assemblage of mountain ranges together with their associated plateaus and intermontane basins." SOAs within the Cordillera lie within four major geologic provinces: (1) the Rocky Mountains; (2) the Colorado Plateau; (3) Basin and Range (Great Basin); and (4) the Mojave Desert. As one might expect, the topography and associated climate within these SOAs is highly variable, being characterized by mountain ranges adjacent to broad valleys or basins. Climate varies from arid to cool and temperate. SOAs at Eglin AFB are in a humid-temperate climate with warm temperatures and rainfall averaging about 65 in per year.

Climatic regions of most southwestern SOAs fall into three categories: arid and semi-arid (desert and steppe), Mediterranean, and temperate. Some of the higher elevation mountain regions may have experienced glacial or tundra climate regimes during the ice ages. Most areas of interest to this study, however, have modern annual rainfalls that average less than about 20-25 in. The low elevation regions are generally arid to semi-arid, with annual rainfalls less than about 10 in, and the higher elevation, mountain and plateau, regions have annual rainfall averages of 10-25 in. Consequently, most of the soils and near-surface deposits will be dry for much of the year, and partially-to-fully saturated during the rainy season. Stream channels and playa lake beds may have a shallow water table, and therefore, deposits may be saturated at shallow depths all year round, or at least during the wet season. In the arid regions the rainfall is highly variable, and some years may pass without significant or measurable precipitation. The character of the rainfall in the adjoining mountainous regions and the underground aquifer are important in determining the level of the water table in all these areas.

Elevations of SOAs in the southern Rocky Mountains, White Sands (WS) and Valentine (V) vary from about 3,000 ft to almost 9,000 ft. Interior basins of these areas are undrained; streams flowing into them do not reach the sea, but may form intermittent lakes that eventually dry up. Few thunderstorms from Pacific storms reach these areas during the winter dry season; most of the rainfall comes from the Gulf of Mexico during summer. As in all of the regions, rainfall is higher in the mountains, although White Sands, being surrounded by mountain ranges, lies in a rain shadow and is arid. Valentine, which is on the east flank of the mountains, varies from semi-arid at low elevations to cool and temperate at higher elevations.

The Colorado Plateau is a flat, elevated region that slopes gently from elevations that average about 8,000 ft in the south to elevations that average about 6,000 ft in the north. Peaks within the Reserve SOA (R) reach above 10,000 ft. Because of its higher elevations, rainfall is generally greater in the Colorado Plateau SOAs than in other SOAs at lower elevations, and its climate is semi-arid to cool and temperate.

The Basin and Range province consists of north-south trending mountain ranges with peaks that may exceed 10,000 ft in elevation, and intervening basins that may extend below sea level (Death Valley, for example). The Great Basin is the part of the larger Basin and Range province that lies

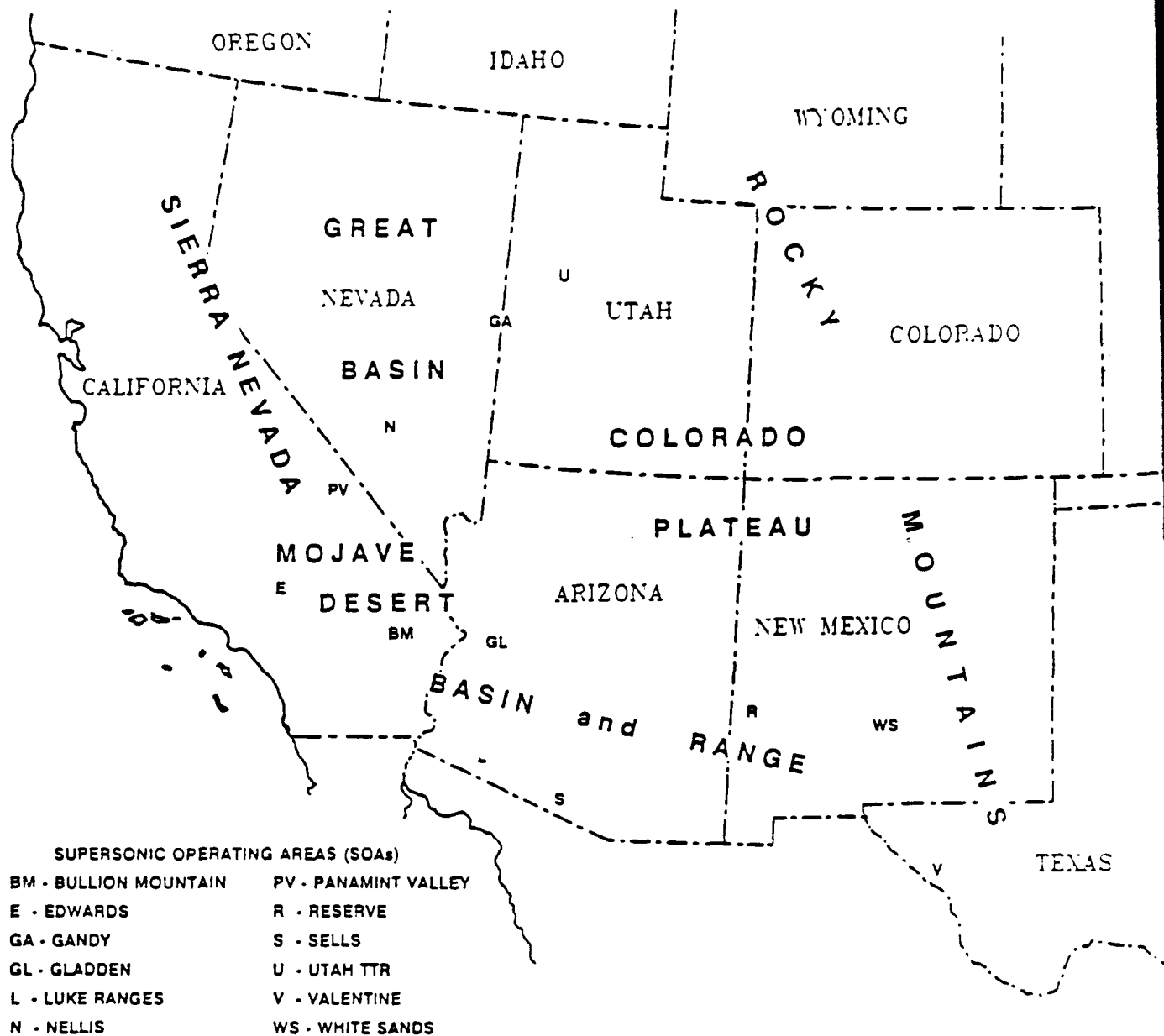


Figure 2-3. Map Showing Location of Supersonic Operating Areas (SOAs) and the Major Geologic Provinces in the Western United States (see page 19).

between the Colorado Plateau and the Sierra Nevada. Most basins in the Basin and Range province are internal and undrained; the streams empty into these internal basins where the water percolates into the ground or is evaporated. Only the Colorado River, with its tributaries, passes through the area and reaches the sea. During wetter climates of the past, large freshwater lakes filled some of these basins, such as Pleistocene Lake Bonneville in the Utah area. The Bonneville salt flats and the Great Salt Lake are remnants of this ancient lake.

The Mojave Desert is a small province in eastern California, similar in character to the Basin and Range province, but it is generally elevated above about 4,000 ft. Because it is in the rain shadow of the Sierra Nevada and other mountains to the west, it has an arid climate.

2.2.2 Depositional Environment

One of the most successful techniques used by geologists to categorize sedimentary deposits is the concept of depositional environment--the environment under which the sediments were actually transported and deposited. Topographic relief and climate are major factors in determining the depositional environment. Major categories of depositional environment (Table 2-3) include: *aeolian* or wind derived; *alluvial* or water transported; *fluvial* or river/stream transported; *lacustrine* or lake deposits; *glacial* and *glacio-fluvial*, deposits from streams fed by glaciers; and *colluvial* or locally weathered and transported, such as slope wash deposits. The major categories listed in Table 2-3 are in approximate order of increasing relief or elevation. For this study, specific depositional settings will be considered, which are sub-categories of the above depositional environments. These include: alluvial fans--stream and debris flow deposits at the foot of mountains where stream valleys enter the valley or basin floor; bajadas, pediments or terraces--relatively flat-lying deposits at the foot of mountains, on basin floors or slightly elevated above the basin or valley floor; fluvial--stream channels, flood plains, stream terraces, and inland deltas associated with active and intermittent streams; aeolian--sand dunes or loess deposits; lacustrine--modern and ancient lake bed deposits, playa lake deposits; other alluvium-sediments on mesas, ridges, hills, or landslides; and bedrock slopes--colluvium or thin soils over bedrock outcrops on mountain faces, and so forth. These categories are consistent with the sedimentary units described in the soils reports provided by the Soils Conservation Service (Appendix B). Depositional environments appropriate for Eglin AFB, Florida include deltaic; estuarine or drowned river valley; or clastic shoreline including beaches, barrier islands, tidal flats and lagoons.

Table 2-3. Depositional Environments.

Representative Geologic Conditions and Soil Types

Transitional--Marine/Non-Marine

Deltaic

Estuarine

Clastic Shoreline

Lacustrine--Ancient and Modern Lakes

Ancient and Playa Lake Deposits

Fluvatile--Stream Channels, Flood Plains, Stream Terraces

Fluvial Deposits

Aeolian--Wind-borne Sediments

Sand Dunes

Loess

Alluvial--Water-borne Sediments

Young Alluvial Fans

Older Alluvial Fans

Other Alluvium--Plains, Hills, Mesas, Ridges, and Terraces

Other Basin Deposits--Bajada and Pediment

Glacial and Glacio-Fluvial

Glacial Deposits

Bedrock and Colluvium--Mountains and Foothills

Bedrock Deposits--Clastic Sedimentary

Bedrock Deposits--Carbonate/Evaporite Sedimentary

Bedrock Deposits--Volcanic and Metamorphic and Mixed

The character of the sedimentary materials is directly related to the energy involved in sedimentation, both transportation and deposition. High energy streams that flow through mountain valleys and canyons keep fine-grained material in suspension and allow only heavy, coarse-grained material, such as gravel or boulders, to settle out. Slow moving streams in more level areas will deposit finer-grained material such as sand. Quiet water sites, such as lakes or overbank areas on flood plains, are locations where fine-grained silts and clays will settle. Waves and ocean currents on beaches will redistribute sediment from river deltas, spreading sands along beaches and washing fine-grained silts and clays out to the deep sea.

In the arid and semi-arid southwestern United States where rainfall is rare, occasional cloudbursts occur. These may produce very rapid, high energy deposition from flash floods or mud and debris flows that consist of inhomogeneous mixtures of sediments and rock fragments of various sizes, including boulders. Such materials are often channeled down steep mountain valleys and deposited along the base of the mountains into the adjoining basins as "alluvial fans." Continued erosional and depositional processes on these fan surfaces can redistribute some of the more fine-grained sediments farther out into the valleys and basin troughs. Coalescence of numerous alluvial fans on the edge of a mountain front form a "bajada." During especially wet seasons, temporary lakes may form in the basins, allowing the most fine-grained sediment, silts and clays to slowly settle out in the quiet waters. Later, evaporation will dry out these "playa" lakes, leaving layers of evaporite minerals such as gypsum, carbonates, or other salts that are common in the arid southwest basins. In addition, steady winds carry fine sands or silts to form sand dunes in some areas and loess deposits in others. These fine-grained minerals are also deposited in the cracks and spaces between the larger gravel or boulder deposits on fan surfaces, or between mud cracks on dry lake beds.

Because the climate has alternated between wet and dry, and tectonic movements have uplifted the mountain ranges many times during the geological past, ancient depositional environments may be found at different elevations and locations than modern ones. Fluvial terraces of uplifted ancient stream channel and flood plain deposits are found along the sides of mountain valleys and basins. Similar terraces, formed of beach deposits of ancient lakes, are also common in some areas, especially around the shores of ancient Lake Bonneville in Utah. Flat areas where erosion has planed off ancient bedrock surfaces exist as terraces (small areas) or pediments (large areas), with colluvial or weathered bedrock covers. Tectonic uplift and erosion have also exposed large areas of bedrock consisting of many different rock types in the mountainous areas of the

Cordillera. Along the Florida Gulf coastal area, changing sea levels during the Pleistocene glaciation-ice ages--shifted ancient beach and other shoreline environments inland from the present shoreline. Migrating rivers spread deltaic deposits over wide areas of the coast.

2.2.3 Source Rocks

The types of source rocks from which the sediments are derived determines the mineralogy of the sediments, and the related grain sizes, shapes, and weathering character. Minerals in most rocks weather (a natural chemical reaction) to clays of one sort or another, although some minerals, such as quartz, are chemically more stable and remain unaltered. In addition, mechanical weathering processes, such as frost-wedging or abrasion, break up bedrock into rock fragments of various sizes. Clay minerals are especially resistant to further weathering and therefore persist in soils. Quartz sand grains are very resistant to abrasion, because of their hardness, and so, may endure thousands of years of abrasion during wind and stream transport. Resulting dune or beach sands are mostly quartz minerals, whereas sand grains in deposits closer to their original source rock, such as on alluvial fans, may be composed of many mineral types.

If the region has abundant shell life, calcium carbonate shell detritus may be an important constituent of the deposits. Likewise, if the source rocks are limestones, the sediments will be rich in calcium carbonates (calcareous). In some areas, particular types of source rocks provide unique weathering products. An example is the gypsum sands of the White Sands Missile Range area that are weathered from nearby outcrops of hard gypsum rock.

2.2.4 Age and Geological History--Weathering and Formation of Soils

After deposition of the sediments, continued exposure to moisture and dissolved minerals allow the "alluvium" or other rock material to be altered--the weathering process. This continued weathering may result in soil formation. The original minerals of the deposit continue to break down both chemically and mechanically into more stable minerals, such as clays. Percolation of meteoric waters (from rainfall, groundwater, or runoff) which contain dissolved minerals allows redeposition of some of these minerals, such as calcium carbonate or silica, to form cements that bind the sediment grains together. Fine-grained weathering products such as the clay minerals are also washed downward within the sediment pile to some level where they can no longer pass between the

sediment grains. At this level, the clays accumulate. With time, the redistribution of these minerals forms distinct horizons, or horizontal levels within the soil, that have distinct character. The development of these horizons, with particular depth, color, and other attributes, are related to the age of the soil (how long the soil has been developing at the location). Very young soils will not have a noticeable clay layer, and will consist mostly of the recently deposited alluvium. Such deposits are most likely to occur along active stream channels such as in washes or arroyos, or in very steep areas covered by frequent rockfalls. Young soils that show minor soil development may occur on recently active alluvial fans or bajadas. Older alluvial fans and elevated terraces or pediments on long exposed bedrock slopes of hills and mountains have well-developed soils with prominent horizons. Quartz sand deposits from ancient or modern beaches have developed little soil because of the chemical stability of quartz, and the permeability of the sands allows other dissolved minerals to easily wash away.

2.2.5 Depth of Burial--Compaction and Induration

Depth of burial is related to the amount of compaction that a sediment has undergone; compaction results in greater densities and seismic velocities. Age and geological history are related to the "induration" of the sediment. Induration is the process of hardening of a deposit by cementation, compaction, heat (recrystallization), or other process. All of these processes take time and so older deposits tend to be "well-indurated."

Climate is also an important factor, both modern and ancient, in the compaction and induration of the sediments. Climatic factors, including rainfall (or snowfall) and temperature, affect the rates at which rocks weather and the transportation of these rock fragments or sediment grains through the area. Freezing accelerates breakdown of bedrock by splitting the larger rocks along cracks through the action of "frost-wedging." Modern climate is also important in determining the saturation (with water) of the soil or near-surface sediment deposits (alluvium or colluvium) which, in turn, affects the rates of dissolution or precipitation of minerals in the soil.

The soluble minerals and salts in the alluvium that are removed from the near-surface layers by percolation of water and precipitated deeper in the soil contribute to the induration of soil layers. These precipitates, typically of calcium carbonate (lime) or silica, may form a "hardpan"-- a more compact and hard, low-porosity layer within the soil profile that resists further downward percolation

of water. Calcareous hardpans are called "caliche" by soil scientists. Again, because time is required for such deposits to accumulate, the depth, thickness, and degree of induration of this hardpan depends on the age as well as mineralogy of the alluvium in which the soil is developing.

2.2.6 Biological Activity

Plants, animals, and humans have important effects on soil formation and near-surface geology. Earthworms, rodents and other burrowing animals stir up the soil, increasing its porosity and aiding in the weathering process. Bacteria and other microorganisms are active in mineral alteration associated with weathering, too. Plant life adds important organic matter to the upper soil levels, although in the arid parts of many SOAs, plant life is minimal. The elevated, wetter mountain regions and Florida Gulf Coast have more abundant plant and animal life, resulting in thicker, organic-rich soils. Humans have a major influence on the soils, especially where large tracts of land have been tilled and irrigated for farming. Consolidation of near-surface soils for construction of road beds, buildings or airport runways, will change the physical properties of the soil and the associated seismic velocities. Overgrazing by cattle, diversion of stream channels, road building, and poor soils management have resulted in accelerated soil erosion in some desert areas.

2.3 Properties of the Soil Profile

Properties of the soils and near-surface geology that affect the seismic velocities and Rayleigh wave phase velocities include: mineralogy, grain size and shape, porosity and pore fluid, saturation and moisture content. Detailed descriptions of actual soil profiles from representative areas within or near SOAs are presented in Appendix B. This section discusses the significance of the soil parameters in terms of computing the Rayleigh wave phase velocities.

2.3.1 Mineralogy

Mineralogy affects the seismic velocity of the solid matrix in the soil; representative seismic velocities of some minerals are shown in Table 2-1. The mineral content of the sediment grains also plays a role in the density determination of the material. Hard, rigid, quartz sand grains are unlikely to deform with the modest loading of shallow overburden, whereas pliable, flat, mica or clay mineral grains may be easily bent and shaped to compact more tightly with overburden. Thus, a sand or

young sandstone is typically much more porous than a clay or shale (clay rock); oil companies have exploited this character, recognizing that sandstone acts as a reservoir for petroleum deposits that are often capped by a more dense, compact, shale deposit. Mineralogy also affects the dissolution, recrystallization, and cementation properties of the soil as described above.

2.3.2 Grain Size and Shape

Grain size and shape affect the compaction ability of the soil or sediment. It is related to the mineralogy as described above. The hardness of the mineral grains and the time spent in redistribution and sedimentation determine the size of the sediment particles in a particular deposit. Furthermore, winnowing action by wind, stream currents or waves, will selectively remove fine-grained sediments to more quiet depositional environments such as lake beds, and leave behind the more coarse-grained deposits such as cobbles, gravel, and sands, in the stream channels. Uniform spheres have a limited number of close packing arrangements that result in a minimum porosity. Distribution of grain size in a sediment or soil is important because a wide range of grain sizes (called well graded in geological terms) can be more tightly compacted with less pore space, having the finer grains fill in the gaps between the larger grains. Shape is important because thin flat grains, as in mica and clays, will compact more tightly than uniform spheres. Finer-grained sediments, such as sands, silts, and clays, generally have lower densities and seismic velocities than more coarse-grained deposits, such as gravel and conglomerates. Because clay particles are flat-shaped, however, with a small amount of compaction, clays may have lower porosity and higher seismic velocities than some sands.

2.3.3 Porosity and Pore Fluid

Porosity, which relates to all of the above parameters, is very important in determining the elastic properties of the sediment or soil (Wyllie et al., 1958). The bulk density and seismic velocities of a deposit are weighted averages of the individual values for mineral grains and pore fluid. Higher porosity deposits will have lower seismic velocities because more volume is occupied by low density or low velocity pore fluid. Conversely, low-porosity, highly-compacted or well-indurated (hard, well-cemented) deposits have higher bulk density and seismic velocity. Even though the mineralogy of a given sedimentary deposit may vary widely, variations in porosity and pore fluid content have much greater effect in determining the elastic properties. Pore fluid composition is very important because even minor amounts of gas within a saturated sediment can cause appreciable decrease in the seismic

velocities (Anderson and Hampton, 1980), particularly the compressional velocity. The shear wave velocity is more sensitive to the overall porosity. The compressional wave velocity of a sediment will increase significantly with water saturation whereas the shear velocity may remain about the same, because any fluid, gas or water, has zero shear velocity. At depth in a sediment column, increase of pore fluid pressure caused by water (or other liquid) saturation may help to maintain porosity and keep relatively lower seismic velocities, whereas a dry sediment may be more easily compacted and show an increase in these velocities. With regard to the sonic boom seismic coupling, porous, air-filled, near-surface soils or sediments show greater coupling than water saturated or compacted sediments (Sabatier et al., 1986a and b). Porous, air-filled soils, however, are not likely to extend more than a few meters in depth because of compaction. Yet porous, air-filled soils over saturated, deeper sediments with significant porosity maintained by pore fluid pressure may provide the best low-velocity seismic waveguide for strong seismo-acoustic coupling. Real deposits of this nature may be present in the playa lake beds of the intermontane basins, where the water table is relatively shallow, and the depositional conditions are relatively uniform over wide areas.

2.3.4 Saturation and Moisture Content

Water saturation in sediments has a more complicated effect on seismic velocity than a simple linear increase in seismic velocity with increasing saturation. Ross et al. (1987) found that the elastic properties, including seismic velocity, increased to a maximum at a relatively low saturation (between 5 and 10%), and then decreased to near the dry value as the saturation was increased. They attributed this effect to the presence of gas in the saturated sediment. Petroleum exploration geophysicists have recognized that small amounts of gas can have dramatic effects on the seismic velocities of saturated sediments (Anderson and Hampton, 1980). Considering that near-surface soils and sediments are likely to contain some gas, even when water-saturated, this same effect would be expected for real, "in-situ" soils, and so the maximum seismic velocities may occur at somewhat less than 100% saturation. Increased water saturation also may help to maintain porosity of the sediment, even when buried to a significant depth by increasing the pore fluid pressure. Very permeable soils, such as beach sand deposits, drain quickly, so that water saturation will tend to be very low.

2.4 Representative Soil and Geologic Profiles

Soil profiles for areas in the vicinity of several SOAs were examined in this study in order to develop a representative set of near-surface seismic velocity profiles for computation of the Rayleigh wave phase velocity curves. A list of published soil surveys and several detailed soil descriptions categorized by depositional environment are presented in Appendix B. In addition to the soil surveys, geologic maps for some areas were obtained that showed the near-surface geological conditions. These maps were also used to develop the representative near-surface geologic conditions and depositional environments as described in the preceding sections. Seismic velocity profiles prepared for computation of the Rayleigh wave phase velocities were derived from actual measured profiles in a number of areas that represent the major depositional environments likely to experience Rayleigh wave coupling. A few "bedrock" velocity profiles were also prepared using models of the seismic velocity structure of the earth's crust derived from earthquake seismology. These models are important to bracket the full range of Rayleigh wave phase velocities that may be encountered in SOAs. Furthermore, these models were also added to the base of the near-surface soil velocity profiles to provide geologic structure relevant to the low frequency band of the Rayleigh wave spectrum. This deep structure governs the character of the Rayleigh wave dispersion curves at frequencies below 1 Hz, and so, has no effect on our conclusions regarding the sonic boom-coupled Rayleigh wave resonance phenomenon.

Rayleigh wave phase velocities are proportional to the body wave, i.e., compressional and shear wave velocities of the surficial geologic materials. For simplicity, the real earth is modeled as a continuum, composed of a number of horizontal, laterally homogeneous layers of material. Each layer has a set of physical parameters including bulk density, compressional (P) and shear (S) wave seismic velocities that are used to determine the Rayleigh wave phase velocity, as a function of frequency, for the particular near-surface structure being modeled. The thickness of the layer is also a fundamental parameter used to calculate the Rayleigh wave velocities. Layer thickness depends on depositional environment, degree of weathering, and other geologic processes described previously.

For this study, theoretical Rayleigh wave phase velocities that a given soil or near-surface geologic profile may have were computed and compared with the sonic boom carpet trace speeds to determine at what frequencies the resonance condition may occur. Including the actual measured seismic velocity profiles and other "representative" velocity profiles constructed using realistic seismic

velocities of typical earth/soil materials, a total of 29 different models for computing Rayleigh wave phase velocity dispersion curves were prepared (Table 2-4; Appendix D). As expected, Rayleigh wave phase velocities as low as nominal sonic boom carpet trace speeds (about 300-850 m/sec) occur only for models with low seismic velocity surface layers, such as clay lake beds, sandy soils, or other porous, unconsolidated sediments. Those models with bedrock at the surface (basic earth crustal models) have Rayleigh wave phase velocities much higher than nominal sonic boom carpet trace speeds, and would, therefore, be unlikely to experience the resonant condition.

Table 2-4. Representative Seismic Velocity Models.

Model	Location/Name	Depositional Environment	Reference
1	Edwards AFB	Playa Lake Bed (10-m thick clay)	1
1a	Edwards AFB	Playa Lake Bed (100-m thick clay)	1
1b	Edwards AFB	Playa Lake Bed (1-m thick clay)	1
2	Tonto Forest	Weathered Granitic Bedrock	1
3	Tonto Forest	Weathered Granitic Bedrock	1
11	Mojave Desert	Deep Crust with Igneous Bedrock	2
12	Mojave Desert	Model 11 with Sedimentary Bedrock	2
13	Mojave Desert	Deep Crust w/LVZ, Sediment. Bedrock	2
14	Mojave Desert--EXP-0	Model 13 with Alluvial Fan (Older)	2
15	Mojave Desert--Baldy Mesa	Younger Alluvial Fan	2
16	Mojave Desert--TRASH	Basin Alluvium	2
17	Mojave Desert--EXP-0	Same as Model 14, without Deep Crust	2
21	Colorado Plateau	Deep Crust with Sedimentary Bedrock	3
22	Near Albuquerque	Thin Soil over Weathered Bedrock	4
23	Site 1	Thick Soil, Basin Alluvium	4
24	Site 2	Thick Soil, Basin Alluvium	4
25	Sandy Soil	Stream Channel or Young Fan or Beach/Delta	4
26	Univ. Mississippi	Thick Soil over Sedimentary Bedrock	5
27	A & B Average	Thin Soil, Older Alluvium	5
28	Near Albuquerque	Pumice Layer with Weathered Bedrock	6
29	Great Basin	Deep Crust w/Weathered Bedrock	4,7
30	Great Basin	Deep Crust w/Older Fan	7
31	Imperial Valley	Deep Basin, Marine/Lacustrine	8
41	Shallow Salt #1	Lacustrine, Evaporite Basin	9
42	Shallow Salt #2	Lacustrine, Evaporite Basin	9
43	Deep Salt	Lacustrine, Evaporite Basin	9
44	Antelope Valley	Older Alluvium	10
45	Antelope Valley	Older Alluvium	10

¹Goforth and McDonald, 1968

²Hadley, 1978

³Langston and Helmberger, 1974

⁴Sabatier et al., 1986a

⁵Sabatier et al., 1986b

⁶Sabatier and Raspé, 1988

⁷Priestley and Brune, 1978

⁸Boore and Fletcher, 1982

⁹Hays et al., 1978

¹⁰Fumal and Tinsley, 1985

2.4.1 Near-Surface Waveguide

Goforth and McDonald (1968) reasoned that because the near-surface geology and soil conditions vary over relatively short distances, the sonic boom-coupled Rayleigh wave resonance would be unable to generate damaging levels of ground shaking. Their observations on a small dry lake at Edwards Air Force Base, which had suitably low near-surface seismic velocities, showed significant resonant coupling at only one location, whereas another nearby location on the same clay lake bed had a more complicated seismic character. It is possible that, for this small playa lake, the variations of geological conditions over short distances, including possible thickness changes in the surficial low-velocity layer, would change the resonant frequencies of Rayleigh wave propagation. The strong resonant coupling problem may occur, however, if a surficial low-velocity geological layer exists that has a uniform seismic character over a substantial distance, i.e., for many seismic wavelengths.

The simplest waveguide case is for a single low-velocity layer over bedrock or other hard substrate. Water over a hard bottom, such as limestone, as in a lake or sea is a good example of a simple waveguide where seismic energy may be trapped and propagate over great distances with little attenuation. Soil or weathering layers over bedrock may act as low velocity waveguides, but these layers are usually very thin. Goforth and McDonald (1968) measured sonic boom-coupled seismic waves at the Tonto Forest Observatory where seismographs were located on weathered granitic bedrock, but sonic boom-coupled Rayleigh wave resonance was absent at these sites even though the weathered layer was as much as 60 m thick. Lateral variability in the seismic properties of the near-surface layers may have prevented strong, coupled surface waves to build up. The widespread sandy soil of Eglin AFB may represent an extensive low-velocity surficial layer, but deeper low-velocity deltaic deposits have significant lateral variability that may disrupt strong resonant coupling.

For this analysis, simple layer models with few sedimentary layers over an equally simple upper crust (deep bedrock geology) will be used to estimate the Rayleigh wave phase velocities. More complex layering in alluvium arises from climatic cycles that alternate deposition with erosion or non-deposition, as on playa lake beds. River channels migrate, too, so that alternating layers of channel deposits and overbank or flood plain deposits are found in an area. Because wavelengths for Rayleigh waves at frequencies of interest range from a few tens of meters to a kilometer, there is no point in trying to model the surficial geology at a spacing finer than a few meters. One example,

however, was computed for a very thin, low-velocity surface layer, to show that the Rayleigh waves affected by thin layers have very high resonant frequencies (100 Hz or greater). Likewise, for deeper earth structure, because only low-frequency (long wavelength) Rayleigh waves are affected, the layers in simple models typically get much thicker with depth. Thin, buried layers are generally unnoticeable in the dispersion curves. For example, the differences between the dispersion curves for the simple 5-layer Mojave Desert crustal model and the more complex 9-layer model, with a low-velocity zone at about 11 km depth, are unrecognizable at the frequencies of interest for this study. In fact, for this study, the deeper, crustal, velocity structure in all of the soil models could probably be ignored, because the deep crust affects only the dispersion curves at frequencies lower than 1 Hz. Sonic boom acoustic waves have very little energy at such low frequencies, and the deep crustal Rayleigh wave phase velocities are much higher than typical sonic boom carpet trace speeds.

2.5 Rayleigh Wave Dispersion Curves

Rayleigh waves are seismic surface waves--they travel along the surface of the earth. This is in contrast to seismic body waves, such as P-waves and S-waves that propagate within and through the body of the earth. The phase velocity of Rayleigh waves is proportional to the seismic velocity within the earth materials and typically is between 90% and 95% of the shear wave velocity. Because the earth's surface is composed of differing geologic materials that usually have seismic velocities that increase with depth, Rayleigh waves of different wavelengths (or frequencies) travel at different velocities. This phenomenon is called "dispersion." The Rayleigh wave phase velocity for a given frequency is an integrated average of the seismic velocities of the near-surface materials within about one wavelength of the ground surface. Because the low-velocity soils are shallow, the resulting dispersion means that high-frequency (short wavelength) Rayleigh waves travel more slowly than low-frequency (long wavelength) Rayleigh waves. With time, dispersion causes a pulse of Rayleigh wave energy to spread out into a wave train of varying frequencies with the low frequency waves arriving first and the higher frequencies arriving later.

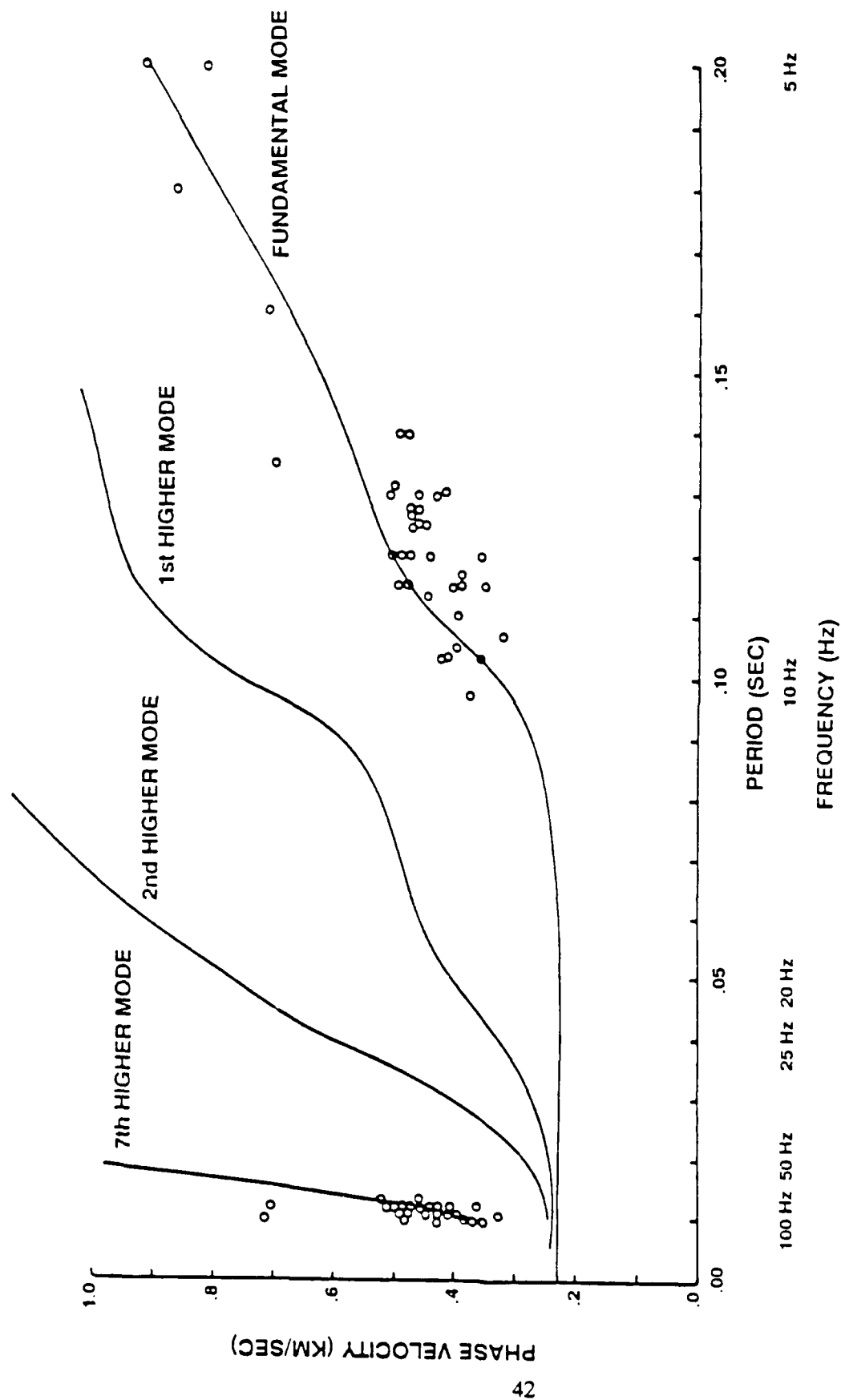
Dispersion is slightly more complicated than the simple explanation above because the seismic energy in a Rayleigh wave travels at the "group velocity" and not the "phase velocity." The difference between group velocity and phase velocity was shown in Figure 1-2 and can be visualized in terms of the wake of a motorboat. Close inspection of the wave propagation in a motor boat wake shows the dispersion phenomenon. The group velocity is the speed at which the wave energy travels; it is

the speed that the front of the boat wake travels. The phase velocity is the speed that the individual wave crests within the wake travel. Phase velocity is often faster than the group velocity, and, for the boat wake, one can see that individual wave crests appear at the end of the wave train, propagate forward at a speed faster than the front of the wake, and then disappear when reaching the front of the wake.

Using the principles of seismology (c.f., Ewing et al., 1958; Aki and Richards, 1980), theoretical Rayleigh wave dispersion curves can be calculated for simple models of earth structure consisting of laterally-homogeneous, parallel, horizontal layers. The theoretical dispersion curves can then be compared with Rayleigh wave dispersion observed on seismograms following earthquakes, explosions, or sonic booms. Figure 2-4 shows a comparison of theoretical and measured Rayleigh wave phase velocities for sonic boom-coupled seismic waves recorded at Edwards Air Force Base (Goforth and McDonald, 1968).

A special case of surface waves can exist where the near-surface geology consists of a thin, low-velocity soil layer that overlies a hard, high-density, high-velocity substrate. In this situation, the soil layer acts as a "waveguide" in which the seismic energy becomes trapped, reflecting back-and-forth between the free surface and the bottom of the waveguide, and propagating with very little attenuation. In cases where the natural resonant frequencies of the waveguide reverberation, called "normal modes," match the frequency spectra of the source energy (earthquake or sonic boom N-wave), strong resonant coupling may occur and the resulting ground motions can be amplified substantially. This phenomenon has been observed in some areas during earthquakes and the resultant heavy destruction of buildings and other structures caused great loss of life. If such resonant conditions could be generated by sonic boom-Rayleigh wave coupling, the shaking intensity, although far weaker than that of a large earthquake, could reach a level that would increase damage to affected structures. One of the principal goals of this project is to identify the conditions under which such resonance might occur.

The following figures show examples of Rayleigh wave dispersion curves computed for representative near-surface geologic or soil conditions in SOAs. A number of different dispersion curve characteristics may be noted in these examples. For all cases, the Rayleigh wave phase velocity curves flatten out toward higher frequencies and asymptotically approach the value of about 90% the



SOURCE: Golorth and McDonald, 1968

Figure 2-4. Theoretical Rayleigh Wave Dispersion Curves and Observed Seismic Wave Frequency Versus Aircraft Velocity for the Dry Lake Area at Edwards AFB.

shear wave velocity of the shallowest layer. These high frequency Rayleigh waves are the non-dispersive, classical Rayleigh waves first described by Lord Rayleigh (1885). The shape of a seismic waveform generated by supersonic aircraft with sonic boom carpet trace speeds at this velocity will be non-dispersive; the seismic waveform will be similar to the N-wave in character. The amplitude of the seismic wave may be determined by the transfer functions derived by other researchers (Press and Ewing, 1951a and b; Baron et al., 1966; Goforth and McDonald, 1968), although amplification of the higher frequency, resonant component of the N-wave may occur. Any slight variation of near-surface seismic velocity or aircraft sonic boom carpet trace speed will prevent significant buildup of the surface wave energy by changing the resonant conditions. The coupled surface waves will tend to be locally generated and not propagate over large distances, being attenuated or scattered by variations in the surficial geology.

At lower frequencies (longer wavelengths), the Rayleigh wave phase velocities increase toward values about 90% of the shear wave velocity of the deepest (and thickest) sublayer. The low-frequency limit for most of the models considered herein is well below 1 Hz, corresponding to wave periods of several seconds to minutes. Because these surface waves have phase velocities much greater than supersonic aircraft and their nominal sonic boom carpet trace speeds, such low-frequency surface waves are of greater interest to earthquake seismologists (for studying the structure of the deep earth) than they are to Air Force planners concerned with possible building damage caused by sonic boom-coupled seismic waves. High carpet trace speeds associated with some maneuvers could reach these values, but they would occur only for short distances. Furthermore, these low frequencies are below the resonant frequencies of most structures that could be affected by sonic booms. Lastly, the typical energy in sonic booms is much too low to excite significant ground oscillations at such long wavelengths.

For the intermediate range of frequencies lying between the two asymptotic parts of the dispersion curves, the Rayleigh wave phase velocity curves may cross the range of nominal sonic boom carpet trace speeds. The primary frequency band of interest is frequencies between 1 Hz and 30 Hz (and slightly greater) that are comparable to the natural response of small buildings and other light structures. In this range, a given sonic boom carpet trace speed will be resonant with Rayleigh waves of one particular frequency for each Rayleigh wave mode excited. This is the classical resonant condition, where highly monochromatic seismic waves (harmonic ground oscillations at a single frequency) are generated. These conditions may allow amplification of the ground motions by

continued resonant coupling between the sonic boom and the ground, provided that the surficial geologic conditions remain constant for many wavelengths' distance and the aircraft also maintains uniform speed over the same distance. At these frequencies and velocities, wavelengths range from 10 m (300 m/sec divided by 30 Hz) to 850 m (850 m/sec divided by 1 Hz). Thus, aircraft speeds and soil conditions must remain steady or consistent over distances of about 1 km or more. Such conditions may occur, for example, in depositional settings such as lake beds, where relatively constant thicknesses of uniform sediments are deposited over large areas; stream channels and flood plains where uniform sediment thicknesses are spread over long, but narrow distances; and recent volcanic ash falls of relatively constant thickness that cover areas of level bedrock or older, consolidated sedimentary layers. The following discussion explains the character of the Rayleigh wave dispersion curves for several representative near-surface geologic profiles in the context of the sonic boom coupling problem.

Figure 2-5 shows the Rayleigh wave phase velocities for the fundamental ($n = 0$) and 8 higher modes ($n = 1-8$) for a simple 1-layer over substrate model similar to the clay lake bed model at Edwards AFB described by Goforth and McDonald (1968). This model was used as the first test case to verify the accuracy of the dispersion curve computational algorithm. Comparison of Figure 2-5 with Figure 2-4 shows the same result as Goforth and McDonald (1968) for these conditions. Apparent differences in the two figures are solely the result of using different abscissa (bottom axes): a frequency scale is used to report the results of this study whereas a period scale is used in other study curves. Because the character of the phase velocity curves in the frequency band from 1 to 30 Hz is the region of interest, instead of using wave period, the data are plotted as a function of wave frequency. Curves plotted versus wave period, the reciprocal of frequency, tend to expand the low frequency part of the data and compress the high frequency part. For easier comparison with the Goforth and McDonald (1968) dispersion curves, dispersion curves are plotted with frequency decreasing to the right, so that the low frequency (long period) values lie farthest from the phase velocity axis.

To better observe the character of the phase velocity curves in the frequency range of interest, the data have been replotted for the frequency interval .020 Hz to 10 Hz (Figure 2-6) for the fundamental and first higher modes. Group velocity (U) has also been plotted in Figure 2-6 to show how it differs from phase velocity (V). Because group velocity is slower than phase velocity, the individual wave crests will travel faster than the seismic energy leading to the phenomenon such

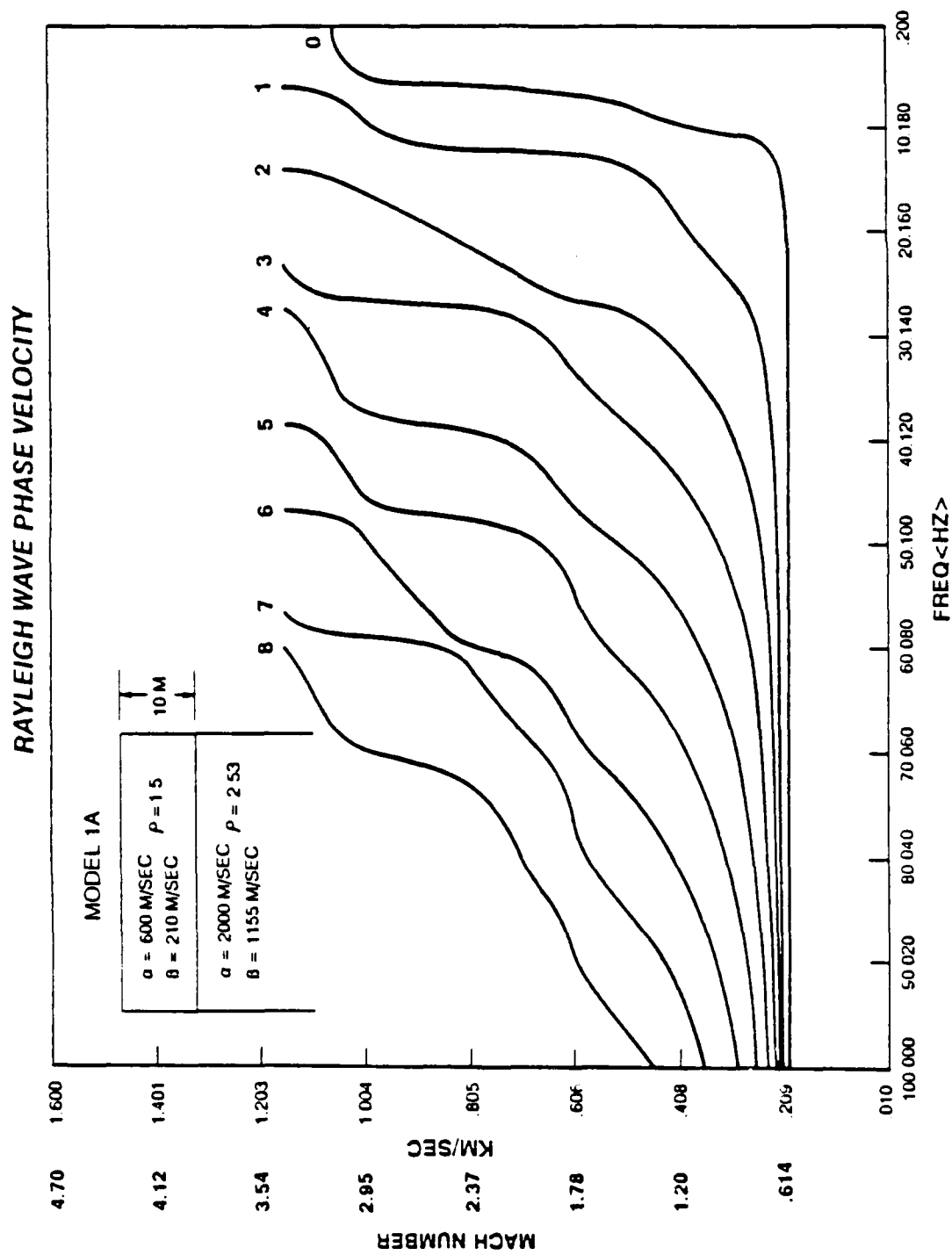


Figure 2-5. Rayleigh Wave Phase Velocity Dispersion Curves for the Simple Clay Lake Bed in Model Shown in the Inset. The frequency axis has been reversed with low frequencies at the far right. The numbers 0, 1, ..., 8 represent the mode numbers (n) for layer model.

RAYLEIGH WAVE DISPERSION CURVES

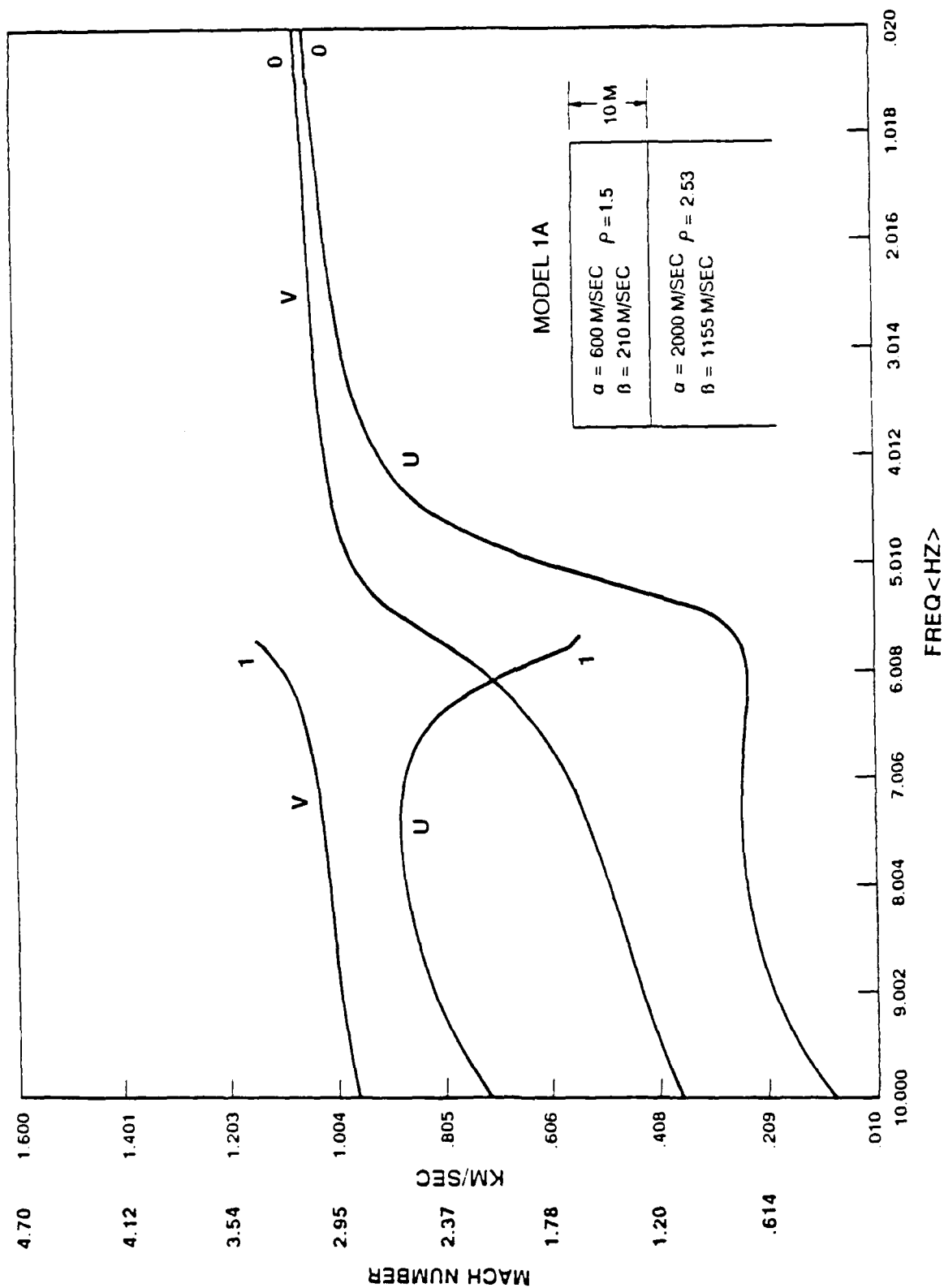


Figure 2-6. Rayleigh Wave Dispersion Curves for Phase Velocity (V) and Group Velocity (U) for the Simple 10-m Thick Clay Lake Bed Model Shown in the Inset.

as the motor boat wake described previously. In terms of sonic boom-coupled Rayleigh waves, this means that the first arrivals of coupled seismic waves reach a location simultaneously with the acoustic wave. The dispersed train of Rayleigh waves will follow the acoustic pulse for some time related to the difference between the group and phase velocities, and the distance over which the resonant coupling has occurred.

In some areas, seismic energy was observed to arrive slightly ahead of the acoustic wave (Goforth and McDonald, 1968; Grover, 1973). In these situations, the group velocity exceeds the local phase velocity. It is possible that these precursory seismic waves were generated by the resonance condition at a location where the group velocity or carpet trace speed was higher and propagated ahead of the slowing acoustic wave.

These curves show the expected asymptotic behavior at limiting values of high and low frequencies. At frequencies below about 5 Hz, the curves flatten out and approach the Rayleigh wave velocity for the underlying high-velocity substrate. These low-frequency and long-period Rayleigh waves propagate as if no low-velocity surface layer existed. At frequencies higher than about 12 Hz, the curves flatten out toward the Rayleigh wave velocity of the low-velocity surface layer; the high-frequency waves are unaffected by the higher-velocity substrate. Because the phase velocity of these high-frequency Rayleigh waves is less than Mach 1.0, the sonic boom resonant condition will not generate these high-frequency Rayleigh waves. The low-frequency waves could be generated by sonic booms at high Mach numbers (about $M = 3.1$). In the range of about 6 Hz to 12 Hz, the Rayleigh wave phase velocities match the aircraft speeds in the Mach 1.0 to 2.5 range; resonant coupling could occur as observed by Goforth and McDonald (1968). Because the resonant frequency changes with changing phase velocity and carpet trace speed, strong resonant coupling is likely only if the geologic conditions and aircraft speed are constant over a distance of several wavelengths (about 500-1,000 m). Goforth and McDonald (1968) noted significant variations in seismic wave character between two of the clay lake bed sites that were separated by only about 300 m, suggesting that near-surface geologic variability existed and prevented significant amplification of the coupled seismic waves at this location. Variability in aircraft speed could also inhibit strong coupling, although at speeds of Mach 2.0 to 2.5, where the dispersion curve is very steep, the resonant frequency changes more slowly with changing aircraft speed and may be more favorable for strong coupling.

Higher mode Rayleigh waves are usually poorly developed, and so, only the first higher mode ($n = 1$) is included in the subsequent dispersion curves. Goforth and McDonald (1968) observed higher frequency seismic waves which could correspond to the seventh higher mode Rayleigh waves, but because none of the lower modes ($n = 1-6$) was apparent, it is more likely that the higher frequency oscillations have a different origin. For example, a thin, near-surface soil layer may exist which was unresolved by their seismic refraction data.

Rayleigh wave dispersion curves shown in Figures 2-7 and 2-8 represent the same model as above, only with the surface layer thickness increased to 100 m (Figure 2-7) and decreased to 1 m (Figure 2-8). The shape of the curves is the same. However, the curves change from the high phase velocities to the lower phase velocities at different frequency ranges. For the thick layer, this transition occurs in the range of 0.5 Hz to 1.2 Hz; for the thin layer, in the range of 50 Hz to 120 Hz. As shown by the simple, 1-dimensional waveguide frequency equation (1-1), this change is linearly (inversely) related to the waveguide thickness. Thus, the simple waveguide equation provides a useful estimate of thickness associated with resonant coupling at frequencies of concern for a known surface low seismic velocity layer and aircraft velocity. For seismic velocities associated with this clay lake bed, thicknesses of about 5 m to 50 m would have resonant frequencies in the 1 Hz to 10 Hz range.

A model of the Mojave Desert deep crustal structure (Hadley, 1978) was used to prepare the Rayleigh wave dispersion curves in Figure 2-9. This model includes a thick surface layer of sedimentary rock. The high seismic velocities of this bedrock model are greater than typical aircraft sonic boom carpet trace speeds, and so, this type of geologic structure is unlikely to experience the resonant condition. Special maneuvers, such as dives or accelerations, may cause local resonance as the carpet trace speed reaches these velocities. Because these conditions are only locally achievable, however, strong ground motion amplification is unlikely.

Figure 2-10 shows dispersion curves for a model (after Hadley, 1978) of an alluvial fan area of the Mojave Desert, south of Edwards AFB. The deep crustal seismic structure is included in this model to provide more complete dispersion data at low frequencies. Resonant frequencies associated with nominal supersonic flight speeds are low (1-2 Hz) for this model. The relatively thick (37-127 m) near-surface layers have seismic velocities somewhat higher than the clay lake bed model. This site represents an older alluvial fan with more consolidated or well-indurated alluvium. Because the

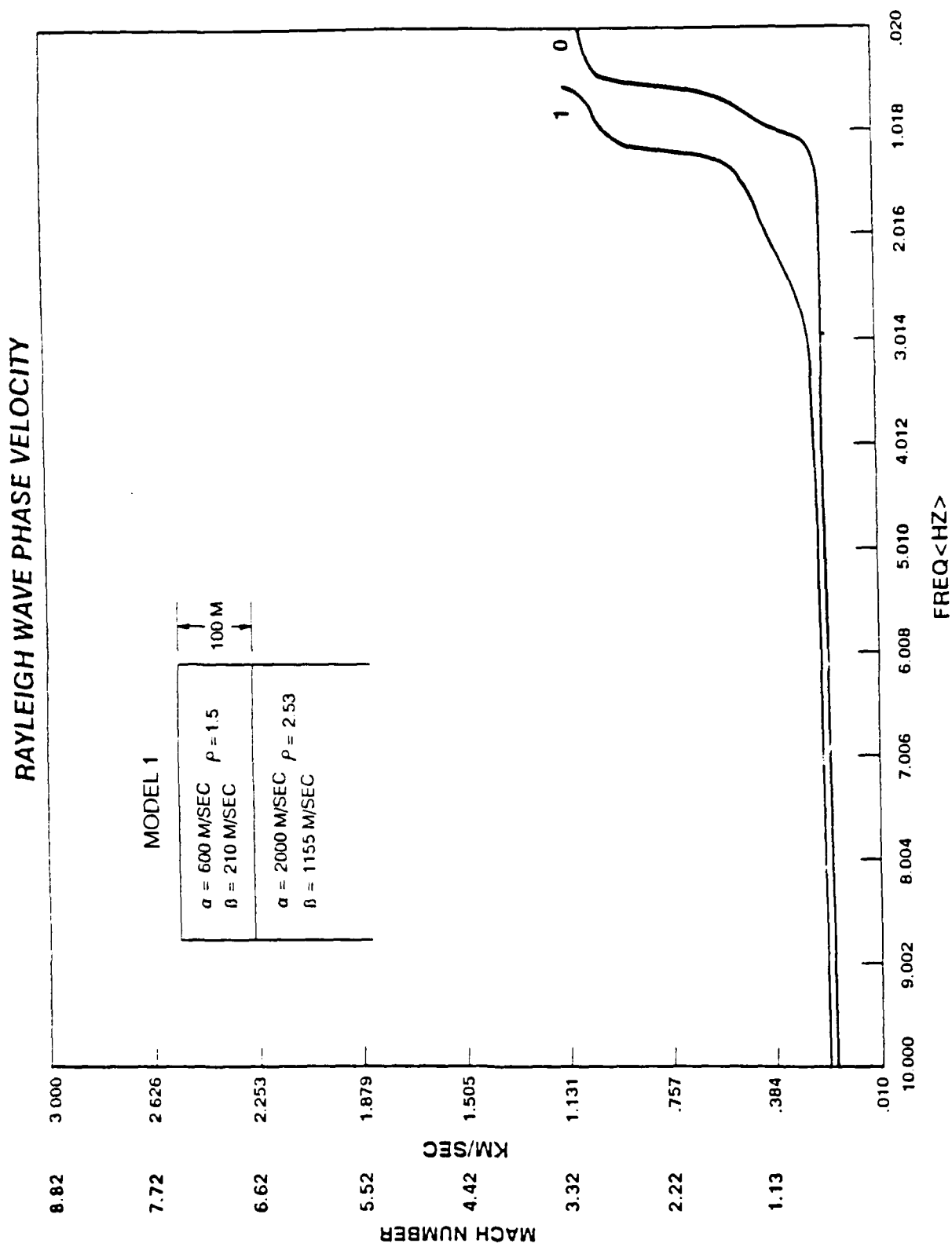


Figure 2-7. Rayleigh Wave Phase Velocity Dispersion Curves for the Simple 100-m Thick Clay Lake Bed Model Shown in the Inset.

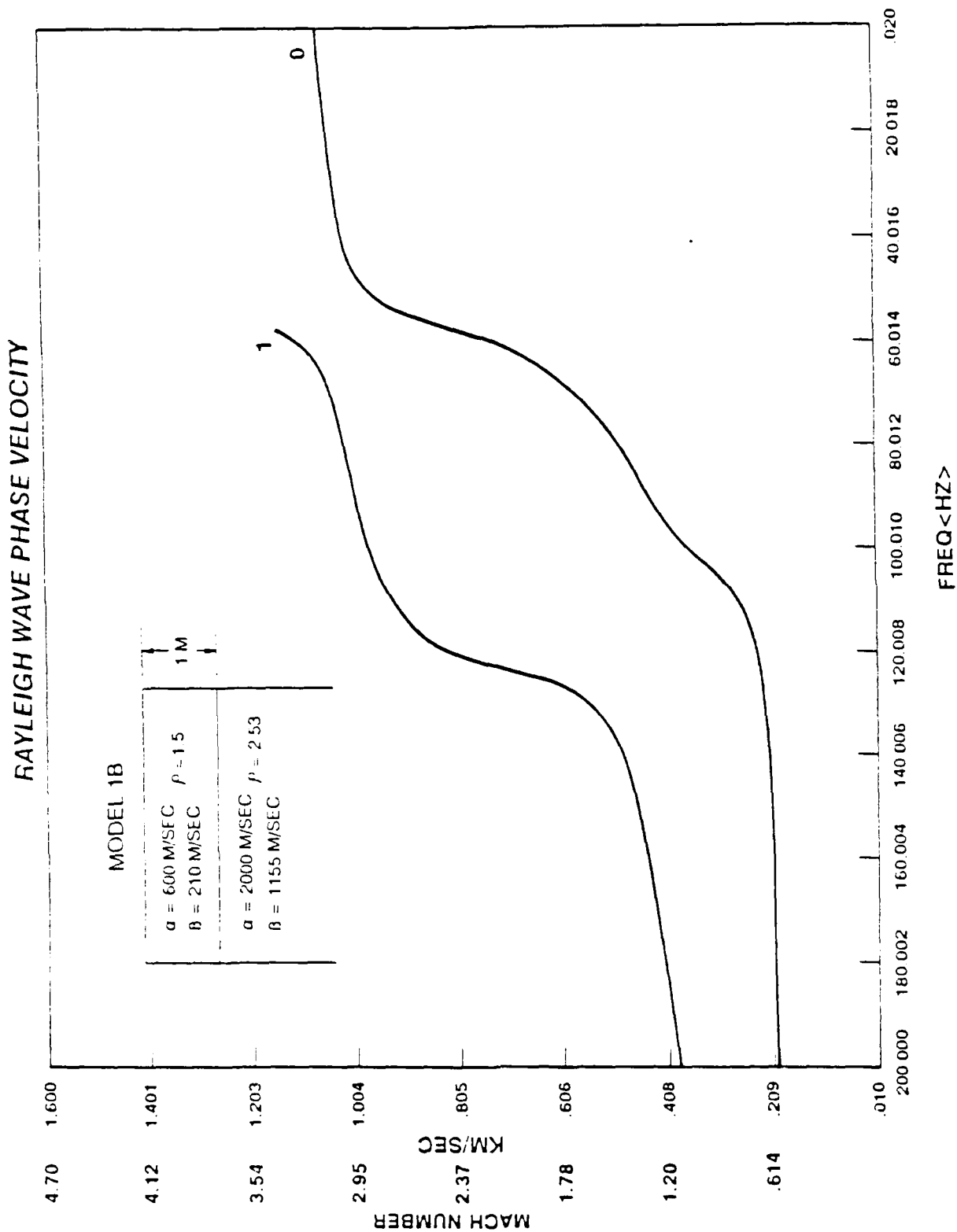


Figure 2-8. Rayleigh Wave Phase Velocity Dispersion Curves for the Simple 1-m Thick Clay Lake Bed Model Shown in the Inset.

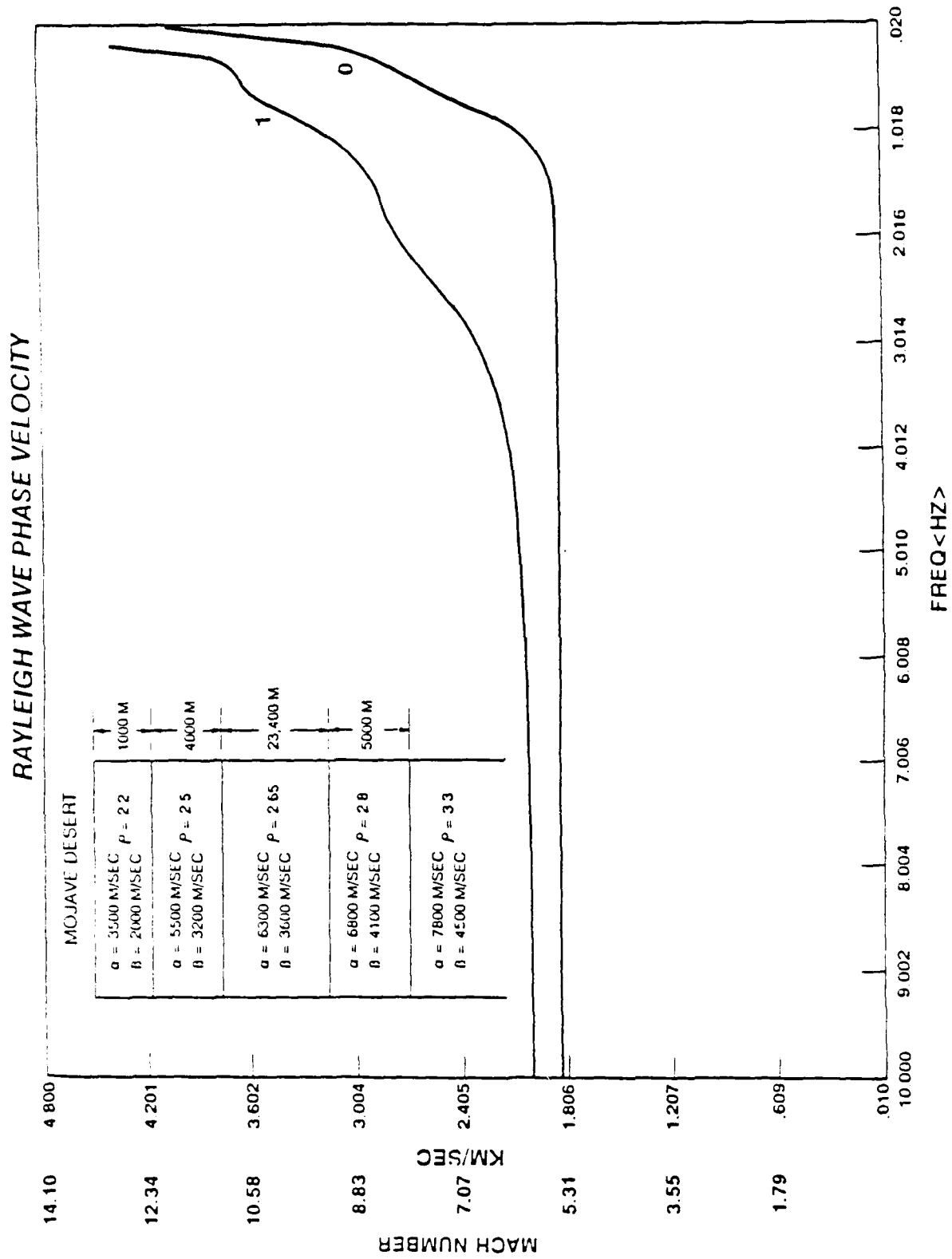


Figure 2-9. Rayleigh Wave Phase Velocity Dispersion Curves for the Mojave Desert Crustal Structure Shown in the Inset (after Hadley, 1978).

RAYLEIGH WAVE PHASE VELOCITY

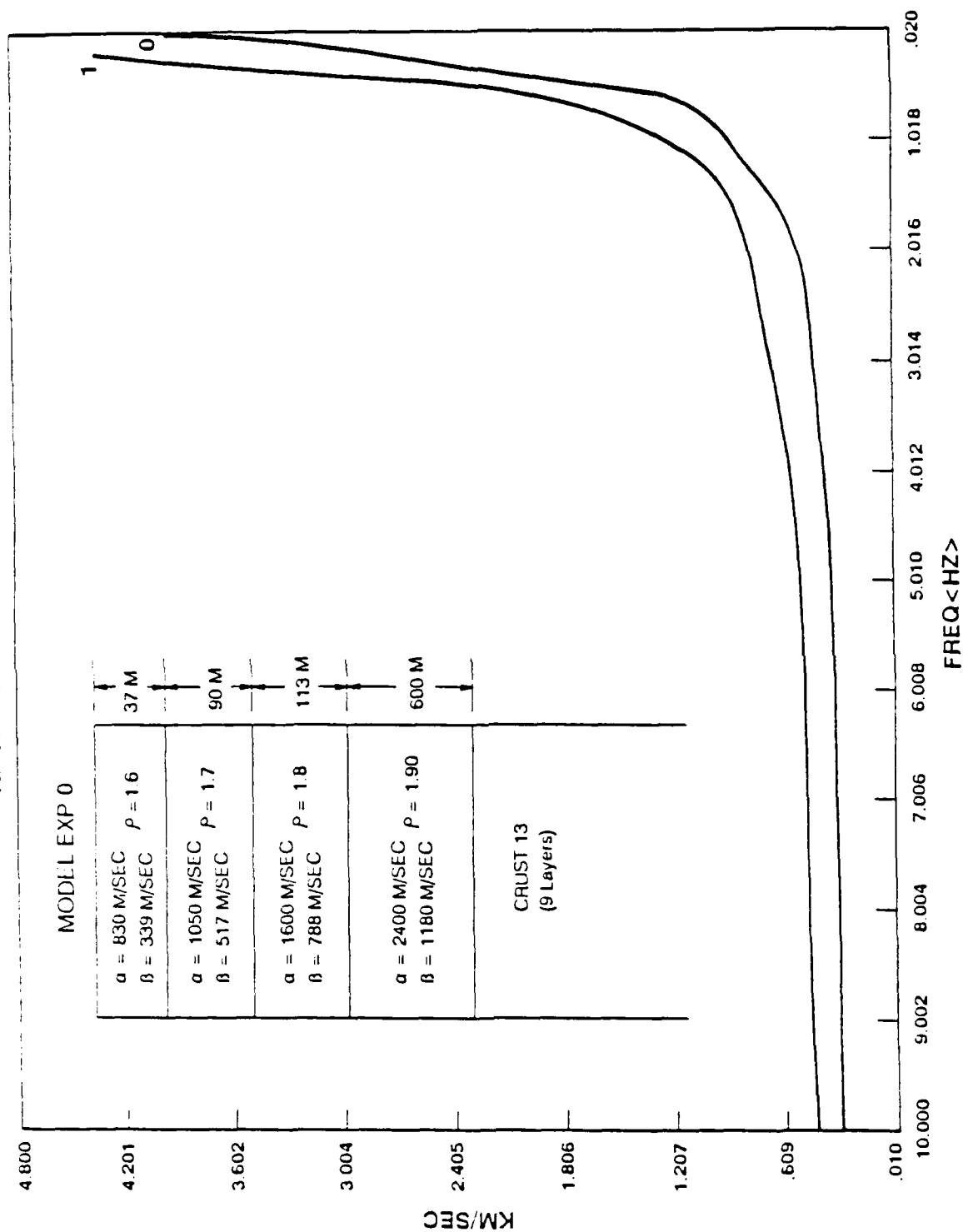


Figure 2-10. Rayleigh Wave Phase Velocity Dispersion Curves for the Mojave Desert Near-surface Geologic Structure Shown in the Inset (after Hadley, 1978). See Appendix B for a description of the 9 layer, crust 13 model.

Rayleigh wave phase velocities for resonant frequencies greater than about 3 Hz are near to Mach 1.0, non-dispersive sonic boom coupling may occur. Nevertheless, because alluvial fans typically have substantial lateral variations in surficial geology, with accompanying variability in seismic velocity structure, strong coupling is unlikely for this depositional environment. Furthermore, the aircraft must also maintain a constant speed, within less than 10% variability of the resonant velocity, for a significant distance. (Note that this model includes a more complex, 9-layer deep crust. This deep crust shows virtually identical phase velocity dispersion, at frequencies greater than 1 Hz, as the simple, 5-layer crust shown in Figure 2-9.)

Figure 2-11 shows the dispersion curves for a younger alluvial basin area in the Mojave Desert near Edwards AFB. The seismic velocity model (after Hadley, 1978) has a thinner layer of lower velocity alluvial sediments than the previous model. The fundamental mode Rayleigh wave resonance, at supersonic aircraft speeds, occurs in the frequency range 2 Hz to 5 Hz. If the resonant earth structure is laterally persistent, strong sonic boom-Rayleigh wave coupling could occur in such deposits.

Figure 2-12 shows Rayleigh wave dispersion curves for thin soils in weathered granitic bedrock located near Albuquerque, NM (after Sabatier et al., 1986b). The thin soil layers show resonance at frequencies of 20 Hz to 40 Hz. As discussed in Section 4, some structural elements may have resonances in this same frequency band. This simple model is similar to that at Tonto Forest seismological observatory where Goforth and McDonald (1968) noted the absence of sonic boom resonant coupling. The lack of strong, resonant coupling may result from lateral variability in the depth or seismic velocity of the weathering layers. Figure 2-13 shows dispersion curves for a similar model, with increased thickness to the soil/weathering layers and an added, very low velocity, low density, pumice layer. The thicker layers with the low velocity pumice have created a strong resonance condition at about 3 Hz. The steep knee in these curves (at 3 Hz) is indicative of a waveguide, where the seismic energy is trapped and the resonant frequency is relatively constant over a wide range of phase velocities. Aircraft flying supersonically, with carpet trace speeds in the range of Mach 1.0 to 3.5 could generate strong, sonic boom-coupled surface waves if such near-surface geological conditions were laterally persistent. Although the model presented is somewhat artificial, real geologic conditions, where a thin, low velocity sediment or soil layer overlies more competent material may be encountered in SOAs.

Figure 2-14 shows the dispersion curves for a thin, sandy soil, overlying a thicker alluvial layer (after Sabatier et al., 1986a). Rayleigh waves at frequencies less than 10 Hz are unaffected by the thin soil layer and resonant conditions for realistic sonic boom carpet trace speeds would only occur at low frequencies (<2 Hz) associated with the thicker alluvial layer. This model is appropriate for the geologic conditions at Eglin AFB, although a thinner deltaic layer (2nd layer) would allow resonance at frequencies in the 1 to 10 Hz range.

Figure 2-15 shows the dispersion curves for a young, alluvial fan setting in the Antelope Valley area of California (after Fumal and Tinsley, 1985). The two uppermost, low-velocity layers of alluvium account for the knee in the fundamental mode dispersion curve at about 3 Hz. Resonant coupling could occur for sonic boom carpet trace speeds in the higher Mach number ranges (2.0 and greater). The higher frequency, slightly dispersive part of the curves suggests possible resonance at lower Mach numbers, but uniform geologic and aircraft flight character would be necessary to achieve significant amplification.

Rayleigh wave dispersion curves for the last two models shown (Figures 2-16 and 2-17) represent waveguide conditions. Figure 2-16 represents a thin waveguide (30-m thick), and Figure 2-17, a thick waveguide (130-m thick). The waveguide is formed by a low-velocity soil or alluvial layer overlying a thick layer of salt. Salt has a very high seismic velocity (about 4,600 m/sec), and forms an excellent substrate for trapping near-surface seismic energy. Layers of salt, or other evaporites such as anhydrite, do exist in many areas of the arid western United States where ancient lakes have dried up leaving a thick residue of the formerly dissolved minerals. An excellent example is the Bonneville salt flats associated with ancient Lake Bonneville in Utah. As noted previously, the waveguide accounts for a sharp knee in the dispersion curves that occurs at the resonant frequency of the waveguide. The dashed curve shows the theoretical dispersion curve for a perfect, simple waveguide of 30-m thickness and 200 m/sec shear velocity; its close fit to the Rayleigh wave curves shows that this model represents nearly perfect waveguide conditions. Strong resonant coupling between the sonic boom and the Rayleigh waves could occur under such conditions, *provided that the conditions are laterally persistent*. The resonance occurs over a wide range of phase velocities, so that the aircraft flight conditions are less critical for resonance. Because the resonance occurs over a very narrow frequency band, the waveguide thickness must be appropriate for the natural response frequency of structures in the area for the resonance to be likely to inflict damage. Waveguides of

RAYLEIGH WAVE PHASE VELOCITY

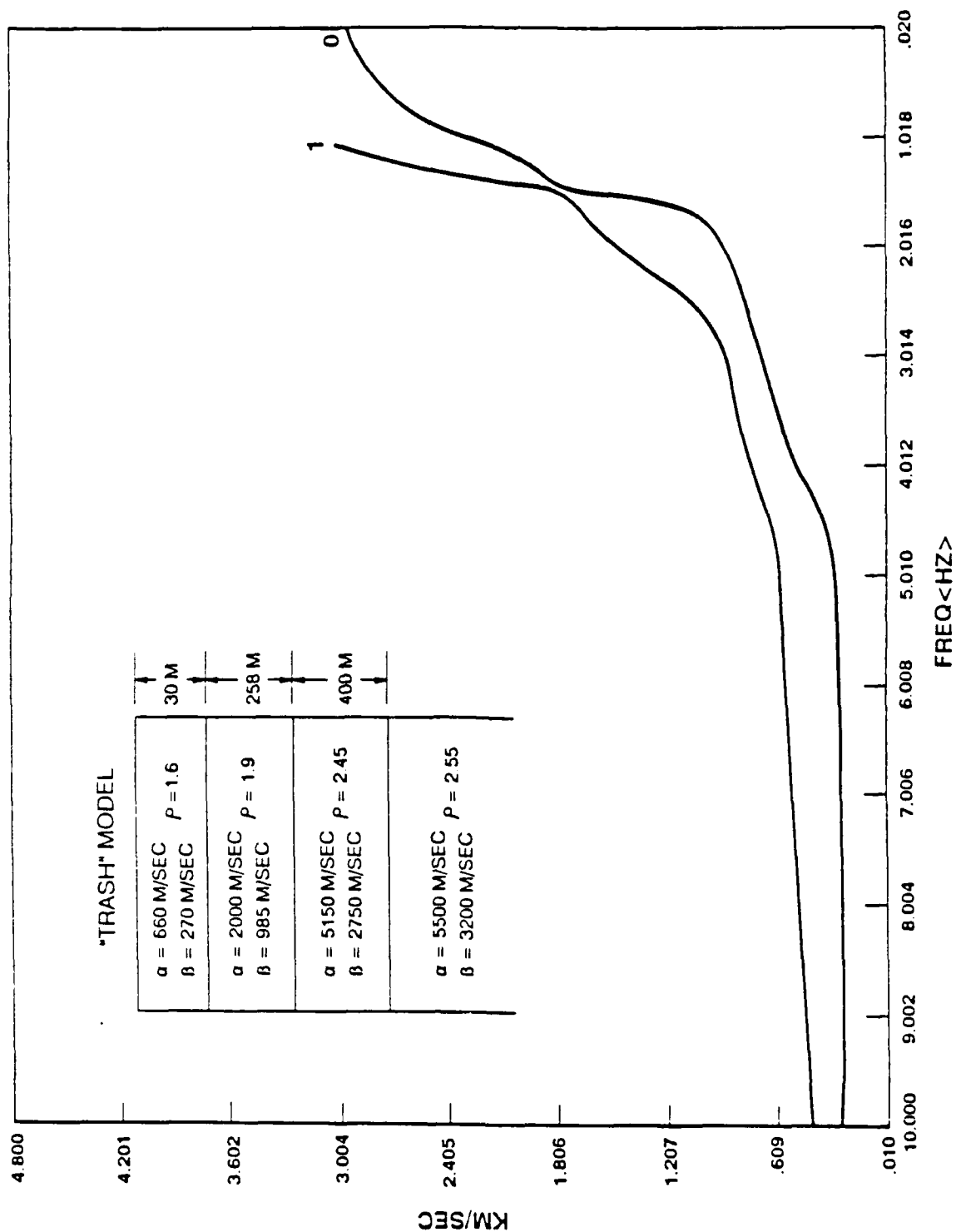


Figure 2-11. Rayleigh Wave Phase Velocity Dispersion Curves for the Mojave Desert Near-Surface Geologic Structure Shown in the Inset (after Hadley, 1978).

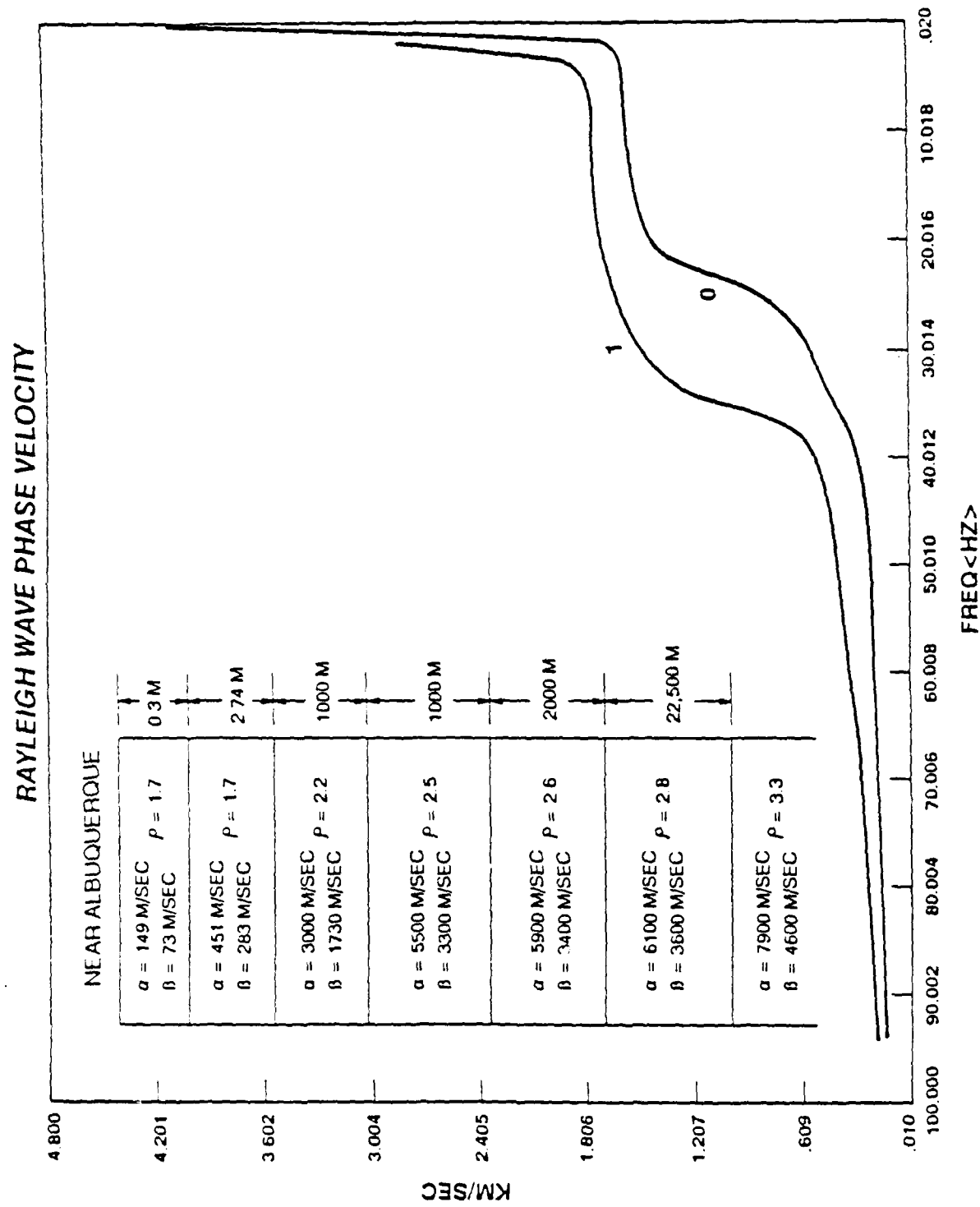


Figure 2-12. Rayleigh Wave Phase Velocity Dispersion Curves for the Near-Surface Geologic Structure Shown in the Inset (after Sabatier et al., 1986b).

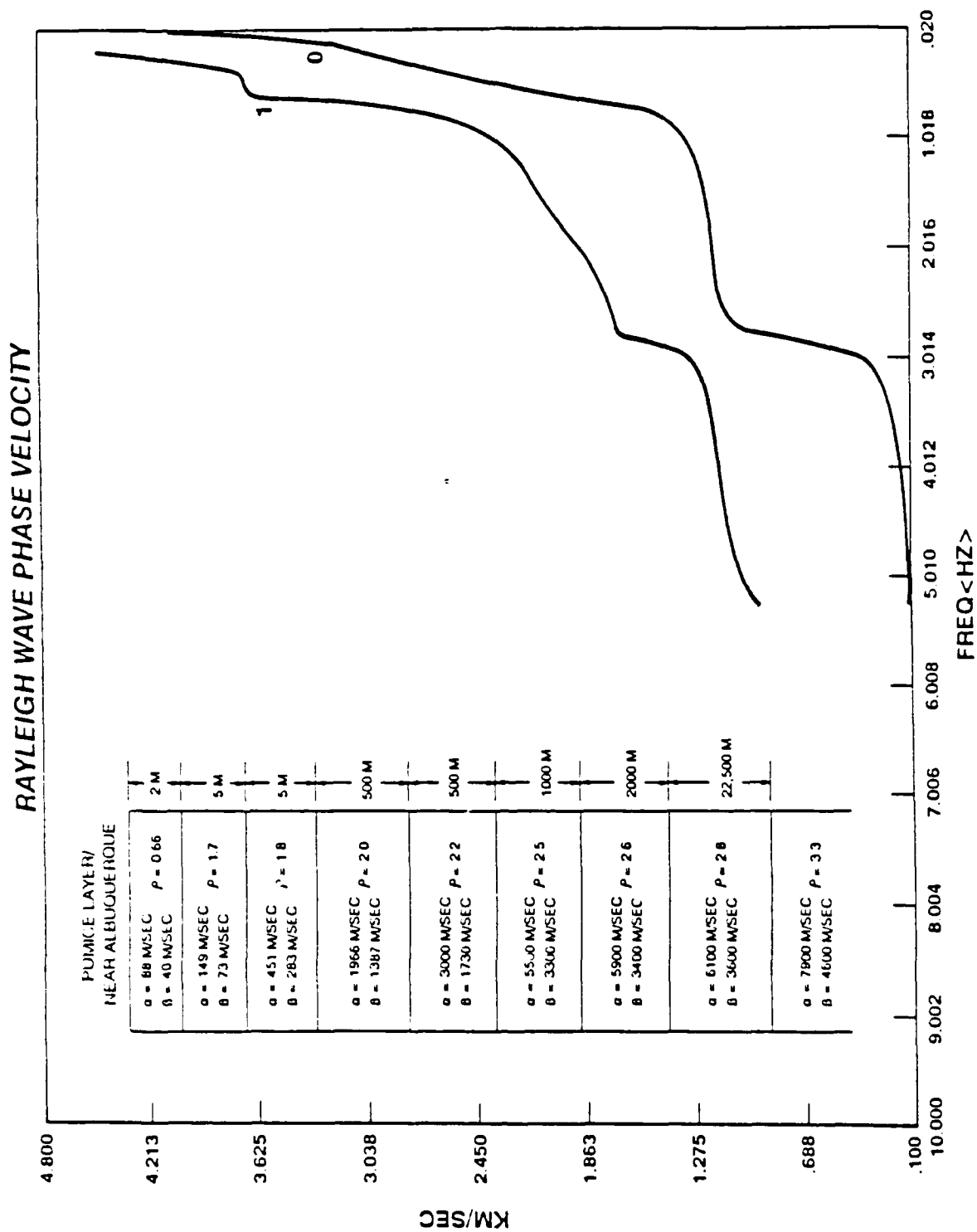


Figure 2-13. Rayleigh Wave Phase Velocity Dispersion Curves for the Near-Surface Geologic Structure Shown in the Inset (after Sabatier and Raspel, 1988).

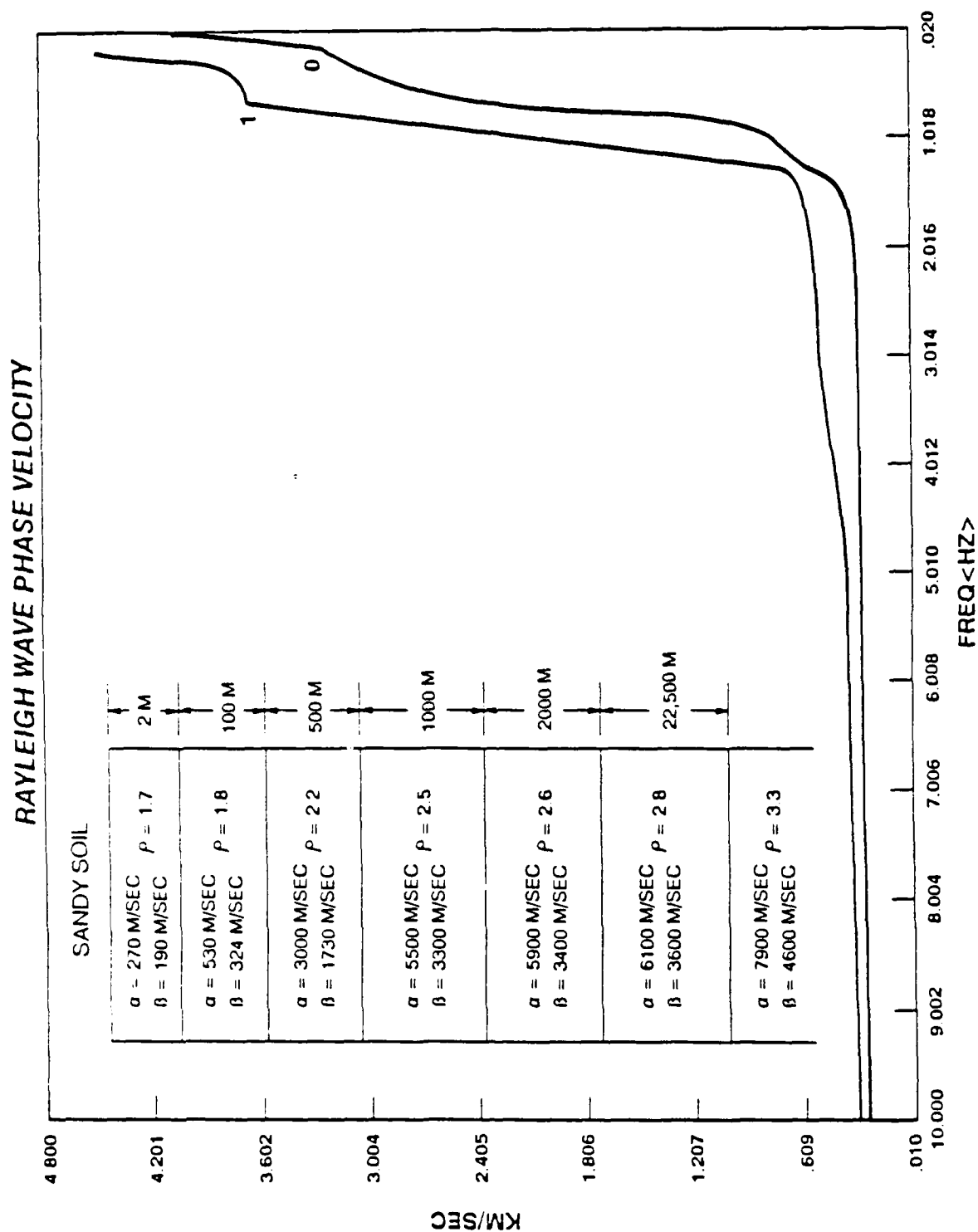


Figure 2-14. Rayleigh Wave Phase Velocity Dispersion Curves for the Near-Surface Geologic Structure Shown in the Inset (after Sabatier et al., 1986a).

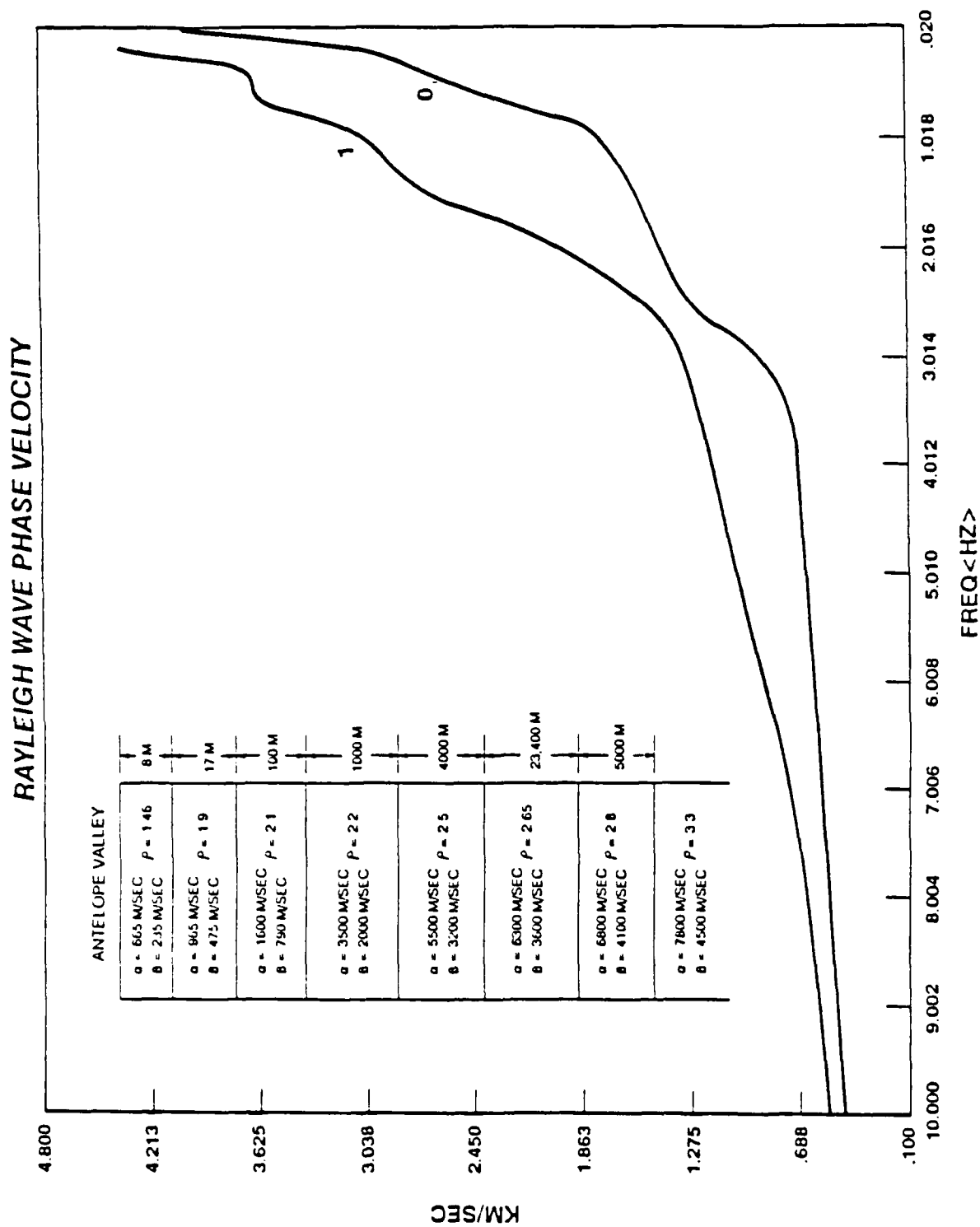


Figure 2-15. Rayleigh Wave Phase Velocity Dispersion Curves for the Near-Surface Geologic Structure Shown in the Inset (after Fumal and Tinsley, 1985).

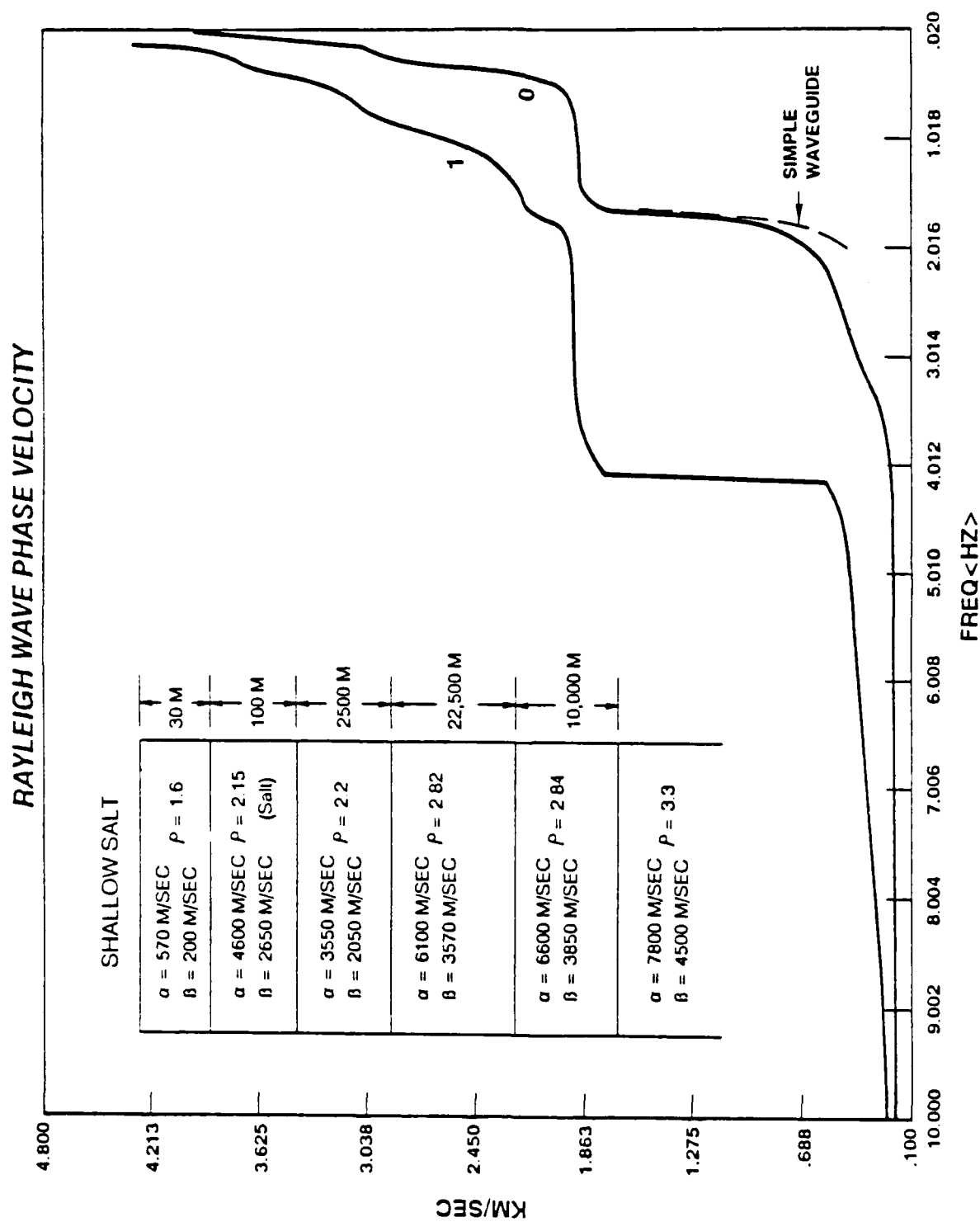


Figure 2-16. Rayleigh Wave Phase Velocity Dispersion Curves for the Near-Surface Waveguide Structure Shown in the Inset (modified from Hays et al., 1978).

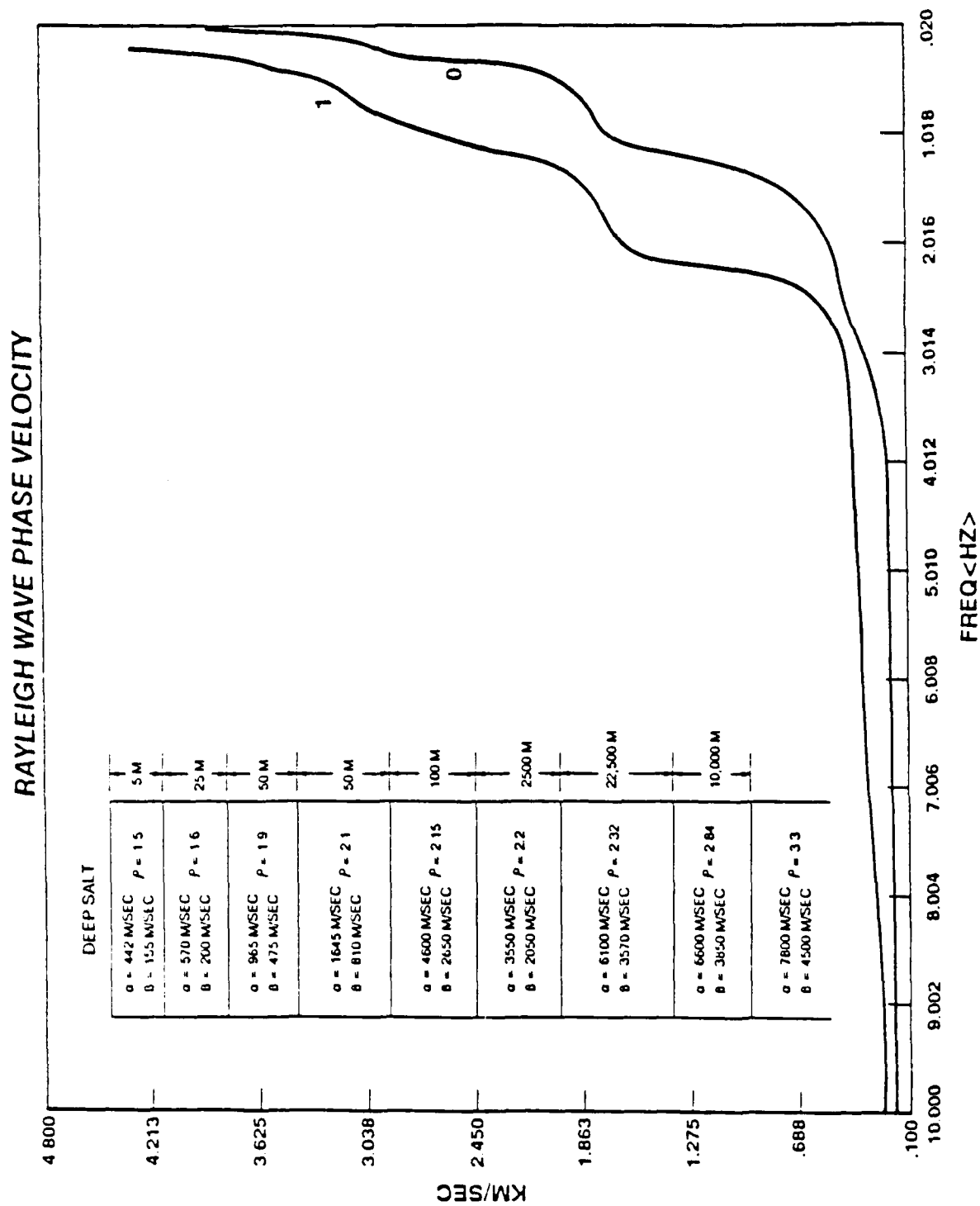


Figure 2-17. Rayleigh Wave Phase Velocity Dispersion Curves for the Near-Surface Waveguide Structure Shown in the Inset (modified from Hays et al., 1978).

2 m to 50 m thickness, with these low seismic velocities, could have resonances at the natural response frequencies of structures.

2.6 Amplitudes of Resonant Sonic Boom-Coupled Rayleigh Waves

Amplitudes of ground shaking that could be achieved under the condition of the sonic boom-coupled Rayleigh wave resonance are unknown. Measured seismic ground motions induced by sonic booms have been substantially lower than damage thresholds of most structures (Goforth and McDonald, 1968; Espinosa et al., 1968), but strong resonant coupling was not observed in these experiments. Theoretical estimates of the amplitudes achievable under the conditions of strong resonant coupling are of limited value because the theory predicts infinite amplitudes at the point of exact resonance (Baron et al., 1966). Such extreme amplifications are unlikely in the real world because of inelastic and other nonlinear effects. For the purpose of this study, a very crude, order-of-magnitude estimation of maximum amplitudes of ground shaking that might occur under a strong resonant coupling condition was made. Such amplification factors calculated by Baron et al. (1966) could exceed 10 to 20 in some instances near the conditions of exact resonance. These high amplification factors occur for buildings of short natural response period (about 0.2 sec or 5 Hz) which corresponds to the light construction most vulnerable to sonic boom-coupled Rayleigh waves. Donn et al. (1971) observed resonant amplification factors in excess of 10 at 4 Hz, from sonic boom seismic waves coupled over a distance of 10 km. Applying the empirical relationship of Goforth and McDonald (1968) between ground motion amplification and sonic boom overpressure, an overpressure of 10 psf could produce a ground motion of about 1 mm/sec (.04 in/sec). If the resonant condition allows this to be amplified by a factor of 20, the resulting shaking at 2 cm/sec (0.8 in/sec) exceeds damage criteria for some of the more vulnerable structural types (see Section 4).

Because these conditions are marginal in their ability to cause damage, and the boom conditions postulated are higher than nominal, sonic boom-coupled Rayleigh wave resonance is unlikely to cause damage in most instances. Nevertheless, because the ground motion amplitude estimates given above are very crude, and amplifications may be greater than are here postulated in some waveguides, it must be concluded that damage to some structural elements caused by strong resonant coupling conditions may occur in some uncommon instances. These strong ground vibrations occur directly under the sonic boom carpet. Rapid dissipation of the seismic waves by

geometrical attenuation and scattering due to variability in soil conditions will reduce the threat to structures away from the carpet.

2.7 Conclusions--Geologic Conditions Conducive to Rayleigh Wave Resonance

Geological processes in the western United States where most SOAs are located provide numerous areas of low-velocity surficial deposits. Deposition of alluvium during recent geologic time provides a general layer of low-velocity material over large areas within the basins, troughs, and valleys of the North American Cordillera. Weathering processes and soil formation also may enhance the development of low-velocity near-surface layers that may be conducive to the sonic boom-coupled Rayleigh wave resonance phenomenon. Saturation of the uppermost soils may decrease the likelihood of the resonant condition by increasing the seismic velocity, relative to air-filled porous sediments, yet saturation deeper in the sediment column may improve the likelihood of coupling because the pore fluid pressure acts to resist compaction, allowing the deeper layers to maintain low densities and seismic velocities.

Strong amplification from resonant coupling requires that the resonance condition be laterally persistent; the near-surface geological condition must remain uniform over significant distances, on the order of 1 km or more. Depositional environments most likely to provide such uniform sedimentary character are provided by basin sediments such as flood plains, lake beds (both modern and ancient), and the basinward deposits of alluvial fans. Although weathering of ancient bedrock outcrops may produce relatively thick layers of low-velocity material, the non-uniform nature of the weathering process and the non-uniform distribution of the bedrock materials may diminish the likelihood that the sonic boom-coupled resonance condition would be achieved. Widespread areas of sandy soils in the Eglin AFB area would be conducive to resonant couplings, but lateral variability in underlying deltaic deposits could prevent strong amplification of the coupled seismic waves.

A situation of particular concern is that of a waveguide: a uniform, low-velocity layer overlying a hard, high-seismic velocity substratum (base layer). In this situation, the seismic energy may become trapped, reflecting incessantly between the bottom hard layer interface and the surface, low-density, air-ground interface. When the Rayleigh wave phase velocity in this situation matches the sonic boom trace speed, continued amplification of the ground motion may occur as the sonic boom is resonantly coupled to the ground. For a simple waveguide, the Rayleigh wave dispersion

curve shows that the phase velocity varies rapidly over a very narrow frequency range; the resonant condition is less affected by variations in aircraft speed, but the resonance occurs over a very narrow frequency range that is strongly dependent on the waveguide thickness and seismic velocity. Thus, the supersonic aircraft could have a more variable carpet trace speed and still maintain the resonant condition. An example was shown representing a waveguide formed by low-velocity lake sediments overlying a thick salt layer (very high seismic velocity) such as may be found in the ancient Lake Bonneville area of Utah. Other waveguides could occur where low-velocity sediments overly hard bedrock, such as stream deposits in volcanic rock areas or thick soils over limestone (as in west Texas). If the resonant frequency of the waveguide, which is directly related to the thickness and seismic velocity of the waveguide, matches a natural response frequency of a structure, then increased potential for damage could result by the strong amplification of the resonant vibration.

It is beyond the scope of this project to map, in detail, areas within all SOAs that may have geologic conditions susceptible to the sonic boom-coupled Rayleigh wave resonance condition. That problem is analogous to the microzonation problem in earthquake engineering, where a mapping of areas most susceptible to strong ground shaking by earthquakes may be used for planning and emergency response procedures. A project to map areas affected by supersonic operations, containing surficial deposits, soils, alluvium, and so forth, that may be conducive to the resonant coupling at frequencies potentially damaging to structures could be initiated by the Air Force. Such maps would be based upon existing soils and other near-surface geologic maps, identifying the relevant soil types and depositional environments as presented in this study. It should be recognized that such maps only identify areas containing deposits that *may* be susceptible to the resonant condition. The exact locations of such deposits would require site-specific investigations, which are very expensive and impractical for the environmental planner. Based upon the conservative mapping program, the Air Force planner could avoid areas where the resonant coupling might occur with resonant frequencies potentially damaging to structures. If no structures exist in an area, or the resonant frequencies are outside the band of concern to structures in the area, supersonic operations could proceed without restriction. Because the carpet trace speed that may induce the resonant coupling can be predicted, knowing the geologic conditions, it would also be possible to restrict maneuvers in some areas to those that would not create the undesirable carpet trace speeds.

Amplitudes of sonic boom-coupled Rayleigh wave resonant ground motions are unknown at present, although values measured in a few instances were significantly less than structural damage

criteria (Goforth and McDonald, 1968). Strong resonant coupling was not observed in those cases, and continued resonant coupling, over distances of many wavelengths, might increase the ground motions substantially. Theoretical amplification factors of 10-100 or more have been calculated (Baron et al., 1966) for the resonant coupling, but inelastic and nonlinear effects in real earth materials may prevent such large amplifications. An experimental program to measure the ground motions induced by resonant coupling in a "worst-case" geologic condition, such as a strong waveguide, could show that the amplitudes remain below even the strictest structural damage criteria.

Such an experiment would, at least, provide a calibration of the theoretical calculations so that amplitudes in other geologic environments could be estimated.

3.0 RANGE OF SONIC BOOM FOOTPRINT CHARACTERISTICS

Pilots training to operate modern fighter airplanes and trained pilots flying to maintain combat efficiency must be able to operate supersonically at relatively low altitudes (less than 30,000 ft AGL) if they are to achieve or maintain combat proficiency requirements. These maneuvers take place within an airspace having the approximate shape of a right elliptical cylinder. The intended floor for these maneuvers is 10,000 ft AGL and the ceiling is, typically, a height on the order of 50,000 ft MSL. Airplanes performing combat maneuver training within this airspace can be at any point and any airspeed within the aircraft's operating envelope.

Aircraft typically will fly supersonically at higher altitudes on initial target acquisition, will slow to subsonic conditions during combat maneuvers, then, after simulated weapon release, will make a supersonic dash for disengagement from a lower altitude. The first part of a typical maneuver involves full power acceleration in a straight line, either in level flight or diving, to low supersonic speeds. The combat maneuver is performed at a reduced throttle setting. Thus, the aircraft typically decelerates as it turns and is subsonic before the turn is complete (Galloway, 1983; Plotkin, 1985).

A review of a sample of these maneuvers (96 sorties) at Nellis AFB and at Luke AFB indicates that supersonic flight produces sonic booms which reach the ground for only a small portion of each sortie. During the time on the range, on average, 2.3% of the flight time produces sonic booms that reach ground level. The highest percentage (13.4%) of flight time producing sonic booms reaching ground level was reported for F-4s flying out of Luke AFB; the lowest percentage (0.6%) reported was for F-15 sorties from Nellis AFB. A major difference between Luke and Nellis is that the average ground elevation at Luke is 750 ft above mean sea level, while the average elevation at Nellis is 4,000 ft (Galloway, 1983).

Certain maneuvers can generate concave wavefronts which cause ray focusing. These include acceleration and the inside of curved flight paths such as pushovers and turns. Deceleration and the outside of turns have a defocusing effect. Overpressures are amplified at focal points. Although there are a number of theoretically possible types of focuses, only a simple focus is typical of combat training maneuvers. A simple focus, or caustic, is a three-dimensional surface along which the wave is focused. If the caustic intercepts the ground, a focal zone exists. (Not all maneuvers which can

produce a focus will produce a focus at ground level.) Focal zone U-wave signatures typically occur over areas of tenths or hundredths of a square mile. The total area where carpet boom overpressures are exceeded is typically less than 1 mi². In characterizing sonic boom footprints the maneuver is more important than the specific aircraft type (Plotkin, 1985).

All of the factors previously alluded to underline the conclusions of a number of investigators: sonic booms of any magnitude are less common than one might be led to believe simply by counting the number of training sorties, and the likelihood that any particular region will be subjected to high-overpressure, maneuver-enhanced sonic booms is smaller still. In this study, we are concerned about the possibility of coupling the sonic boom acoustical energy with seismic waves in a manner that increases the potential for damage. The concern is that, under the right type of conditions, enough energy can be coupled into the ground so that a structure is subjected not only to a brief (acoustical) sonic boom but also a concurrent sustained seismic wave of sufficient amplitude to produce additional damage or annoyance.

The following factors related to the (acoustic) sonic boom affect this possibility: (1) the match between the sonic boom trace velocity and the Rayleigh wave phase velocity, (2) the distance along the earth's surface for which a match occurs (affects how much energy is coupled into the seismic wave), (3) the amplitude of the sonic boom, and (4) the frequency spectrum of the sonic boom. The nature of these factors further emphasizes the importance of the type of training maneuver (as distinct from the particular type of aircraft). Consequently, in the following material the nature of the maneuver rather than aircraft types is emphasized.

Two generic types of aircraft, fighters and fighter bombers, are employed for tactical training. For the purpose of this chapter maneuvers involving representative aircraft from these two classes will be considered. No attempt will be made to distinguish the differences among aircraft within a class.

3.1 Characteristics of the Sonic Boom Footprint

Evaluation of the potential for resonant seismic coupled waves from supersonic aircraft maneuvers requires an appropriate characterization of the sonic boom footprint. A complete

description of the sonic boom footprint would specify the overpressure time history at every affected point. Such a description would incorporate answers to the following important questions:

What is the peak overpressure at each point?

What is the duration of the sonic boom at each point?

What is the velocity of the leading edge of the sonic boom wave as it moves across the ground?

Answers to these questions vary with the particular maneuvers an aircraft is performing as well as with atmospheric conditions. Figure 3-1 shows an idealized normal sonic boom N-wave signature together with extreme variations due to atmospheric conditions--a peaked signature and a highly rounded signature. Figure 3-2 illustrates the evolution of a sonic boom signature from a peaked signature to a rounded signature within a fraction of a second--all of the signatures depicted show the influence of the atmosphere.

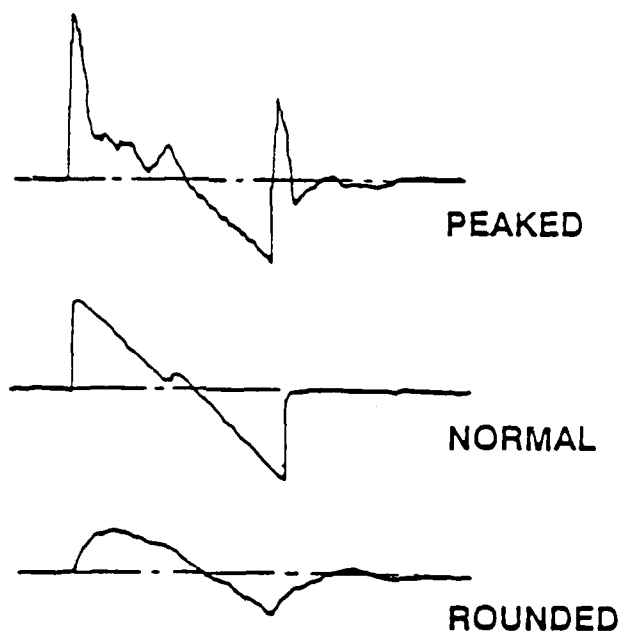


Figure 3-1. Selected Sonic Boom Waveforms (Maglieri and Hubbard, 1965).

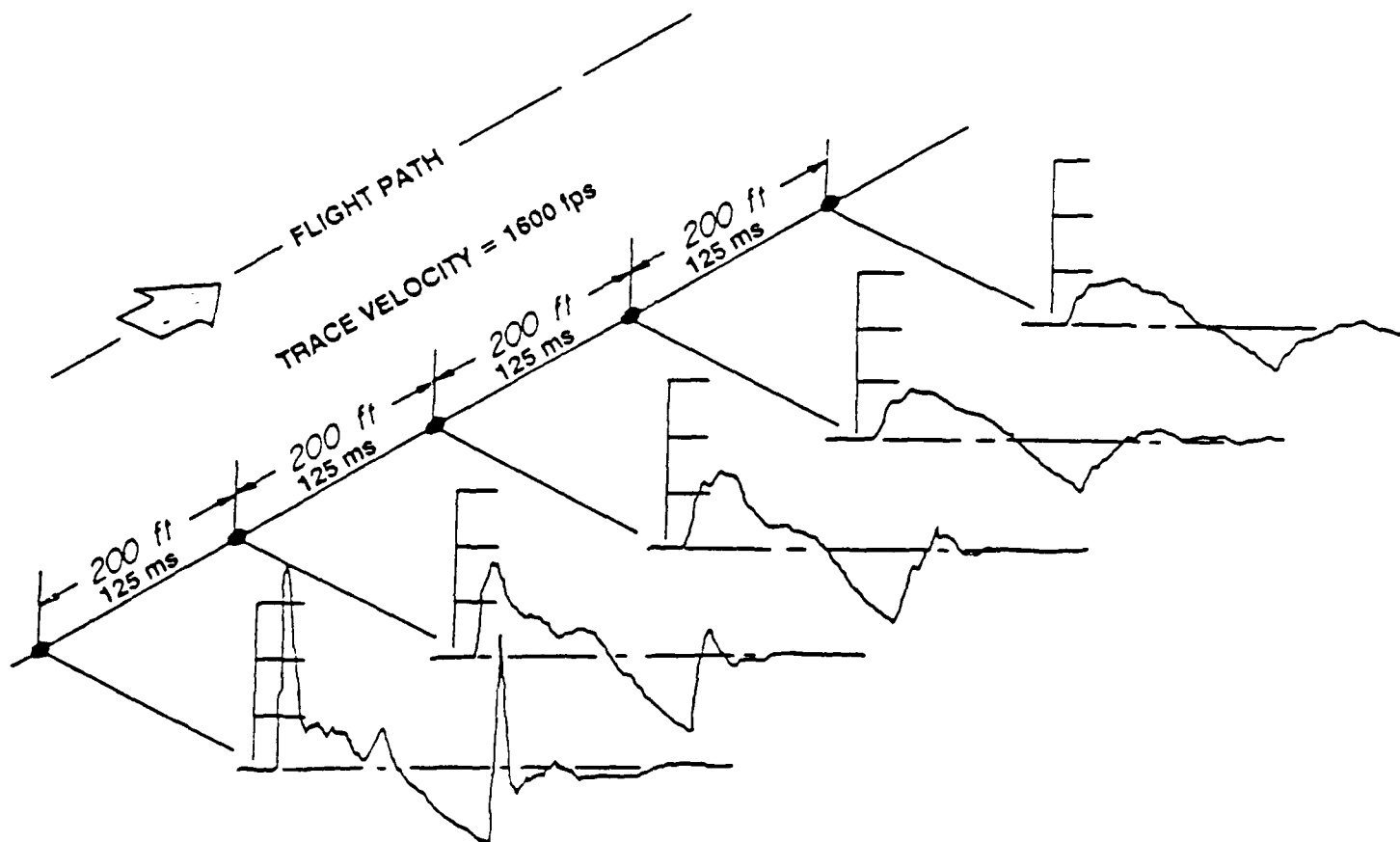


Figure 3-2. Measured Sonic-Boom Pressure Signatures at Several Points Along the Ground Track of Airplane A in Steady-Level Flight (Hilton et al., 1964).

Notwithstanding the waveform complexities that can be introduced by atmospheric conditions, analysis of the waveforms can be simplified by considering standardized representations. In the following material, waveforms will be characterized as normal or focused waveforms with a specified peak overpressure, duration, and trace velocity.

For the purpose of this characterization, aircraft supersonic maneuvers were considered to be one of the following classes of simplified, idealized maneuvers:

Level, constant speed, supersonic flight

Level, constant acceleration, supersonic flight

Constant dive angle, constant acceleration, supersonic flight

Constant angular turn rate, constant speed, supersonic flight

In selecting maneuvers for consideration, a primary consideration was, that for efficient and effective seismic coupling to occur the trace velocity and the phase velocity of the seismic waves must be nearly equal (within a tolerance of $\pm 10\%$) over some relatively significant (several wavelengths) distance. Thus, an emphasis was placed on maneuvers producing either a constant trace speed or a slowly varying trace speed.

In order to obtain an indication of overpressures, trace speeds and sonic boom wave durations, PCBOOM (Bishop, 1988) was used to simulate a broad range of maneuvers for a representative fighter and a representative fighter bomber. The initial set of maneuvers examined is identified in Table 3-1. These simulations were supplemented by analytical calculations and the analyses of previous investigators.

Table 3-1. Maneuvers Simulated with PCIBOOM.

MANEUVER	INITIAL ALTITUDE	INITIAL SPEED	ACCELERATION	DIVE ANGLE	TURN RATE
Constant Speed, Level Flight	500 ft	M = 1.01, 1.05, 1.15, 1.2, 1.25, 1.4, 1.6, 2., 2.5	0	0	0
Constant Speed, Level Flight	1,000 ft	M = 1.01, 1.05, 1.15, 1.2, 1.25, 1.4, 1.6, 2., 2.5	0	0	0
Constant Speed, Level Flight	5,000 ft	M = 1.01, 1.05, 1.15, 1.2, 1.25, 1.4, 1.6, 2., 2.5	0	0	0
Constant Speed, Level Flight	10,000 ft	M = 1.01, 1.05, 1.15, 1.2, 1.25, 1.4, 1.6, 2., 2.5	0	0	0
Constant Speed, Level Flight	15,000 ft	M = 1.01, 1.05, 1.15, 1.2, 1.25, 1.4, 1.6, 2., 2.5	0	0	0
Constant Speed, Level Flight	30,000 ft	M = 1.01, 1.05, 1.15, 1.2, 1.25, 1.4, 1.6, 2., 2.5	0	0	0
Constant Speed, Level Flight	45,000 ft	M = 1.01, 1.05, 1.15, 1.2, 1.25, 1.4, 1.6, 2., 2.5	0	0	0

Table 3-1. Maneuvers Simulated with PCBOOM (continued).

MANEUVER	INITIAL ALTITUDE	INITIAL SPEED	ACCELERATION	DIVE ANGLE	TURN RATE
Level Flight, Constant Acceleration	500 ft	M = 1.01	0.1, 0.3, 0.5 gs	0	0
Level Flight, Constant Acceleration	1,000 ft	M = 1.01	0.1, 0.3, 0.5 gs	0	0
Level Flight, Constant Acceleration	5,000 ft	M = 1.01	0.1, 0.3, 0.5 gs	0	0
Level Flight, Constant Acceleration	10,000 ft	M = 1.03	0.1, 0.3, 0.5 gs	0	0
Level Flight, Constant Acceleration	45,000 ft	M = 1.05, 1.15, 1.30	0.1, 0.3, 0.5 gs	0	0

Table 3-1. Maneuvers Simulated with PCBOOM (concluded).

MANEUVER	INITIAL ALTITUDE	INITIAL SPEED	LINEAR ACCELERATION	DIVE ANGLE	TURN RATE
Dive, Constant Acceleration	12,000 ft	M = 1.01	0.1, 0.5, 1.0 gs	10°	0
Dive, Constant Acceleration	20,000 ft	M = 1.01, 1.4	0.1, 0.5, 1.0 gs	10°, 20°	0
Dive, Constant Acceleration	45,000 ft	M = 1.01, 1.4	0.1, 0.5, 1.0 gs	10°, 20°, 30°, 45°, 60°	0
Constant Speed Turn	10,000 ft	M = 1.1, 1.4, 1.7	0	0	1, 1.1, 1.5 g's
Constant Speed Turn	45,000 ft	M = 1.1, 1.4, 1.7	0	0	1, 1.1, 1.5 g's

The maneuvers presented in Table 3-1 were supplemented by an analytical characterization of the trace speeds for accelerated level flight, dives and climbs, and an examination of theoretical and empirical characterizations of sonic booms from tactical aircraft maneuvers developed by previous investigators (Plotkin, 1985; Maglieri and Hubbard, 1965; Lee et al., 1989; Kane and Palmer, 1964; Haglund and Kane, 1971; Lansing and Maglieri, 1965; and Carlson et al., 1966).

3.2 Supersonic Maneuvers

3.2.1 Straight, Level, Non-accelerating Flight

The sonic boom carpet trace speed of an aircraft flying at a constant speed along a straight, level flight path is equal to that of the aircraft. Because the speed of sound in air varies with atmospheric properties which are a function of altitude, trace speed will vary slightly with altitude for a fixed aircraft Mach number. Figure 3-3 shows the variation of trace speed with altitude and Mach

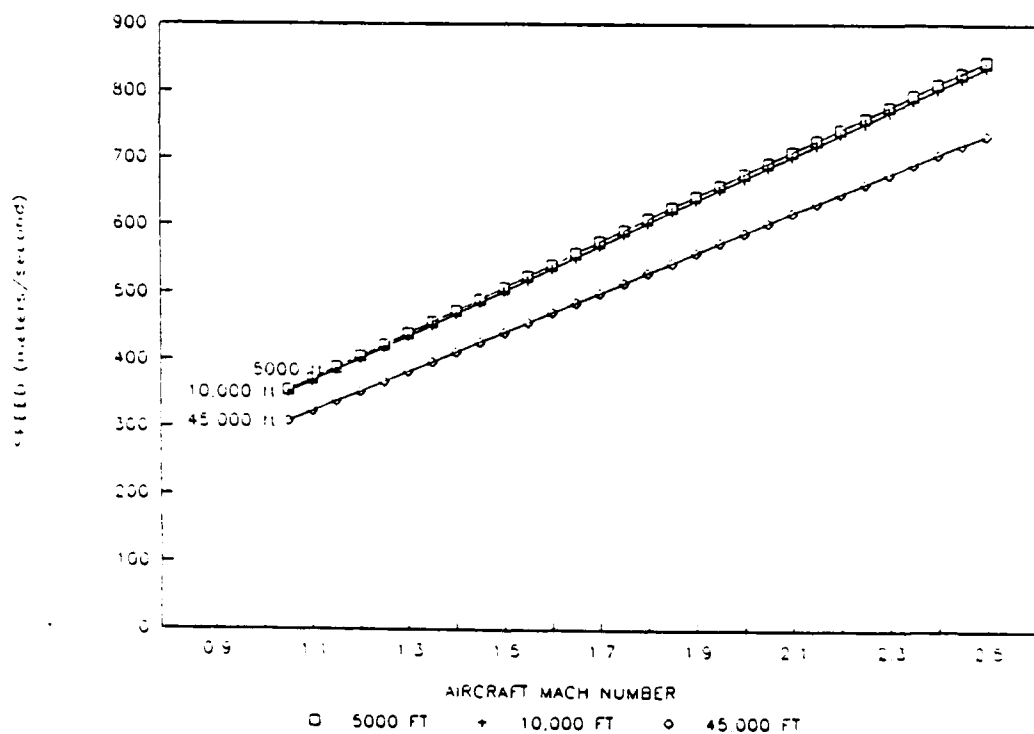


Figure 3-3. Trace Speed as a Function of Speed and Altitude for Constant Speed, Constant Altitude Level Flight.

number. The figure indicates for constant speed level flight that trace speeds fall within the range from 300 m/sec to just under 900 m/sec. (As a practical matter, the upper bound on trace velocities for these conditions is probably closer to 700 m/sec; supersonic flight at these higher speeds is very unusual at low elevations because of the energy requirements.)

Figures 3-4 and 3-5 depict the relationships between peak ground overpressure and flight altitude and flight speed for a fighter (F-15) and a fighter-bomber (FB-111). Figures 3-6 and 3-7 depict a similar functional relationship for sonic boom duration. Notice that the sensitivity of overpressure to both aircraft altitude and speed increases with decreasing altitude. A consequence of this correlation is that while it is easy to define a floor for supersonic operations that will protect a population with a high degree of confidence, deliberate or accidental supersonic operations at lower altitudes may produce substantially higher overpressures; the exact magnitude may be quite sensitive to the actual altitude and speed and maneuver flown. These figures indicate that aircraft flying at or above the 10,000 ft floor will produce overpressures of less than 10 psf in level constant speed flight. Maglieri et al. (1966) reports on a set of ground measurements made for 2 different supersonic fighters flying at constant altitudes and speeds in the altitude range from about 50 ft to 890 ft for a Mach number range of about 1.05 to 1.16. The highest reported measured overpressure was 120 psf from an overflight at 110 ft at a Mach number of 1.13; typical overpressures measured for overflights at 500 ft were 30 to 40 psf.

Figures 3-6 and 3-7 indicate the strong dependence of sonic boom wavelength on the exact speed at low Mach numbers and the decreasing sensitivity at higher Mach numbers. As for peak overpressure, the altitude dependence is greatest at low altitudes. The wavelength at sea level (duration) for level flight ranges from approximately 0.06 sec (16 Hz) to 0.24 sec (4 Hz), corresponding to distances from approximately 18m (60 ft) to 72m (235 ft).

3.2.2 Straight, Level, Accelerating Flight

Unlike constant speed flight, the trace speed for accelerating, level flight is dependent on not only the speed of the aircraft, but also on the aircraft acceleration and the flight altitude. The acceleration of the aircraft has 2 effects. It directly alters the trace speed and it affects the rate of

change of the Mach cone angle and hence the initial direction of propagation. The initial angle of the shock wave changes in accord with the equation

$$\sin \mu = 1 / M \quad (3-1)$$

Representative examples of level accelerated flight were examined for altitudes ranging from 5,000 ft MSL to 45,000 ft MSL, for Mach numbers in the range from 1.01 to 2.5, and accelerations ranging from approximately 0.15 gs to approximately 1.0 gs. (All simulations were based on the ground being at sea level; acceleration was expressed as the time rate of change of Mach number \dot{M} .)

All cases examined have a number of common characteristics, as illustrated in Figure 3-8, which depicts a plot of the trace speed as a function of the distance along the flight track for level flight at constant acceleration ($\dot{M} = 0.01/\text{sec}$) at an altitude of 10,000 ft MSL. The maneuver begins with the aircraft traveling just slightly faster than the cutoff Mach number (the speed at which the sonic boom wavefront refracts upward at ground level) and continues to a speed of Mach 2.5. The initial trace speed is negative and large in magnitude. As the aircraft accelerates, the location of the sonic boom initially decreases slightly and the trace speed rapidly first declines to zero and then begins to increase. (Zero trace speed will occur at the ground level focus.) As the aircraft continues to accelerate, the location of the sonic boom ground intersection advances smoothly in the downtrack direction and the trace speed increases relatively slowly.

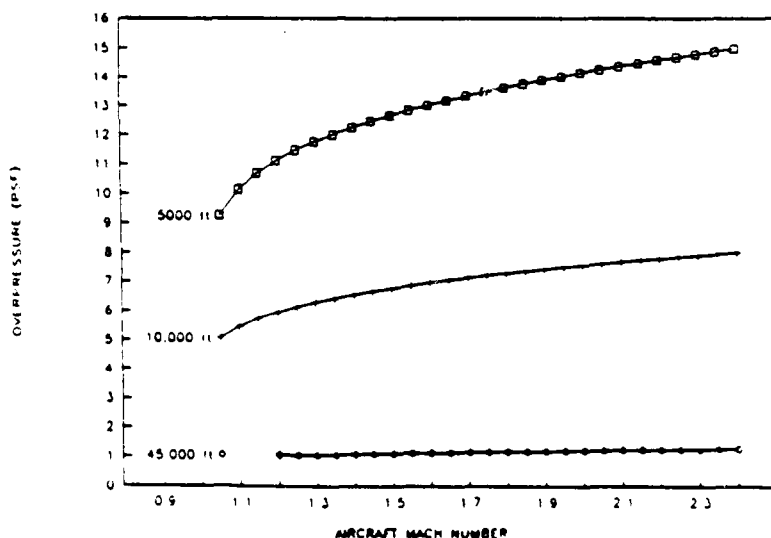


Figure 3-4. Peak Overpressure as a Function of Speed and Altitude for a Fighter (F-15) Flying at a Constant Speed and a Constant Altitude.

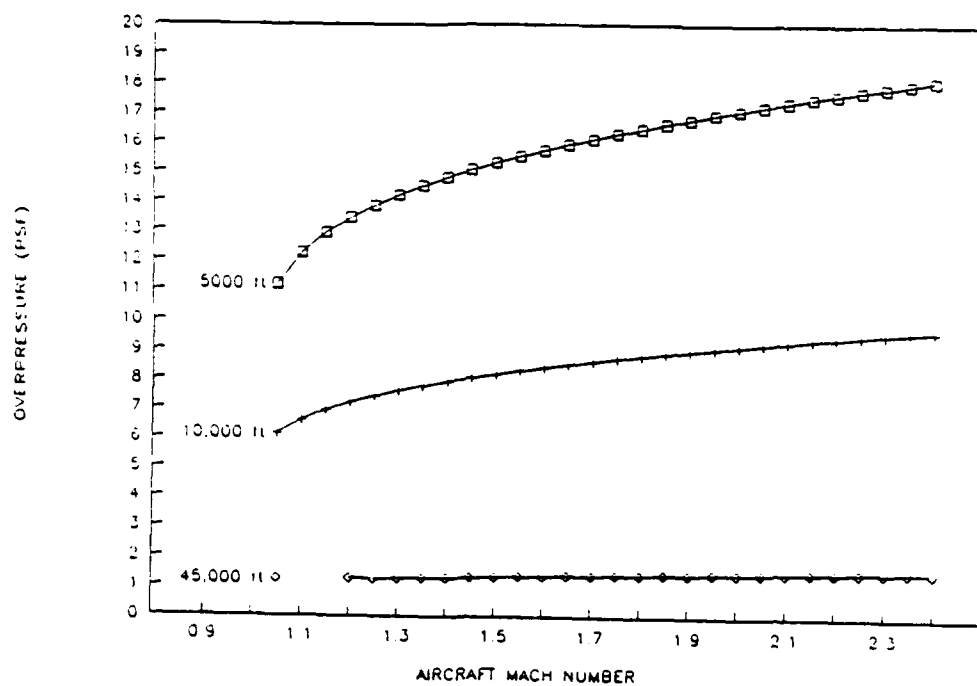


Figure 3-5. Peak Overpressure as a Function of Speed and Altitude for a Fighter-Bomber (FB-111) Flying at a Constant Speed and a Constant Altitude.

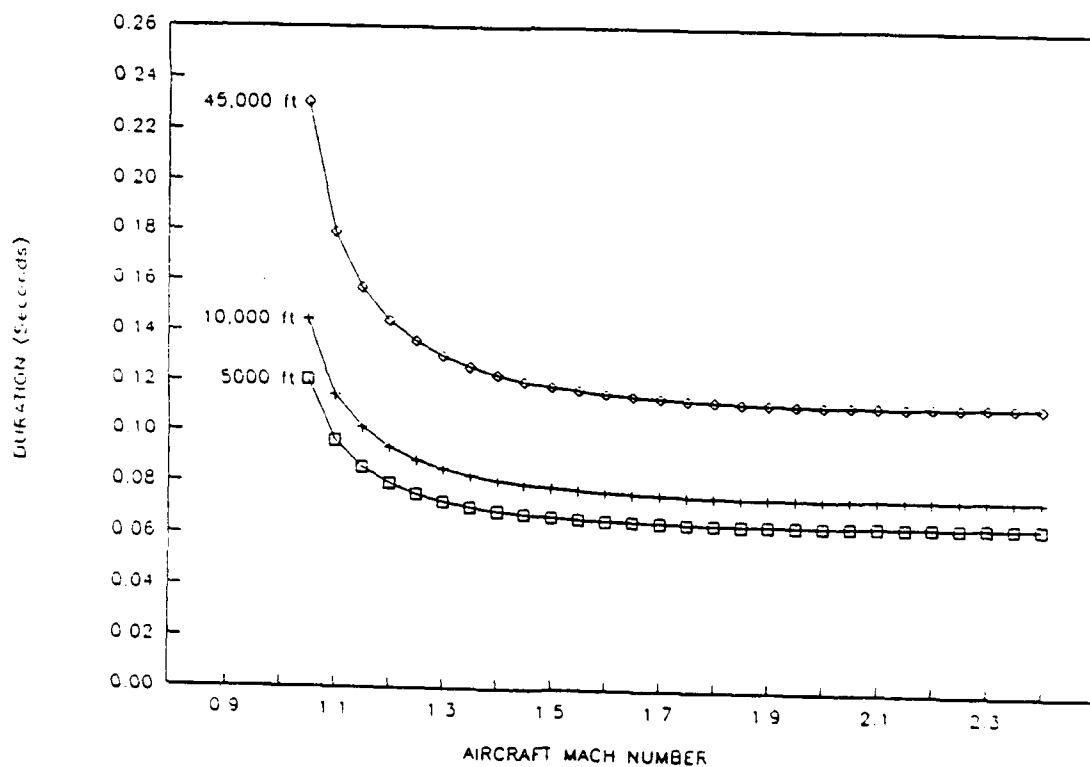


Figure 3-6. Sonic Boom Signature Durations as a Function of Speed and Altitude for a Fighter (F-15) Flying at a Constant Speed and Altitude.

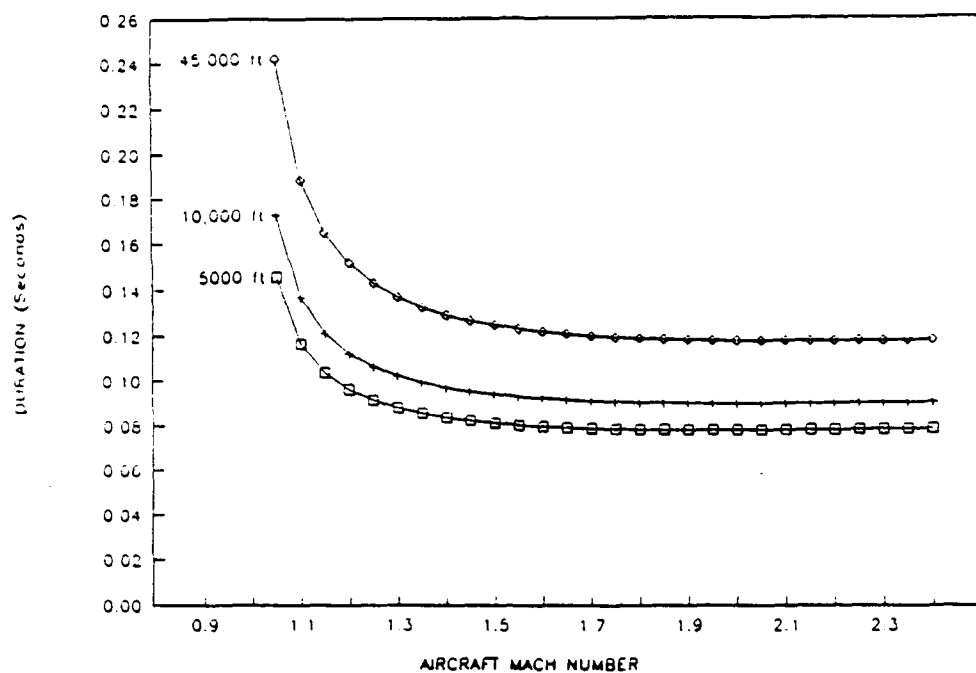


Figure 3-7. Sonic Boom Signature Durations as a Function of Speed and Altitude for a Fighter-Bomber (FB-111) Flying at a Constant Speed and Altitude.

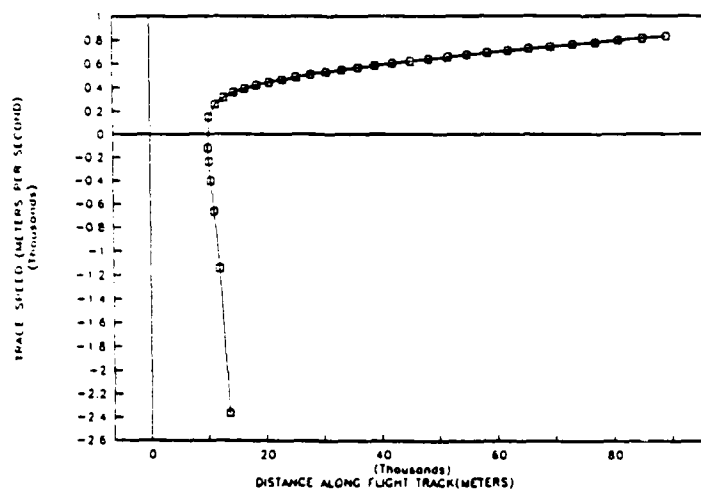


Figure 3-8. Trace Speed as a Function of Distance Along the Flight Track for Level Accelerated Flight at an Altitude of 10,000 Ft MSL ($M=0.01$ per sec).

Figure 3-9 shows a detail of this plot ranging out to approximately 20 km downtrack from the focus. Notice that beginning at a distance of a few kilometers downtrack from the focus, that the trace velocity is within the $\pm 10\%$ range for a distance on the order of at least 2 km.

Figure 3-10 depicts a plot of the trace velocity against ground track distance for the same type of maneuver at an acceleration of $\dot{M} = 0.015$. The higher acceleration results in a larger trace velocity and larger distance from the focus before the trace velocity rate of change with distance along the ground track levels off.

Figures 3-11 and 3-12 illustrate the trace speed versus ground track distance for the same maneuvers at 45,000 ft MSL. Notice that these trace curves follow the same pattern depicted for the maneuvers at 10,000 ft MSL.

In order to understand the behavior of overpressures associated with accelerated flight, it is useful to understand the geometry of the surface along which focusing occurs. In the most general case, accelerated flight initially produces a focus aloft. As the aircraft accelerates, the focus location descends until it first reaches the ground level and then "moves underground." In a "no-wind" atmosphere, the focus along the flight track reaches the ground before the offtrack portion of the focus. Thus, while the focus along the flight track consists of a point, away from the flight track it consists of a pair of points located symmetrically about the flight track.

Figure 3-13 depicts the relationship between the focus location beneath the flight track, trace speed and the type of signature. As the aircraft begins to accelerate, the focus is above ground and thus, the initial ground signature is a post-focus signature attenuated to a level less than the carpet boom; the trace speed in this region is negative and changes rapidly with distance along the flight track. The peak overpressure is associated with the focus at the ground level; the trace speed at this location is zero. Continued acceleration causes the focus to "move underground," making the ground level signatures prefocus, maneuver-enhanced signatures. (This region will have reflected above-ground focuses.) The degree of enhancement varies with the distance from the ground level focus. Initially, the trace speed changes rapidly with down track distance from the ground level focus and then more gradually. A similar pattern occurs at locations laterally displaced from the flight track.

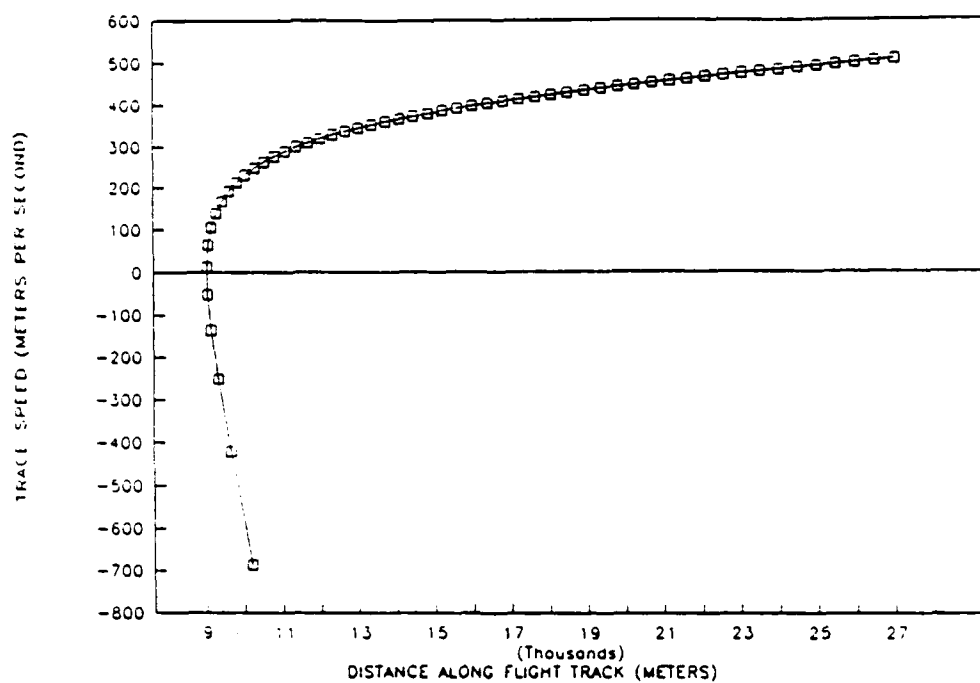


Figure 3-9. Detail of Trace Speed versus Distance (Altitude=10,000 Ft MSL, $\dot{M}=0.01$ per sec).

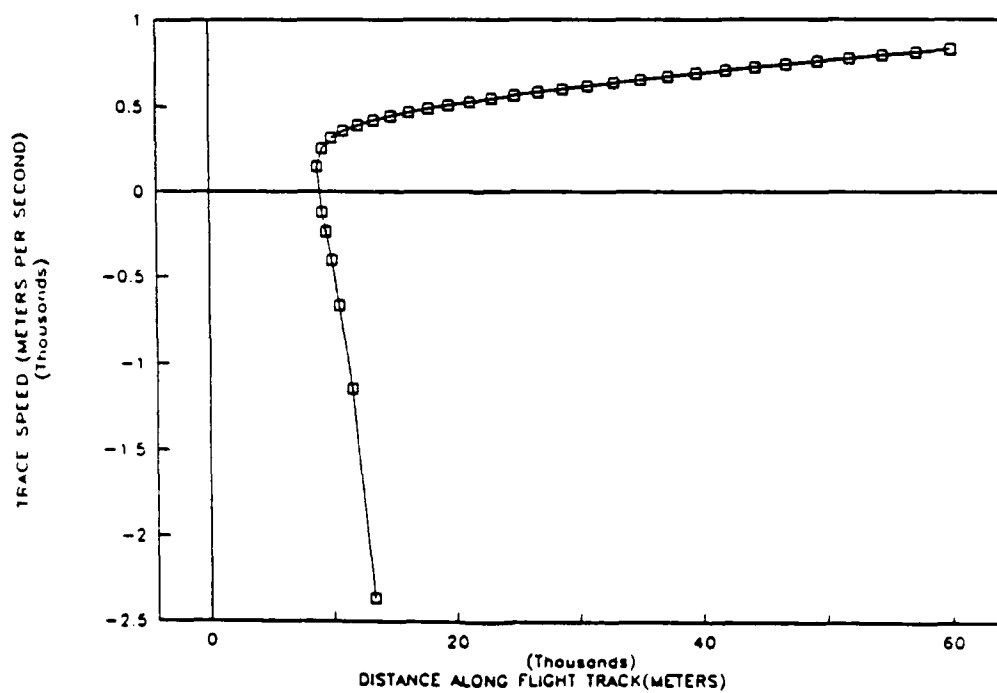


Figure 3-10. Trace Speed as a Function of Distance Along the Flight Track for Level Accelerated Flight at an Altitude of 10,000 Ft MSL ($\dot{M}=0.015$ per sec).

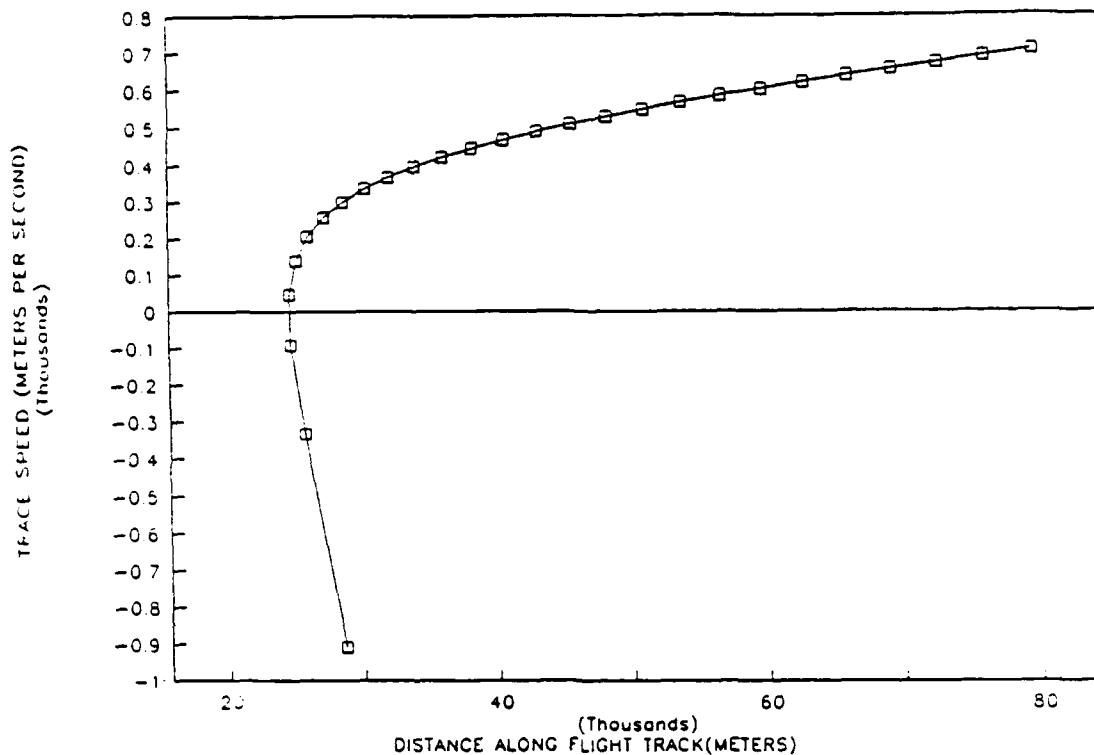


Figure 3-11. Trace Speed as a Function of Distance Along the Flight Track for Level Accelerated Flight at an Altitude of 45,000 Ft MSL ($\dot{M}=0.01$ per sec).

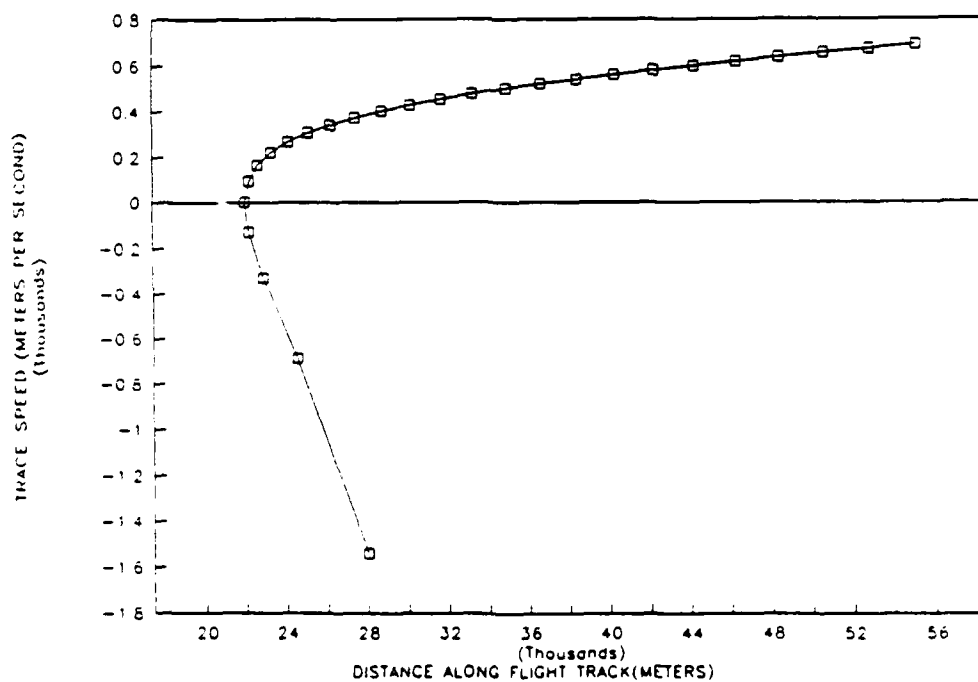


Figure 3-12. Trace Speed as a Function of Distance Along the Flight Track for Level Accelerated Flight at an Altitude of 45,000 Ft MSL ($\dot{M}=0.015$ per sec).

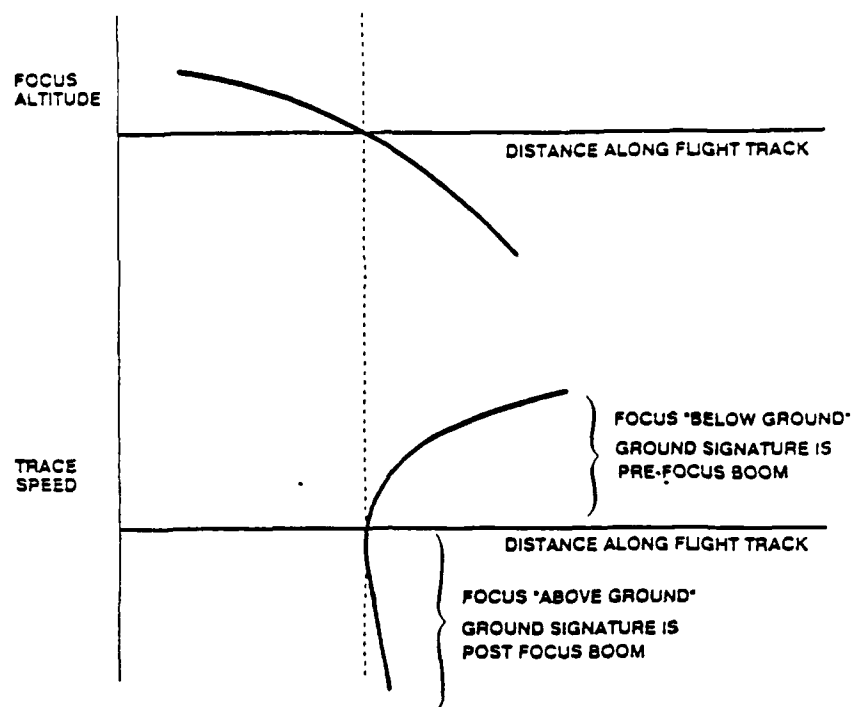


Figure 3-13. Relationship Between Focus Location and Trace Speed Plots.

The same basic focus surface geometry characterizes diving acceleration. The major difference between the two maneuvers is the changing aircraft altitude which changes the distance of propagation. As a consequence of the similarities, the sonic boom footprints and trace speed plots of the two types of maneuvers are very similar.

A previous study (Plotkin, 1985) reports prefocus and focus maneuver footprints for a collection of representative tactical aircraft maneuvers. The overpressure for the highest overpressure zone reported for an F-15 in level accelerated flight at 10,000 ft above the ground was 14 psf; for an F-15 in level accelerated flight at 45,000 ft it was 5 psf. Figures 3-14 and 3-15 illustrate the footprints for these two maneuvers. Notice that while the zone of enhanced overpressure is approximately 2,000 ft along the flight track, the width of the zone decreases rapidly with lateral displacement from the flight track. Figure 3-14 also indicates that within the region of enhanced overpressures, the peak overpressures decrease rapidly with distance from the focus. In particular, notice that the highest overpressure contour is barely separable from the next level.

3.2.3 Diving Acceleration

A diving (or climbing) maneuver differs from level flight in three important ways. First, the flight path angle is either elevated or depressed; it is not parallel to the earth's surface. The second effect is more subtle. The speed of sound changes slowly with altitude. This changes the relationships between aircraft speed, Mach number, and Mach cone angle. Third, at lower Mach numbers the portion of the wavefront originating above a diving aircraft will reach the ground; for aircraft in level flight or climbing this will occur only if the wave is refracted back to the ground by an inversion.

A dive at a constant Mach number produces a constant trace speed. Espinosa et al., 1968, describe relationships between constant Mach number climbs and dives. At low Mach numbers (Mach numbers less than 1.3), they indicate that these maneuvers can produce constant trace velocities ranging from a few hundred m/sec to arbitrarily large values. As the orientation of the wavefront becomes nearly parallel to the ground, the trace velocities grow without limit.

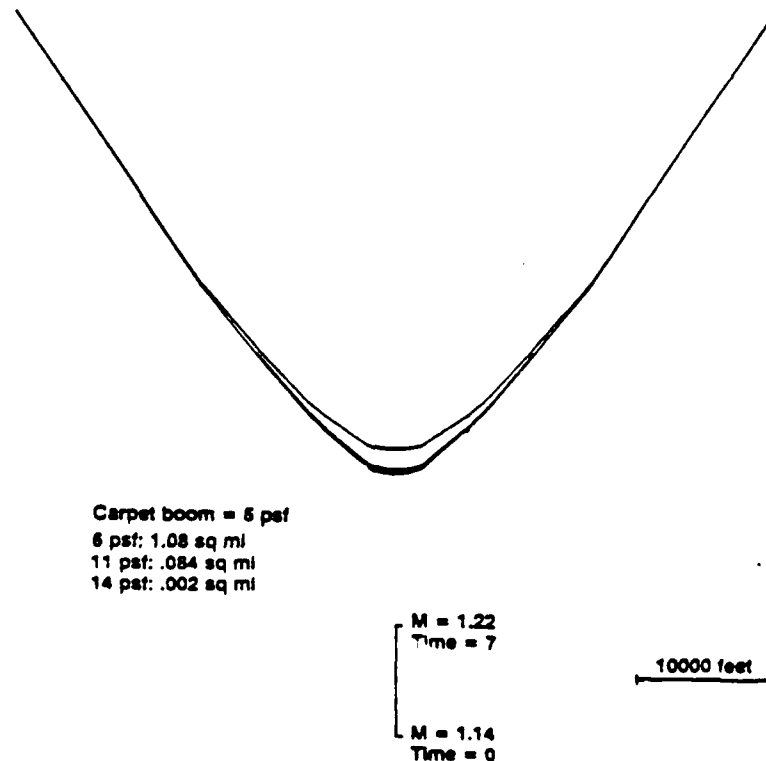
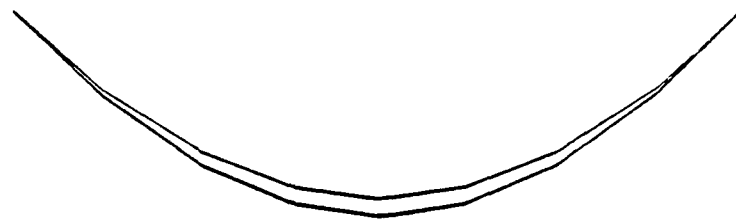


Figure 3-14. F-15 Level Acceleration at 10,000 Ft (Plotkin, 1985).



Carpet boom = 1.2 psf
2 psf: 1.26 sq mi
5 psf: 0.033 sq mi

10000 feet

M = 1.25
Time = 5
M = 1.23
Time = 0

Figure 3-15. F-15 Level Acceleration at 45,000 Ft (Plotkin, 1985).

The trace velocity plots for the shock wave originating beneath the aircraft for constant acceleration, constant dive angle maneuvers are similar in form to those for the constant acceleration level flight with the following notable differences. Accelerating dives originating at low supersonic speeds and continuing long enough will produce wavefronts that go through the following evolution. The wave normals produced at the start of the dive will have a component pointing in the forward direction. As the aircraft accelerates, the wavefront first becomes parallel to the ground and then develops a component in the reverse direction, producing a discontinuity in the trace speed as the wave front moves through paralleling the ground. A second important difference is the relatively larger rates of change of the trace velocity with distance along the ground track. Nevertheless, relatively constant trace velocities are maintained for fairly substantial distances as long as the region is sufficiently down track from a focus. Dives originating at higher speeds or of shorter duration will exhibit only a portion of this pattern.

Figures 3-16 and 3-17 display trace speed versus distance along the flight track for accelerating 45° dives (at an acceleration of \dot{M} equals 0.01) from initial altitudes of 15,000 ft and 35,000 ft respectively. Both trace speed plots have the same general form. The assumption of a floor on dives at 10,000 ft results in the lower dive terminating

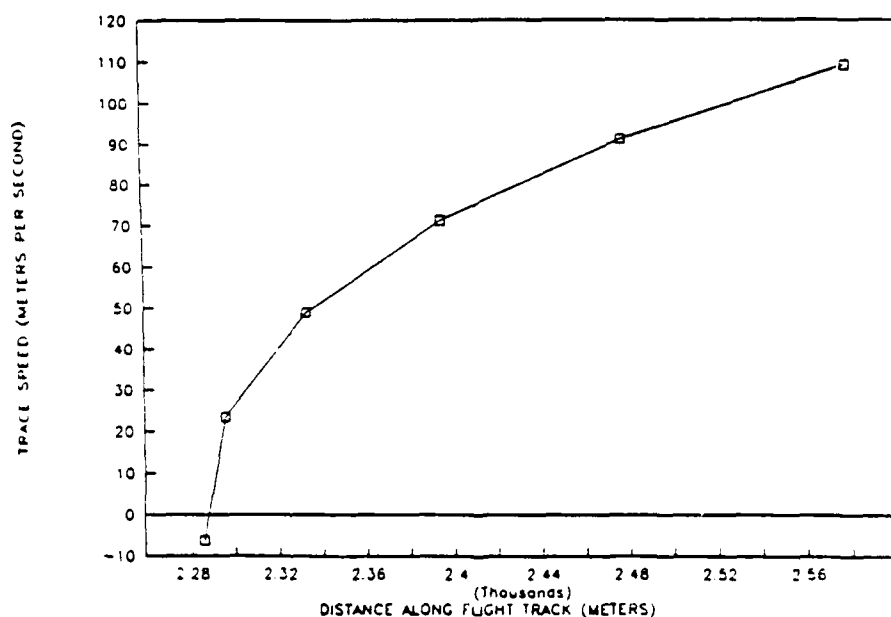


Figure 3-16. Trace Speed as a Function of Distance Along the Flight Track for an Accelerated Dive from 15,000 Ft at a Dive Angle of 45° ($\dot{M}=0.01$ per sec).

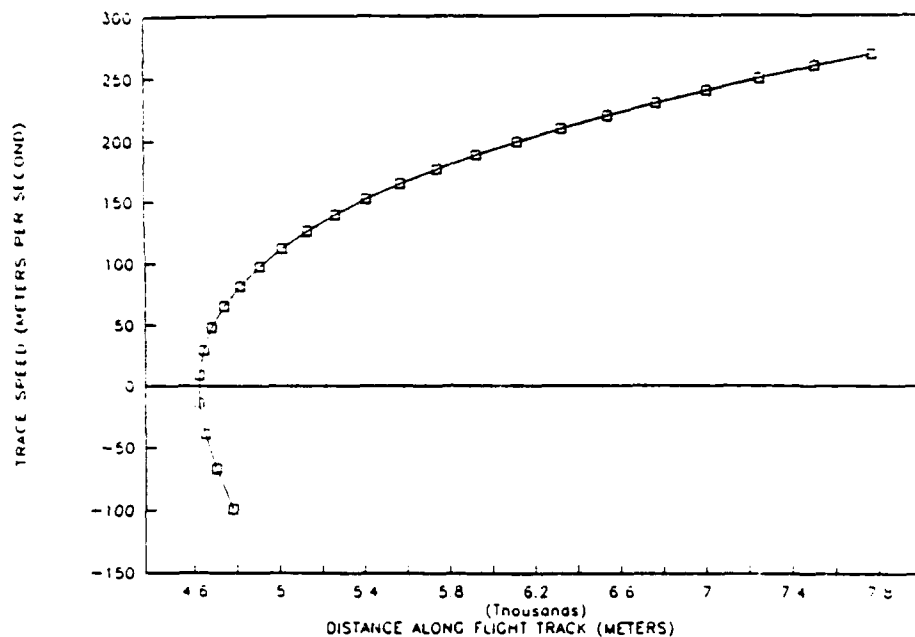


Figure 3-17. Trace Speed as a Function of Distance Along the Flight Track for an Accelerated Dive from 35,000 Ft at a Dive Angle of 45° ($M=0.01$ per sec).

just as the rate of trace velocity change with distance has begun to slow down and stabilize, while the dive from the higher altitude produces a longer trace at a more slowly changing trace speed.

The trace plots of accelerated climbs are similar to those of accelerated level flight with the difference that the climb angle increases the aircraft speed required for the sonic boom to reach the ground. While accelerated climbs do occur, decelerated climbs are somewhat more common for protracted climbs at supersonic speeds. In a decelerated climb, the trace speed is affected by the same factors that affect accelerated flight; however, the factors operate in the opposite fashion. Deceleration reduces the aircraft speed which tends to reduce the trace speed. The increased Mach cone angle associated with the reduced aircraft speed tends to increase the trace speed. After sufficient deceleration, the aircraft speed approaches the effective cutoff Mach number and the wavefront becomes parallel to the ground. The trace speed is relatively constant until the aircraft speed approaches the effective cutoff Mach number. At this point the trace speed approaches infinity.

Based on the results of a previous study (Plotkin, 1985), a fighter in a 10° dive from 15,000 ft produces overpressures in the focal zones of about of 11 to 16 psf; characteristic overpressures of

peak overpressure zones for a 30° fighter dive from 30,000 ft are in the range from 8 to 11 psf. In general, the greater the accelerations the smaller the focal areas. Figures 3-18 through 3-20 display a collection of footprints for fighter dives. As for the case of level acceleration, overpressures decline rapidly with distance from the focus.

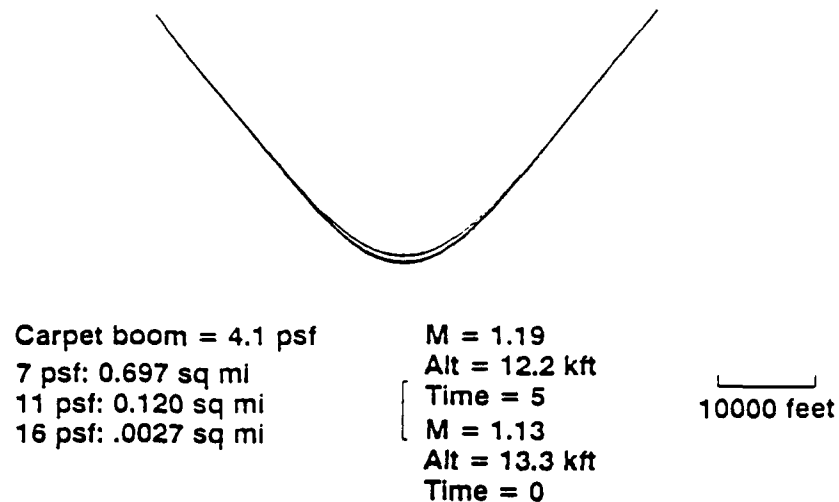


Figure 3-18. F-4 10° Dive from 15,000 Ft (Plotkin, 1985).

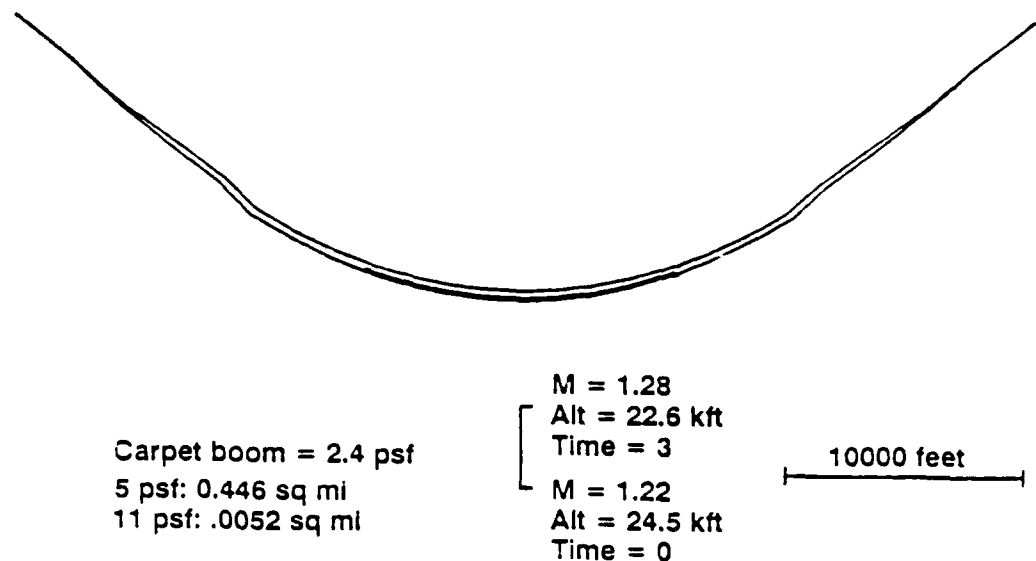


Figure 3-19. F-4 30° Dive from 30,000 Ft (Plotkin, 1985).

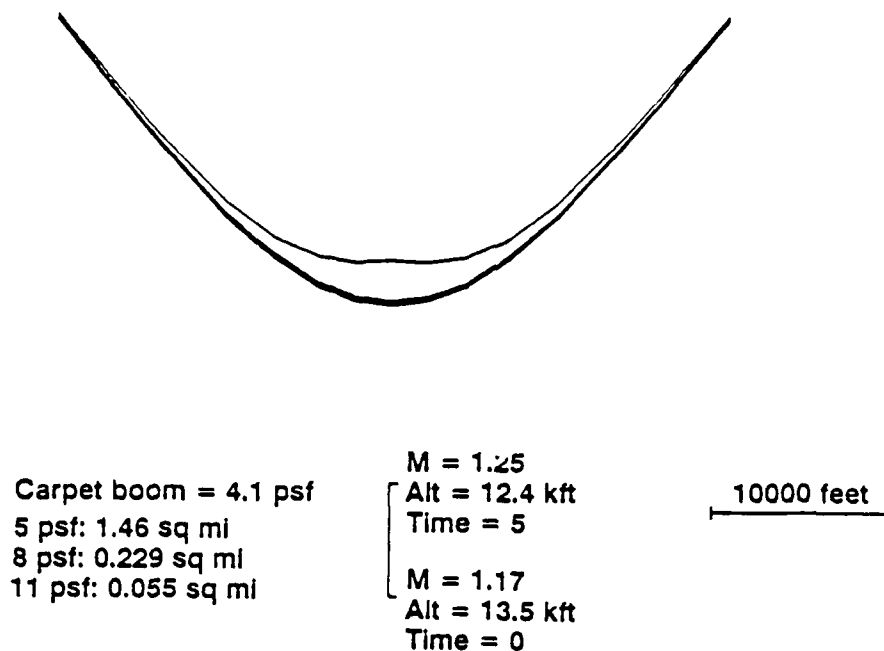


Figure 3-20. F-15 10° Dive from 15,000 Ft (Plotkin, 1985).

3.2.4 Constant Speed Turns

The trace speed characteristics of turns are substantially more complicated to characterize in detail than linear maneuvers, because different portions of the sonic boom footprint are responsible for successive wavefronts striking the ground along a particular direction. Nevertheless, it is easy to demonstrate that away from the focus, typical constant speed turns have relatively constant trace velocities for distances on the order of at least 2 km. The component of a velocity, v , in a direction x , after the aircraft has turned through an angle ϕ , is $v \cos \phi$. The criterion which allows a variation of $\pm 10\%$ is equivalent to stating that the velocity is within the criterion, providing that the turn angle is no more than $\phi = \cos^{-1} 0.8$, or approximately 37° . The "standard turn rate" of $3^\circ/\text{sec}$ corresponds to approximately 12.5 sec flight time. At a speed of Mach 1 the turn rate corresponds to a distance of approximately 3 km; at higher speeds it corresponds to greater distances.

The more typical situation of a decelerating turn will reduce the distance over which trace speeds are relatively constant. The exact combination of turn parameters and acceleration will govern

the amount of reduction. Figure 3-21 depicts an example of overpressure contours from a decelerating turn.

3.3 Summary

As can be seen from the previous discussion, significant portions of a large number of maneuvers--steady level flight, accelerated level flight, accelerated dives and climbs, decelerated climbs, and constant speed turns--produce trace speeds which are sufficiently constant over moderately significant distances to be favorable to Rayleigh wave resonance. In no case examined were steady trace velocities found in the neighborhood of a focus. In contrast to these simulations, aircraft have been flown at constant or nearly constant speeds at the threshold Mach number for

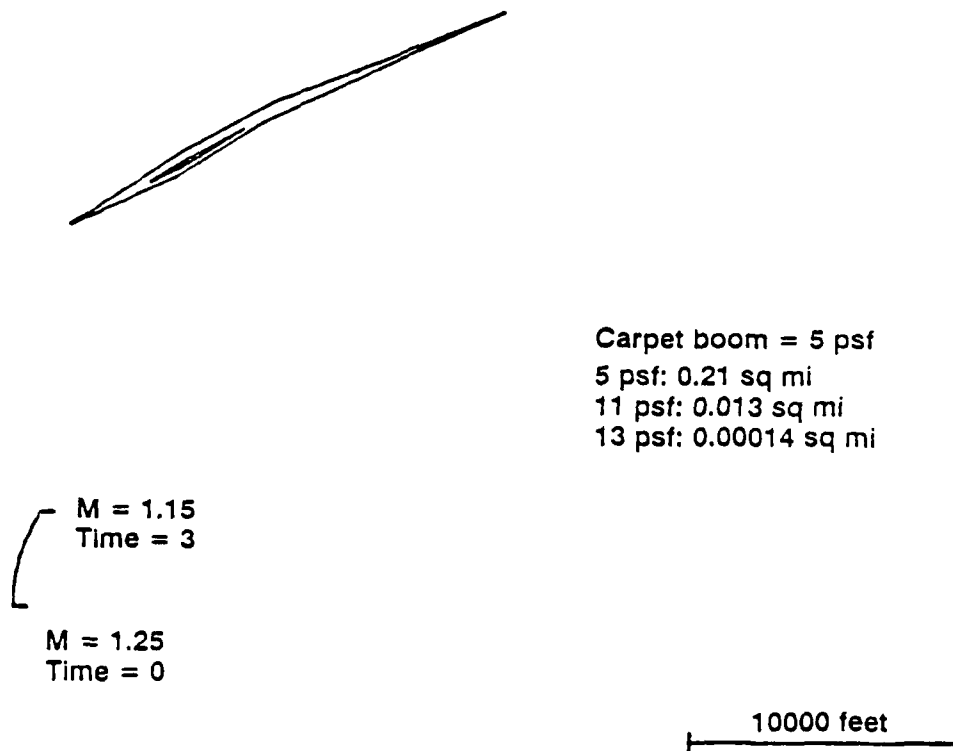


Figure 3-21. F-15 Level Turn at 10,000 Ft (Plotkin, 1985).

research purposes. This type of flight will produce steady trace velocities with focus type signatures. This type of flight is not anticipated for realistic training maneuvers. Thus, while signatures containing maneuver enhanced overpressures may be associated with Rayleigh wave resonance, it is unlikely that signatures within a focal zone will be involved in Rayleigh wave resonance.

4.0 RESONANT CHARACTERISTICS OF TYPICAL STRUCTURES

4.1 Introduction

The response of a structure or a portion of a structure to acoustic or seismic waves is directly related to the potential for annoying vibrations or damage. The details of the response of a structure to a loading waveform are dependent upon the distribution of mass and stiffness within the structure and the degree of damping in the various elements. The structural motion is governed by a second-order, differential equation. (The complete motion of the structural components is characterized by a matrix formulation of this equation; however, it is frequently simplified using an overall composite mass and stiffness and solving an approximating single degree of freedom, scalar equation.)

Natural frequencies of the building and building elements describe the rate at which the mass will freely oscillate when it is displaced. Damping characterizes the amount of continued free vibration. A critically damped structural element will return to its equilibrium position without oscillating. Real elements are characterized by some damping level at a fraction of critical damping, which is indicative of the amount of continued oscillation before the element stabilizes in its equilibrium position. Solution of the governing equation characterizes the time history responses of the structural elements. Damage estimates are typically based on the peak value of a response parameter (displacement, velocity, or acceleration). For sustained vibration, however, it is important to recognize that the duration of the loading is related to the number of structural element oscillations that will occur. Thus, duration is closely related to damage.

The overall structural response correlates with plaster cracking potential; midwall motion correlates with window sashes rattling, picture frames tilting, dishes jiggling, and bric-a-brac falling (Siskind et al., 1980). Damage to unconventional structures, other than buildings, may be more configuration-dependent.

While the damage potential to any particular structure depends on the response characteristics of that particular structure, regulations are written in terms of the maximum ground motion to which a particular type of structure should be subjected. These standards have been inferred by combinations of theoretical and empirical evaluations of structural response to various loads. Figure

4.2 Conventional Structures

The Uniform Building Code (UBC), 1988 edition, gives equation (4-1) for the natural response period of various buildings:

$$T = C_t (h_n)^{0.75} \quad (4-1)$$

where T is the period of the fundamental mode in seconds, and h_n is the height of the building in feet. The values for the coefficient C_t depend on the type of construction as follows:

C_t	Type of Construction
-------	----------------------

0.035	Structures with steel moment-resisting frames
-------	---

0.030	Reinforced concrete moment-resisting and eccentric braced frames
-------	--

0.020	All other buildings
-------	---------------------

Discussions with representatives of the Structural Engineers Association of California (SEAOC) suggest that the coefficients C_t can range from roughly 80% to 100% of their nominal values. Based on the height and type of building construction, one can estimate the ranges of fundamental periods and natural frequencies (i.e., natural frequency = $1/T$) of the building response to vibration. An evaluation of these equations for low-rise and light conventional structures suggests a range of fundamental frequencies of approximately 1 to 10 Hz. A Bureau of Mines study (Siskind et al., 1980) reports measured natural frequencies for more than 50 houses in 2 directions (N-S and E-W); the reported resonant frequencies were in the range of 4 to 10 Hz. The Bureau of Mines study also reports the results of measurements from 2 other investigators. These results were similar to those measured by the Bureau of Mines except that one investigator (Medearis, 1976) reported results extending to slightly higher frequencies: for 1-story homes he reported a range of 8 to 18 Hz, for 1½-story homes a range of 7 to 14 Hz, and for 2-story homes a range of 4 to 11 Hz. Damping for the full structures is reported by these investigators to range from 2% to 10% of critical damping.

The Bureau of Mines study also reports natural frequencies for the response of midwalls. These range from 12 to 26 Hz. Damping is reported as ranging from 2% to 6%.

Sutherland et al. (1990) estimate the resonant frequencies of plaster ceilings to be in the range of approximately 13 to 15 Hz.

Also reported in the Bureau of Mines study is an assessment of damage thresholds based on measurements involving more than 350 buildings. Three levels of damage were defined as follows:

- | | |
|------------|--|
| Threshold: | Loosening of paint; small plaster cracks at joints between construction elements; lengthening of old cracks. |
| Minor: | Loosening and falling of plaster; cracks in masonry around openings near partitions; hairline to 3mm cracks (0 to 0.125 in); fall of loose mortar. |
| Major: | Cracks of several millimeters in walls; rupture of opening vaults; structural weakening; fall of masonry, e.g., chimneys, load support ability affected. |

Figure 4-2 depicts regression curves depicting the particle velocities required to produce each of the three damage levels as a function of vibration frequency. Notice that in the low frequency range two sets of curves are depicted. One set corresponds to wallpapered walls; the second corresponds to walls stripped of wallpaper, plaster walls and masonry. Figure 4-3 depicts the fit of a lognormal distribution to damage prediction for the combined data set **independent of vibration frequency**.

Based on the following set of assumptions, the criteria depicted in Figure 4-4 are proposed as safe vibration levels: safe vibration is interpreted to mean that interior cracking or other damage is unlikely. Structures are assumed to be sited on a **firm** foundation, to be no more than two stories, to have dimensions of typical residences, and wave trains are assumed to be no longer than a few seconds.

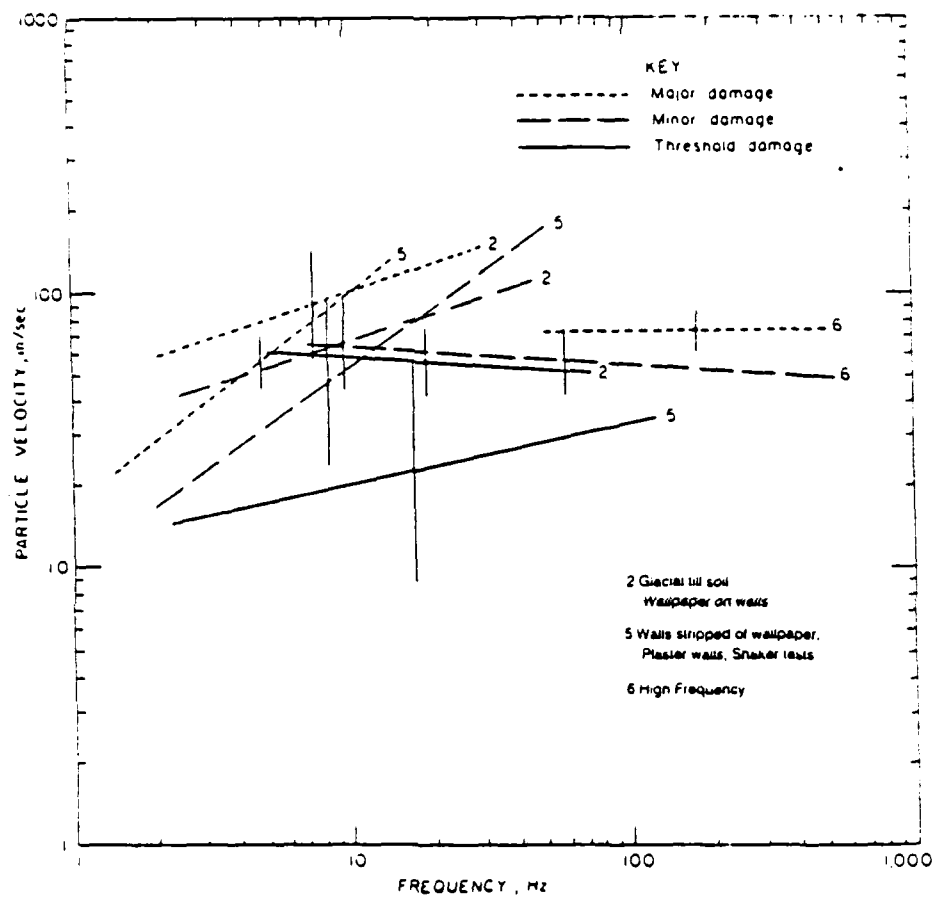


Figure 4-2. Particle Velocities Resulting in Damage (Siskind et al., 1980).

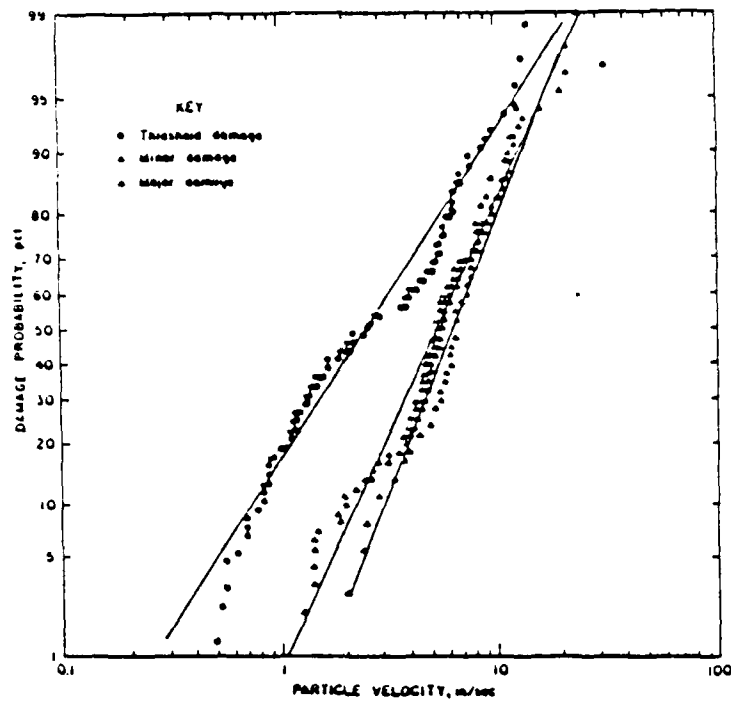


Figure 4-3. Probability Damage Analysis Summary (Siskind et al., 1980).

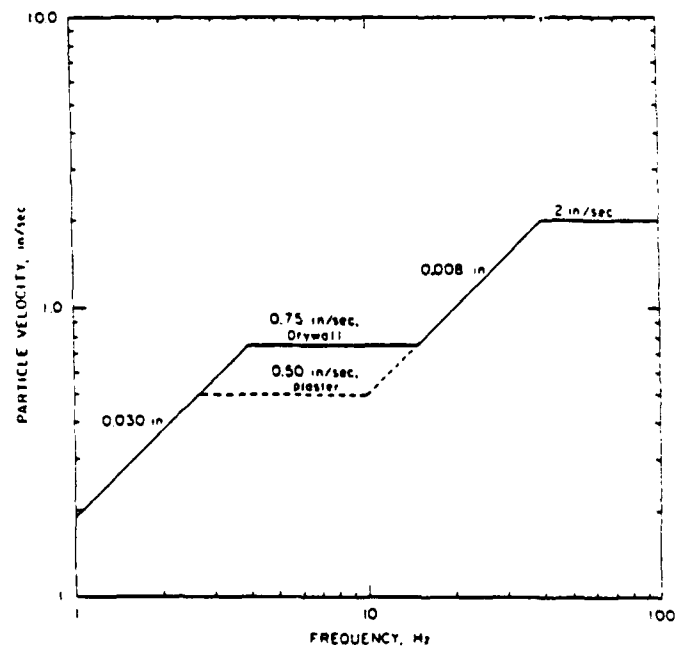


Figure 4-4. Safe Levels of Blasting Vibration for Houses Using a Combination of Velocity and Displacement (Siskind et al., 1980).

Other investigators have defined a variety of levels for damage. For example, an alternative set of criteria are the values listed in Table 4-1, reproduced from Siskind et al. (1980), which were originally published in Langefors and Kihlstrom (1963).

The Bureau of Mines study also provides some test results from a variety of sources which provide an indication of the vulnerability of foundations. Several investigators are quoted as having measured the threshold of damage to stone mortar and to concrete block walls at a particle velocity of between 3 and 4.5 in/sec. Minor damage is reported to have occurred at a particle velocity of 7 in/sec and major damage at a particle velocity of 10 in/sec. Poured concrete is reported to be considerably less vulnerable. The observed damage threshold was 10 in/sec. These damage thresholds are far in excess of any ground motions likely to be induced, even by resonant sonic boom-coupled Rayleigh waves.

Table 4-1. Damage Levels from Blasting.

Damage Effects	Peak Particle Velocity (in/sec)		
	Sand, gravel, clay, below water level; c=1,000-1,500 m/sec	Moraine, slate, soft limestone; c=2,000-3,000 m/sec	Granite, hard limestone, or diabase; c=4,500- 6,000 m/sec
No noticeable crack formation	0.71	1.4	2.8
Fine cracks and falling plaster threshold	1.2	2.2	4.3
Crack Formation	1.6	3.2	6.3
Severe Cracks	2.4	4.5	9.1

4.3 Unconventional Structures

Sutherland et al. (1990) assembled data characterizing resonant frequencies for a variety of unconventional structures. This study reports estimates of mean resonant frequency and 20 times the

standard deviation of the logarithm of the resonant frequency for each category of structures. By interpreting these data as describing a log normal distribution of -3σ to $+3\sigma$, ranges of frequencies will have the form of:

$$10^{\log(\text{Mean Resonant Frequency}) - 3 (\text{Std Dev Log(Resonant Frequency)})}$$

to

$$10^{\log(\text{Mean Resonant Frequency}) + 3 (\text{Std Dev Log(Resonant Frequency)})}$$

Mean reported resonant frequencies for historic buildings range from 12 Hz for brick buildings to 25 Hz for masonry stone buildings. The three-sigma limits calculated from Sutherland's et al. (1990) table by the formula indicated above are approximately 4 Hz on the low end (brick walls) to approximately 56 Hz (masonry stone walls). In the following material, the three-sigma limits are shown in parentheses after the mean. A mean resonant frequency of 10 Hz (4 to 24 Hz) is reported for a woodframe bridge.

Prehistoric structures are described as being either adobe or masonry stone structures. Resonant frequencies reported for these two types of structures are almost the same. The masonry/stone structures have mean resonant frequencies of 5.1 Hz (1.4 to 18.8 Hz); the adobe structures have mean resonant frequencies of 5.4 Hz (1.5 to 19.9 Hz).

Free-standing adobe walls are characterized by resonant frequencies in the range from 3 to 21 Hz; free-standing masonry walls are characterized by resonant frequencies in the 0.5 to 5 Hz range. Observed natural frequencies vary with the exact composition of the walls and the dimensions of the walls. Bariola and Sozen (1990) report the results of seismic tests of adobe walls. The measured natural frequencies were within the range reported by Sutherland et al. (1990). It is interesting to note that walls of comparable dimensions subjected to the same load histories exhibited similar natural frequencies, even when the adobe mixture was from widely separated geographical areas. Adobe walls which had been subjected to a single, simulated earthquake exhibited lower frequencies than new adobe walls.

Utility buildings are characterized as being concrete block, wood frame, or metal frame structures. The mean natural frequency reported for metal frame structures is 14 Hz (7.3 to 26.9 Hz).

for wood frame structures, 15 Hz (6.3 to 35.6 Hz) and for concrete block structures, 25 Hz (11.1 to 56.1 Hz).

Water wells and tanks are characterized by a mean resonant frequency of 25 Hz (3 to 200 Hz). A set of supplementary calculations indicates that sloshing in moderate size tanks will have a lower resonant frequency (0.1 to 2.5 Hz).

The only sensitive equipment for which resonant frequency was reported by Sutherland et al. (1990) are radio telescopes. These have been characterized as having a mean natural frequency of 5 Hz (2.6 to 9.6 Hz).

The Bureau of Mines study cites four sets of standards which relate to unconventional structures. The most stringent of these are the German vibration standards (DIN 4150). The standards are reportedly so strict that they are not enforced; moreover, no technical data support these standards. Esteves (1978) proposes safe vibration values in terms of pseudo-vector sum peak particle velocity, depending on the soil supporting the structure. For special cases such as historical monuments, hospitals, and very tall buildings, he proposes the values shown in Table 4-2.

Table 4-2. Safe Vibration Levels (Esteves, 1978).

Type of Soil	Peak Particle Velocity (in/sec)
Incoherent loose soils, soft coherent soils, rubble mixtures: $c < 1,000$ m/sec	0.10
Very hard to medium consistence coherent soils, uniform or well-graded sand: $c = 1,000$ - $2,000$ m/sec	0.20
Coherent hard soils and rock: $c > 2,000$ m/sec	0.40

Ashley (1976) recommends a limit of peak particle velocities of 0.30 in/sec for ancient and historic monuments. No adjustment factor is indicated for type of soil. While neither of these references presents supporting empirical data, they are reasonably consistent with each other.

Figure 4-5 presents vibration criteria for a variety of sensitive equipment and indicates that the vibration tolerance of this type of equipment is typically below the human perception threshold. Thus, buildings housing this type of equipment are typically specially designed to isolate this equipment from vibration. This vibration isolation would also protect such sensitive equipment from sonic boom-coupled seismic waves.

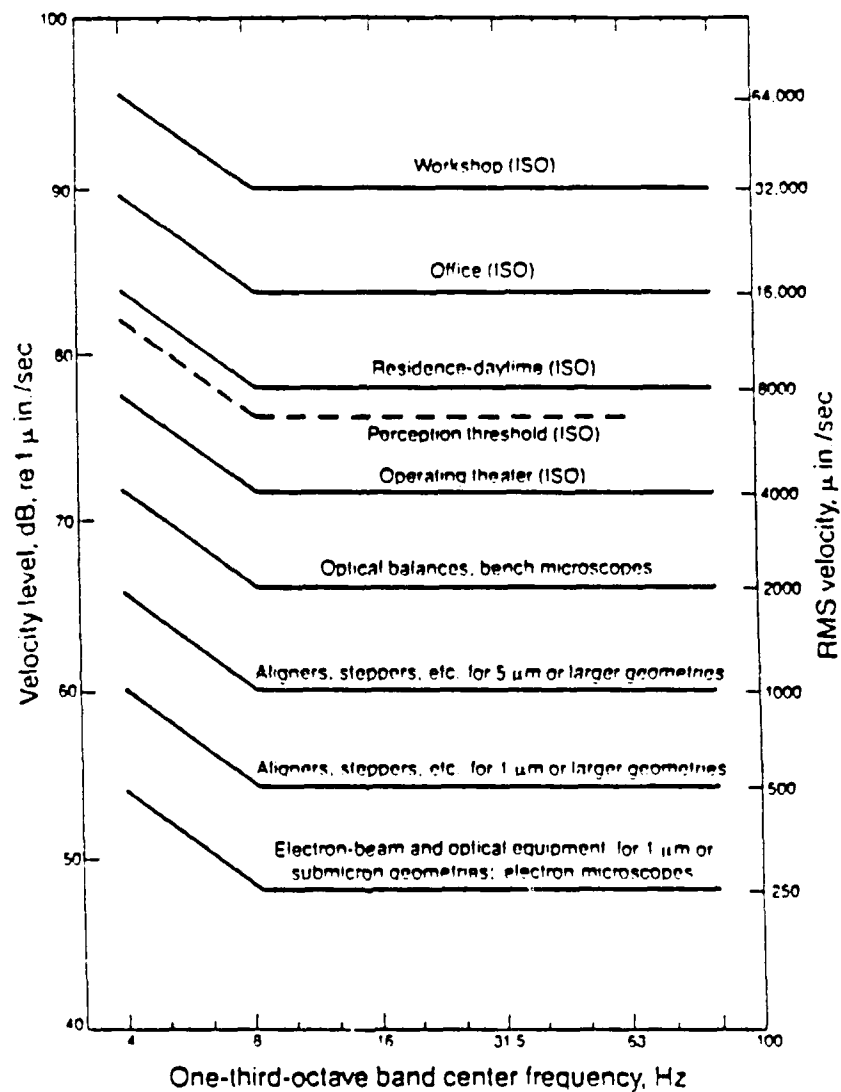


Figure 4-5. Vibration Criteria for Sensitive Equipment (Unger, 1985).

4.4 Human Tolerance

Completeness in evaluation of the effects of sonic boom coupled Rayleigh waves requires consideration of the effects of vibration on humans. Although the levels at which human annoyance is produced are lower than those associated with damage to structures, they are greater than vibration levels which affect sensitive equipment. Figure 4-6 depicts International Organization for Standardization (ISO) human vibration tolerance standards for vibrations exceeding 1 min duration. Figure 4-7 displays relationships developed in the Bureau of Mines report for human tolerance to vibration as a function of the duration of the vibration. Figures 4-8 and 4-9 depict the results of two alternative interpretations of exploratory research (Fidell et al., 1983) regarding the effect of repetitive exposures to vibration on human tolerance.

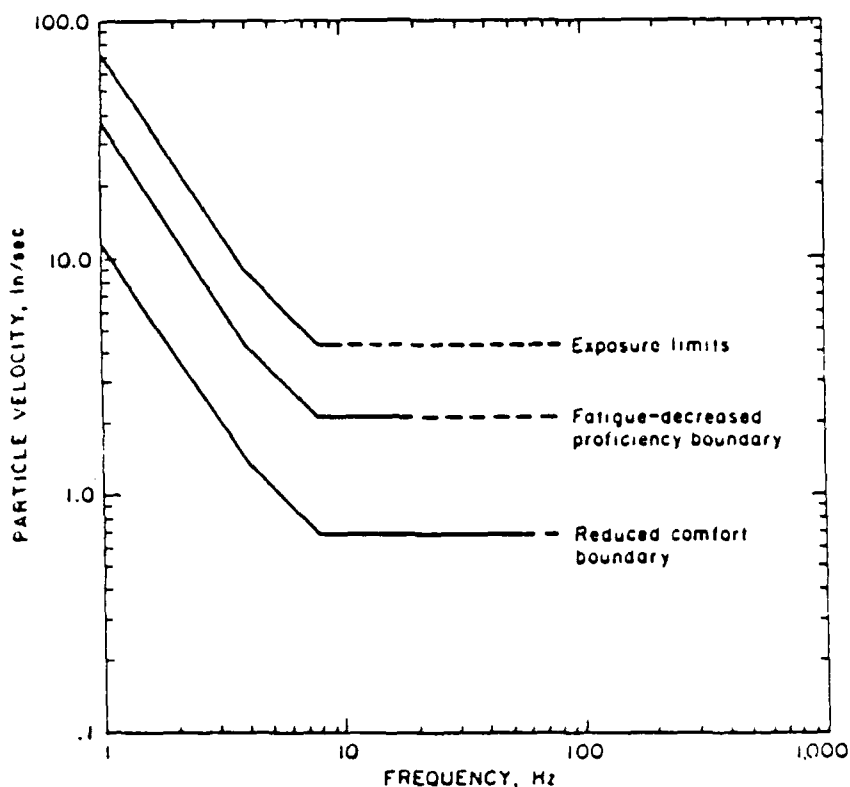


Figure 4-6. Human Tolerance Standards for RMS Vibrations Exceeding 1-Min Duration (Siskind et al., 1980).

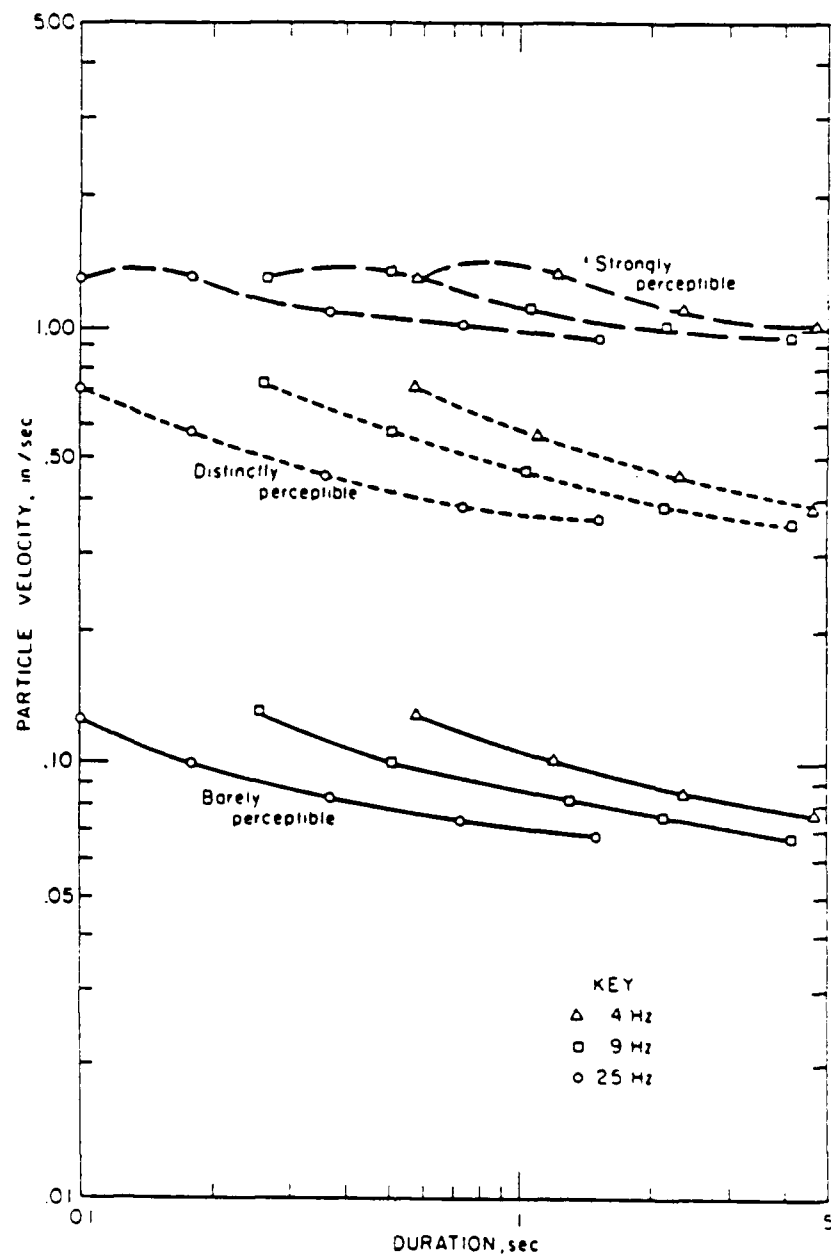


Figure 4-7. Human Response to Transient Vibration Velocities of Various Durations (Siskind et al., 1980).

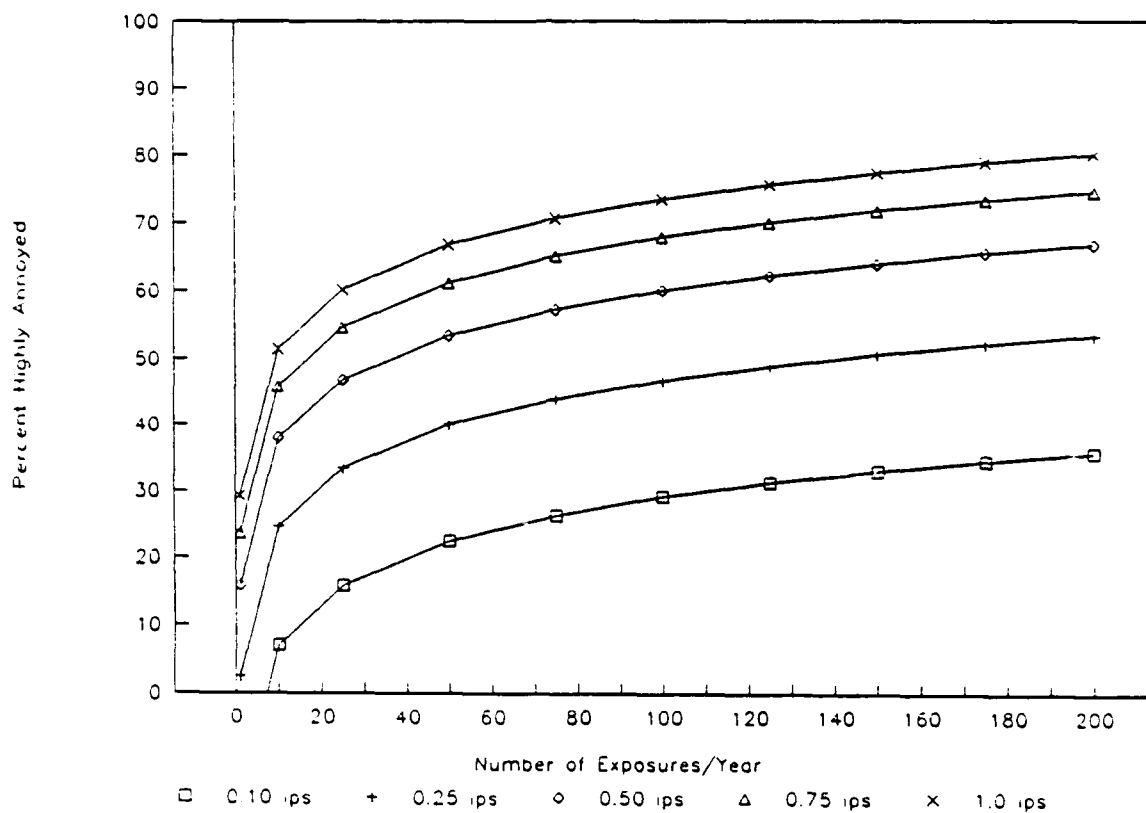


Figure 4-8. Tentative Relationship Between Annoyance and Number of Exposures to Blast Vibration Levels (Fidell et al., 1983).

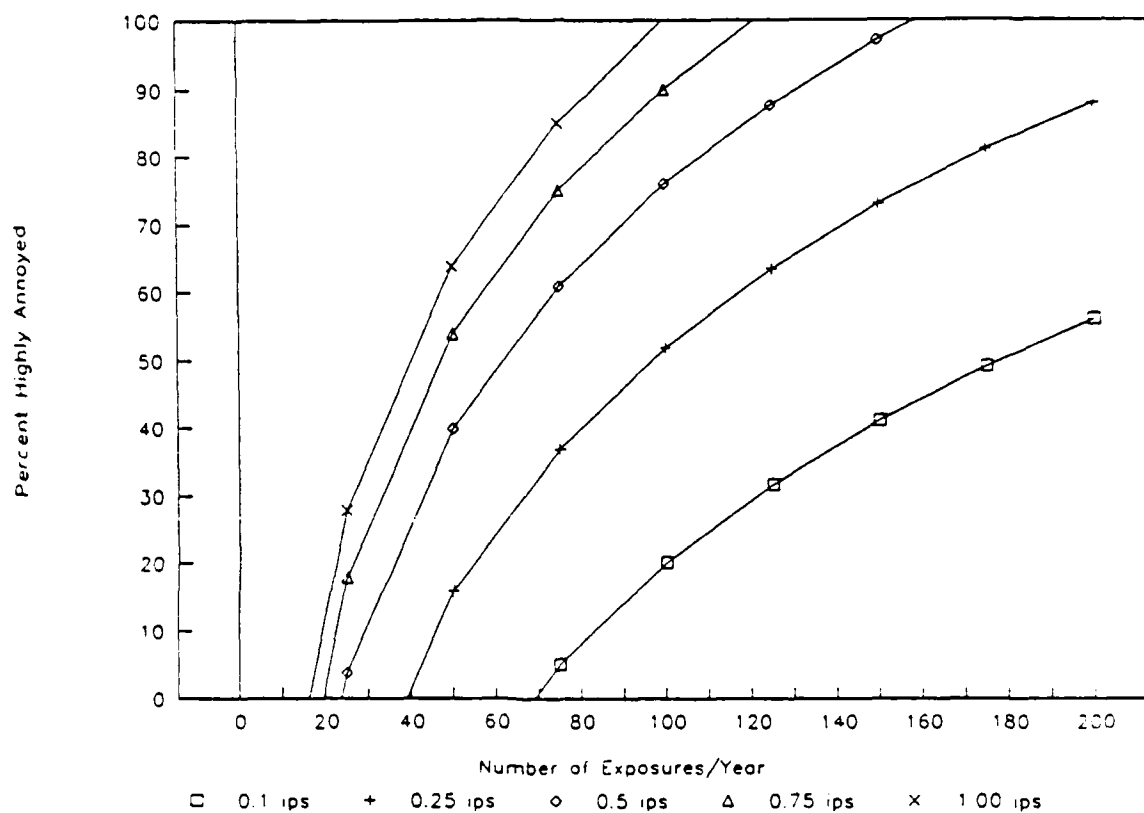


Figure 4-9. Alternative Relationship of Annoyance and Number of Exposures to Blast Vibration Levels (Fidell et al., 1983).

4.5 Summary

Rayleigh wave frequencies in the range of 1 to 10 Hz are expected to be most important based on typical structural response. Some structures or structural elements have higher resonant frequencies; most of these fall within the frequency band of 10 to 40 Hz. Isolated cases exist of higher resonant frequencies.

Levels of vibration which produce a potential damage threat or a source of annoyance vary significantly depending on soil type, frequency, and the item in question. For plaster and wallboard the damage threshold may be as low as a displacement of 0.03 in and a peak particle velocity of 0.2 in/sec for frequencies of 1 Hz. The vibration sensitivity decreases for higher frequencies. Levels as low as 0.1 in/sec have been proposed as a threshold of damage for historical monuments. While sensitive equipment has still lower thresholds, it is normally protected by vibration isolation techniques. Thus, each case must be considered in the context of its vibration isolation environment.

Building foundations are considerably less vulnerable and damage to these elements is very unlikely at the low levels of ground shaking induced by sonic boom-coupled Rayleigh waves, even for the resonant condition. Foundations are somewhat more vulnerable to ground failures, such as landslides. The potential for sonic boom-induced landslides is unknown at present.

5.0 CONCLUSIONS AND RECOMMENDATIONS

Review of USAF environmental assessment documents showed few public concerns directly related to the coupled Rayleigh wave phenomenon. Indirectly related concerns focused upon specific structural types that may be damaged, including archaeological sites, historical structures, old adobe buildings, water wells and storage tanks, house trailers, and radio telescopes. A top-level review of litigation and claims history found no pertinent litigation or claims regarding the sonic boom-coupled Rayleigh wave phenomenon.

Sonic boom-coupled Rayleigh wave resonance, where the carpet trace speed of the sonic boom matches the Rayleigh wave phase velocity, has been observed. The resonant condition requires a low-velocity surficial layer or waveguide. Lateral variability in geologic conditions that alters the resonant conditions prevents substantial amplification of the seismic energy in most cases. The strongest resonant coupling may occur where a laterally-uniform, low-velocity surface layer overlies a more competent (compacted soil or hard rock) high-velocity layer, forming a waveguide in which the seismic energy can be trapped and propagate with little attenuation. For a simple waveguide, the Rayleigh wave dispersion curve shows that the phase velocity varies rapidly over a very narrow frequency range. The resonant condition is relatively unaffected by variations in aircraft speed, but the resonant frequency is inversely proportional to the thickness of the waveguide and directly proportional to the seismic shear wave velocity in the waveguide.

Strong amplification of seismic waves from sonic boom coupling requires that the resonance condition be laterally persistent; the near-surface geological condition must remain uniform over distances of several seismic wavelengths, on the order of 1 km or more. Depositional environments most likely to provide such uniform sedimentary character are basin sediments such as flood plains, lake beds (both modern and ancient), and the basinward deposits of alluvial fans. Although weathering of bedrock outcrops may produce relatively thick layers of low-velocity material, the non-uniform nature of the weathering process and the non-uniform distribution of the bedrock materials diminish the likelihood that the sonic boom-coupled resonance condition would be achieved in these materials. Other low-velocity surficial deposits may experience resonant coupling over large distances, but attenuation of seismic energy by "leaking" out of the base of these imperfect waveguides reduces the potential for strong amplification. Ideal waveguides, with laterally-extensive, low-velocity surface

layers of uniform thickness overlying a hard, high-velocity substratum, provide the best opportunity for strong resonant coupling.

Porous, air-filled soils show greater seismic coupling to acoustic waves than predicted by simple acoustic impedance mismatch. Flooding or water saturation of the topsoil may decrease the likelihood of the resonant condition by increasing the seismic velocity, relative to air-filled porous sediments; yet saturation deeper in the sediment column may improve the likelihood of coupling because the pore fluid pressure acts to resist compaction, allowing the deeper layers to maintain low densities and seismic velocities.

Because surface-wave propagation within a waveguide is dispersive, with many different frequencies each associated with a particular phase velocity, there will be at least one particular frequency associated with the sonic boom carpet trace speed in general. If the near-surface geology has relatively high Rayleigh wave phase velocities, then only special maneuvers, such as the climbing or diving maneuvers that increase the carpet trace speed to high values, would cause the resonant condition. Significant portions of a large number of maneuvers--steady level flight, accelerated level flight, accelerated dives and climbs, decelerated climbs, and constant speed turns--produce trace speeds which are sufficiently constant over moderately significant distances to be favorable to Rayleigh wave resonance. In no case examined were steady trace velocities found in the neighborhood of a focus. Maneuver enhanced overpressures, however, can occur over sufficient distances with steady trace velocities.

For the sonic boom-coupled surface waves to be potentially damaging, the resonant sonic boom-coupled Rayleigh wave frequencies must be similar to that of structures in the area affected. Rayleigh wave frequencies in the range of 1 to 10 Hz are expected to be most important based upon typical structural response of houses and low-rise construction. Some structures or structural elements, such as midwalls and ceilings, have somewhat higher resonant frequencies; most of these fall in the frequency band of 1 to 40 Hz. Rayleigh wave frequencies of shallow, thin (1-m to 100-m thick), low-velocity (10 to 500 m/sec) soil layer waveguides overlap this band. Because the surface waves are coupled to the sonic boom, affected structures will be shaken by the seismic waves at the same time the airborne acoustic pressure pulses strike. Therefore, the combined effect of these two loadings should be considered.

Levels of vibration which produce a potential damage threat vary depending on soil type, frequency, and the item in question. For plaster and wallboard, the damage threshold may be as low as 0.03 in and a peak particle velocity of 0.2 in/sec for frequencies of 1 Hz; the vibration sensitivity decreases for higher frequencies. Levels as low as 0.1 in/sec have been proposed as a threshold of damage for historical monuments. While sensitive equipment has still lower thresholds, it is normally protected by vibration isolation techniques; each case must be considered in the context of its vibration isolation environment. Building foundations are much less vulnerable to seismic shaking; damage thresholds are greater than 3 to 4.5 in/sec.

Amplitudes of resonant sonic boom-coupled Rayleigh wave ground motions are unknown at present, although values measured in a few instances were significantly less than structural damage criteria (Goforth and McDonald, 1968). Strong resonant Rayleigh wave coupling in laterally uniform waveguides may exceed the lower damage thresholds for some structural types. The potential for resonant sonic boom-coupled Rayleigh waves triggering landslides or avalanches is unknown, but may be significant on unstable slopes.

5.1 Summary of Major Conclusions

Resonant sonic boom seismic coupling may be common because:

- Numerous realistic near-surface geologic conditions have Rayleigh wave phase velocities in the range of nominal sonic boom carpet trace speeds;
- Portions of most tactical supersonic flight maneuvers produce carpet trace speeds that match these Rayleigh wave phase velocities; and
- The Rayleigh wave frequencies at these phase velocities are in the range of the natural response frequencies of some types of structures.

Strong resonant coupling that could cause amplification of the ground motion to damaging levels is uncommon because:

- Near-surface geological conditions are laterally varying so that the resonant conditions change too rapidly for strong amplification of ground motion;
- Carpet trace speeds of supersonic maneuvers that produce focused, large overpressure, sonic booms vary rapidly so that the resonant condition is only locally met, and resonant amplification is diminished;
- Due to atmospheric perturbations, pressure signatures of real sonic booms vary significantly over short distances, even for level, non-accelerating flight conditions; and
- Sonic booms reach ground level in only a small proportion of supersonic flights, and these may miss geologic areas susceptible to the resonant condition.

Potential damage to structures due to sonic boom-coupled Rayleigh wave resonance may occur under special conditions because:

- Low-velocity seismic waveguides, where the sonic boom-coupled seismic energy is trapped and propagates with little attenuation allowing strong amplification to occur, may exist in SOAs;
- Resonant frequencies for these waveguides, which depend on the thickness and seismic velocity in the waveguide, may match the natural response frequencies of structures in the same area;
- Aircraft and carpet trace speeds have less effect on the surface wave resonance in a "perfect" waveguide so that most supersonic maneuvers could cause the resonant condition over significant distances; and
- Near-surface geologic conditions that constitute a seismic waveguide are known to exist.

Uncertainty in evaluating the potential for damage from sonic boom-coupled Rayleigh waves exists in:

- Estimating the amplitudes of ground motions that may be generated by the resonant coupling;
- Estimating the distance over which the uniform resonant coupling conditions must extend in order to get strong amplification;
- Measuring the lateral extent of uniform geologic conditions conducive to strong resonant coupling in the real earth; and
- Predicting the locations of real seismic waveguides in Supersonic Operating Areas.

5.2 Recommendations

An experimental program to measure the ground motions induced by resonant coupling in a "worst-case" geologic condition, such as a strong waveguide, could show that the amplitudes remain below even the strictest structural damage criteria. Such an experiment would, at least, provide a calibration of the theoretical calculations so that amplitudes in other geologic environments could be estimated.

A program to map areas affected by supersonic operations that may contain surficial deposits conducive to the resonant coupling at frequencies potentially damaging to structures could be accomplished based upon existing soils and other near-surface geologic maps. Relevant soil types and depositional environments as presented in this study could be delineated on maps of the SOAs. These maps could be used in environmental assessment documents or to plan future supersonic operations that would avoid areas where the resonant coupling might occur with resonant frequencies potentially damaging to structures. In addition, the potential for sonic boom-induced landslide or avalanche should be evaluated.

APPENDIX A - ANNOTATED BIBLIOGRAPHY

Seismo-Acoustics and Air-Coupled Rayleigh Waves

Battis, J. C., 1983, Seismo-acoustic effects of sonic booms on archeological sites, Valentine Military Operations Area: U.S. Air Force Geophysics Laboratory, Technical Report *AFGL-TR-83-0304*, ERP, No. 858, Hanscom AFB, Massachusetts, 36 pp.

Abstract--Seismo-acoustic recordings of sonic booms were made at two sites in the Valentine Military Operations Area (MOA). Each location was selected as representative of a class of significant archeological sites found within the MOA. These studies indicate that sonic booms are unlikely to cause damage to the archeological finds. The expected motions are, at worst, 8% of the limits set by strict blasting codes and comparable to velocities that could be produced by local earthquakes which have occurred in the Valentine area. At these levels of motion, competent rock will be unaffected by the transmission of seismic waves. The predicted velocity levels are unlikely to initiate either fracture or spalling in rocks. However, it is possible that in rocks where natural meteorological action has initiated these erosive mechanisms, the sonic boom induced motion could accelerate the processes to some small, and probably insignificant, degree.

Baron, M.L., H. H. Bleich & J. P. Wright, 1966, An investigation of ground shock effects due to Rayleigh Waves generated by sonic booms: NASA Contractor Report, *CR-451*, Weidlinger Consulting Engineers, New York, NY. 49 pp.

Abstract--Expressions are derived for the steady state vertical displacements produced at the surface of an elastic half-space by a line load of finite length, which moves with a constant velocity in a direction either parallel or perpendicular to its length. These expressions are used to estimate the response of structures to the seismic disturbances produced by a sonic boom which moves at speeds close to the speed of surface waves in the medium. Shock amplification factors for the accelerations imparted to the structure are obtained for a range of parameters. The results show that the accelerations produced at these speeds are generally quite small and that the resonance peak which occurs when the applied load moves with the surface wave speed is extremely narrow.

Cook, J. C. & T. T. Goforth, 1970, Ground motion from sonic booms: *Journal of Aircraft*, Vol. 7, pp. 126-129.

Abstract--To ascertain the degree of hazard to structures from sonic-boom-induced ground vibrations, seismic measurements were made under NASA support during a series of sonic boom tests in 1967 and 1968. The maximum ground vibration velocity observed was 340 $\mu\text{m/sec}$ at 90 Hz, corresponding to a sonic boom overpressure of 3.5 lb/ft², which is less than 1% of the structural damage threshold established experimentally by the U.S. Bureau of Mines and others, of 50,800 $\mu\text{m/sec}$. It is therefore very unlikely that any structural damage to slabs, foundations, wells, etc., can occur because of sonic booms. Incidental to the study, seismic precursor waves were observed which provide a possible basis for automatic warnings of approaching sonic booms, to reduce their startle effect.

Crowley, F. A. & H. A. Ossing, 1969, On the application of air-coupled seismic waves: Air Force Cambridge Research Laboratories, *Environmental Research Papers*, No. 302.

Abstract--Seismic measurements taken on Rogers Lake Playa, Edwards AFB, California, were prompted by a concern that ground vibrations excited by F-1 rocket engines might affect the role of playa cracking. These measurements relate to other USAF interests. Specifically, the note characterizes seismic waves excited by F-1 rockets, sonic booms, and atmospheric explosions to: (1) Playa landing areas; (2) Ground conditions affecting sonic booms and rocket firings sensed in buildings; (3) Detection of acoustic sources using seismic systems; (4) The playa's selective distortion of acoustic wave characteristics; and (5) Consideration of a playa seismic alarm system.

Donn, W. L., I. Dalins, V. McCarty, M. Ewing & G. Kaschak, 1971, Air-coupled seismic waves at long range from Apollo launchings: *Geophysics*, Vol. 26, pp. 161-171.

Abstract--Microphones and seismographs were colocated in arrays on Skidaway Island, Georgia, for the launchings of Apollo 13 and Apollo 14, 437 km to the south. Simultaneous acoustic and seismic waves were recorded for both events at times appropriate to the arrival of the acoustic waves from the source. Significant comparisons of the true signals are (1) the acoustic signal is relatively broadband compared to the nearly monochromatic seismic signal; (2) the seismic signal is much more continuous than the more pulse-like acoustic signal; (3) ground loading from the pressure variations of the acoustic waves is shown to be too small to account for the seismic waves; (4) the measured phase velocities of both acoustic and seismic waves across the local instrument arrays differ by less than 6% and possibly 3% if experimental error is included. It is concluded that the seismic waves are generated by resonant coupling to the acoustic waves along some 10 km of path on Skidaway Island. The thickness of unconsolidated sediment on the island is appropriate to a resonant ground wave frequency of 3.5 to 4 Hz, as observed. Under appropriate conditions, ground wave observations may prove more effective means of detecting

certain aspects of acoustic signals in view of the filtering of wind noise and amplification through resonance.

- Espinosa, A. F., P. J. Sierra & W. V. Mickey, 1968, Seismic waves generated by sonic booms: A geoacoustical problem: *Journal of the Acoustical Society of America*, Vol. 44, No. 4, pp. 1074-1082.

Abstract--Low and very low-frequency air-coupled seismic waves were efficiently generated on different occasions by jet fighter planes flying at high altitudes and at Mach numbers greater than 1.2. The experiments presented in this investigation were clearly recorded on a geophone array containing up to twelve short-period vertical component stations, and a singular station recording the transverse and radial type of motion. A higher-mode, seismic, coupled wave from sonic booms has been observed for the first time. Correlation is made between the acoustical signal registered at the microphone stations in Cape Kennedy and the first impulsive onset of the seismic waves recorded at the array setup. The seismic waves coupled from sonic booms are explained as a constructive interference phenomenon in the surficial ground layers. Fourier-transform techniques are applied to some of the seismograms, and some interesting features are delineated.

- Kanamori, H., J. Mori, D. Anderson, T. Heaton & L. Jones, 1989, Seismic response of the Los Angeles basin to the shock wave caused by the Space Shuttle Columbia: *Transactions of the American Geophysical Union*, Vol. 70, No. 43, pp. 1191-2.

Abstract--Shock waves generated by the Space Shuttle Columbia on its return to Edwards Air Force base on August 13, 1989, were recorded by the southern California Seismic Network. The arrival times can be best explained with Mach cones propagating N40E across the Los Angeles basin. From the propagation velocity of the Mach cone and its shape, we determined the velocity and the altitude of the Space Shuttle to be 800 m/sec (Mach 2.35), and about 20 km respectively. The seismograms recorded at the stations in the Los Angeles basin exhibit reverberations before and after the shock wave, while those from stations outside the basin show no reverberations. The broadband record obtained at the IRIS-TERRAscope station at Pasadena shows a distinct pulse having a period of about 3 sec which arrived 12.5 sec before the shock wave. The distinct onset, the particle motion direction and the arrival time of this pulse indicate that this pulse originated from a point near downtown Los Angeles. This pulse is followed by shorter period reverberations which have spectral peaks at 0.76, 1.17, 1.62, and 2.00 Hz. The reverberations can be interpreted as the response of the Los Angeles basin to the shock wave. A simple calculation using the Thomson-Haskell method shows that the observed spectrum at frequencies higher than 1 Hz is consistent with a soft superficial layer with a two-way P-wave travel time of about 2 sec.

Press, F. & W. M. Ewing, 1951a, Ground roll coupling to atmospheric compressional waves: *Geophysics*, Vol. 16, pp. 416-430.

Abstract--A theoretical treatment of ground roll originating from air shots and hole shots is given. It is shown that coupling of ground roll to compressional waves in the atmosphere exists for both air shots and hole shots. Experimental data obtained in the field are in excellent agreement with theoretical results namely, that the effective coupling exists for surface waves whose phase velocity is equal to the speed of sound in air. In regions where Rayleigh wave velocities vary with period due to layering in such a way that they are less than the speed of sound in air for short periods and exceed this value for longer periods, this coupling gives rise to a unique surface wave pattern on seismic records. It is shown that body wave and surface wave character is almost independent of charge elevation in the range from 0 (on the ground) to 30 feet. In a reciprocal manner ground roll from hole shots was recorded with air microphones as predicted by the theory.

Press, F. & W. M. Ewing, 1951b, Theory of air-coupled flexural waves: *Journal of Applied Physics*, Vol. 22, pp. 892-899.

Abstract--The theory of air-coupled flexural waves in a floating ice sheet is derived for the case of an impulsive point source situated either in the air or in the water. It is found that new branches are introduced to the dispersion curve of flexural waves as a result of coupling to compressional waves in the atmosphere. Experimental data are briefly reviewed.

Press, F. & J. Oliver, 1956, Model study of air-coupled surface waves: *Journal of the Acoustical Society of America*, Vol. 27, pp. 43-46.

Abstract--Flexural waves generated in a thin plate by a spark source are used to investigate properties of air-coupled surface waves. Both ground shots and air shots are simulated in the model. Effects of source elevation, fetch of air pulse, and cancellation by destructive interference are studied.

Raspet, R. & G. E. Baird, 1988, The acoustic surface wave above a complex impedance ground surface: *Journal of the Acoustical Society of America*, Vol. 85 (2), pp. 638-640.

Abstract--A surface wave like term arises in the analysis of spherical wave propagation above a complex impedance plane. Whether this wave is a true independently propagating surface wave, or a reaction to the incident air wave, has been the subject of discussion for a number of years.

In this article, it is demonstrated that this term is a true surface wave that can exist independent of the body wave in air.

Sabatier, J. M., H. E. Bass & L. N. Bolen, 1986, Acoustically induced seismic waves: *Journal of the Acoustical Society of America*, Vol. 80 (2), pp. 646-649.

Abstract--When an airborne acoustic wave is incident at the ground surface, energy is coupled into the ground as seismic motion. In a previous publication [Sabatier et al., J. Acoust. Soc. Am. 78, 1345-1352 (1986)] the ground surface was modeled as an air-filled poroelastic layer overlying a semi-infinite, nonporous elastic substrate. In this work, the model is extended to include calculations of the normal seismic transfer function (ratio of the normal soil particle velocity at a depth d to the acoustic pressure at the surface). Measurements of the seismic transfer function for three sites are considered and compared to the predicted values. Generally good agreement between theory and experiment is achieved by best fits assuming the soil or seismic attenuation, which is accomplished by specifying the ratio of the imaginary to real part of the measured seismic P - and S -wave speeds. The seismic transfer functions quite typically exhibit minima and maxima which are associated with the seismic layering of the ground surface. Typical layer depths are 1-2 m. An analytical expression predicting the location of these maxima is offered based on hard substrate and the experimental and theoretical comparisons are reasonable.

Sabatier, J. M. & H. E. Bass, 1986, On the location of frequencies of maximum acoustic-to-seismic coupling: *Journal of the Acoustical Society of America*, Vol. 80 (4), pp. 1200-1202.

Abstract--Measurements of the acoustic-to-seismic transfer function (ratio of the normal soil particle velocity at a depth d to the acoustic pressure at the surface) for outdoor ground surfaces quite typically reveal a series of maxima and minima. In a publication (Sabatier et al., J. Acoust. Soc. Am. 80, 646-649 [1986]), the location and magnitude of these maxima are measured and predicted for several outdoor ground surfaces using a layered poroelastic model of the ground surface. In this paper, the seismic transfer function for a desert site is compared to the seismic transfer function for holes dug in the desert floor which were filled with pumice (volcanic rock). The hole geometry was rectangular and the hole depths varied from 0.25-2.0 m. The P - and S -wave speeds, densities, porosities, and flow resistivities for the desert floor and pumice were all measured. By varying the hole depth and the fill material, the maxima in the seismic transfer function can be shifted in frequency and the locations of the maxima compare reasonably with that of a hard-backed layer calculation. The area or extent of the acoustic-to-seismic coupling for pumice was determined to be less than 1 m².

Sabatier, J. M. & R. Raspet, 1988, Investigation of possibility of damage from the acoustically coupled seismic waveform from blast and artillery: *Journal of the Acoustical Society of America*, Vol. 84, pp. 1478-1482.

Abstract--This article examines the source of ground vibrations in regions adjacent to artillery fire or explosive operations. Measurements have been performed to evaluate the possibility of damage from high levels of ground-borne vibration in the vicinity of residential homes. The result of these measurements demonstrates that the acoustically coupled seismic wave is much larger than the directly coupled seismic wave from large scale impulsive sources. The theory of acoustic-to-seismic coupling is extended to impulsive sources, in order to investigate the damage potential of the acoustic-to-seismic coupled wave with respect to the airborne wave. The results of the theory are compared to controlled measurements made using a small scale impulsive source. In addition, the theory and experiment are shown to be in good agreement with the large scale impulsive source with reasonable assumed values of the seismic velocities and layer depths. The theory is used to develop the acoustic-to-seismic coupling ratio for a typical blast wave over the expected range of wave speeds and porosities normally encountered. Worst-case scenarios are developed. It is demonstrated that it is unlikely that damage will occur to houses due to the acoustically coupled seismic wave unless the acoustic pulse pressure exceeds 162 dB.

Weber, G., 1972, Sonic boom exposure effects II.1: Structures and terrain: *Journal of Sound and Vibration*, Vol. 20, pp. 505-509.

Abstract--Effects on structures due to pressure waves from explosions and guns have been known and studied for a long time. Experience has shown that peak overpressures from 5 to 15 kN/m² might crack panes and cause superficial damage to houses. The pressure waves from supersonic aircraft with peak overpressures in the order of 50-150 N/m² would thus seem to be too low to create structural damage. Nevertheless, a growing number of damage claims have been recorded. Extensive data on sonic boom damage have now been accumulated from many investigations which have taken place over the past ten years. Available data show some features which are relatively easy to define and attempts are made in this document to make conclusive statements concerning sonic boom exposures and the occurrence of damage on structures. In many areas, where it is not easy to obtain adequate data, suggestions are made concerning suitable research. Three general sets of parameters determine the effect of sonic booms on structures and terrain: (i) the generation; (ii) the propagation of shock waves; (iii) the characteristics of the structures. The first two of these parameters are better known than the third. If the specific aircraft design, flight and weather conditions are known, the free field pressure wave characteristic can be predicted. In following the effect of sonic booms on topographical features and ground motion effects on structures will be evaluated and then the structural parameters will be discussed.

Earthquake Strong-Motion

Bard, P.-Y., M. Campillo, F. J. Chavez-Garcia & F. Sanchez-Sesma, 1988, The Mexico earthquake of September 19, 1985--A theoretical investigation of large- and small-scale amplification effects in the Mexico City Valley: *Earthquake Spectra*, Vol. 4, No. 3, pp. 609-633.

Abstract--The linear, large-scale and small-scale amplification effects in the Mexico City valley, related to both the surficial clay layer and the underlying thick sediments, are investigated with 2-dimensional (2D) models and compared with the results of simple 1-dimensional (1D) models. The deep sediments are shown to be responsible, on their own, for an amplification ranging between 3 and 7, a part of which is due to the 2D effects in case of low damping and velocity gradient. This result is consistent with the observed relative amplification around 0.5 Hz at CU stations with respect to TACY station. The amplification due to the clay layer is much larger (above 10), and the corresponding 2D effects have very peculiar characteristics. On the one hand, the local surface waves generated on any lateral heterogeneity exhibit a strong spatial decay, even in case of low damping (2%), and the motion at a given site is therefore affected only by lateral heterogeneities lying within a radius smaller than 1 km. On the other hand, these local 2D effects may be extremely large, either on the very edges of the lake bed zone, or over localized thicker areas, where they induce a duration increase and an overamplification. The main engineering consequences of these results are twofold: i) microzoning studies in Mexico City should take into account the effects of deep sediments, and ii) as the surface motion in the lake bed zone is extremely sensitive to local heterogeneities, 1D models are probably inappropriate in many parts of Mexico City.

Celebi, M., J. Prince, C. Dietel, M. Onate & G. Chavez, 1987, The culprit in Mexico City--Amplification of motions: *Earthquake Spectra*, Vol. 3, No. 2, pp. 315-328.

Abstract--Mexico City has repeatedly suffered from the long-distance effects of the earthquakes that originate as far away as the subduction trenches near the Mexican Pacific Coast. The Michoacan, Mexico earthquake of 19 September 1985 was no exception and caused extensive damage to property and numerous loss of lives. The unique subsurface condition resulting from the historical lake bed has distinct resonant low frequencies around 0.5 Hz. The strong earthquake motions from long distances as well as the locally originating weak motions cause large amplifications at resonant low frequencies in the subsurface environment of Mexico City lake bed. In this paper, the resonant frequencies and associated amplifications of motions in Mexico City are quantified in terms of spectral ratios using 19 September 1985 strong-motion data and weak motions recorded in January, 1986. These ratios confirm that the amplifications of motions at resonant frequencies due to the subsurface conditions is indeed the culprit.

Lermo, J., M. Rodriguez & S. K. Singh, 1988, The Mexico earthquake of September 19, 1985-- Natural period of sites in the Valley of Mexico from microtremor measurements and strong motion Data: *Earthquake Spectra*, Vol. 4, No. 4, pp. 805-834.

Abstract--The period at which peak in the microtremor Fourier velocity spectra occurs in the transition and lake bed zones of the valley of Mexico is found to be the natural period of the site. These periods in the valley are compiled from the microtremor measurements carried out by Instituto de Ingenieria, UNAM and scientists from Japan (for a total of 181 sites). Using this data and the natural periods estimated from strong motion recordings (36 sites), an isoperiod contour map of the valley of Mexico is presented. This map may be useful in future design of important structures.

Romo, M. P., A. Jaime & D. Resendiz, 1988, The Mexico earthquake of September 19, 1985-- General soil conditions and clay properties in the Valley of Mexico: *Earthquake Spectra*, Vol. 4, No. 4, pp. 731-752.

Abstract--We present and discuss the results of resonant column and cyclic triaxial tests on clay samples obtained from different sites within the Lake zone in the Valley of Mexico. Of particular interest are the nearly elastic behavior and low damping ratio even for shear strain amplitudes as high as 0.3 (%). A hyperbolic model reproduces adequately well the resulting shear modulus vs strain curves. Degradation of shear modulus caused by load repetition is negligible for strains lower than about 1 (%) but increases significantly for higher strains. A power-type expression fits well the modulus degradation vs number of cycles curves. Results from static triaxial tests indicate that for compression stress paths the induced pore water pressure is uniquely related to axial strains. Analyses of ground motions show that one dimensional wave propagation models may be used to predict free field seismic motions in most parts of the Lake zone.

Rukos, E. A., 1988, The Mexico earthquake of September 19, 1985--Earthquake behavior of soft sites in Mexico City: *Earthquake Spectra*, Vol. 4, No. 4, pp. 771-786.

Abstract--From the September 19, 1985 earthquake there are several acceleration records for the soft (lake bed) sites in Mexico City. One-dimensional propagation models of the incident seismic accelerations incorporate the wave propagation profiles at three of those sites. The undamped computed surface acceleration spectra compare well with the recorded ones for two sites. The other one does not produce adequate results, which is probably due to incomplete information on the shear wave velocities. Further investigation with the site impulse function indicates that the surface accelerations during the September 19, 1985 event had a frequency content determined, to a certain extent, by the natural periods of the site. Direct inspection of the

recorded spectra for the September 19, 1985 earthquake at the studied sites shows that the relation between spectral periods corresponds to the closed form solution of a homogeneous layer with a fixed base. This relation may be different for other earthquakes recorded at these sites.

Sanchez-Sesma, F., S. Chavez-Perez, M. Suarez, M. A. Bravo & L. E. Perez-Rocha, 1988. The Mexico earthquake of September 19, 1985--On the seismic response of the Valley of Mexico: *Earthquake Spectra*, Vol. 4, No. 3, pp. 569-589.

Abstract--In order to explain damage and observed ground motions in Mexico City during the 1985 Michoacan earthquake, simultaneous consideration must be given to source, path, and site conditions, which is clear from teleseismic records and local vertical displacements. Incident waves had an important part of energy in the frequency band of 0.3-1 Hz. Damage distribution and observed motion in the lake bed zone cannot be satisfactorily explained using 1-dimensional theory. The effects of lateral irregularities are required. To assess its effects we describe the stratigraphic setting of the valley and discuss some features of damage distribution with results for 1- and 2-dimensional wave propagation models. These are useful to establish on quantitative basis the importance of lateral heterogeneity.

Seed, H. B., H. M. P. Romo, J. I. Sun, A. Jaime & J. Lysmer, 1988. The Mexico earthquake of September 19, 1985--Relationships between soil conditions and earthquake ground motions: *Earthquake Spectra*, Vol. 4, No. 4, pp. 687-729.

Abstract--Comparisons are presented between the characteristics of ground motions at five sites underlain by clay at which ground motions were recorded in Mexico City in the earthquake of September 16, 1985 and for which analyses of ground response have been made, based on the measured properties of soils and the motions recorded on hard formations at the National University of Mexico. It is shown that the ground response in areas of Mexico City underlain by clay is extremely sensitive to small changes in the shear wave velocity of the clay; it is suggested that a probabilistic approach which allows for uncertainties in shear wave velocity measurements and in the characteristics of the motions on the hard formations is desirable to assess these effects of local soil conditions on the characteristics of ground motions likely to develop at sites underlain by soft clays. The use of these procedures also provides a useful basis for estimating the general nature of the ground motions in the extensive heavy damage zone of Mexico City in the 1985 earthquake.

Singh, S. K., J. Lermo, T. Dominguez, M. Ordaz, J. M. Espinosa, E. Mena & R. Quaas, 1988. The Mexico Earthquake of September 19, 1985--A study of amplification of seismic waves in the Valley of Mexico with respect to a hill zone site: *Earthquake Spectra*, Vol. 4, No. 4, pp. 653-673.

Abstract--Since the installation of an extensive digital strong motion array by Fundacion Javier Barros Sierra in 1987, three moderate earthquakes have been recorded by the array and by the accelerographs operated by Instituto de Ingenieria, UNAM. Using this new data and results from the analysis of previous accelerograms we present spectral ratios at 40 sites in the valley of Mexico with respect to a hill zone site in Ciudad Universitaria (CU). Clear evidence for nonlinear behavior of the clay is found at Central de Abastos Oficina (CDAO) site during the great Michoacan earthquake ($M_s=8.1$). At four other lake bed sites this behavior is not seen, either because none occurred or because of poorer quality of data. The spectral ratio at a given site appears to be roughly independent of magnitude (except, perhaps, during great earthquakes when lake bed sites may behave nonlinearly), azimuth, and depth of earthquakes with epicenters ≥ 200 km from the city. On the lake bed sites of the valley the relative amplification (RA) varies between 8 and 56 and the natural period lies between 1.4 to 4.8 sec. Relative amplification maps at periods centered at 3, 2.5, 2, 1.5, and 1 seconds are presented. The area where severe damage and collapse of buildings in the city was concentrated during the Michoacan earthquake correlates well with the area with $RA \geq 14$ in the period range of 1.75 to 2.75 sec.

Geology and Soils Information

Bassett, A. M., D. H. Kupfer & F. C. Barstow, 1959, Core logs from Bristol, Cadiz, and Canby Dry Lakes, San Bernardino County, California: U.S. Geological Survey, Geologic Investigations in the Mojave Desert and Adjacent Region, California, *Bulletin 1045-D*, pp. 97-138.

A detailed description of cores from a chain of three dry lake basins.

Benda, W. K., R. C. Erd & W. C. Smith, 1960, Core logs from five test holes near Kramer, California: U.S. Geological Survey, Geologic Investigations in the Mojave Desert and Adjacent Region, California, *Bulletin 1045-F*, pp. 319-393.

Detailed logs of drill cores of Quaternary alluvium and Tertiary colemanite-bearing sediments--*Abstract*--"In 1957, five test holes were drilled near Kramer, Calif., in the western Mojave Desert, for the U.S. Geological Survey. The drill sites are in topographic basins where gravimetric and geologic surveys indicated the presence, beneath alluvium, of a thick section of Quaternary and Tertiary sedimentary and volcanic rocks. Two holes, which were deeper tests at sites drilled in 1954, cored only silts, sands and gravel: Four Corners test hole 1 was drilled in sec. 20, T. 10 N., R. 6 W., to a depth of 3,500 feet. Four Corners test hole 2, in sec. 5, T. 10 N., R. 8 W., was drilled to 2,328 feet. Three holes which were drilled at new sites north of Kramer Junction, the intersection of U.S. Highways 395 and 466 and locally known as Four Corners, penetrated colemanite-bearing sediments. The location and total depth of these holes are as follows: Four

Corners test hole 3, sec. 18, T. 11 N., R. 6 W., depth 2,568 feet; Four Corners test hole 4, near the north edge of sec. 30, T. 11 N., R. 6 W., depth 3,500 feet; Four Corners test hole 5, near the south edge of sec. 30, depth 1,604 feet. The sections of rocks penetrated in these 3 holes are similar. In each, the colemanite is in fine-grained sediments; these lie below sands and gravel, which are about 600 to 800 feet thick, and are underlain by sandstones and conglomerates. Colemanite is most abundant in the cores from Four Corners test hole 5, particularly in the 76 feet of core recovered between depths of 1,051 and 1,131 feet. Chemical analysis indicates that in this section of core the average content of B_2O_3 is above 14%. In addition to colemanite, the cores contain sulfides of arsenic, an unusual iron sulfide, and zeolites. This mineral content of the colemanite-bearing sediments north of Kramer Junction (Four Corners), together with the general lithology of the lake beds and the occurrence of the sediments as a tilted section of beds below sands and gravel, supports correlation with the upper or marginal parts of the borate-bearing sediments at the Kramer borate mining district, which have similar features. There is, however, no evidence that any beds are exactly equivalent in age."

Bortugno, E. J. & Spittler, T. E., 1986, Geologic map of the San Bernardino Quadrangle: California Division of Mines and Geology, Regional Geologic Map Series, *Map No. 3A*, Scale 1:250,000.

Cohen, P., 1963, Specific-yield and particle-size relations of Quaternary alluvium, Humboldt river valley, Nevada: U.S. Geological Survey, Contributions to the Hydrology of the United States, *Water-Supply Paper 1669-M*, 24 pp.

Cooley, M.E., 1973a, Map showing distribution and estimated thickness of alluvial deposits in the Tucson area, Arizona: U.S. Geological Survey, Miscellaneous Investigations Series, *Map I-844-C*, Scale 1:250,000.

Cooley, M.E., 1973b, Map showing distribution and estimated thickness of alluvial deposits in the Phoenix area, Arizona: U.S. Geological Survey, Miscellaneous Investigations Series, *Map I-845-C*, Scale 1:250,000.

Dickey, D. D., 1957, Core logs from two test holes near Kramer, San Bernardino County, California: U.S. Geological Survey, Geologic Investigations in the Mojave Desert and Adjacent Region, California, *Bulletin 1045-B*, pp. 63-79.

Detailed logs of drill cores of Quaternary and Tertiary sediments--*Abstract*--"Between July 1954 and May 1955 two test holes were drilled near Kramer, Calif., on the Mojave Desert. Four Corners test hole 1 was drilled in sec. 20, T. 10 N., R. 6 W., San Bernardino base line and meridian, to a depth of 1,561 feet in a basin filled with Quaternary and Tertiary sediments. The

core is predominantly sand and conglomerate composed of mostly unweathered quartz monzonite debris. Four Corners test hole 2 was drilled in sec. 5, T. 10 N., R. 8 W., in a separate sediment-filled basin. The core from this hole is less consolidated and more weathered. It is predominantly clay, silt, sand, and gravel composed of quartz monozonitic and volcanic material. Detailed logs of the cores are given in this report."

Dohrenwend, J. C., 1982, Surficial geology, Walker Lake 1° by 2° Quadrangle, Nevada-California: U.S. Geological Survey, Miscellaneous Field Studies, *Map MF-1382-C*, Scale 1:250,000.

Fernald, A. T., G. S. Corchary & W. P. Williams, 1968, Surficial geologic map of Yucca Flat, Nye and Lincoln Counties, Nevada: U.S. Geological Survey, Miscellaneous Geologic Investigations, *Map I-550*, Scale 1:48,000.

Haines, D. V., 1959, Core logs from Searles Lake, San Bernardino County, California: U.S. Geological Survey, Geologic Investigations in the Mojave Desert and Adjacent Region, California, *Bulletin 1045-E*, pp. 139-317.

Detailed logs of drill cores of Quaternary evaporites and sediments--*Abstract*--"Forty-one drill holes in the saline deposit on Searles Lake, San Bernardino County, Calif., were cored and logged. Drill holes averaged about 100 feet in depth; the majority are located around the margins of the dry lake. The saline deposit consists of an upper salt body about 39 square miles in area, of which 12 square miles are exposed in the central part of the lake, and a lower salt body of approximately the same areal extent found at greater depth. The 2 salt bodies are separated by a seam of clay or marl averaging about 12 feet thick. Isopach maps show the salt bodies are slightly elongated to the north; maximum thicknesses of the upper and lower salt bodies are 95 and 54 feet, respectively. Core logs, in written and graphic form, show the chief minerals of the saline bodies are halite, trona, hanksite, borax, and burkeite; relatively minor quantities of 13 additional minerals are described. The 41 drill-hole logs are shown graphically in columnar sections which give thicknesses, mineralogy, and mineral percentages; 15 representative written logs are published in full."

Jennings, C. W., 1977, Geologic Map of California: California Division of Mines and Geology, California Geologic Data Map Series, *Map No. 2*, Scale 1:750,000.

Madsden, B. M., 1970, Core logs of three test holes in Cenozoic lake deposits near Hector, California: U.S. Geological Survey *Bulletin 1296*.

Abstract--"Cores and cuttings from three holes drilled into upper Cenozoic lake deposits in the Mojave Desert near Hector, Calif., were relogged and examined in detail mineralogically. An evaporite section penetrated by one of the holes consists of beds of laminated and massive anhydrite rock, mudstone, claystone, calcite rock, sandstone, and colemanite rock. Colemanite ($\text{Ca}_2\text{B}_6\text{O}_{11} \cdot 5\text{H}_2\text{O}$) is the only borate mineral present except for a few blebs of howlite. A minor amount of celestite occurs throughout the core. Beds of tuff in the cored intervals have been altered to clay minerals or the zeolites clinoptilolite, analcime, erionite, and chabazite."

Muessig, S., G. N. White & F. M. Byers, Jr., 1957, Core logs from Soda Lake, San Bernardino County, California: U.S. Geological Survey, Geologic Investigations in the Mojave Desert and Adjacent Region, California, *Bulletin 1045-C*, pp. 81-96.

A description of the cores from a desert basin and an interpretation of the late Pleistocene physical history of the basin and contiguous areas.

Smith, G. I. & W. P. Pratt, 1957, Core logs from Owens, China, Searles, and Panamint Basins, California: U.S. Geological Survey, Geologic Investigations in the Mojave Desert and Adjacent Region, California, *Bulletin 1045-A*, pp. 1-62.

Detailed logs of drill cores of Quaternary lake sediments--*Abstract*--"Detailed logs of drill cores are presented in this report. The drill cores are of sediments from four basins that were occupied during the Pleistocene by a continuous chain of lakes. Owens Lake basin (one hole, 920 feet) contains fine-grained sediments and includes locally many diatoms and ostracodes. China Lake basin (one hole, 700 feet) contains silt- to sand-sized clastic sediments and some calcite and gaylussite; a few diatoms, ostracodes, and mollusks are present. Searles Lake basin (one hole, 875 feet) contains many layers of gaylussite- or pirssonite-bearing sediments intercalated with beds of halite, trona, and lesser amounts of other minerals peculiar to Searles Lake; the top 120 feet consists of thicker evaporite bodies with a more complex mineralogy. Panamint basin (three holes, 500, 375, 995 feet) contains clastic deposits ranging from clay to gravel, a small amount of gypsum, anhydrite, a trace of bassanite, and thick bodies of halite in the basin center; a few diatoms and ostracodes are present."

Stewart, J. H. & J. E. Carlson, 1978a, Geologic Map of Nevada: U.S. Geological Survey, Scale 1:500,000.

Stewart, J. H. & J. E. Carlson, 1978b, Sources of data for geologic map of Nevada: U.S. Geological Survey, *Map MF-930*, Scale 1:1,000,000.

- Williams, T. R. & M. S. Bedinger, 1984, Selected geologic and hydrologic characteristics of the Basin and Range province, western United States, Pleistocene lakes and marshes: U.S. Geological Survey, Miscellaneous Investigations Series, *Map I-1522-D*, Scale 1:2,500,000.
- Witkind, I. J., W. R. Hemphill, C. L. Pillmore & R. H. Morris, 1960, Isopach mapping by photogeologic methods as an aid in the location of swales and channels in the Monument Valley area, Arizona: U.S. Geological Survey, Procedures and Studies in Photogeology, *Bulletin 1043-D*, pp. 57-85.

APPENDIX B - SOILS AND GEOLOGIC INFORMATION

Table B-1. Points-of-Contact: Soils Conservation Service.

West National Technical Center	Portland, Oregon 97204	
	Gary Muckel	423-2851
Arizona	SCS, Phoenix, Arizona 85012	
STATE SOIL SCIENTIST	Davie L. Richmond	(602) 379-3059
		FTS 261-5187
Tucson SCS		(602) 670-6602
California	SCS, Davis, California 95616	
STATE SOIL SCIENTIST	Ronald R. Hoppes	(916) 449-2872
Asst. St. Soil Scientist	Richard C. Herriman	(916) 449-2871
Florida	SCS, Gainesville, Florida 32601	(904) 377-1092
STATE SOIL SCIENTIST	Wade Hurt	(904) 377-1092
Nevada	SCS, Reno, Nevada 89505	
STATE SOIL SCIENTIST	Jack W. Rogers	(702) 784-5875
		FTS 470-5875
Asst. St. Soil Scientist	William E. Dollarhide	FTS 470-5875
New Mexico	SCS, Albuquerque, New Mexico 87102-3157	
STATE SOIL SCIENTIST	Tommie Parham	(505) 766-3277
		FTS 474-1846
Asst. St. Soil Sci.		FTS 474-1846
Texas	SCS, Temple, Texas 76501-7682	
STATE SOIL SCIENTIST	Richard D. Babcock	(817) 774-1261
		FTS 736-1261
Utah	SCS, Salt Lake City, Utah 84138	
STATE SOIL SCIENTIST	Ferris P. Allgood	(801) 524-5064
		FTS 588-5064

Table B-2. List of Published Soil Surveys Near SOAs.

Arizona

- 1986 Aquila-Carefree Area, Parts of Maricopa and Pinal Counties
- 1986 Colorado River Indian Reservation, Arizona-California
- 1977 Maricopa County, Central Part
- 1973 Organ Pipe Cactus National Monument
- 1972 Tucson-Avra Valley Area
- 1976 Yavapai County, Western Part
- 1980 Yuma-Wellton Area

California

- 1986 Colorado River Indian Reservation, Arizona-California
- 1981 Kern County, Southeastern Part
- 1980 San Bernardino County, Southwest Part
- 1986 San Bernardino County, Mojave River Area

Florida

- 1980 Santa Rosa County
- 1989 Walton County

Nevada

- 1980 Big Smoky Valley Area, Part of Nye County
- 1975 Fallon-Fernley Area
- 1985 Las Vegas Valley Area
- 1976 Meadow Valley Area
- 1980 Virgin River, Parts of Clark and Lincoln Counties

New Mexico

- 1985 Catron County, Northern Part
- 1989 Socorro Area
- 1976 White Sands Missile Range

Texas

- 1988 Brewster County
- 1977 Jeff Davis County
- 1980 Reeves County

Table B-3. Geologic References for Supersonic Operating Areas.

The following list of geologic references was derived from U. S. Geological Survey, Geologic Map Indexes for the states of Arizona, California, Nevada, Texas, and Utah, and the U. S. Geological Survey Index of Water Resources Investigations for the State of New Mexico. The listings have been grouped by MOA and surrounding counties. The number (or letter) preceding each entry refers to the number on the U.S.G.S. geologic map index sheets.

ARIZONA--Gladden (Luke AFB)

Maricopa, La Paz, Yavapai, and Yuma Counties, Arizona.

- 76. Lasky, S.G., and Webber, B.N., 1944, Manganese deposits in the Artillery Mountains region, Mohave county, Arizona: U.S. Geological Survey Bulletin 936-R, pl. 62, scale 1:31,680.
- 77. Lasky, S.G., and Webber, B.N., 1949, Manganese resources of the Artillery Mountains region, Arizona: U.S. Geological Survey Bulletin 961, pl. 1, scale 1:31,680.
- 78. Wolcott, H.N., Skibitzke, H.E., and Halpenny, L.C., 1956, Water resources of Bill Williams River valley near Alamo, Arizona: U.S. Geological Survey Water-Supply Paper 1360-D, pl. 21, Scale 1:62,500.
- 92. Babcock, H.M., and Brown, S.C., 1947, Ground-water resources of Peeples Valley, Arizona: U.S. Geological Survey open-file report, pl. 1, scale 1:60,000.
- 99. Babcock, H.M., and Brown, S.C., 1948, Water supply of Date Creek area, Yavapai County, Arizona: Arizona State Land Dept., pl. 1, scale 1:31,680.
- 108. Metzger, J.H., 1948, Geology and ground-water resources of the northern part of the Ranegras Plain, Yuma County, Arizona: U.S. Geological Survey open-file report, pl. 1, scale 1:62,500. (NC)
- 109. Bancroft, Howland, 1911, Reconnaissance of the ore deposits in northern Yuma County, Arizona: U.S. Geological Survey Bulletin 451, Fig. 14, scale 1:18,000.
- 177. Metzger, D.G., 1957, Geology and ground-water resources of the Harquahala Plains area, Maricopa and Yuma Counties: Arizona State Land Dept. Water Resources Report 3, pl. 1, scale 1:125,000.

ARIZONA--Luke Ranges (Luke AFB)

Pima and Yuma Counties, Arizona

- 51. Wilson, E.D., 1933, Geology and mineral deposits of southern Yuma County, Arizona: Arizona Bur. Mines Bull. 134, pl. 5, scale 1:24,000, pl. 9, scale 1:14,400, pl. 16, scale 1:7,000, Fig. 2, scale 1:1,000, Fig. 7, scale 1:62,500.
- 371. Olmstead, F.H., Loeltz, O.J., and Irelan, Burdge, 1973, Geohydrology of the Yuma area, Arizona and California: U.S. Geological Survey Prof. Paper 486-H, pl. 3, scale 1:125,000.

ARIZONA--Sells (Luke AFB)

Pima County, Arizona

- 58. Gilluly, James, 1937, Geology and ore deposits of the Ajo quadrangle: Arizona Bur. mines Bull. 141, Geol. Ser. 9, pl. 1, scale 1:62,500.
- 62. Romslo, T.M., and Robinson, C.S., 1952, Copper Giant deposits, Pima County, Arizona: U.S. Bur. Mines Rept. Inv. 4850, Fig. 2, scale 1:1800.

CALIFORNIA--Bullion Mountain (George AFB)

San Bernardino County, California

- 33. Hazzard, J.C., 1933, Notes on the Cambrian rocks of the eastern Mohave Desert: California University, Dept. Geological Sciences Bulletin, v. 23, no. 2, Map 1, scale 1:187,500.
- 479. Gale, H.S., 1951, Geology of the saline deposits, Bristol dry lake, San Bernardino County: California Division of Mines Special Report 13, pl. 1, scale 1:62,500.
- 569. Kupfer, D.H., and Bassett, A.M., 1962, Geologic reconnaissance map of part of the southeastern Mojave Desert, California: U.S. Geological Survey Misc. Field Studies Map MF-205, scale 1:125,000.

- 586. Riley, F.S., 1956, Data on water wells in Lucerne, Johnson, Fry, and Means Valleys, San Bernardino County, California: U.S. Geological Survey open-file Report 56-100, pl. 1, scale 1:95,000.
- 617. Dibblee, T.W., Jr., 1967, Geologic map of the Joshua Tree quadrangle, San Bernardino and Riverside Counties, California: U.S. Geological Survey Misc. Geological Invest. Map I-516, scale 1:62,500.
- 618. Bader, J.S., and Moyle, W.R., 1960, Data on water wells and springs in Yucca Valley--Twentynine Palms area, San Bernardino and Riverside Counties, California: California Dept. Water Resources Bulletin, no. 91-2, Fig 2, scale 1:62,500.
- 778. Dyer, H.B., Bader, J.S., and Giessner, F.W., 1963, Wells and springs in the lower Mojave Valley area, San Bernardino County, California: California Dept. Water Resources Bulletin 91-10, Fig. 2, scale 1:125,000.
- 780. Parker, R.B., 1963, Recent volcanism at Amboy Crater, San Bernardino County, California: California Division of Mines and Geology Special Report 176, pl. 1, scale 1:31,680.

CALIFORNIA--Edwards (Edwards AFB)

Kern, Los Angeles, and San Bernardino Counties, California

- 591. Smith, G.I., 1956, Geology and petrology of the Lava Mts., San Bernardino County, California: U.S. Geological Survey Open-file Report 56-109, pl. 2, scale 1:24,000, pl. 1, scale 1:250,000.
- 642. Dutcher, L.C., 1959, Data on water wells in the Fremont Valley area, Kern County.: U.S. Geological Survey Open-file Report 59-135, pl. 1, scale 1:62,5000.
- 680. Mabey, D.R., 1960, Gravity survey of the western Mojave Desert, California: U.S. Geological Survey Professional Paper 316-D, pl. 11, scale 1:130,000.
- 693. Page, R.W., and Moyle, W.R., Jr., 1960, Data on water wells in the eastern part of the middle Mojave Valley area, San Bernardino County, California: California Dept. Water Resources Bull. 91-3, pl. 2, scale 1:62,500.

778. Dyer, H.B., Bader, J.S., and Giessner, F.W., 1963, Wells and springs in the lower Mojave Valley area, San Bernardino County, California: California Dept. Water Resources Bull. 91-10, Fig. 2, scale 1:125,000.
877. Dibblee, T.W., Jr., 1967, Areal geology of the western Mojave Desert, California: U.S. Geological Survey Prof. Paper 522, pl. 1, scale 1:125,000.
890. California Department of Water Resources, 1967, Mojave River ground water basins investigations: California Dept. Water Resources Bull. 84, pl. 2, scale 1:140,000.
897. Moyle, W.R., Jr., 1963, Data on water wells in Indian Wells Valley area, Inyo, Kern, and San Bernardino Counties, California: California Dept. Water Resources Bull. 91-9, Fig. 2, scale 1:62,500.
914. Smith, G.I., Troxel, B.W., Gray, C.H., Jr., and von Huene, Roland, 1968, Geologic reconnaissance of the Slate Range, San Bernardino and Inyo Counties, California: California Div. Mines and Geology Spec. Rept. 96, pl. 1, scale 1:62,500.
919. Dutcher, L.C., and Moyle, W.R., Jr., 1973, Geologic and hydrologic features of Indian Wells Valley, California: U.S. Geological Survey Water-Supply Paper 2007, pl. 1, scale 1:125,000.
920. Kunkel, Fred, and Chase, G.H., 1969, Geology and ground water in Indian Wells Valley, California: U.S. Geological Survey Open-file report 69-329, Fig. 2, scale 1:125,000. (NC, SF, LA; Water Resources Div., Menlo Park.)
946. Duffield, W.A., and Bacon, C.R., 1981, Geologic map of the Coso volcanic field and adjacent areas, Inyo county, California: U.S. Geological Survey Misc. Investigations Ser. I-1200, scale 1:50,000.
996. Renner, J.L., 1971, Lithologic units useful for solar evaporation pond construction at Searles Lake, San Bernardino County, California: U.S. Geological Survey Open-file Report 71-238, pl. 1, scale 1:62,500. (NC, Da, M, LA, SF, U.)
1026. Moyle, W.R., Jr., 1971, Water wells in the Harper, Superior, and Cuddeback Valley areas, San Bernardino County, California: California Dept. Water Resources Bull. 91-19, Map scale 1:63,360.
1077. Kundert, C.J., 1955, Geologic map of California, Trona sheet: California Dept. Nat. Res., Div. Mines and Geology, scale 1:250,000.

1256. Burke, D.B., Hillhouse, J.W., McKee, E.H., Miller, S.T., and Morton, J.L., 1982, Cenozoic rocks in the Barstow Basin area of southern California--Stratigraphic relations, radiometric ages, and paleomagnetism: U.S. Geologic Survey Bull. 1529-E, pl. 2, scale 1:125,000.

CALIFORNIA--Panamint Valley (George AFB)

Inyo County, California

62. Ball, S.H., 1907, A geologic reconnaissance in southwestern Nevada and eastern California: U.S. Geological Survey Bulletin 308, pl. 1, scale 1:250,000.
73. Hopper, R.H., 1947, Geologic section from the Sierra Nevada to Death Valley, California: Geological Society of America Bulletin, v. 58, no. 5, pl. 1, scale 1:220,000.
82. Murphy, F.M., 1932, Geology of a part of Panamint Range, California: California Division of Mines Report 28, Map, p. 330, scale 1:125,000.
752. Drewes, Harald, 1964, Geology of the Funeral Peak quadrangle, California, on the east flank of Death Valley: U.S. Geological Survey Professional Paper 413, pl. 1, scale 1:62,500.
798. Hunt, C.B., and Mabey, D.R., 1966, Stratigraphy and structure, Death Valley, California: U.S. Geological Survey Professional Paper 494-A, pl. 1, scale 1:96,000.
934. Moyle, W.R., Jr., 1969, Water wells and springs in Panamint, Searles, and Knob Valleys, San Bernardino and Inyo Counties, California: California Dept. Water Resources Bulletin 91-17, Maps 1-33, scale 1:63,360.
1022. Wright, L.A., Troxel, B.W., Burchfiel, B.C., Chapman, R.H., and Labotka, T.C., 1981, Geologic cross section from the Sierra Nevada to the Las Vegas valley, eastern California to southern Nevada: Geological Society of America Map and Chart Series MC-28M, scale 1:250,000.
1036. Hunt, C.B., and others, 1966, Hydrologic basin, Death Valley, California: U.S. Geological Survey Professional Paper 494-B, pl. 1, scale 1:96,000.
1098. Waring, C.A., 1917, Geologic map of Inyo County: California Min. Bureau Map, scale 1:250,000.

1101. Jennings, C.W., 1958, Geologic map of California, Death Valley sheet: California Division of Mines and Geology, scale 1:250,000.
1161. Cook, J.R., 1980, Hydrogeochemical and stream sediment reconnaissance Death Valley 1"x2" NTMS area, California and Nevada: E. I. du Pont de Nemours and Co., Savannah River Laboratory, for DOE Report GJBX-135(80), pl 1A, scale 1:250,000.
1188. Carlisle, Donald, Kettler, R.M., and Swanson, S.C., 1980, Geological study of uranium potential of the Kingston Peak Formation, Death Valley region, California: University of California, Los Angeles, for DOE Report GJBX-37(81), pl. 1-3, scale 1:31,680.

NEVADA--Nellis (Nellis AFB)

Clark, Lincoln, and Nye Counties, Nevada

138. Maxey, G.B., and Jameson, C.H., 1948, Geology and water resources of Las Vegas, Pahrump, and Indian Spring Valleys, Clark and Nye Counties, Nevada: Nevada State Engineer Water Resources Bull. 5, pl. 1, scale 1:125,000.
177. Intermountain Association of Petroleum Geologists, 1952, Guidebook to the geology of Utah No. 7, Cedar City, Utah, to Las Vegas, Nevada: Utah Geol. and Mineralog. Survey, Pl. 10, scale 1:62,500.
288. Longwell, C.R., Pampeyan, E.H., Bowyer, Ben, and Roberts, R.J., 1965, Geology and mineral deposits of Clark County, Nevada: Nevada Bur. Mines Bull. 62, pl. 1, scale 1:250,000.
289. Bowyer, Ben, Pampeyan, E.H., and Longwell, C.R., 1958, Geologic map of Clark County: U. S. Geological Survey Mineral Inv. Field Studies Map MF-138, scale 1:200,000.
432. Burchfiel, B.C., and others, 1974, Geology of the Spring Mountains, Nevada: Geological Society of America Bulletin, v. 85, n. 7, fig. 3, scale 1:63,360.

NEW MEXICO--White Sands (Holloman AFB)

NEW MEXICO--Reserve (Holloman AFB)

Catron, Cibola, and Socorro Counties, New Mexico

- H. Ground water resources of Cibola County, New Mexico.
- L. Ground-water resources of the plains of San Agustin and adjacent areas, Catron and Socorro County, New Mexico.

NEW MEXICO/TEXAS--Valentine (Holloman AFB)

Jeff Davis, Presidio, Culberson, Hudspeth, Reeves, Brewster Counties, Texas

UTAH/NEVADA--Gandy (Hill AFB)

Elko County, Nevada

- 146. Hains, C.F., Van Sickle, D.M., and Ryals, W.G., 1949, Range water resources of part of Elko grazing district, Elko county, Nevada: U.S. Geol. Survey, Open-file rept. Pl. 2, 1:250,000. [NC; Nevada State Engineer's Office.]
- 223. Berge, J.S., 1960, Stratigraphy of the Ferguson Mountain area, Elko County, Nevada: Brigham Young Univ. Research Studies Geol. Ser. v. 7, n. 5, Pl 4, 1:19,500.
- 291. Hood, J.W., and Waddell, K.M., 1969, Hydrologic reconnaissance of Deep Creek valley, Tooele and Juab Counties, Utah, and Elko and White Pine Counties, Nevada: Utah Dept. Nat. Resources Tech. Pub. 24, Pl. 1, 1:250,000.
- 368. Hope, R.A., 1970, Preliminary geologic map of Elko County, Nevada: U.S. Geol. Survey, Open-file map, 1:200,000. (NC, Da, LA, M, SF, U; Mackay School of Mines.
- 414. Granger, A.E., Bell, M.M., Simmons, G.C., and Lee, Florence, 1957, Geology and mineral resources of Elko County, Nevada: Nevada Bur. Mines Bull. 54, Pl. 1, 1:250,000.

Juab and Tooele Counties, Utah

- 77. Reagan, A.B., 1929, Geology of the Deep Creek Reservation and its environs: Kansas Academy of Sciences, Transactions, v. 32, Map p. 105, scale 1:187,500.
- 93. Nolan, T.B., 1935, The Gold Hill mining district, Utah: U.S. Geological Survey Professional Paper 177, plate 1, scale 1:62,500, plate 2, scale 1:24,000.
- 192. Stokes, W. L., ed., 1951, Geology of the Canyon, House, and Confusion Ranges, Millard County, Utah: Utah Geological and Mineralogical Survey Guidebook 6, plate 2, scale 1:187,500.
- 491. Bick, K.F., 1966, Geology of the Deep Creek Mountains, Tooele and Juab Counties, Utah: Utah Geological and Mineralogical Survey Bulletin 77, plate 1, scale 1:62,500.
- 876. Percival, T.J., and Bright, J.H., 1982, National uranium resource evaluation--Elko quadrangle, Nevada and Utah: Uranium Services Co., for U.S. Department of Energy, Report PGJ/F-046(82), plate 6, scale 1:500,000.
- 903. Karfunkel, B.S., compiler, 1983, Geology and mineral resources of the Caliente, Ely, Klamath Falls, Vya, and Wells 1° x 2° NTMS quadrangles: E.I. du Pont de Nemours and Co., for U.S. Department of Energy, Report GJBX-7(83), plate 1, Caliente, scale 1:500,000, plate 3, Ely, scale 1:500,000, plate 10, Wells, scale 1:500,000.

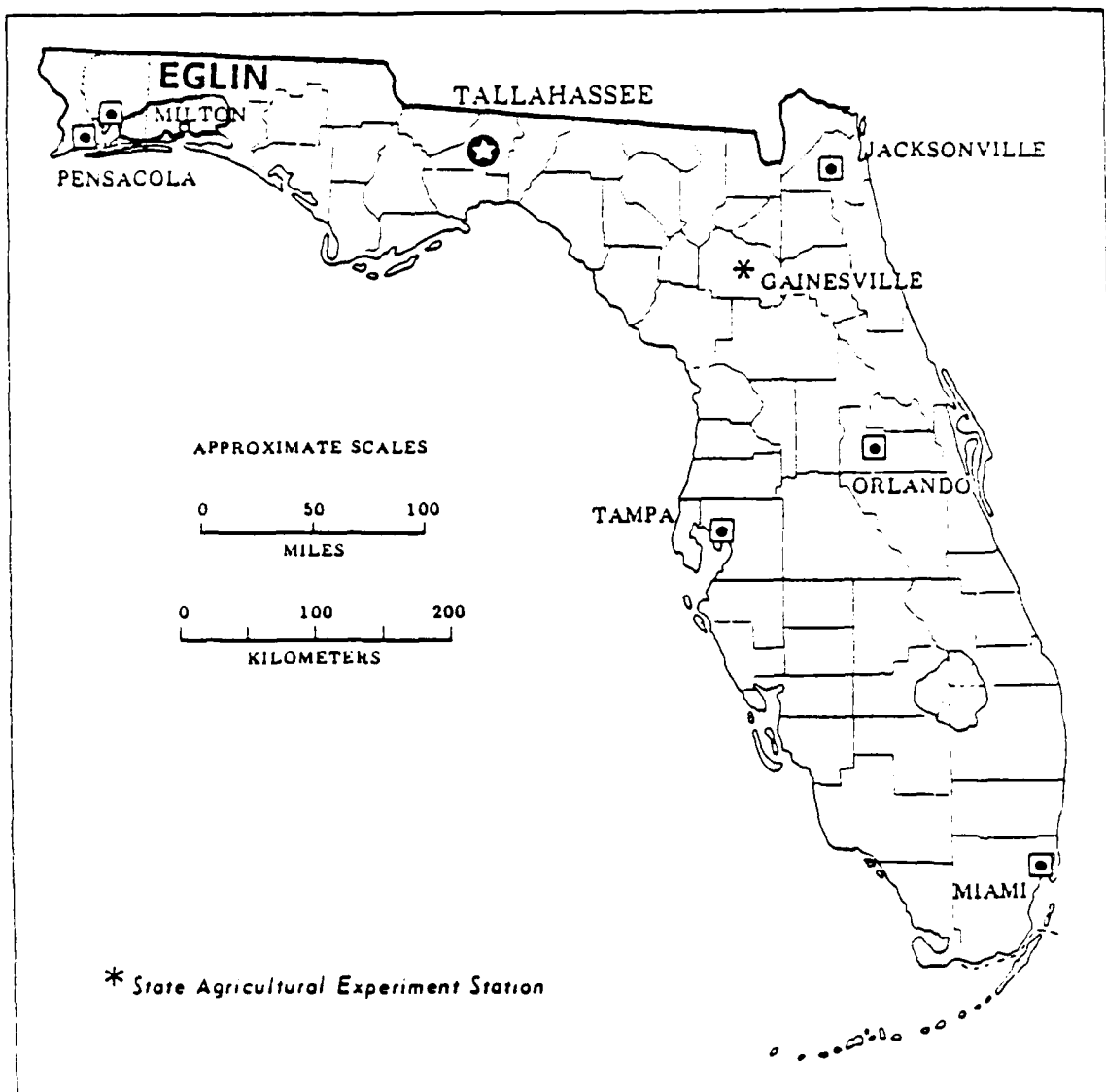
UTAH--Utah TTR (Hill AFB)

Tooele and Juab Counties, Utah

- 192. Stokes, W. L., ed., 1951, Geology of the Canyon, House, and Confusion Ranges, Millard County, Utah: Utah Geological and Mineralogical Survey Guidebook 6, plate 2, scale 1:187,500.
- 401. Staatz, M.H., and Carr, W.J., 1964, Geology and mineral deposits of the Thomas and Dugway Ranges, Juab and Tooele Counties, Utah: U.S. Geological Survey Professional Paper 415, plate 1, scale 1:31,680.
- 547. Allmendinger, R.W., and Jordan, T.E., 1984, Mesozoic structure of the Newfoundland Mountains, Utah--Horizontal shortening and subsequent extension in the hinterland

of the Sevier belt: Geological Society of America Bulletin, v. 95, p. 1280-1292, fig. 2, scale 1:130,000, fig. 4, scale 1:60,000.

- 582. Morris, H.T., 1978, Preliminary geologic map of the Delta 2° quadrangle, west-central Utah: U.S. Geological Survey Open-file Report 78-705, map, scale 1:250,000.
- 786. Moore, W.J., and Sorensen, M.L., 1979, Geologic map of the Tooele 1° x 2° quadrangle, Utah: U.S. Geological Survey Miscellaneous Investigations Series Map I-1132, scale 1:250,000.
- 882. Lindsey, D.A., 1982, Tertiary volcanic rocks and uranium in the Thomas Range and northern Drum Mountains, Juab County, Utah: U.S. Geological Survey Professional Paper 1221, fig. 2, scale 1:150,000, fig. 15, scale 1:40,000.
- 883. Lindsey, D.A., 1983, Geologic map and cross-sections of Tertiary rocks in the Thomas Ranges and northern Drum Mountains, Juab County, Utah: U.S. Geol. Survey Miscellaneous Investigations Series Map I-1176, scale 1:62,500.
- 895. Pampeyan, E.H., 1984, Geologic map of the Lynndyl 30x60 minute quadrangle, Tooele, Juab, Utah, and Millard Counties, Utah: U. S. Geological Survey Open-file Report 84-660, map, scale 1:100,000. (NC, Da, M, Db, U; Utah survey.)



Location of Santa Rosa County in Florida.

Figure B-1. Map Showing Location of Eglin AFB and Santa Rosa County, Florida.

EGLIN
Representative Geologic Conditions and Soil Types
Santa Rosa County, Florida

Areas Dominated by Sandy, Droughty Soils

Lakeland-Troup (Nearly level to strongly sloping soils; some are excessively drained and sandy throughout, and some are well drained and have at least 40 in of sand over a loamy subsoil; broad areas of rolling sandhills interspersed with long, narrow bottom lands surrounded by steep side slopes; mostly on Eglin AFB)

Ortega-Kureb (Nearly level to gently sloping, moderately well drained and excessively drained soils that are sandy throughout; flatwoods in the southern part of Santa Rosa County)

Areas Dominated by Well Drained Soils That Have a Loamy Subsoil

Red Bay-Lucy (Nearly level to sloping, well drained loamy and sandy soils that have a red or dark red, loamy subsoil; cleared and cultivated farmland in the northwestern part of Santa Rosa County)

Troup-Orangeburg-Dothan (Sloping to strongly sloping, well drained sand and loamy soils that have a loamy subsoil; undulating sandy soils on sides of steep hills separated by long, narrow stream bottoms)

Dothan-Orangeburg (Nearly level to sloping, well drained loamy soils that have a loamy subsoil at a depth of less than 20 in; undulating soils scattered north of U.S. Highway 90)

Troup-Dothan-Bonifay (Gently sloping to strongly sloping, well drained soils; some have 40 in of sand over a loamy subsoil, and some are sandy or loamy and have a loamy subsoil at a shallow depth; mainly undulating soils, higher than the surrounding soils)

Areas Dominated by Somewhat Poorly Drained to Very Poorly Drained Sandy and Loamy Soils

Pactolus-Rutledge-Mulat (Level to gently sloping, somewhat poorly drained to very poorly drained soils that are sandy and loamy throughout; broad, flat areas of soils that are normally wet during most years)

Areas Dominated by Soils Subject to Flooding

Bibb-Kinston-Johns (Level soils; some are poorly drained and are stratified loamy and sandy material, and some are somewhat poorly drained and loamy; swamps and on flood plains and stream terraces throughout most of Santa Rosa County except the southern

and southeastern parts; lower than surrounding soils, areas generally long and narrow and commonly surrounded by steep slopes or abrupt drop-offs from the uplands; sometimes flooded)

Dorovan-Pamlico (Nearly level, very poorly drained organic soils that are underlain by sandy material; heavily vegetated swamps in wet depressional areas adjacent to the alluvial flood plains; mainly in southern Santa Rosa County)

Bohicket (Level, very poorly drained clayey soils that are underlain by sandy and loamy materials; low lying, wet soils in salt marshes; along the coast and the mouth of major rivers and streams in the southern part of Santa Rosa County; thoroughly dissected by numerous small bayous and streams)

Chewacla-Wahee-Riverview (Level, somewhat poorly drained and well drained loamy soils; alluvial swamps; lower than the surrounding soils; along the western boundary of Santa Rosa County; unit has a network of sloughs and old river beds that have been cut off from the main channel; numerous lakes that are almost always filled with water)

GANDY, NELLIS

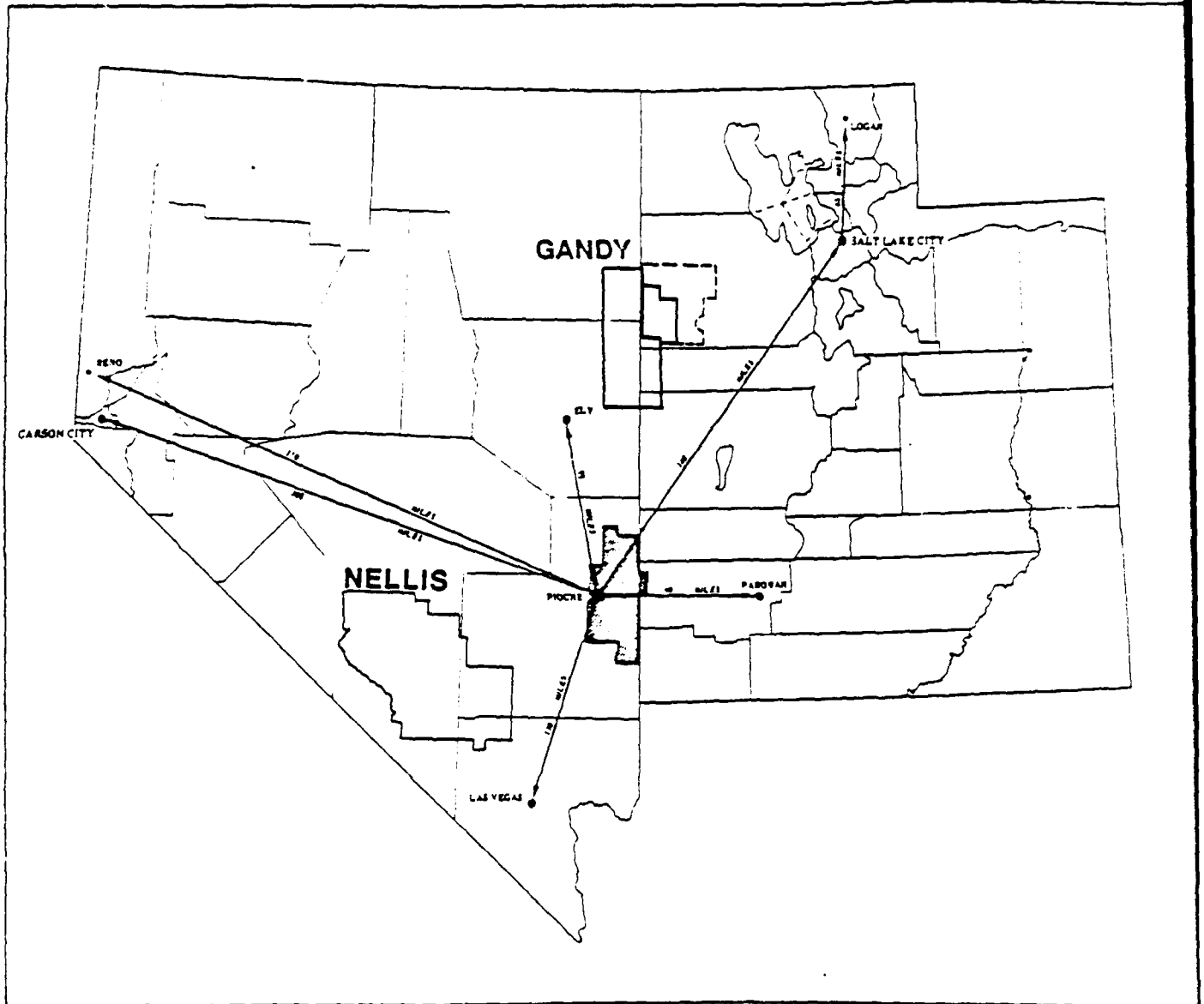


Figure B-2. Map showing location of Gandy and Nellis SOAs and the Meadow Valley Area.

GANDY, NELLIS
Representative Geologic Conditions and Soil Types
Meadow Valley Area, Nevada-Utah

Soils on High Mountains and on Foothills

Tica-Rock outcrop-Hamtah association (Very shallow to very deep, well-drained and somewhat excessively drained, moderately steep to steep soils and rock outcrops; on foothills and mountain faces; Ann. Rainfall--14" to 22")

Winu-Rock outcrop-Winz association (Moderately deep to very deep, well-drained, strongly sloping to very steep soils and rock outcrops; on mountain faces; Ann. Rainfall--14" to 24")

Soils on Low Mountains and on Foothills

Itca-Rock outcrop-Cedaran association (Very shallow to moderately deep, well-drained, gently sloping to steep soils and rock outcrops; on foothills and mountain faces; Ann. Rainfall--10" to 16")

Soils on Upper Terraces and on Alluvial Fans

Acana-Roval-Seval association (Shallow and moderately deep, well-drained, nearly level to moderately sloping soils on terraces and alluvial fans and moderately deep, well-drained, steep soils on terrace side slopes; Ann. Rainfall--8" to 14")

Badland-Linco-Acana association (Shallow to very deep, well-drained to excessively drained, strongly sloping to very steep soils on terrace side slopes and gently sloping to moderately sloping soils on terrace tops; Ann. Rainfall--8" to 12")

Basket-Satt-Decathon association (Very deep, well-drained, moderately steep and steep soils on terrace side slopes and moderately deep, well-drained, gently sloping to moderately steep soils on terraces; Ann. Rainfall--10" to 16")

Cath-Timpahute-Jarab association (Shallow to very deep, well-drained, nearly level to strongly sloping soils on terraces, terrace side slopes and alluvial fans; Annual Rainfall--8" to 14")

Decan-Uana-Shroe association (Moderately deep to very deep, well-drained, gently sloping to moderately steep soil on terrace tops, alluvial fans, side slopes; Ann. Rainfall--10" to 16")

Homestake-Lize-Buster association (Very deep, well-drained, nearly level to steep soils on terrace tops and terrace side slopes; Ann. Rainfall--8" to 14")

Minu-Vil association (Shallow, well-drained, nearly level to moderately sloping soils on terraces; Ann. Rainfall--8" to 12")

Ursine-Denmark-Sieroclip association (Shallow and moderately deep, well-drained, nearly level to moderately steep soils on terrace tops, terrace side slopes and alluvial fans; Ann. Rainfall--8" to 12")

Soils on Flood Plains, on Lower Terraces, and on Alluvial Fans

Geer-Heist-Patter association (Very deep, well-drained and moderately well-drained, nearly level to moderately sloping soils on flood plains and short alluvial fans; Ann. Rainfall--8" to 12")

Hottle-Fanu-Poorma association (Very deep, well-drained, nearly level to moderately sloping soils on flood plains, low alluvial terraces, and alluvial fans; Ann. Rainfall--8" to 12")

Descriptions of Soils
Meadow Valley Area, Nevada-Utah

Young Alluvial Fans

Cliffdown Series (gravelly sandy loam, sandy loam, very gravelly stratified sandy loam and loamy sand, pebbles and pan fragments; alkaline and calcareous)

Cliffdown-Geer association (CG) (70% Cliffdown gravelly sandy loam, 2 to 8% slopes, 20% Geer fine sandy loam, 0 to 2% slopes, 10% Heist soils)

Deerlodge-Ursine association (DH) (50% Deerlodge gravelly sandy loam, 4 to 15% slopes, 40% Ursine gravelly loam, 2 to 15% slopes, 10% Linco soils, Badland and Alluvial land)

Fanu Series (gravelly fine sandy loam, loam, light sandy clay loam, heavy loam, sandy loam, coarsely stratified sandy clay loam; moderately alkaline, calcareous)

Fanu gravelly fine sandy loam, 0 to 8% slopes (FAC) (long, narrow areas on flood plains and low alluvial fans, with 10% other Fanu soils and Alluvial land)

Geer Series (silt loam, stratified loamy sand, very fine sandy loam, loam; moderately to very strongly alkaline, calcareous)

Geer fine sandy loam, gravel substratum (GE) (short alluvial fans with 5% to 30% gravel below 20", 5% Heist soils and other Geer soils)

Geer silt loam (Gf) (flood plains and alluvial fans, with 6% saline-affected Geer soils and other Geer soils with hummocky, fine sandy loam surface layer and slopes up to 4%)

Geer silt loam, slightly saline (Gg) (small, narrow sections on flood plains and shore alluvial fans, with 10% other Geer soils; shallow water table)

Geer-Heist association (GM) (flood plains and alluvial fans, 50% Geer fine sandy loam, 0 to 2% slopes, 35% Heist gravelly sandy loam, 0 to 8% slopes, 15% other Geer and Heist soils)

Heist Series (gravelly sandy loam, sandy loam; alkaline, calcareous)

Heist gravelly sandy loam, 0 to 8% slopes (HDC) (short alluvial fans with 5% Geer and other Heist soils)

Heist gravelly sandy loam, sand substratum, 0 to 8% slopes (HEC) (short alluvial fans, with very friable loamy sand under 20 to 35 in, 15% Geer and other Heist soils)

Hottle Series (loam, silt loam, lime coated nodules; neutral to alkaline, calcareous)

Holtle loam, 0 to 8% slopes (HOC) (flood plains and short alluvial fans, with 5% other Holtle-like soils)

Patter-Geer association (PN) (50% Patter loam, 0 to 4% slopes, 35% Geer fine sandy loam, 0 to 2% slopes, 15% Heist and other Geer soils)

Patter-Shroe association (PR) (65% Patter loam, 0 to 4% slopes, 30% Shroe gravelly loam, 2 to 15% slopes, 5% Acoma soil and some alluvium)

Poorma Series (very fine sandy loam, silt loam, hard, firm, brittle silica and lime cemented durinodes; alkaline, calcareous)

Poorma very fine sandy loam, 0 to 4% slopes (PTB) (alluvial fans and flood plains, with 10% similar Poorma soils)

Umil Series (gravelly loam, loam, indurated hardpan, gravelly loamy sand, silica laminae; calcareous, alkaline)

Umil gravelly loam, 2 to 4% slopes (UMB) (alluvial fans and terraces, with 10% Fanu soils)

Ursine Series (gravelly loam, loam, very gravelly loam, gravel, indurated hardpan, gravelly loamy sand, gravelly sandy loam, weakly lime and silica cemented; calcareous, alkaline)

Older Alluvial Fans

Aned Series (sandy loam, loam, clay loam, gravelly loamy sand, gravelly sandy loam; silica and lime cement; neutral to strongly alkaline and calcareous)

Aned sandy loam, 2 to 8% slopes (ANC) (moderately dissected valley-fill terraces and alluvial fans, with 15% Decan and Fanu soils)

Bit Series (fine sandy loam, very fine sandy loam, weakly cemented gravelly loam, indurated to weakly cemented gravelly material, sandy loam; silica and lime cement; very strongly alkaline, calcareous)

Cedaran-Decan association (CD) (50% Cedaran cobbly loam, 4 to 30% slopes, 35% Decan gravelly clay loam, 2 to 15% slopes, 15% Rock outcrop and Alluvial land)

Decan Series (gravelly clay loam, clay loam, very sticky and very plastic clay, slightly hard loam, sandy loam; strongly cemented with silica, lime segregations; slightly acid to strongly alkaline)

Decan-Uana association (DA) (40% Decan gravelly clay loam, 2 to 15% slopes, 30% Decan gravelly clay loam, 15 to 30% slopes, 20% Uana gravelly loam, 2 to 15% slopes, 10% Fanu, Tica, Uana soils with gravelly clay loam surface, and Alluvial land)

Denmark Series (gravelly loam, loam, hardpan, very gravelly fine sandy loam; weakly to strongly cemented with lime and silica, alkaline)

Denmark gravelly loam, 2 to 15% slopes (DMD) (strongly dissected terraces and some alluvial fans, with 15% Cath soils, other Denmark soils with gravelly sandy loam surfaces, Badland and Alluvial land)

Denmark-Linco association (DN) (60% Denmark cobbly loam, 2 to 15% slopes, 30% Linco gravelly sandy loam, 15 to 30% slopes, 10% other Denmark soils with gravelly loam surfaces, other Linco soils with slopes less than 15%, and Alluvial land)

Jarab Series (cobbly loam, gravelly loam, gravelly clay loam, pan fragments, hardpan with silica laminae, weakly and strongly cemented with lime, soft, calcareous gravelly loam; alkaline, calcareous)

Jarab cobbly loam, 2 to 15% slopes, (JCD) (moderately dissected terraces, with 5% Cath soils and Alluvial land)

Lien Series (gravelly fine sandy loam, very gravelly fine sandy loam, duripan cemented with silica and lime, loamy fine sand; alkaline, calcareous)

Lien gravelly fine sandy loam, 2 to 4% slopes (LAB) (alluvial fans and terrace tops, with 5% similar soils and alluvium in drainage ways)

Met Series (very fine sandy loam, loam, gravelly fine sandy loam, hardpan, gravelly loamy fine sand; lime and silica cemented, alkaline)

Pamsdel Series (gravelly loam, loam, clay loam, very gravelly clay loam, strongly lime cemented gravelly material, indurated silica layer; lime and silica cement, alkaline)

Pamsdel gravelly loam, 2 to 8% slopes (PMC) (dissected alluvial fans, with 10% Sieroclip and Denmark soils)

Sieroclip Series (gravelly sandy loam, light clay loam, gravelly loam, hardpan, strongly cemented, indurated, very gravelly hardpan; cemented with lime and silica, alkaline)

Sieroclip gravelly sandy loam, 2 to 8% slopes (SKC) (old dissected alluvial fans, with 5% Jarab soils)

Stampede Series (gravelly loam, clay loam, clay, silica laminae capping moderately coarse material strongly to weakly cemented; calcareous, moderately alkaline)

Stampede gravelly loam (ST) (alluvial fans, with 5% Shroe soils and similar Stampede soils)

Timpahute Series (gravelly loam, clay loam, clay, indurated gravelly hardpan, loamy sand, sandy loam, very gravelly and cobbly loamy sand; alkaline, calcareous)

Ursine gravelly loam, 2 to 15% slopes (URD) (moderately to strongly dissected alluvial fans, with 15% Linco soils and some Badland)

Ursine gravelly loam, 15 to 30% slopes (URE) (strongly dissected alluvial fans, with 20% Badland and alluvium)

Vil Series (gravelly loam, gravelly heavy sandy clay loam, weakly cemented gravelly loam, strongly cemented hardpan, gravelly loamy sand, very coarse sand, very gravelly; calcareous, alkaline)

Lacustrine, Modern, Ancient, and Playa Lake Deposits

Acana Series (gravelly sandy loam, very friable, slightly plastic sandy clay loam, gravelly loamy sand, very gravelly loamy sand, hardpan; silica and lime cementation; alkaline)

Acana gravelly sandy loam, 2 to 8% slope (ACC) (moderately and strongly dissected terraces, with Cath, Heist, Linco, and Ursine soils and Badland)

Acana-Ursine association (AE) (75% Acana gravelly sandy loam, 2 to 8% slopes, 20% Ursine gravelly loam, 2 to 15% slopes, 5% Heist and Linco soils and Badland)

Badland (Strongly dissected terrace remnants of the Panaca--Pliocene lake bed, and Muddy Creek Formations and terrace side slopes)

Badland (BA) (strongly dissected, rough, complex exposures of the Panaca Formation, with 20% Acana, Cath, Geer, Heist, Cliffcown, Denmark, Ursine, Linco, and Sieroclip soils)

Rough Broken Land (gullies cut into soft ancient lake bed material)

Seval Series (very gravelly sandy loam, gravelly sandy clay loam, gravelly clay, brittle gravelly sandy loam, indurated hardpan, strongly cemented with silica cap, weakly cemented, very gravelly material of fine sand, loamy sand, and loam; calcareous, neutral to alkaline)

Seval very gravelly sandy loam, 30 to 50% slopes (SEF) (sides of terraces, with 5% similar Seval soils)

Other Basin Deposits

Fluvial Deposits

Alluvial land (river-washed material, very gravelly and cobbly, and medium-textured to coarse-textured soils and alluvium)

Alluvial land (AL) (highly stratified material in long, narrow areas or adjacent to streams or intermittent drainage ways)

Bicondoa Series (silt loam, silty clay loam, very plastic clay, silty clay; shallow water table; slightly alkaline to alkaline and calcareous)

Bicondoa sandy loam (Bm) (small, narrow areas on nearly level flood plains, 5% other Bicondoa soils; shallow water table 5-6 ft)

Bicondoa silty clay loam, drained (Bn) (as above, with 5% other Bicondoa soils; deeper water table below 6 ft)

Bicondoa complex (Bo) (70% Bicondoa silty clay loam, 0 to 2% slopes, 25% Bicondoa peat, 0 to 2% slopes, 5% other Bicondoa soils; very shallow water table, 0-2 ft)

Buster Series (fine sandy loam, heavy loam, sandy clay loam, clay loam, weakly cemented loam, gravelly loamy coarse sand; neutral to alkaline and calcareous)

Buster Rough broken land association (BR) (55% Buster fine sandy loam, 0 to 2% slopes, 25% Rough broken land, 20% Holtle loam and Linco soil)

Cath Series (gravelly loam, clay loam, gravelly clay loam, very gravelly sandy clay loam; lime and silica cement, neutral to alkaline and calcareous)

Cath gravelly loam, 2 to 8% slopes (CAC) (moderately dissected terraces, with 15% Acana, Heist, and Jarab soils and Alluvial land)

Four Star Series (loam, gravelly coarse sandy loam, silty clay loam, sandy loam, fine gravelly loam, fine sandy loam, coarse sandy loam, silt loam, coarse sand, finely stratified fine sandy loam, fine sand, very fine sandy loam; slightly acid; shallow water table, up to 4 ft)

Geer silt loam, strongly saline (Gh) (narrow areas on flood plains, with Pahrnagat soils, other similar Geer soils; shallow water table--4 to 6 ft)

Geer silt loam, wet (Gk) (small, narrow spots on flood plains, nonsaline to moderately saline, silt loam, stratified silt loam, very fine sandy loam, with 5% other Geer soils; shallow water table--2 to 5 ft)

Holtle-Four Star association (HR) (small, narrow areas on bottom lands within narrow valleys, 70% Holtle loam, 0 to 8% slopes, 30% Four Star loam, 0 to 4% slopes, small percentage of Alluvial land)

Pahrnagat Series (sandy root mat, silty clay loam, clay loam, sandy loam, silt loam, clay loam, clay with occasional fine pebbles; alkaline, calcareous)

Pahrnagat silt loam, drained, strongly saline (Pa) (silt loam, clay loam, clay, with 5% Geer soils and other Pahrnagat soils; water table below 30", saline and alkali affected)

Pahranagat silt loam, strongly saline (Pd) (silt loam, strongly saline and alkali affected, with 2% other Pahranagat soils; water table below 4 ft)

Pahranagat silty clay loam (Pe) (flood plains and bottom lands, with 5% other Pahranagat soils, poorly drained)

Pahranagat silty clay loam, drained (Pg) (less stratified above 40", sandy loam, loam below 40", with 5% other Pahranagat soils; water table below 4 to 5 ft)

Patter Series (loam, very fine sandy loam, silt loam; saline and alkali affected, calcareous)

Patter-Heist association (40% Patter silty clay loam, 0 to 2% slopes, strongly saline, 30% Heist gravelly sandy loam, 0 to 8% slopes, 20% Geer fine sandy loam, 0 to 2% slopes, 10% other Patter and Geer soils and some alluvial soil material)

Poorma Variant (silt loam, clay, white salt and gypsum crystals; strongly saline and alkali affected)

Poorma silt loam, clay variant (PV) (flood plains, with 3% Poorma and Holtle soils)

Glacial Deposits

Other Alluvium

Acoma Series (gravelly sandy loam, gravelly sandy clay, very gravelly sandy clay loam; mildly alkaline, neutral to calcareous)

Acoma gravelly sandy loam, 2 to 15% slopes (AGD) (moderately and strongly dissected terraces, with 20% Linco, Heist, and Geer soils)

Badland-Bit association (BB) (50% Badland, 40% Bit fine sandy loam, 0 to 8% slopes, 10% Sierocliiff soils and Alluvial land)

Badland-Buster association, eroded (BD2) (30% Badland, 25% Buster loamy sand, 0 to 8% slopes, 25% Holsine gravelly sandy loam, 0 to 8% slopes, 20% Holtle, Usine, Fanu, Poorma, and other Buster soils)

Basket Series (gravelly sandy loam, gravelly fine sandy loam, very gravelly sandy clay loam, very gravelly sandy loam, very gravelly coarse sand; neutral to strongly alkaline and calcareous)

Basket gravelly fine sandy loam, 30 to 50% slopes (BKF) (long narrow areas on terrace side slopes, with 10% Decathon and other Basket soils, soils with clay horizons on moderately sloping and strongly sloping terrace foot slopes)

Basket-Lize association (BL) (30% Basket gravelly sandy loam, 30 to 50% slopes, 30% Lize stony fine sandy loam, 30 to 50% slopes, 30% Satt very stony sandy loam, 4 to 15% slopes, with 10% Holtle soils and Rough broken land)

Decathon Series (gravelly loam, clay loam, sandy loam, heavy loam, gravelly sandy loam, very gravelly loamy sand, hardpan; neutral to alkaline, lime cement)

Decathon gravelly loam, 2 to 8% slopes (DCC) (intermediate terraces, with 20% Basket and Fanu soils)

Decathon-Basket association, moderately steep (DED) (60% Decathon gravelly loam, 2 to 8% slopes, 20% Basket gravelly sandy loam, 15 to 30% slopes, 20% Holtle and other Basket soils)

Decathon-Basket association, steep (DEE) (40% Decathon gravelly loam, 2 to 8% slopes, 40% Basket gravelly fine sandy loam, 30 to 50% slopes, 20% Holtle and other Basket soils)

Deerlodge Series (gravelly sandy loam, sandy clay loam, gravelly sandy clay loam, indurated hardpan; lime cemented, moderately alkaline)

Deerlodge association (DG) (60% Deerlodge gravelly sandy loam, 4 to 15% slopes, 35% Deerlodge gravelly loam, 15 to 30% slopes, 5% Deerlodge soils with steeper slopes, shallow hardpan, and Alluvial land)

Holsine Series (gravelly sandy loam, very gravelly coarse sandy loam, very fine sandy loam; calcareous, moderately alkaline)

Holsine-Usine association (HN) (45% Holsine gravelly sandy loam, 0 to 8% slopes, 30% Usine cobbly sandy loam, 0 to 30% slopes, 20% Buster loamy sand, 0 to 8% slopes, eroded, 5% Fanu and Poorma soils and Badland)

Homestake Series (gravelly sandy loam, gravelly light sandy clay loam, gravelly clay loam, very gravelly clay, very gravelly heavy clay loam, very cobbly sandy clay loam, weakly cemented very cobbly and gravelly light sandy clay loam, weakly cemented very cobbly loamy sand; neutral to alkaline, calcareous)

Homestake gravelly sandy loam, 4 to 8% slopes (HSC) (terrace tops, with 20% Basket and Lize soils)

Homestake very stony sandy loam, 2 to 8% slopes (HTC) (terrace tops, with 10% Holtle and other Homestake soils)

Linco Series (gravelly sandy loam, gravelly loam, slightly brittle gravelly fine sandy loam, gravelly fine sandy loam, sandy loam, loamy sand; alkaline, calcareous)

Linco-Acana association (LC) (45% Linco gravelly sandy loam, 15 to 30% slopes, 35% Acana gravelly sandy loam, 2 to 8% slopes, 20% other Linco soils, Badland, and alluvium)

Linco-Badland association (LD) (45% Linco gravelly sandy loam, 4 to 15% slopes, 20% Linco gravelly sandy loam, 15 to 30% slopes, 20% Badland, 15% Acana and Cath soils and some alluvium)

Lize Series (stony fine sandy loam, slightly hard gravelly loam, hard gravelly clay loam, hard gravelly sandy loam; calcareous, neutral to moderately alkaline)

Lize association (LE) (60% Lize stony fine sandy loam, 15 to 30% slopes, 30% Lize stony fine sandy loam, 30 to 50% slopes, 10% Badland)

Lize-Tica association (LT) (50% Lize stony fine sandy loam, 15 to 30% slopes, 45% Tica very stony loam, 15 to 30% slopes, 5% other Lize and Tica soils and some alluvial soil material)

Met-Ursine association (MU) (50% Met very fine sandy loam, 0 to 4% slopes, 35% Ursine gravelly loam, 2 to 15% slopes, 15% Linco and Met soils, some alluvial soil material, and Badland)

Minu Series (stony sandy loam, gravelly clay loam, strongly cemented gravelly hardpan, gravelly loamy sand; silica and lime cement, alkaline)

Minu gravelly sandy loam, 2 to 8% slopes (MVC) (dissected terraces, with 10% other Minu soils, some alluvium and Linco similar soil)

Minu stony sandy loam, 0 to 8% slopes (dissected terraces, with 20% Timpahute, Poorma, and other Minu soils)

Nevu Series (gravelly sandy loam, fine gravelly loam, gravelly clay loam, indurated hardpan, gravelly sandy loam; alkaline, calcareous)

Nevu gravelly sandy loam, 4 to 15% slopes (NSD) (dissected terraces, with 10% Fanu and other Nevu soils)

Roval Series (gravelly loam, gravelly clay loam, indurated hardpan, very gravelly loamy sand; lime and silica cemented, alkali)

Roval gravelly loam, 2 to 15% slopes (RRD) (dissected high valley-fill terraces, with 20% Linco and Acana soils, some Badland and alluvium)

Roval-Acana association (RV) (55% Roval gravelly loam, 2 to 15% slopes, 25% Acana gravelly sand loam, 2 to 8% slopes, 20% Geer and Linco soils)

Satt Series (very stony sandy loam, gravelly sandy clay loam, gravelly clay, very gravelly sandy clay, very gravelly sandy clay loam, indurated hardpan, strongly cemented hardpan with pockets and seams of weakly cemented loamy fine sand; alkaline, calcareous)

Satt stony sandy loam, 4 to 15% slopes, eroded (SAD2) (dissected upland terraces, with 5% other non-eroded Satt soils)

Satt stony fine sandy loam, 2 to 8% slopes, eroded (SCC2) (dissected terraces, shallow hardpan, with 10% Basket and other Satt soils)

Satt association (SD) (45% Satt stony sandy loam, 4 to 15% slopes, eroded, 45% Satt extremely stony sandy loam, 15 to 30% slopes, 10% Holtle soils)

Shroe Series (gravelly loam, gravelly sandy clay loam, sandy clay loam, gravelly clay, very gravelly sandy clay loam, fine tuff fragments, loam; neutral)

Shroe gravelly loam, 2 to 15% slopes (SGD) (dissected sides of terraces, with 10% Decan soils)

Shroe-Badland association (SH) (50% Shroe cobbley sandy clay loam, 15 to 30% slopes, 15% Shroe gravelly loam, 2 to 15% slopes, 15% Badland, 20% similar Shroe soils and some alluvium)

Slickens (SL) (Miscellaneous accumulations of fine-textured materials separated in ore mill operations)

Swisbob Series (very stony loam, gravelly light clay loam, clay, gravel and cobbles strongly cemented by silica and lime, cobbley and gravelly sandy loam; calcareous, moderately alkaline)

Swisbob very stony loam, 4 to 8% slopes (SWC) (ancient high terraces, with 10% Holtle soils)

Timpahute gravelly loam, 0 to 4% slopes (TTB) (moderately dissected terraces, with 20% Minu and Patter soils)

Uana Series (gravelly loam, sandy clay loam, clay, clay loam, weakly clay loam, indurated silica laminae capping sandy loam weakly to strongly cemented by lime, sandy loam; calcareous, alkaline)

Ursine-Badland association (US) (60% Ursine gravelly loam, 2 to 15% slopes, 20% Badland, 20% Heist, Geer, and Linco soils)

Usine Series (cobblely sandy loam, gravelly very fine sandy loam, very gravelly loamy sand, very gravelly sand; calcareous, moderately alkaline)

Vicu Series (stony sandy loam, gravelly sandy loam, gravelly and cobblely sandy clay, very gravelly sandy clay, very gravelly coarse sandy loam, very gravelly loamy sand, strongly cemented, very gravelly hardpan; neutral to moderately alkaline, calcareous)

Vicu stony sandy loam, 2 to 8% slopes (high alluvial terraces and fans, with 10% Tica and Umil soils)

Vil gravelly loam, 2 to 8% slopes (high dissected terraces, with 5% Acana soil and alluvial soil material)

Bedrock Deposits--Clastic Sedimentary

Pioche Series (extremely stony loam, cobblely clay loam, cobblely clay, quartzite bedrock; neutral)

Pioche-Rock outcrop complex (PS) (65% Pioche extremely stony loam, 8 to 30% slopes, 25% Rock outcrop, 10% similar deeper Pioche soils)

Bedrock Deposits--Carbonate/Evaporite Sedimentary

Kyler Series (very cobblely loam, cobblely loam, gravelly loam, limestone bedrock; alkaline, calcareous)

Kyler-Rock outcrop complex (KO) (55% Kyler very cobblely loam, 15 to 30% slopes, 30% Rock outcrop, with 15% other Kyler soils and similar soils)

Kyler-Rock outcrop association (KR) (35% Kyler stony loam, 30 to 50% slopes, 20% Kyler very stony loam, moderately deep variant, 50 to 75% slopes, 25% Rock outcrop, with 20% other Kyler and similar soils)

Kyler Variant (very stony and gravelly loam, many pan fragments, very gravelly loam weakly cemented with lime, gravelly and very gravelly heavy loam, hard bedrock; alkaline, calcareous)

Urtah Series (very stony loam, very gravelly loam, hard limestone bedrock; moderately alkaline)

Urtah-Rock outcrop association (UT) (45% Urtah very stony loam, 30 to 50% slopes, 40% Rock outcrop, 15% similar Urtah soils)

Bedrock Deposits--Volcanic and Metamorphic and Mixed

Cedaran Series (cobbley loam, gravelly clay loam, hard tuff; neutral)

Cedaran-Rock outcrop complex (CE) (50% Cedaran cobbley loam, 4 to 30% slopes, 35% Rock outcrop, 15% Itca soils, remnant Fanu and Patter soils)

Hamtah Series (very stony clay loam, gravelly clay loam, gravelly clay, very gravelly clay, very gravelly clay loam, weathered rhyodacitic ignimbrite; neutral to slightly acid)

Hamtah-Tica association (HA) (50% Hamtah very stony clay loam, 30 to 50% slopes, 25% Tica very stony loam, 15 to 30% slopes, 15% Rock outcrop, with 10% Nevtah and Udel soils)

Hamtah-Udel association (HC) (50% Hamtah very stony clay loam, 30 to 50% slopes, 25% Udel very gravelly sandy loam, 30 to 50% slopes, 15% Rock outcrop, with 10% Nevtah and Tica soils)

Itca Series (stony loam, gravelly clay loam, gravelly clay, hard ignimbrite bedrock; neutral)

Itca stony clay loam, 2 to 15% slopes (IND) (foothill faces, with 15% Rock outcrop, gravelly, medium-textured soil and other Itca soils)

Itca-Cedaran association (IO) (45% Itca stony loam, 15 to 30% slopes, 25% Cedaran stony loam, 15 to 50% slopes, 25% Rock outcrop, with other Itca soils, Aned soils, and Alluvial land)

Itca-Rock outcrop association (IR) (60% Itca very stony loam, 15 to 50% slopes, 25% Rock outcrop, with Minu and other Itca soils and Alluvial land)

Nevtah Series (stony loam, gravelly loam, weathered ignimbrite, very gravelly loam, hard ignimbrite bedrock; neutral to slightly acid)

Nevtah-Rock outcrop association (NR) (30% Nevtah stony loam, 4 to 15% slopes, 30% Nevtah very stony loam, 15 to 30% slopes, 20% Rock outcrop, 20% Udel and other Nevtah soils)

Rock Land (RO) (Rock outcrop, rubble land, some alluvium, very shallow soils)

Tica Series (very stony loam, stony loam, stony light clay, cobbley heavy sandy clay loam, hard rhyodacitic ignimbrite--welded tuff; neutral)

Tica-Nevtah association (TN) (30% Tica very stony loam, 15 to 30% slopes, 30% Nevtah very stony loam, 15 to 30% slopes, 30% Rock outcrop, 10% Udel and Holtle soils)

Tica-Rock outcrop association (TR) (70% Tica very stony loam, 15 to 30% slopes, 25% Rock outcrop, 5% Itca soils and some alluvium)

Udel Series (gravel, cobbles, stones, very gravelly sandy loam, ignimbrite bedrock; neutral)

Udel-Rock outcrop association (UK) (60% Udel very gravelly sandy loam, 30 to 50% slopes, 35% Rock outcrop, 5% Nevta soils)

Urwil Series (stony fine sandy loam, clay loam, gravelly clay, gravelly sandy clay, weathered rhyodacitic ignimbrite; neutral to slightly acid)

Urwil stony fine sandy loam, 2 to 15% slopes (UWD) (foothills, with 10% volcanic Rock outcrop)

Wilpar Series (very stony sandy loam, gravelly heavy sandy loam, gravelly clay, very gravelly clay, very gravelly sandy clay, very gravelly sandy clay loam, weathered coarse fragments, weathered ignimbrite bedrock; neutral to mildly alkaline)

Wilpar very stony sandy loam, 30 to 50% slopes (WMF) (mountain faces, with 20% Tica and Hamta soils, volcanic rock outcrops)

Winu Series (very stony loam, gravelly clay loam, gravelly heavy clay loam, sandy loam, hard bedrock--weathered rhyodacitic ignimbrite; neutral to slightly acid)

Winu extremely stony loam, 50 to 75% slopes (WNG) (very steep mountain faces, with 20% Udel and other Winu soils, Rock outcrop)

Winu-Rock outcrop association (WR) (30% Winu very stony loam, 15 to 30% slopes, 30% Winu extremely stony loam, 30 to 50% slopes, 20% Rock outcrop, 20% Nevta, Udel, and Winz soils)

Winz Series (tuff, very stony sandy loam, very gravelly coarse sandy loam, very gravelly clay, extremely cobbly clay; slightly acid)

Winz association (WS) (45% Winz very stony sandy loam, 30 to 50% slopes, 45% Winz extremely stony sandy loam, 50 to 75% slopes, 10% Rock outcrop)

Zoate Series (cobbly loam, gravelly heavy clay loam, gravelly clay, indurated silica laminae, strongly cemented material, volcanic bedrock; mildly alkaline)

Zoate cobbly loam, 15 to 50% slopes (ZOF) (foothill and mountain slopes, with 20% Kyler soils, similar Zoate soils, Rock outcrop)

Zoate-Rock outcrop association (ZR) (40% Zoate stony loam, 15 to 50% slopes, 20% Zoate cobbly loam, 4 to 15% slopes, 30% Rock outcrop, 10% similar Zoate soils)

RESERVE

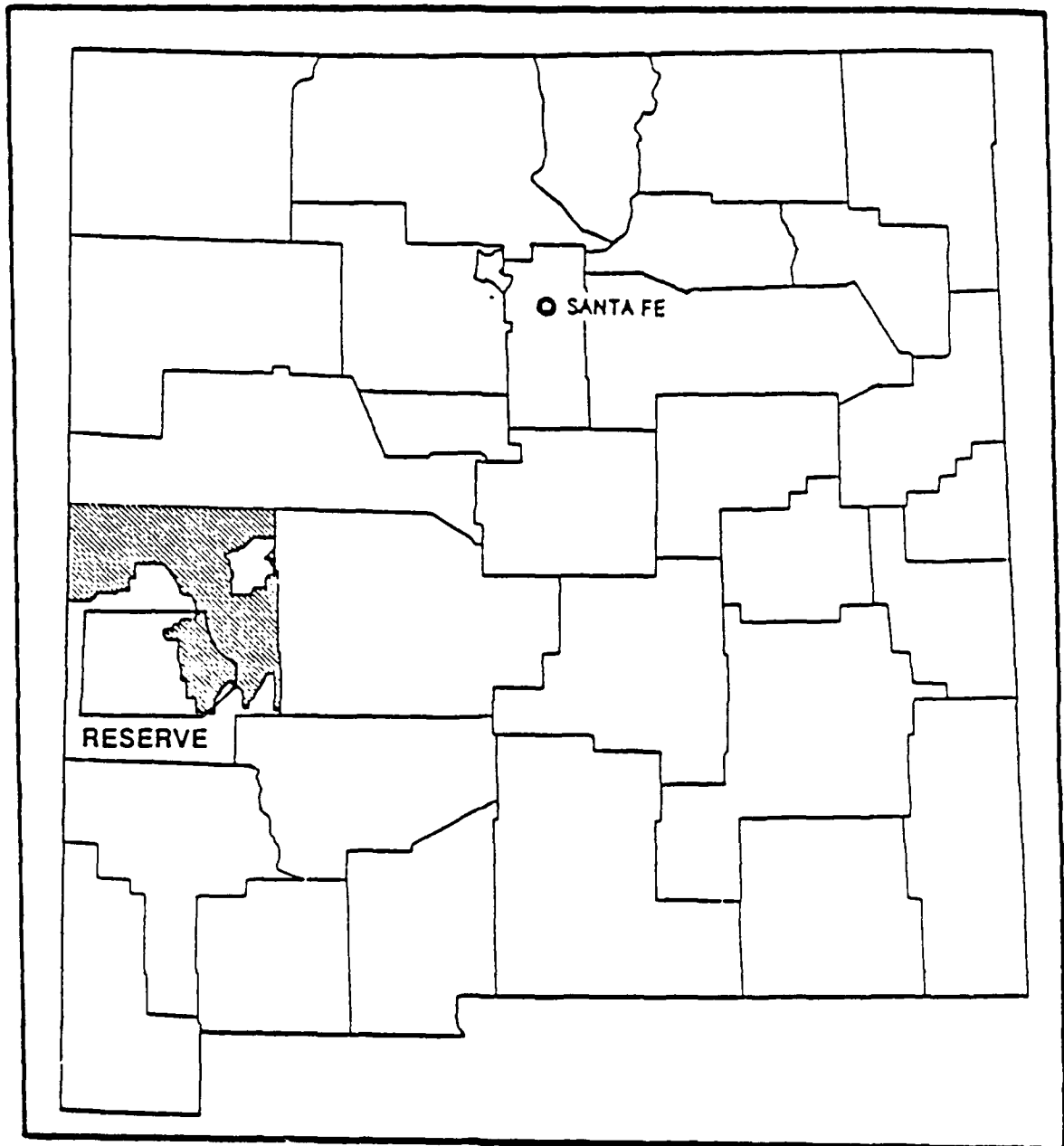


Figure B-3. Map showing location of Reserve MOA and Catron County, New Mexico.

RESERVE
Representative Soil Types and Mapped Soil Units
Catron County (northern part), New Mexico

Soils of Alluvial Fans, Plains, Hills, and Mountains

Cabezon-Datil-Hubbell (Shallow and deep, well drained, sloping to steep soils; mainly on mesas, hills, and alluvial fans; Ann. Rainfall--12" to 15"; Cabezon--volcanic residuum, cobbley clay loam, clay, unweathered basalt; Datil--alluvium, fine sandy loam, loam, gravelly clay loam, sandy clay loam; Hubbell--volcanic ash and cinders, loamy sand, stratified loamy sand, sandy loam, loam)

Celacy-Datil-Typic Ustorthents (Shallow to deep, well drained, sloping to steep soils, mainly on plains, alluvial fans, and hills; Ann. Rainfall--12" to 15"; Celacy--sandstone and shale residuum, fine sandy loam, sandy clay loam, weathered soft bedrock; Datil--alluvium, fine sandy loam, loam, gravelly clay loam, sandy clay loam; Typic Ustorthents--alluvium, fine sandy loam, loam, weakly cemented volcanic debris)

Flugle-Loarc-Typic Ustorthents (Shallow to deep, well drained, level to steep soils; on alluvial fans, hills, and ridges; Ann. Rainfall--12" to 15"; Flugle--alluvium, sandy loam, sandy clay loam; Loarc--wind modified alluvium, sandy loam, sandy clay loam, gravelly sandy loam, loamy sand; Typic Ustorthents--alluvium, fine sandy loam, loam, weakly cemented volcanic debris)

Motoqua-Datil-Abrazo (Shallow to deep, well drained, sloping to steep soils; on alluvial fans, hills, plains, and ridges; Ann. Rainfall--12" to 15"; Motoqua--tuff residuum, very gravelly loam, very cobbley clay loam, rhyolitic tuff; Datil--alluvium, fine sandy loam, loam, gravelly clay loam, gravelly sandy clay loam; Abrazo--tuff residuum and local alluvium, gravelly loam, cobbley clay, cobbley clay loam, unweathered tuff)

Mion-Jacee-Rock outcrop (Shallow and moderately deep, well drained, level to steep soils; on ridges, hills, plains, and alluvial fans; Ann. Rainfall--12" to 15"; Mion--sandstone and shale residuum and alluvium, gravelly clay loam, clay loam, clay, weathered, soft shale; Jacee--sandstone and shale residuum and local alluvium, loam, silty clay, clay, weathered shale; Rock outcrop--sandstone and shale)

Penistaja-Veteado (Deep, well drained, sloping soils; on plains and alluvial fans; Ann. Rainfall--9" to 12"; Penistaja--old basalt flow alluvium, sandy loam, sandy clay loam; Veteado--fine textured alluvium, sandy loam, clay, sandy clay loam)

Telescope-Loarc-Augustine (Deep, well drained, level to sloping soils; on alluvial fans and hills; Ann. Rainfall--12" to 15"; Telescope--alluvium and eolian material, loamy sand, sandy loam; Loarc--alluvium and eolian material, sandy loam, sandy clay loam, gravelly sandy loam, loamy sand; Augustine--alluvium, fine sandy loam, clay loam, loam)

Tolman-Smilo-Pleioville (Shallow and moderately deep, well drained, level to steep soils; on hills, mountains, alluvial fans, and plains; Ann. Rainfall--16" to 20"; Tolman--tuff residuum, extremely cobbly loam, very cobbly clay loam, unweathered tuff; Smilo--basalt residuum, cobbly sandy loam, loam, cobbly clay, cobbly clay loam, gravelly clay, unweathered basalt; Pleioville--conglomerate residuum, gravelly sandy loam, gravelly clay, gravelly clay loam, very gravelly clay, very gravelly clay loam, conglomerate)

Soils of Valleys and Basins

Catman-Manzano-Hickman (Deep, well drained, level to sloping soils; in swales, drainage ways, and playas; Ann. Rainfall--12" to 15"; Catman--fine textured alluvium, clay, silty clay loam, clay loam, silty clay, silt loam; some areas strongly saline or alkaline; Manzano--alluvium, loam, clay loam; Hickman--alluvium, loam, stratified clay loam, sandy clay loam, sandy loam)

RESERVE
Descriptions of Soils
Catron County (northern part), New Mexico

Young Alluvial Fans

- Flugle-Typic Ustorthents association, 2 to 15% slopes (340) (40% Flugle fine sandy loam, 2 to 15% slopes, 35% Typic Ustorthents, 5 to 15% slopes, 25% Manzano, Jacques soils, Rock outcrop and other Flugle soils)
- Flugle-Jacques association, 1 to 5% slopes (341) (45% Flugle sandy loam 3 to 5% slopes, 35% Jacques clay loam, 1 to 3% slopes, loarc and Manzano soils)
- Datil-Dioxice complex, 1 to 5% slopes (347) (50% Datil fine sandy loam, 30% Dioxice gravelly sandy loam, 20% Guy, similar Dioxice, and Manzano soils)
- Smilo-Adman complex, 0 to 9% slopes (371) (40% Smilo cobbley sandy loam, 0 to 4% slopes, 30% Adman cobbley loam, 2 to 9% slopes, 30% Rock outcrop, and similar Smilo and Adman soils, Bryman soils)
- Gustspring-Guy-Typic Ustorthents complex, 1 to 10% slopes (373) (25% Gustspring loamy sand, 1 to 5% slopes, 25% Guy gravelly sandy loam, 3 to 10% slopes, 20% Typic Ustorthents, 1 to 10% slopes, 30% Datil, Dioxice, Flugle, Lapdun, Aridic Ustochrepts, Albinas, Hickman, and Manzano soils)
- Datil gravelly fine sandy loam, 1 to 6% slopes (382) (gravelly fine sandy loam, gravelly clay loam, gravelly sandy clay loam, with 15% Majada, Maia, and Manzano soils)
- Hubbell loamy sand, 1 to 9% slopes (408) (loamy sand, stratified loamy sand, sandy loam, loam, with 15% Ceniza soils and sandstone outcrop)
- Telescope loamy fine sand, 3 to 10% slopes (459) (loamy fine sand, sandy loam, gravelly fine sandy loam, with 15% Augustine and Manzano soils)
- Augustine fine sandy loam, 1 to 6% slopes (479) (fine sandy loam, clay loam, loam, with 20% Gustspring, Datil, and Manzano soils)
- Datil-Guy association, 3 to 15% slopes (482) (40% Datil sandy loam, 3 to 10% slopes, 35% Guy gravelly sandy loam, 3 to 15% slopes, 25% Gustspring, Loarc, similar Guy, and Manzano soils)
- Telescope loamy sand, 0 to 3% slopes (525) (loamy sand, sandy loam, with 25% Loarc, Manzano and similar Telescope soils)

Goldust gravelly sandy clay loam, 2 to 8% slopes (540) (gravelly sandy clay loam, gravelly clay loam, very gravelly clay loam, very cobbly clay, very cobbly sandy loam, with 15% Abrazo and Datil soils)

Maia sandy loam, 1 to 8% slopes (560) (sandy loam, sandy clay loam, clay loam, gravelly clay loam, gravelly loam, with 20% Catman and Manzano soils)

Celsosprings loam, 1 to 8% slopes (565) (loam, clay, clay loam, cobbly clay loam, gravelly clay loam, with 25% Manzano and similar Celsosprings soils)

Brycan loam, 0 to 3% slopes (624) (loam, with 20% clayey soils)

Albinas-Datil complex, 1 to 5% slopes (645) (40% Albinas sandy loam, 30% Datil loam, 30% Guy, Dioxice, and Manzano soils)

Majada-Lapdun very cobbly loams, 1 to 8% slopes (655) (45% Majada very cobbly loam, 35% Lapdun very cobbly loam, 20% Amenson and Gustspring soils)

Veteado-Penistaja sandy loams, 1 to 5% slopes (665) (45% Veteado sandy loam, 1 to 4% slopes, 40% Penistaja sandy loam, 1 to 5% slopes, 15% Catman, saline Catman, and similar Veteado soils)

Loarc-Flugle-Manzano association, 1 to 9% slopes (675) (40% Loarc sandy loam, 2 to 6% slopes, 30% Flugle sandy loam, 2 to 9% slopes, 20% Manzano loam, 1 to 2% slopes, 10% Ralphston soils)

Millpaw-Datil complex, 0 to 7% slopes (690) (45% Millpaw loam, 0 to 7% slopes, 45% Datil fine sandy loam, 1 to 7% slopes, 10% Albinas and Manzano soils)

Gustspring gravelly fine sandy loam, 0 to 5% slopes (720) (gravelly fine sandy loam, gravelly sandy clay loam, gravelly sandy loam, extremely gravelly loamy coarse sand, with 20% Datil, Manzano, Augustine, and similar Gustspring soil)

Older Alluvial Fans

Gustspring-Aridic Ustochrepts complex, 5 to 40% slopes (375) (35% Gustspring very gravelly sandy loam, 5 to 15% slopes, 30% Aridic Ustochrepts, 5 to 40% slopes, 35% Albinas, Hickman, Manzano, Pietown, Guy, and Lapdun soils, and Typic Ustorthents)

Diatee-Flugle association, 1 to 9% slopes (670) (40% Diatee gravelly sandy loam, 1 to 5% slopes, 35% Flugle loam, 3 to 9% slopes, 25% Loarc, Manzano, and Gustspring soils)

Parquat-Tafoya association, 5 to 30% slopes (705) (35% Parquat very cobbly sandy loam, 5 to 15% slopes, 35% Tafoya gravelly sandy loam, 15 to 30% slopes, 30% Majada, Motoqua, and Manzano soils)

Lacustrine--Modern, Ancient, and Playa Lake Deposits

Catman silty clay, 0 to 2% slopes (494) (moderately saline silty clay, with 15% Hickman and Manzano soils)

Loarc-Telescope loamy sands, 0 to 3% slopes (517) (backswamps, 60% Loarc loamy sand, 25% Telescope loamy sand, 15% Augustine, Datil and similar Telescope soils)

Other Basin Deposits

Fluvial Deposits

Pietown-Hickman complex, 0 to 5% slopes (422) (45% Pietown fine sandy loam, 30% Hickman very fine sandy loam, 25% sand dunes, Catman and saline Catman soils)

Manzano clay loam, 0 to 2% slopes (424) (clay loam, with 15% Albinas, Hickman, and Jacques soils)

Catman-Hickman complex, 1 to 5% slopes (425) (50% Catman clay, 25% Hickman clay loam, 25% saline Catman clay and Pietown soils)

Jacques clay loam, 1 to 5% slopes (680) (clay loam, clay, silty clay loam, sandy clay loam, with 20% Catman and Manzano soils)

Glacial Deposits

Other Alluvium--Plains, Hills, Ridges, Mesas, and Plateaus

Tejana-Rock outcrop complex, 3 to 15% slopes (330) (60% Tejana very gravelly loam, 20% Rock outcrop, 20% Celacy and Jacee soils)

Ralphston-Amenson loam, 1 to 9% slopes (335) (50% Ralphston loam, 1 to 9% slopes, 25% Amenson loam, 1 to 4% slopes, 25% Flugle, Albinas, and Dioxice soils)

Celsosprings stony loam, 1 to 8% slopes (366) (stony loam, cobbly clay, clay loam, with 30% Celsosprings loam, Thunderbird and Cabezon soils)

Aridic Argiustolls-Rock outcrop complex, 15 to 45% slopes (385) (60% Aridic Argiustolls, 25% Rock outcrop, 15% Majada and Guy soils, and Aridic Haplustolls)

Ceniza-Gatlin complex, 1 to 15% slopes (409) (55% Ceniza extremely gravelly loam, 35% Gatlin very gravelly loam, 10% Albinas and Hickman soils, and sandstone outcrop)

Goesling-Celacy complex, 0 to 10% slopes (411) (50% Goesling loamy sand, 0 to 10% slopes, 35% Celacy sandy loam, 5 to 10% slopes, 15% Rock outcrop, Jacee and Mion soils)

Datil-Dioxice association, moist, 3 to 15% slopes (463) (35% Datil gravelly loam, 35% Dioxice gravelly loam, 30% Motoqua, Faraway and Dioxice similar soils)

Royosa fine sand, 3 to 15% slopes (497) (fine sand, loamy sand, sand, with 20% Celacy and Travessilla soils)

Bario sandy clay loam, 0 to 5% slopes (550) (sandy clay loam, clay, clay loam, with 20% Pleioville and Brycan soils)

Loarc-Datil complex, moist, 2 to 20% slopes (580) (35% Loarc sandy loam, 2 to 8% slopes, 35% Datil cobbly loam, 4 to 20% slopes, 30% Diatee, Flugle, Manzano, and fine sandy loam Datil soils)

Amenson-Gustspring loam, 2 to 7% slopes (595) (40% Amenson loam, 35% Gustspring loam, 25% similar Amenson, similar Gustspring soil)

Typic Ustorthents-Hickman-Majada association, 1 to 25% slopes (650) (30% Typic Ustorthents, 3 to 25% slopes, 30% Hickman loam, 1 to 3% slopes, 15% Majada very cobbly sandy loam, 15 to 25% slopes, 25% Manzano and Pietown soils, and Rock outcrop)

Datil-Loarc association, 1 to 15% slopes (660) (40% Datil sandy loam, 1 to 15% slopes, 40% Loarc sandy loam, 1 to 8% slopes, 20% Manzano and Guy soils)

Alegros-Alegros Variant complex, 1 to 10% slopes (710) 60% Alegros cobbly loam, 20% Alegros Variant extremely cobbly loam, 20% soils with no calcium carbonate, with dark surface layer or with shallow bedrock)

Guy gravelly loamy fine sand, 0 to 12% slopes (715) (gravelly loamy fine sand, gravelly fine sandy loam, with 30% Dioxice, Manzano, and Maia soils)

Bedrock Deposits--Clastic Sedimentary

Valnor-Midnight association, 1 to 25% slopes (486) (45% Valnor fine sandy loam, 1 to 7% slopes, 30% Midnight very gravelly loam, 3 to 25% slopes, 25% Brycan soils and sandstone and shale outcrop)

Jacee-Celacy-Rock outcrop association, 0 to 9% slopes (492) (40% Jacee loam, 0 to 5% slopes, 20% Celacy fine sandy loam, 2 to 9% slope, 20% Rock outcrop, 0 to 9% slopes, 20% Catman, Jacques, Flugle, Royosa, Mion, and Travessilla soils)

Mion-Travessilla-Rock outcrop complex, 2 to 30% slopes (493) (35% Mion gravelly clay loam, 25% Travessilla very gravelly sandy loam, 20% Rock outcrop, 20% Badland, Celacy, Flugle, Jacee, Catman, and Hickman soils)

Mion-Catman association, 2 to 17% slopes (495) (40% Mion gravelly clay loam, 5 to 17% slopes, 25% Catman clay loam, 2 to 5% slopes, 35% sandstone outcrop, Travessilla, Celacy, Flugle, and Jacee soils)

Pleioville gravelly sandy loam, 3 to 15% slopes (551) (gravelly sandy loam, gravelly clay, gravelly clay loam, very gravelly clay, very gravelly clay loam, conglomerate, with 20% Brycan, Bario, and similar Pleioville soils)

Celacy-Rock outcrop complex, 2 to 9% slopes (592) (45% Celacy loamy sand, 25% Rock outcrop, 30% Jacee, Mion, and Travessilla soils)

Jacee-Mion-Celacy association, 1 to 10% slopes (635) (30% Jacee loam, 30% Mion loam, 20% Celacy loam, 20% Goesling soils and sandstone and shale outcrop)

Hiarc-Loarc-Typic Ustorthents association, 1 to 9% (700) (35% Hiarc sandy loam, 1 to 5% slopes, 25% Loarc fine sandy loam, 1 to 9% slopes, 20% Typic Ustorthents, 1 to 9% slopes, 20% sandstone Rock outcrop and Manzano soils)

Bedrock Deposits--Carbonate/Evaporite Sedimentary

Bedrock Deposits--Volcanic and Metamorphic and Mixed

Cabezon-Thunderbird-Celsosprings complex, 3 to 25% slopes (365) (45% Cabezon cobbly clay loam, 3 to 25% slopes, 25% Thunderbird loam, 3 to 15% slopes, 15% Celsosprings silt loam, 3 to 8% slopes, 15% Apache and similar Cabezon soils, and Rock outcrop)

Cabezon-Rock outcrop complex, 3 to 50% slopes (370) (40% Cabezon cobbly loam, 40% Rock outcrop, 20% Thunderbird and similar Cabezon soils)

Rock outcrop-Aridic Ustochrepts complex, 10 to 25% slopes (387) (40% Rock outcrop, 40% Aridic Ustochrepts, 20% Brycan, Smilo, and Adman soils)

Rudd-Modyon complex, 3 to 15% slopes (390) (40% Rudd gravelly loam, 30% Modyon cobbly loam, 30% Apache and Cabezon soils, Rock outcrop)

Faraway-Motoqua-Rock outcrop complex, 8 to 30% slopes (471) (30% Faraway very stony loam, 25% Motoqua very cobbly loam, 25% Rock outcrop, 20% similar Faraway and Motoqua soils with few rock fragments)

Abrazo-Rock outcrop complex, 15 to 50% slopes (472) (60% Abrazo gravelly loam, 25% Rock outcrop, 15% Apache, Faraway, Motoqua and similar Abrazo soils)

Ustic Torriorthents-Rock outcrop-Badland complex, 20 to 100% slopes (487) (30% Ustic Torriorthents, 30% Rock outcrop, 25% Badland, 15% Hickman, Manzano, Pietown and Majada soils)

Motoqua-Rock outcrop complex, 8 to 30% slopes (555) (60% Motoqua very gravelly loam, 20% Rock outcrop, 20% similar Motoqua, Faraway and Apache soils)

Joachim-Rock outcrop complex, 3 to 15% slopes (575) (50% Joachim gravelly sandy loam, 30% Rock outcrop, 20% Motoqua, Abrazo, and Apache soils)

Abrazo-Apache complex, 2 to 15% slopes (585) (35% Abrazo loam, 2 to 10% slopes, 30% Apache gravelly sandy loam, 6 to 15% slopes, 35% Datil, Motoqua soils and Rock outcrop)

Penistaja-Viuda-Rock outcrop association, 0 to 9% slopes (590) (30% Penistaja sandy loam, 1 to 5% slopes, 25% Viuda gravelly sandy loam, 0 to 3% slopes, 20% Rock outcrop, 0 to 9% slopes, 25% Catman and similar Penistaja soils)

Tolman-Rock outcrop complex, 25 to 60% slopes (606) (45% extremely cobbly loam, 35% Rock outcrop, 25% Coni, Motoqua, and Brycan soils)

Typic Argiborolls-Tolman-Motoqua association, 5 to 60% slopes (612) (35% Typic Argiborolls, 5 to 45% slopes, 25% Tolman extremely cobbly loam, 25 to 60% slopes, 20% Motoqua extremely cobbly loam, 20 to 60% slopes, 20% Brycan, similar Typic Argiborolls, and Rock outcrop)

Coni-Tolman complex, 10 to 40% slopes (625) (50% coni very gravelly sandy loam, 10 to 35% slopes, 30% Tolman cobbly loam, 10 to 40% slopes, 20% Brycan, Adman, Smilo soils and Rock outcrop)

Smilo-Adman complex, moist, 2 to 15% slopes (671) (55% Smilo stony loam, 25% Adman stony loam, 20% Coni and deep clayey soils)

VALENTINE

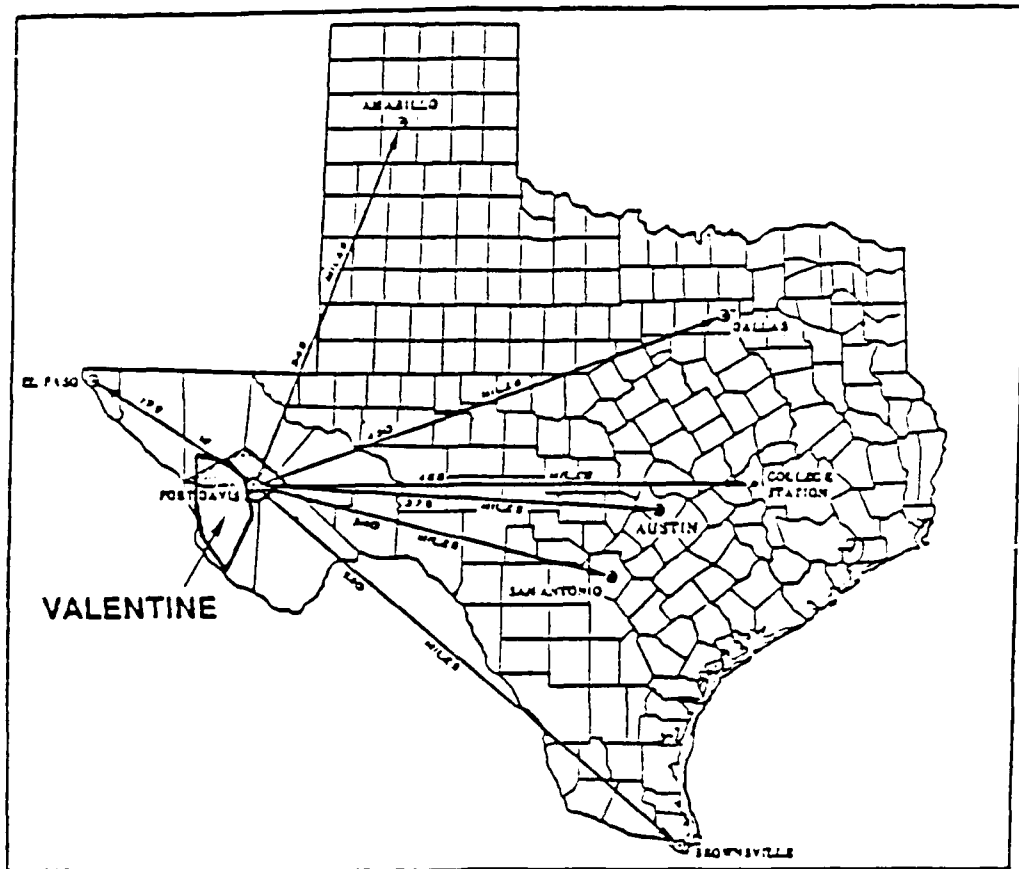


Figure B-4. Map Showing Location of Valentine SOA and Jeff Davis County, Texas.

VALENTINE
Representative Soil Types and Mapped Soil Units
Jeff Davis County, Texas

Soils of Hills and Mountains

- Brewster association (Shallow to very shallow, hilly to steep, noncalcareous soils of arid and semiarid hills; Ann. Rainfall--15")
- Mainstay-Liv-Brewster association (Very shallow to moderately deep, hilly to steep, noncalcareous soils of semiarid hills and mountains; Ann. Rainfall--14" to 20")
- Volco-Brewster-Ector association (Shallow to very shallow, hilly to steep, calcareous to noncalcareous soils of arid and semiarid hills; Ann. Rainfall--7" to 15")
- Puerta-Rock outcrop-Madrone association (Shallow to moderately deep, steep, noncalcareous soils and rock outcrop of semiarid and subhumid hills and mountains; Ann. Rainfall--16" to 22")

Soils of Valleys, Plains, and Basins

- Musquiz-Santo Tomas-Boracho association (Very shallow to deep, nearly level to gently sloping, noncalcareous and calcareous soils of arid and semiarid valleys; Ann. Rainfall--15")
- Redona-Verhalen-Reagan association (Deep, nearly level to gently sloping, calcareous to noncalcareous soils of arid and semiarid valleys and plains; Ann. Rainfall--7" to 14")
- Nickel-Canutio-Vieja association (Very shallow to deep, undulating to hilly, calcareous soils of arid basins; Ann. Rainfall--6" to 10")
- Gageby-Rockhouse association (Deep, nearly level, noncalcareous soils of flood plains; flood plains of the larger streams)

VALENTINE
Descriptions of Soils
Jeff Davis County, Texas

Young Alluvial Fans

Older Alluvial Fans

Boracho Series (gravelly loam, indurated caliche, strongly cemented caliche, very gravelly loam; calcareous)

Boracho-Espy association, gently sloping (BeB) (30% to 70% Boracho gravelly loam, 17% to 40% Espy loam, 0 to 40% similar Boracho soils without caliche, 10% to 30% other soils)

Canutio Series (gravelly loam, very gravelly loam, cobbly loam; calcareous)

Canutio-Badland association, rolling (CbD) (30% to 40% Canutio gravelly loam, 30% to 60% Badland, 10% to 20% Nickel soils and gravelly, stream-washed material)

Canutio-Nickel association, rolling (CID) (60% Canutio gravelly loam, 30% Nickel gravelly loam, 10% gravelly streamwash material; calcareous)

Chispa Series (fine sandy loam, friable sandy clay loam, sandy clay loam, sandy loam; calcareous)

Chispa-Nickel association, undulating (CnC) (68% to 80% Chispa loam, sandy clay loam, 10% to 30% Nickel gravelly loam, gravelly caliche, very gravelly loam, 10% to 30% other soils)

Espy Series (loam, friable clay loam, hard caliche; calcareous)

Hurds Series (gravelly loam, very gravelly sandy clay loam, very gravelly sandy loam, very gravelly loamy sand; slightly acid)

Hurds-Friends association, rolling (HuD) (35% to 45% Hurds gravelly soils, 10% to 30% Friends clayey soils, 10% to 20% Limpia soils, 15% to 25% other soils)

Limpia Series (gravelly loam, firm, very gravelly clay; neutral)

Limpia and Mitre soils, gently sloping (LmB) (40% to 80% Limpia soils, 0 to 40% Mitre soils, and 0 to 30% other soils)

Loghouse Series (mat of leaves and stems, sandy loam, gravelly sandy loam, very gravelly sandy loam; neutral to medium acid)

Loghouse association, rolling (LsD) (30% to 70% Loghouse soils, 20% to 40% dark colored soils, 10% to 30% other soils)

Medley Series (gravelly sandy loam, gravelly loam, calcareous loam; neutral to calcareous)

Mitre Series (gravelly loam, very gravelly clay loam, indurated to strongly cemented caliche; non-calcareous)

Nickel Series (gravelly loam, gravelly caliche, very gravelly loam, lime clayey earth; calcareous)

Nickel-Chispa association, undulating (NcC) (50% to 70% Nickel gravelly loam, 20% to 30% Chispa loam over sandy clay loam, 0 to 20% other soils)

Sanderson Series (gravelly clay loam, gravelly loam; calcareous)

Sanderson-Upton association, undulating (SeC) (30% to 70% Sanderson gravelly loam, 20% to 40% Upton gravelly loam, 10% to 40% other soils)

Santo Tomas Series (very gravelly loam, gravelly loam; calcareous)

Santo Tomas-Medley association, gently sloping (SmB) (20% to 60% Santo Tomas gravelly loam, 30% to 70% Medley loam, 10% to 40% other soils)

Upton Series (gravelly loam, hard caliche--indurated to weakly cemented; calcareous)

Vado Series (gravelly sandy loam, very gravelly sandy loam; calcareous)

Vado-Redona association, undulating (VdC) (50% to 80% Vado soils, 10% to 40% Redona soils, 10% to 40% other soils)

Lacustrine--Modern, Ancient, and Playa Lake Deposits

Verhalen clay, depressional (Vh) (dry lake beds, clay)

Other Basin Deposits

Gullied Land (Gu) (50% eroded soils, 50% slightly eroded soils)

Fluvial Deposits

Anthony Series (fine sandy loam, loamy sand, sandy loam, gravelly sand; calcareous)

Anthony and Glendale Soils (Ag) (Flood plains, 30% to 70% Anthony loam and fine sandy loam, 0 to 50% Glendale loam and clay loam, 5% to 10% gravelly and stony stream-washed material, and 10% to 30% other soils)

Gageby Series (silt loam, friable clay loam, friable loam; neutral to calcareous)

Gageby association (Ga) (Flood plains, 80% to 90% Gageby soils, 0 to 20% other soils)

Glendale Series (loam, friable clay loam; calcareous)

Phantom Series (clay loam, firm clay loam, very firm silty clay loam; calcareous)

Phantom association (Ph) (60% to 90% Phantom soils, 10% to 30% Hodgins soils, 10% to 20% other soils)

Rockhouse Series (loam, very cobbly loamy sand, very cobbly sand; noncalcareous)

Rockhouse association (Rh) (70% to 100% Rockhouse soils, 0 to 30% Gageby soils)

Rockhouse-Gageby association (Rk) (33% to 80% Rockhouse soils, 10% to 40% Gageby soils, 5% to 20% gravelly and stony stream-washed material, 5% to 30% other soils)

Glacial Deposits

Other Alluvium

Dalby Series (clay, very firm clay, silty clay; calcareous)

Friends Series (fine sandy loam, friable loam, clay; slightly acid, noncalcareous)

Hodgins Series (clay loam, friable clay loam, silty clay; calcareous)

Hodgins clay loam, 0 to 1% slopes (HoA) (clay loam, silty clay)

Ima Series (fine sandy loam, gravelly sand; calcareous)

Ima-Hodgins association, gently sloping (IhB) (60% to 80% Ima fine sandy loam, 10% to 40% Hodgins fine sandy loam, loam, clay loam, silty clay, 0 to 30% other soils)

Musquiz Series (loam, clay, clay loam; mildly alkaline)

Musquiz association (Mu) (50% to 70% Musquiz soils, 10% to 30% similar but thicker soils, 0 to 40% other soils)

Reagan Series (clay loam; calcareous)

Reagan-Hodgins association (Rd) (0 to 50% Reagan soils, 10% to 50% Hodgins soils, 30% to 50% other soils)

Redona Series (sandy loam, sandy clay loam, clay loam, loam, gravelly sand; neutral, mildly alkaline to calcareous)

Redona association (Re) (40% to 80% Redona soils, 20% to 60% other soils)

Verhalen Series (clay, very firm clay, friable clay loam; calcareous)

Verhalen clay (Ve) (clay, very firm clay, friable clay loam; calcareous)

Verhalen-Dalby association (Vm) (50% to 80% Verhalen soils, 20% to 30% Dalby soils, 0 to 20% other soils)

Bedrock Deposits--Clastic Sedimentary

Vieja Series (silty clay, clayey shale; moderately alkaline, calcareous)

Vieja-Nickel association, hilly (VnE) (50% to 70% Vieja soils, 30% to 40% Nickel soils, 10% to 20% other soils and land types)

Bedrock Deposits--Carbonate/Evaporite Sedimentary

Ector Series (gravelly loam over limestone bedrock; calcareous)

Ector association, hilly (EcE) (50% to 75% Ector gravelly loam, 0 to 20% Rock outcrop, 10% to 40% other soils)

Lozier Series (gravelly loam over limestone bedrock)

Lozier association, undulating (LtC) (50% to 80% Lozier soils, 0 to 30% Ector soils, 0 to 20% Rock outcrop, 10% to 20% other soils)

Lozier-Rock outcrop association, hilly (LuE) (50% to 70% Lozier soils, 20% to 40% Rock outcrop, 0 to 20% other soils)

Bedrock Deposits--Volcanic and Metamorphic and Mixed

Badland (Bd) (Young, deeply dissected rock surfaces--lava ash and tuff; 70% to 90% volcanic ash, 10% to 20% gravelly and stony, washed material, 10% to 20% Nickel gravelly soils)

Brewster Series (gravelly loam, fractured rhyolite bedrock; neutral)

Brewster-Rock outcrop association, steep (BrF) (40% to 50% Brewster stony loam, 20% to 50% igneous Rock outcrop, 10% to 30% other soils)

Brewster association, hilly (BsE) (40% to 80% Brewster stony loam, 0 to 10% Rock outcrop, 0 to 40% other soils over igneous rock)

Kokernot Series (gravelly sandy loam, gravelly loam, gravelly clay loam, volcanic bedrock)

Kokernot-Brewster association, gently sloping (KbB) (40% to 75% Kokernot loam, 25% to 50% Brewster stony loam, 0 to 20% other soils)

Liv Series (cobbley silt loam, gravelly clay, tuffaceous rock; neutral)

Liv-Mainstay-Rock outcrop association, steep (LrF) (20% to 40% Liv cobbley silt loam, 10% to 20% Mainstay cobbley silt loam, 20% to 40% Rock outcrop, 10% to 50% other soils)

Madrone Series (cobbley silt loam, cobbley loam, cobbley clay, fractured igneous bedrock; neutral to strongly acid)

Mainstay Series (cobbley silt loam, firm gravelly clay, igneous bedrock; neutral)

Mainstay-Brewster association, hilly (MbE) (20% to 40% Mainstay soils, 10% to 40% Brewster gravelly loam, 10% to 30% Liv soils, 10% to 30% other soils and Rock outcrop)

Puerta Series (gravelly silt loam, gravelly loam, gravelly clay, fractured igneous bedrock; neutral to strongly acid)

Puerta-Madrone association, steep (PmF) (30% to 50% Puerta soils, 20% to 40% Madrone soils, 10% to 30% other soils, 5% to 10% Rock outcrop)

Rock Outcrop (igneous rock masses and rubble piles)

Rock outcrop-Brewster association, steep (RoF) (50% to 90% igneous Rock outcrop, 10% to 40% Brewster soils, 0 to 20% other soils)

Sproul Series (clay loam, very firm clay, clay, strongly cemented tuffaceous bedrock; slightly acid)

Sproul-Mainstay association, gently sloping (SnB) (50% to 70% Sproul soils, 20% to 40% Mainstay soils, 10% to 20% other soils)

Volco Series (gravelly loam, friable gravelly loam, platy igneous bedrock; calcareous)

Volco association, hilly (VoE) (60% to 80% Volco gravelly loam, 10% to 30% Brewster stony loam, 10% to 20% other soils or Rock outcrop)

WHITE SANDS

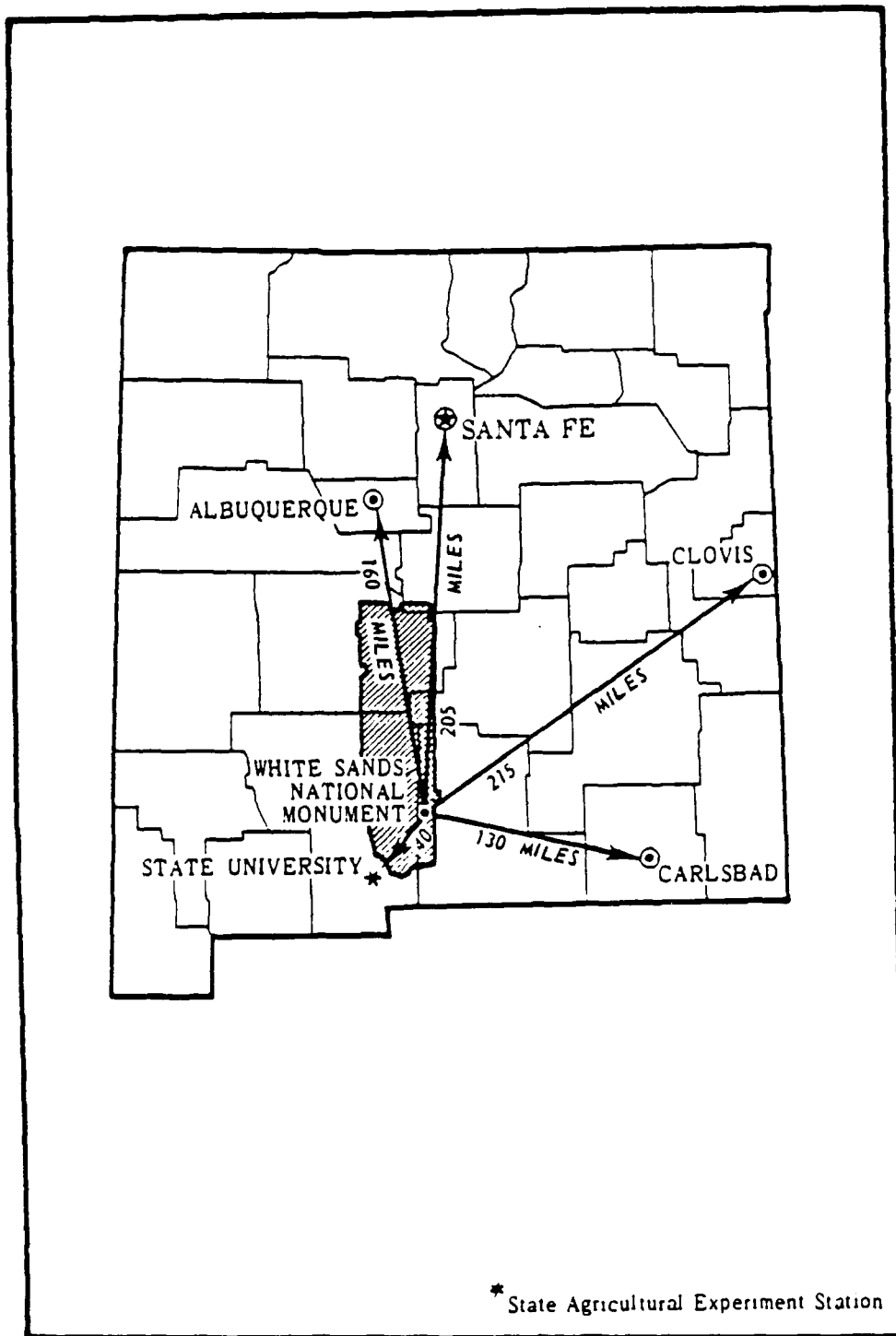


Figure B-5. Map showing location of White Sands Missile Range in New Mexico.

WHITE SANDS
Representative Soil Types and Mapped Soil Units
White Sands Missile Range, New Mexico

Young Alluvial Fans

- Aladdin Series (gravelly loamy sand; neutral)
- Aladdin association (AD) (30% Aladdin, 55% Pinaleno)
- Berino Series (sandy loam/sandy clay loam/loamy sand; calcareous below 2')
- Bluepoint Series (highly permeable loamy fine sand; slight to mod. calcareous)
- Mimbres Series (silt loam/clay loam/silty clay loam; strongly calcareous)
- Mimbres-Glendale association (MG) (55% Mimbres silt loam, 25% Glendale silt loam)

Older Alluvial Fans

- Alicia Series, High Gypsum Substratum Variant (loam/clay loam; calcareous)
- Berino-Dona Ana association (BD) (50% Berino sandy loam, 30% Dona Ana sandy loam)
- Dona Ana Series (sandy loam/clay loam; calcareous)
- Dona Ana-Pajarito-Bluepoint association (DP) (30% Dona Ana sandy loam, 30% Pajarito sandy loam, 25% Bluepoint loamy fine sand)
- Glendale Series (silt loam; strongly calcareous)
- La Fonda Series (loam/clay loam; non- to slight calcareous)
- La Fonda association (LA) (45% La Fonda loam, 40% Alicia loam, high gypsum substratum variant)
- Nickel Series (gravelly fine sandy loam/gravelly loam/very gravelly loam; strongly calcareous)
- Nickel-Tencee association (NT) (60% Nickel gravelly fine sandy loam, 25% Tencee very gravelly loam)
- Onite Series (loamy fine sand/sandy loam/fine sandy loam; calcareous)
- Onite-Bluepoint-Wink association (40% Onite loamy fine sand, 25% Bluepoint fine sand, 20% Wink loamy fine sand)
- Pajarito Series (sandy loam/loamy fine sand; mod. calcareous)
- Pinaleno Series (gravelly sandy loam/gravelly sandy clay loam/very gravelly heavy sandy loam/very gravelly sandy loam; calcareous)
- Russler Series (silt loam/clay loam/silty clay loam/gravelly sandy loam; calcareous)
- Sonoita Series (gravelly sandy loam/gravelly sandy clay loam; calcareous below 1 m)

Sonoita-Pinaleno-Aladdin association (SP) (35% Sonoita gravelly sandy loam, 25% Pinaleno gravelly sandy loam, 20% Aladdin gravelly loamy sand)

Sotim Series (clay loam/gravelly sandy loam; calcareous)

Sotim-Russler association (SR) (60% Sotim clay loam, 25% Russler silt loam)

Tencee Series (very gravelly loam/gravelly loam/indurated caliche; calcareous)

Tencee-Nickel association, gently sloping (TC) (65% Tencee very gravelly loam, 20% Nickel gravelly fine sandy loam)

Tencee-Nickel association, steep (TK) (45% Tencee very gravelly loam, 40% Nickel gravelly fine sandy loam)

Wink Series (loamy fine sand/sandy loam/fine sandy loam; calcareous)

Ancient and Playa Lake Deposits

Gypsum Land (saline, white, chalky earth)

Gypsum land, hummocky (GS) (very fine sandy loam/gypsum beds)

Gypsum land, level (GU) (gypsum over lacustrine sediments, shallow water table)

Gypsum rock land (GV) (50% Gypsum rock land, 35% Rance gravelly loam, shallow variant)

Holloman Series (very fine sandy loam over finely divided gypsum; mod. calcareous)

Marcial Series (heavy silty clay loam/ silty clay/ gypsum; strongly calcareous and saline)

Marcial-Ubar association (MA) (55% Marcial silty clay loam, 35% Ubar silt loam)

Mead Series (silt loam/heavy clay loam/clay over lacustrine material; mod. to slightly calcareous, saline; shallow water in summer rainy season)

Mead silt loam (ME) (saline-alkali soil over lacustrine sediments)

Ubar Series (silt loam/heavy silty clay loam/silty clay; saline and alkali affected)

Other Basin Deposits

Active Dune Land, Gypsum (gypsum sand dunes)

Dune Land (sand dunes)

Dune land-Dona Ana complex (DU) (40% Dune land, 25% Dona Ana sandy loam, 20% Bluepoint loamy fine sand)

Dune land-Yesum association (DY) (55% Dune land, 30% Yesum very fine sandy loam)

Yesum Series (very fine sandy loam/fine sandy loam; slightly calcareous)

Yesum very fine sandy loam (YE)

Yesum-Holloman association (YH) (35% Yesum very fine sandy loam, 30% Holloman very fine sandy loam, 20% Gypsum land, hummocky)

Fluvial Deposits

Mimbres Series (silt loam/clay loam/silty clay loam; strongly calcareous)

Oscura Series (silty clay/clay/heavy silty clay loam/very fine sandy loam; mod. calcareous)

Oscura silty clay (OS) (flood plains of intermittent waterways)

Glacial Deposits

Other Alluvium

Bedrock Deposits--Clastic Sedimentary

Gilland Series (stony loam/weathered shale over sandstone)

Gilland-Rock outcrop complex (GR) (40% Gilland stony loam, 35% Rock outcrop)

Shale Rock Land (SH) (35% barren shale outcrop, 35% stony land, 15% very shallow and shallow soils)

Bedrock Deposits--Carbonate/Evaporite Sedimentary

Deama Series (stony loam/limestone)

Deama-Rock outcrop complex (DO) (40% Deama stony loam, 40% Rock outcrop)

Lozier Series (stony loam/limestone)

Lozier-Rock outcrop complex (LR) (45% Lozier stony loam, 35% Rock outcrop)

Rance Series, Shallow Variant (gravelly loam/loam over hard gypsum bedrock; slightly to mod. calcareous)

Bedrock Deposits--Volcanic and Metamorphic and Mixed

Lava Flows (LF) (geologically recent basalt)

Pinaleno Series, Noncalcareous Variant (gravelly sandy loam/gravelly clay loam/very gravelly sandy clay loam/weathered granitic bedrock)

Rock Land (35% barren rock outcrop, 30% stony land, 20% shallow and very shallow soils)

Rock land, cool (RK) (limestone, acid igneous rock, sandstone, basalt, shale, and gypsum)

Rock land, warm (RL) (limestone, acid igneous rock, sandstone, basalt, shale, gypsum)

APPENDIX C - GLOSSARY OF SOILS AND GEOLOGICAL TERMS

Definitions are from the reports of the United States Soils Conservation Service.

Aeolian soil material--Earthy parent material accumulated through wind action; commonly refers to sandy material in dunes or to loess in blankets on the surface.

Aggregate, soil--Many fine particles held in a single mass or cluster. Natural soil aggregates, such as granules, blocks, or prisms, are called peds. Clods are aggregates produced by tillage or logging.

Alkali (sodic) soil--A soil having so high a degree of alkalinity (pH 8.5 or higher), or so high a percentage of exchangeable sodium (15% or more of the exchangeable bases), or both, that plant growth is restricted.

Alluvial fan--The fanlike deposit of a stream where it issues from a gorge upon a plain or of a tributary stream near or at its junction with its main stream.

Alluvium--Material, such as sand, silt, or clay, deposited on land by streams.

Arroyo--The flat-floored channel of an ephemeral stream, commonly with very steep to vertical banks cut in alluvium.

Association, soil--A group of soils geographically associated in a characteristic repeating pattern and defined and delineated as a single map unit.

Back slope--The geomorphic component that forms the steepest inclined surface and principal element of many hillsides. Back slopes in profile are commonly steep, are linear, and may or may not include cliff segments.

Badland--Steep or very steep, commonly nonstony barren land dissected by many intermittent drainage channels. Badland is most common in semiarid and arid regions where streams are entrenched in soft geologic material. Local relief generally ranges from 25 to 500 feet. Runoff potential is very high, and geologic erosion is active.

Bajada--A broad alluvial slope extending from the base of a mountain range out into a basin and formed by coalescence of separate alluvial fans.

Bedding planes--Fine stratifications, less than 5 millimeters thick, in unconsolidated alluvial, aeolian, lacustrine, or marine sediments.

Bedrock--The solid rock that underlies the soil and other unconsolidated material or that is exposed at the surface.

Bottom land--The normal flood plain of a stream, subject to frequent flooding.

Boulders--Rock fragments larger than 2 feet (60 centimeters) in diameter.

Butte--An isolated small mountain or hill with steep or precipitous sides and a top variously flat, rounded, or pointed that may be a residual mass isolated by erosion or an exposed volcanic neck.

Calcareous soil--A soil containing enough calcium carbonate (commonly with magnesium carbonate) to effervesce (fizz) visibly when treated with cold, dilute hydrochloric acid. A soil having measurable amounts of calcium carbonate or magnesium carbonate.

Caliche--A more or less cemented deposit of calcium carbonate in soils of warm-temperate, subhumid to arid areas. Caliche occurs as soft, thin layers in the soil or as hard, thick beds just beneath the solum, or it is exposed at the surface by erosion.

Canyon--A long, deep, narrow, very steep sided valley with high, precipitous walls in an area of high local relief.

Cemented pan--Strongly cemented or indurated caliche layer.

Clay--As a soil separate, the mineral soil particles less than 0.002 millimeter in diameter. As a soil textural class, soil material that is 40% or more clay, less than 45% sand, and less than 40% silt.

Clay film--A thin coating of oriented clay on the surface of a soil aggregate or lining pores

or root channels. Synonyms: clay coat, clay skin.

Coarse fragments--Mineral or rock particles up to 3 inches (2 millimeters to 7.5 centimeters) in diameter.

Coarse textured (light textured) soil--Sand or loamy sand.

Cobble (or cobblestone)--A rounded or partly rounded fragment of rock 3 to 10 inches (7.6 to 25 centimeters) in diameter.

Cobbly soil material--Material that is 15% to 35%, by volume, rounded or partially rounded rock fragments 3 to 10 inches (7.5 to 25 centimeters) in diameter. Very cobbly soil material is 35% to 60% of these rock fragments, and extremely cobbly soil material is more than 60%.

Colluvium--Soil material, rock fragments, or both moved by creep, slide, or local wash and deposited at the bases of steep slopes.

Concretions--Grains, pellets, or nodules of various sizes, shapes, and colors consisting of concentrated compounds or cemented soil grains. The composition of most concretions is unlike that of the surrounding soil. Calcium carbonate and iron oxide are common compounds in concretions.

Conglomerate--A coarse grained, clastic rock composed of rounded to subangular rock fragments more than 2 millimeters in diameter. It commonly has a matrix of sand and finer

material. Conglomerate is the consolidated equivalent of gravel.

Coppice dunes--Mounds of aeolian or wind-deposited material around desert shrubs; dunes average 3 to 8 feet in height.

Corrosive--High risk of corrosion to uncoated steel or deterioration of concrete.

Cuesta--An asymmetric, homoclinal ridge capped by resistant rock layers of slight to moderate dip.

Desert pavement--A layer of gravel or coarser fragments on a desert soil surface that was emplaced by upward movement of fragments from underlying sediments or remains after finer particles have been removed by running water or wind.

Dip slope--A slope of the land surface, roughly determined by and approximately conforming with the dip of underlying bedded rock.

Drainage, surface--Runoff, or surface flow of water from an area.

Draw--A small stream valley, generally more open and with broader bottom land than a ravine or gulch.

Dune land--Land consisting of sand in ridges and intervening troughs that shifts with the wind.

Ephemeral stream--A stream, or reach of a stream, that flows only in direct response to

precipitation. It receives no long-continued supply from melting snow or other source, and its channel is above the water table at all times.

Erosion--The wearing away of the land surface by running water, wind, ice, or other geologic agents and by such processes as gravitational creep.

Erosion (geologic)--Erosion caused by geologic processes acting over long geologic periods and resulting in the wearing away of mountains and the building up of such landscape features as flood plains and coastal plains. Synonym: natural erosion.

Erosion (accelerated)--Erosion much more rapid than geologic erosion, mainly as a result of the activities of man or other animals or of a catastrophe in nature, for example, fire, that exposes a bare surface.

Erosion (sheet)--Erosion caused by water moving more or less uniformly over the land surface.

Escarpment--A relatively continuous and steep slope or cliff breaking the general continuity of more gently sloping land surfaces and produced by erosion or faulting. Synonym: scarp.

Excess alkali--Excess exchangeable sodium. The resulting poor physical properties restrict the growth of plants.

Fan terrace--A relict alluvial fan, no longer a site of active deposition, incised by younger and lower alluvial surfaces.

Fine textured (heavy textured) soil--Sandy clay, silty clay, and clay.

Flooding--The temporary covering of soil with water from overflowing streams, runoff from adjacent slopes, and tides. Frequency, duration, and probable dates of occurrence are estimated. Frequency is expressed as none, rare, occasional, and frequent. *None* means that flooding is not probable; *rare* that it is unlikely but possible under unusual weather conditions; *occasional* that it occurs on an average of once or less in 2 years; and *frequent* that it occurs on an average of more than once in 2 years. Duration is expressed as *very brief* if less than 2 days, *brief* if 2 to 7 days, and *long* if more than 7 days. Probable dates are expressed in months; *November-May*, for example, means that flooding can occur during the period November through May. Water standing for short periods after rainfall or commonly covering swamps and marshes is not considered flooding.

Flood plain--A nearly level alluvial plain that borders a stream and is subject to flooding unless protected artificially.

Foot slope--The inclined surface at the base of a hill.

Fragipan--A loamy, brittle, subsurface horizon that is very low in organic-matter content and clay but is rich in silt or very fine sand. The layer is seemingly cemented. When dry, it is hard or very hard and has a high bulk density in comparison with the horizon or horizons above it. When moist, the fragipan tends to

rupture suddenly if pressure is applied, rather than to deform slowly. The layer is generally mottled, is slowly or very slowly permeable to water, and has few or many bleached fracture planes that form polygons. Fragipans are a few inches to several feet thick; they generally occur below the B horizon, 15 to 40 inches below the surface.

Friability--Term for the ease with which soil crumbles. A friable soil is one that crumbles easily.

Gravel--Rounded or angular fragments of rock as much as 3 inches (2 millimeters to 7.6 centimeters) in diameter. An individual piece is a pebble.

Gravelly soil material--Material from 15% to 50%, by volume, rounded or angular rock fragments, not prominently flattened, up to 3 inches (7.5 centimeters) in diameter.

Ground water (geology)--Water filling all the unblocked pores of underlying material below the water table, which is the upper limit of saturation.

Gully--A miniature valley with steep sides cut by running water and through which water ordinarily runs only after rains. The distinction between gully and rill is one of depth. A gully generally is an obstacle to farm machinery and is too deep to be obliterated by normal tillage; a rill is of lesser depth and can be smoothed over by ordinary tillage. V-shaped gullies result if the material is more difficult to erode with depth; whereas U-shaped gullies result if

the lower material is more easily eroded than that above it.

Gypsum--Hydrous calcium sulphate.

Hardpan--A hardened or cemented soil horizon, or layer. The soil material is sandy, loamy, or clayey and is cemented by iron oxide, silica, calcium carbonate, or other substance.

Hill--A natural elevation of the land surface, rising as much as 1,000 feet above surrounding lowlands, commonly of limited summit area and having a well-defined outline; hillsides generally have slopes of more than 15%. The distinction between a hill and a mountain is arbitrary and is dependent on local usage.

Hogback--A sharp-crested, symmetrical (homoclinal) ridge formed by highly tilted, resistant rock layers; produced by differential erosion of interlayered resistant and weak rocks and have dips of more than about 25 degrees (45%).

Horizon, soil--A layer of soil, approximately parallel to the surface, having distinct characteristics produced by soil-forming processes. The major horizons of mineral soil are as follows:

O horizon--An organic layer, fresh and decaying, plant residue, at the surface of a mineral soil.

A horizon--The mineral horizon, formed or forming at or near the surface, in which an accumulation of humified organic matter is mixed with the mineral material. Also, a

plowed surface horizon most of which was originally part of a B horizon.

A₂ horizon--A mineral horizon, mainly a residual concentration of sand and silt high in content of resistant minerals as a result of the loss of silicate clay, iron, aluminum, or a combination of these.

B horizon--The mineral horizon below an A horizon. The B horizon is in part a layer of change from the overlying A to the underlying C horizon. The B horizon also has distinctive characteristics caused (1) by accumulation of clay, sesquioxides, humus, or a combination of these; (2) by prismatic or blocky structure; (3) by redder or browner colors than those in the A horizon; or (4) by a combination of these. The combined A and B horizons are generally called the solum, or true soil. If a soil lacks a B horizon, the A horizon alone is the solum.

C horizon--The mineral horizon or layer, excluding indurated bedrock, that is little affected by soil-forming processes and does not have the properties typical of the A or B horizon. The material of a C horizon may be either like or unlike that from which the solum is presumed to have formed. If the material is known to differ from that in the solum the Roman numeral II precedes the letter C.

Rock layer--Consolidated rock beneath the soil. The rock commonly underlies a C horizon, but can be directly below an A or a B horizon.

Humus--The well-decomposed, more or less stable part of the organic matter in mineral soils.

Igneous rock--Rock formed by solidification from molten or partially molten state. Major

varieties include plutonic and volcanic rock. Examples are andesite, basalt, and granite.

Impervious soil--A soil through which water, air, or roots, penetrate slowly or not at all. No soil is absolutely impervious to air and water all the time.

Karst (topography)--The relief of an area underlain by limestone that dissolves in differing degrees, thus forming numerous depressions or small basins.

Knoll--A small, low, rounded hill rising above adjacent landforms.

Lacustrine deposit (geology)--Material deposited in lake water and exposed when the water level is lowered or the elevation of the land is raised.

Landscape--All the characteristics that distinguish a certain kind of area on the earth's surface and give it a distinguishing pattern in contrast to other kinds of areas. Any one kind of soil is said to have a characteristic natural landscape, and under different uses it has one or more characteristic cultural landscapes.

Leaching--The removal of soluble material from soil or other material by percolating water.

Lime concretion--An aggregate cemented by the precipitation of calcium carbonate (CaCO_3).

Loam--Soil material that is 7% to 27% clay particles, 28% to 50% silt particles, and less than 52% sand particles.

Loess--Fine grained material, dominantly of silt-size particles, deposited by wind.

Medium textured soil--Very fine sandy loam, loam, silt loam, or silt.

Mesa--A broad, nearly flat topped and commonly isolated upland mass characterized by summit widths that are more than the heights of bounding erosional scarps.

Metamorphic rock--Rock of any origin altered in mineralogical composition, chemical composition, or structure by heat, pressure, and movement. Nearly all such rocks are crystalline.

Meteoric water--That which occurs in or is derived from the atmosphere. (American Geological Institute, 1976)

Mineral soil--Soil that is mainly mineral material and low in organic material. Its bulk density is more than that of organic soil.

Moderately coarse textured (moderately light textured) soil--Sandy loam and fine sandy loam.

Moderately fine textured (moderately heavy textured) soil--Clay loam, sandy clay loam, and silty clay loam.

Morphology, soil--The physical makeup of the soil, including the texture, structure, porosity, consistence, color, and other physical, mineral, and biological properties of the various horizons, and the thickness and arrangement of those horizons in the soil profile.

Mottling, soil--Irregularly marked with spots of different colors that vary in number and size. Mottling in soils usually indicates poor aeration and lack of drainage. Descriptive terms are as follows: abundance--*few*, *common*, and *many*; size--*fine*, *medium*, and *coarse*; and contrast--*faint*, *distinct*, and *prominent*. The size measurements are these: *fine*, less than 5 millimeters (about 0.2 inch) in diameter along the greatest dimension; *medium*, ranging from 5 millimeters to 15 millimeters (about 0.2 to 0.6 inch) in diameter along the greatest dimension; and *coarse*, more than 15 millimeters (about 0.6 inch) in diameter along the greatest dimension.

Mountain--A natural elevation of the land surface, rising more than 1,000 feet above surrounding lowlands, commonly of restricted summit area (relative to a plateau) and generally having steep sides and considerable bare-rock surface. A mountain can occur as a single, isolated mass or in a group forming a chain or range.

Muck--Dark, finely divided, well-decomposed organic soil material (see Sapric soil material).

Mudstone--Sedimentary rock formed by induration of silt and clay in approximately equal amounts.

Neutral soil--A soil having a pH value between 6.6 and 7.3 (See Reaction, soil).

Organic matter--Plant and animal residue in the soil in various stages of decomposition.

Outwash plain--A landform of mainly sandy or coarse textured material of glaciofluvial origin. An outwash plain is commonly smooth; where pitted, it is generally low in relief.

Pan--A compact, dense layer in a soil that impedes the movement of water and the growth of roots. For example, *hardpan*, *fragipan*, *claypan*, *plowpan*, and *traffic pan*.

Parent material--The great variety of unconsolidated organic and mineral material in which soil forms. Consolidated bedrock is not yet parent material by this concept.

Ped--An individual natural soil aggregate, such as a crumb, a prism, or a block, in contrast to a clod.

Pediment--Gently inclined planate erosion surfaces carved in bedrock and generally veneered with fluvial gravel. (AGI, 1976)

Permeability--The quality that enables the soil to transmit water or air, measured as the number of inches per hour that water moves through the soil. Terms describing permeability are *very slow* (less than 0.06 inch), *slow* (0.06 to 0.20 inch), *moderately slow* (0.20 to 0.6 inch), *moderate* (0.6 to 2.0 inches), *moderately rapid* (2.0 to 6.0 inches), *rapid* (6.0

to 20 inches), and *very rapid* (more than 20 inches).

Phase, soil--A subdivision of a soil series or other unit in the soil classification system based on differences in the soil that affect its management. A soil series, for example, may be divided into phases on the bases of differences in slope, stoniness, thickness, or some other characteristic that affects management. These differences are too small to justify separate series.

pH value--(See Reaction, soil)--A numerical designation of acidity and alkalinity in soil.

Plateau--An extensive upland mass with relatively flat summit area that is considerably elevated (more than 100 meters) above adjacent lowlands and separated from them on one or more sides by escarpments.

Ponding--Standing water on soils in closed depressions. The water can be removed only by percolation or evapotranspiration.

Poorly graded--Refers to a coarse grained soil or soil material consisting mainly of particles of nearly the same size. Because there is little difference in size of the particles, density can be increased only slightly by compaction. Synonym: Well sorted.

Pores--Space not occupied by soil particles or coarse fragments in a bulk volume of soil. Types of pores are:

Interstitial--Irregularly shaped pores that have faces that are curved inward; formed by curved

or angular faces of adjacent mineral grains, peds, or both;

Tubular--Pores that are more or less cylindrical in shape and elongated in one direction;

Vesicular--Pores that are roughly spherical or ellipsoidal in shape and are not appreciably elongated in any direction.

Numbers of pores are expressed as:

Few	1 to 3 per square inch
Common	4 to 14 per square inch
Many	More than 14 per square inch

Porosity, soil--The degree to which the soil mass is permeated with pores or cavities.

Profile, soil--A vertical section of the soil extending through all its horizons and into the parent material.

Reaction, soil--The degree of acidity or alkalinity of a soil, expressed in pH values. A soil that tests to pH 7.0 is described as precisely neutral in reaction because it is neither acid nor alkaline. The degree of acidity or alkalinity is expressed as:

	pH
Extremely acid	Below 4.5
Very strongly acid	4.5 to 5.0
Strongly acid	5.1 to 5.5
Medium acid	5.6 to 6.0
Slightly acid	6.1 to 6.5
Neutral	6.6 to 7.3
Mildly alkaline	7.4 to 7.8
Moderately alkaline	7.9 to 8.4
Strongly alkaline	8.5 to 9.0
Very strongly alkaline	9.1 and higher

Red Beds--Sedimentary strata mainly red in color and composed largely of sandstone and shale.

Regolith--The unconsolidated mantle of weathered rock and soil material on the earth's surface; the loose earth material above the solid rock.

Relief--The elevations or inequalities of a land surface, considered collectively.

Residuum (residual soil material)--Unconsolidated, weathered, or partly weathered mineral material that accumulates over disintegrating rock.

Ridge--A long, narrow elevation of the land surface. It commonly is sharp-crested, has steep sides, and forms an extended upland between valleys. The term is used in areas of both hill and mountain relief (less than and more than 300 meters, respectively).

Rock fragments--Rock or mineral fragments having a diameter of 2 millimeters or more; for example, pebbles, cobbles, stones, and boulders.

Rubble land--Land consisting of areas of stones and boulders. Rubble land commonly is at the base of mountains, but some areas are deposits of cobbles, stones, and boulders left on mountainsides by glaciation or by periglacial processes.

Runoff--The precipitation discharged in stream channels from a drainage area. The water that

flows off the land surface without sinking in is called surface runoff; that which enters the ground before reaching surface streams is called ground-water runoff or seepage flow from ground water.

Saline-alkali soil--A soil that contains a harmful concentration of salts and exchangeable sodium; contains harmful salts and is strongly alkaline; or contains harmful salts and exchangeable sodium and is very strongly alkaline. The salts, exchangeable sodium, and alkaline reaction are in the soil in such location that growth of most crop plants is less than normal.

Sand--As a soil separate, individual rock or mineral fragments from 0.05 millimeter to 2.0 millimeters in diameter. Most sand grains consist of quartz. As a soil textural class, a soil that is 85% or more sand and not more than 10% clay.

Sandstone--Sedimentary rock containing dominantly sand-size particles.

Sapric soil material (muck)--The most highly decomposed of all organic soil material. Muck has the least amount of plant fiber, the highest bulk density, and the lowest water content at saturation of all organic soil material.

Sedimentary rock--Rock made up of particles deposited from suspension in water. The chief kinds of sedimentary rock are conglomerate, formed from gravel; sandstone, formed from sand; shale, formed from clay; and limestone, formed from soft masses of calcium carbonate.

There are many intermediate types. Some wind-deposited sand is consolidated into sandstone.

Seepage--The rapid movement of water through the soil. Seepage adversely affects the specified use.

Series, soil--A group of soils, formed from a particular type of parent material, having horizons that, except for the texture of the A or surface horizon, are similar in all profile characteristics and in arrangement in the soil profile. Among these characteristics are color, texture, structure, reactions, consistence, and mineralogical and chemical composition.

Shale--Sedimentary rock formed by hardening of a clay deposit.

Shoulder (hillslope)--The geomorphic component that forms the uppermost inclined surface at the top of a hillslope. It comprises the transition zone from the back slope to the summit of an upland. The surface is dominantly convex in profile and erosional in origin.

Silica--Silica is a combination of silicon and oxygen. The mineral form is called quartz.

Silt--As a soil separate, individual mineral particles that range in diameter from the upper limit of clay (0.0002 millimeter) to the lower limit of very fine sand (0.05 millimeter). As a soil textural class, soil that is 80% or more silt and less than 12% clay.

Siltstone--Sedimentary rock made up of dominantly silt-sized particles.

Sinkhole--A depression in the landscape where limestone has been dissolved.

Slope--The inclination of the land surface from the horizontal. Percentage of slope is the vertical distance divided by horizontal distance, then multiplied by 100. Thus, a slope of 20% is a drop of 20 feet in 100 feet of horizontal distance.

Soil--A natural, three-dimensional body on the earth's surface that supports plants and that has properties resulting from the integrated effect of climate and living matter acting on earthy parent material, as conditioned by relief over periods of time.

Soil separates--Mineral particles less than 2 millimeters in equivalent diameter and ranging between specified size limits. The names and sizes of separates recognized in the United States are as follows: *very coarse sand* (2.0 millimeters to 1.0 millimeter); *coarse sand* (1.0 millimeter to 0.5 millimeter); *medium sand* (0.5 millimeter to 0.25 millimeter); *fine sand* (0.25 millimeter to 0.10 millimeter); *very fine sand* (0.10 millimeter to 0.05 millimeter); *silt* (0.05 millimeter to 0.002 millimeter); *clay* (less than 0.002 millimeter).

Solum--The upper part of a soil profile, above the C horizon, in which the processes of soil formation are active. The solum in mature soil consists of the A and B horizons. Generally, the characteristics of the material in these

horizons are unlike those of the underlying material. The living roots and other plant and animal life characteristics of the soil are largely confined to the solum.

Stones--Rock fragments 10 to 24 inches (25 to 60 centimeters) in diameter if rounded or 6 to 15 inches (15 to 38 centimeters) in length if flat.

Stratified--Arranged in strata, or layers. The term refers to geologic material. Layers in soils that result from the processes of soil formation are called horizons; those inherited from the parent material are called strata.

Structure, soil--The arrangement of primary soil particles into compound particles or aggregates that are separated from adjoining aggregates. The principal forms of soil structure are *platy* (laminated, *prismatic* (vertical axis of aggregates longer than horizontal), *columnar* (prisms with rounded tops), *blocky* (angular or subangular), and *granular*. *Structureless* soils are either *single grained* (each grain by itself, as in dune sand) or *massive* (the particles adhering without any regular cleavage, as in many hardpans).

Subsoil--Technically, the B horizon; roughly, the part of the solum below plow depth.

Substratum--The part of the soil below the solum.

Tectonic--Of, pertaining to, or designating the rock structure and external forms resulting

from deformation of the earth's crust. (American Geological Institute, 1976)

Terrace (geologic)--An old alluvial plain, ordinarily flat or undulating, bordering a river, a lake, or the sea. A stream terrace is frequently called a second bottom, in contrast with a flood plain, and is seldom subject to overflow. A marine terrace, generally wide, was deposited by the sea.

Texture, soil--The relative proportions of sand, silt, and clay particles in a mass of soil. The basic textural classes, in order of increasing proportion of fine particles, are *sand*, *loamy sand*, *sandy loam*, *loam*, *silt*, *silt loam*, *sandy clay loam*, *clay loam*, *silty clay loam*, *sandy clay*, *silty clay*, and *clay*. The sand, loamy sand, and sandy loam classes may be further divided by specifying "coarse," "fine," or "very fine."

Toe slope--The outermost inclined surface at the base of a hill; part of a foot slope.

Topsoil--The upper part of the soil, which is the most favorable material for plant growth. It is ordinarily rich in organic matter and is used to topdress roadbanks, lawns, and land affected by mining.

Tuff--A compacted deposit that is 50% or more volcanic ash and dust.

Upland (geology)--Land at a higher elevation, in general, than the alluvial plain or stream terrace; land above the lowlands along streams.

Valley fill--In glaciated regions, material deposited in stream valleys by glacial melt water. In nonglaciated regions, alluvium deposited by heavily loaded streams emerging from hills or mountains spreading sediments onto the lowland as a series of adjacent alluvial fans.

Varian, soil--A soil having properties sufficiently different from those of other known soils to justify a new series name, but the limited geographic soil area does not justify creation of a new series.

Water table--The upper limit of the soil or underlying rock material that is wholly saturated with water.

Water table, artesian--A water table under hydrostatic head, generally beneath an impermeable layer. When this layer is penetrated, the water level rises in an uncased borehole.

Water table, perched--A water table standing above an unsaturated zone. In places an upper, or perched, water table is separated from a lower one by a dry zone.

Weathering--All physical and chemical changes produced in rocks or other deposits at or near the earth's surface by atmospheric agents. These changes result in disintegration and decomposition of the material.

Well graded--Refers to a soil or soil material consisting of particles well distributed over a wide range in size or diameter. Such a soil normally can be easily increased in density and bearing properties by compaction. Contrasts

with poorly graded soil. Synonym: Poorly sorted.

American Geological Institute, 1976, Dictionary of Geological Terms: Anchor Press/Doubleday, New York.

APPENDIX D - SEISMIC MODELS FOR COMPUTATION OF RAYLEIGH WAVE DISPERSION CURVES

Simple Test Cases Similar to Edwards AFB Region¹

1. Single Layer over a Half-Space

<u>H(km)</u>	<u>α(km/sec)</u>	<u>β(km/sec)</u>	<u>ρ(gm/cm³)</u>	<u>σ</u>
0.100	0.600	0.210	1.50	.43
--	2.000	1.155	2.53	.25

1a. Single Thin Layer over a Half-Space

<u>H(km)</u>	<u>α(km/sec)</u>	<u>β(km/sec)</u>	<u>ρ(gm/cm³)</u>	<u>σ</u>
0.010	0.600	0.210	1.50	.43
--	2.000	1.155	2.53	.25

1b. Single Very Thin Layer over a Half-Space

<u>H(km)</u>	<u>α(km/sec)</u>	<u>β(km/sec)</u>	<u>ρ(gm/cm³)</u>	<u>σ</u>
0.001	0.600	0.210	1.50	.43
--	2.000	1.155	2.53	.25

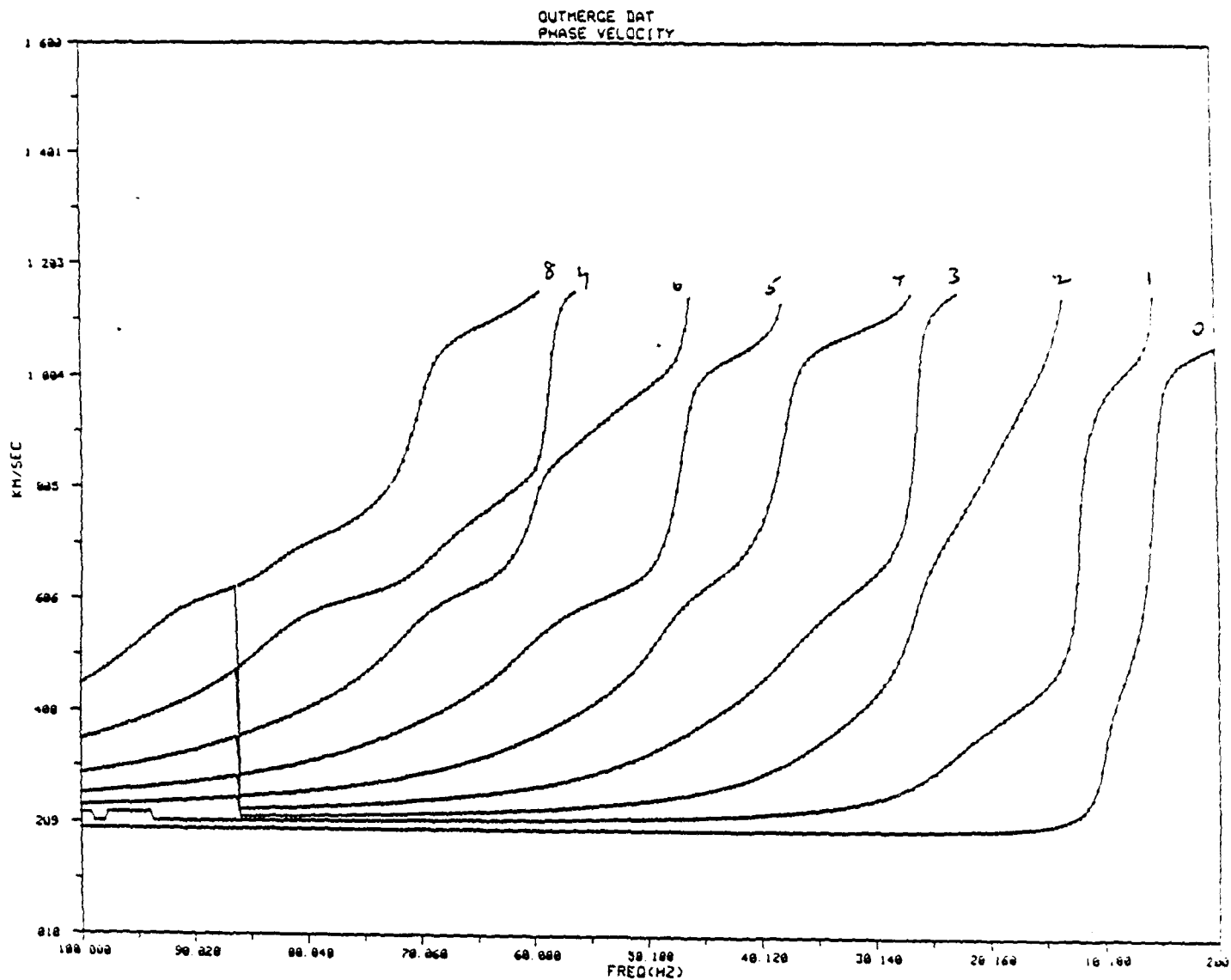
2. Two Layers over a Half-Space

<u>H(km)</u>	<u>α(km/sec)</u>	<u>β(km/sec)</u>	<u>ρ(gm/cm³)</u>	<u>σ</u>
0.020	0.235	0.082	1.50	.43
0.075	0.800	0.320	1.90	.40
--	2.860	1.650	2.60	.25

3. Three Layers over a Half-Space

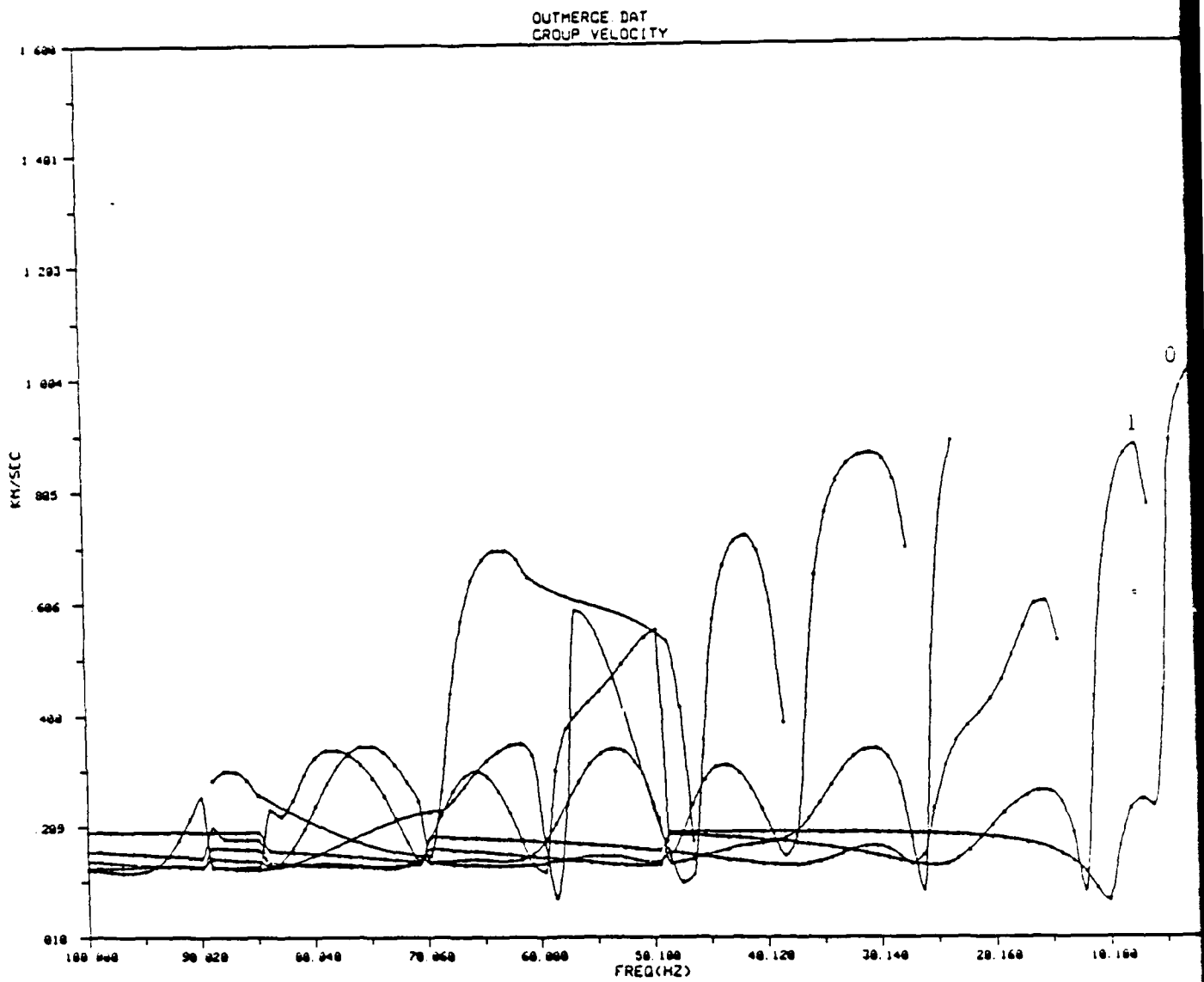
<u>H(km)</u>	<u>α(km/sec)</u>	<u>β(km/sec)</u>	<u>ρ(gm/cm³)</u>	<u>σ</u>
0.015	0.183	0.064	1.20	.43
0.050	0.548	0.192	1.60	.43
0.135	1.020	0.500	1.90	.34
--	3.000	1.830	2.70	.20

¹Goforth, T. T., and J. A. McDonald, 1968, Seismic effects of sonic booms: NASA Report No. CR-1137, Teledyne Geotech, Garland, Texas.



CRUST 1 A NO. OF LAYERS. = 2

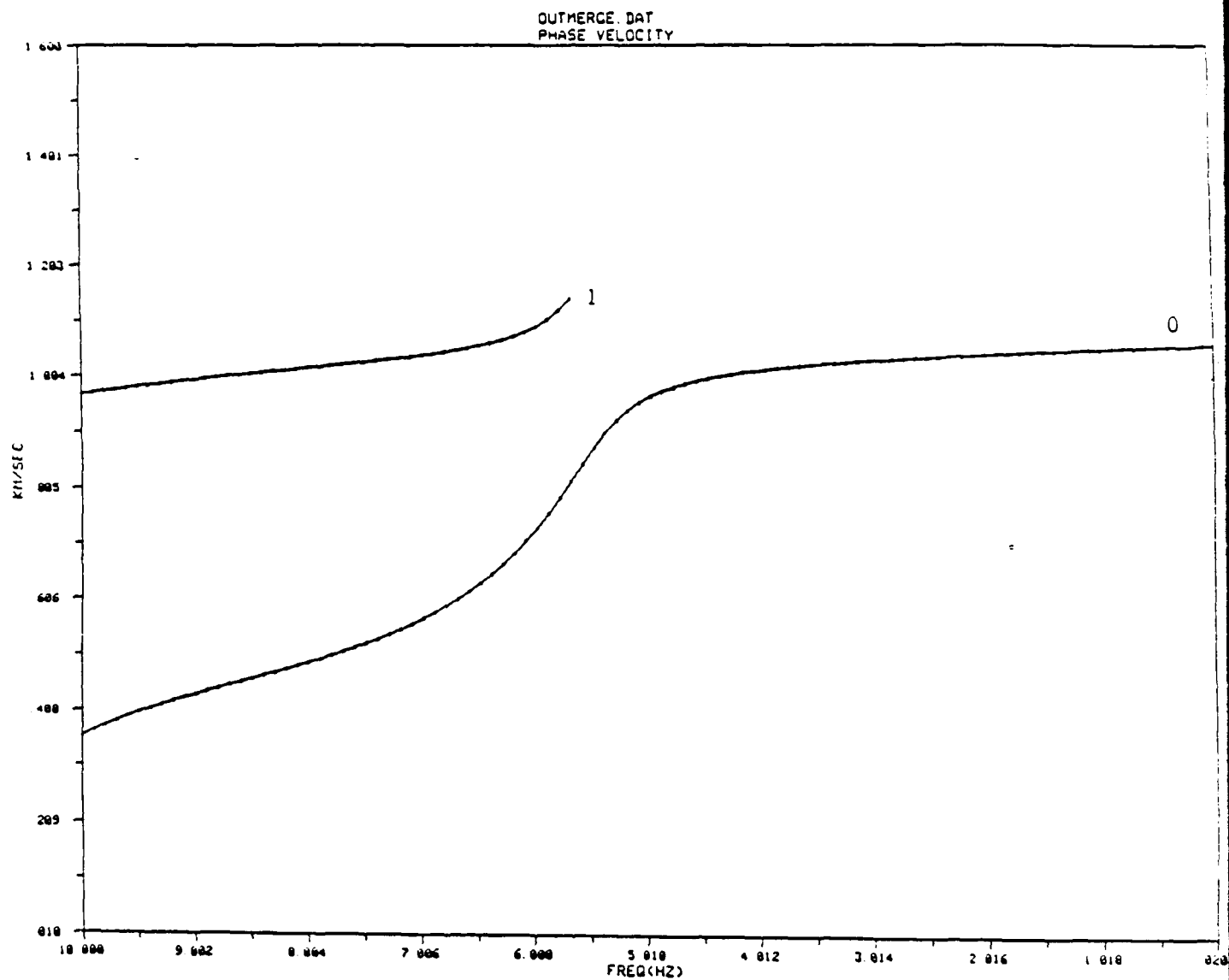
H (km)	VP (km/s)	VS (km/s)	RHO (g/cm ³)
010	600	.210	1.500
100 000	2.000	1.155	2.530



CRUST1A

NO. OF LAYERS = 2

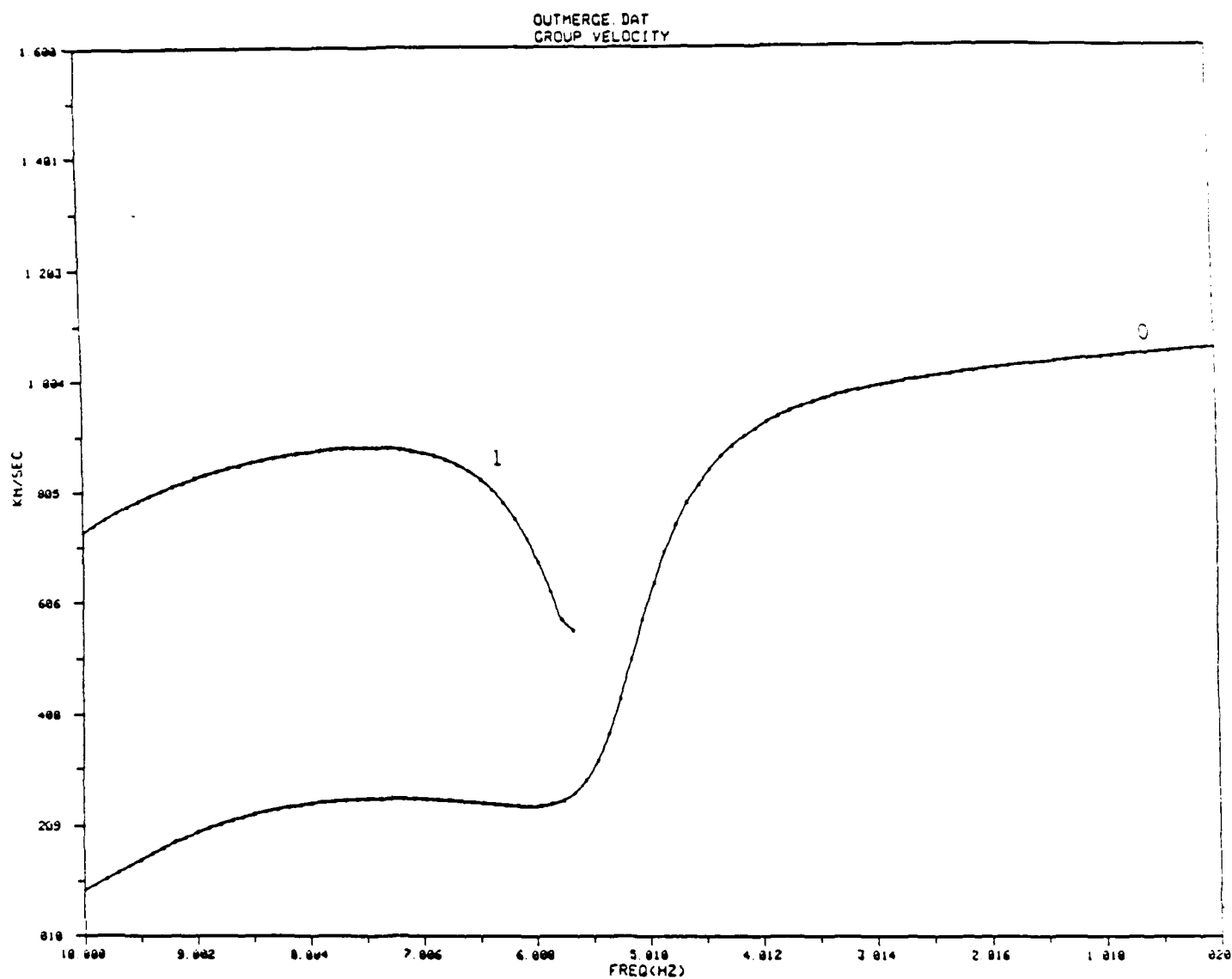
H (km)	VP (km/s)	VS (km/s)	RHO (g/cm ³)
0.10	.600	.210	1.500
100.000	2.000	1.155	2.530



CRUST1A

NO. OF LAYERS = 2

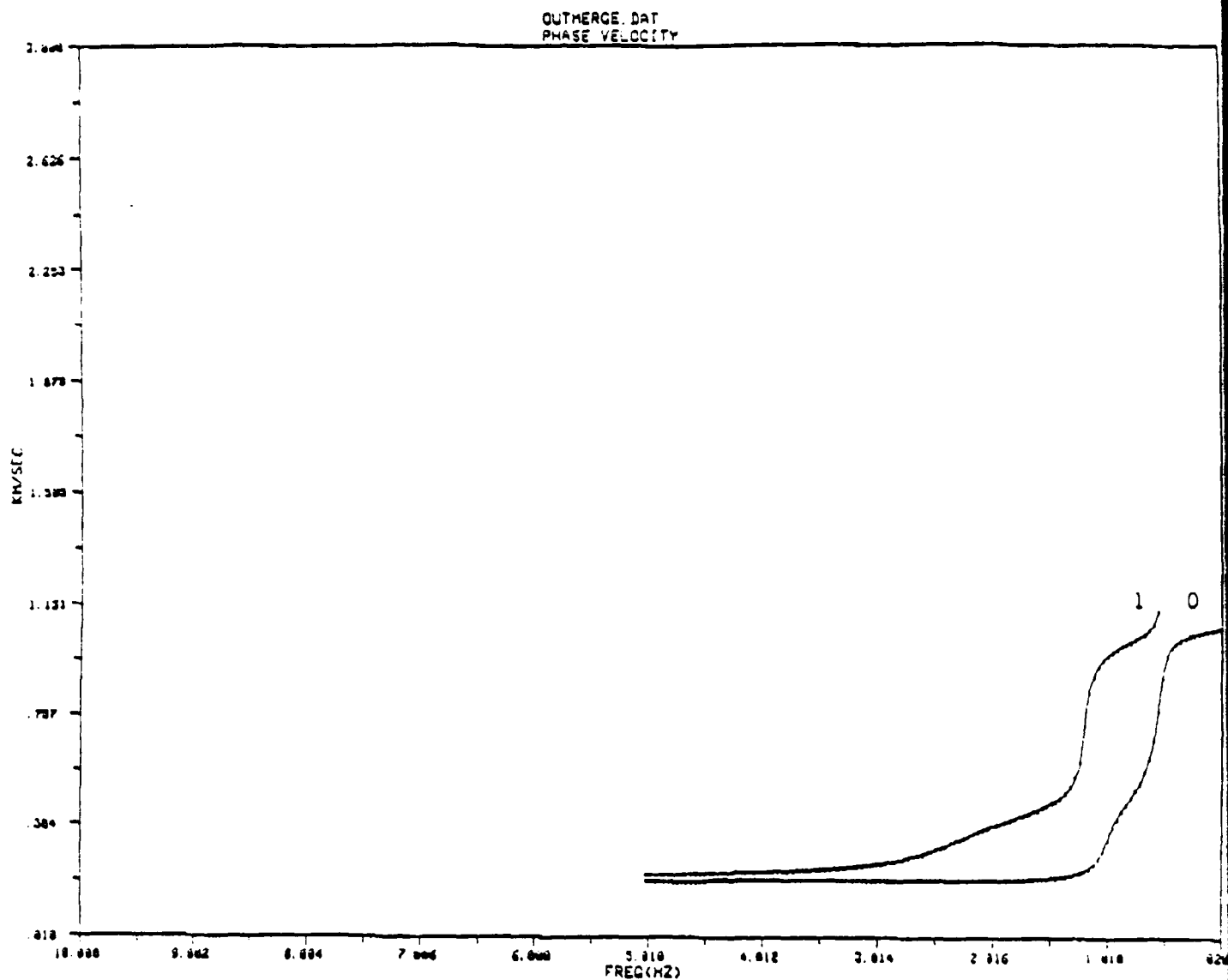
H (km)	VP (km/s)	VS (km/s)	RHO (g/cm ³)
010	600	.210	1.500
100 000	2 000	1 155	2 530



CRUST1A

NO. OF LAYERS = 2

H (km)	VP (km/s)	VS (km/s)	RHO (g/cm ³)
.010	.600	.210	1.500
100.000	2.000	1.155	2.530

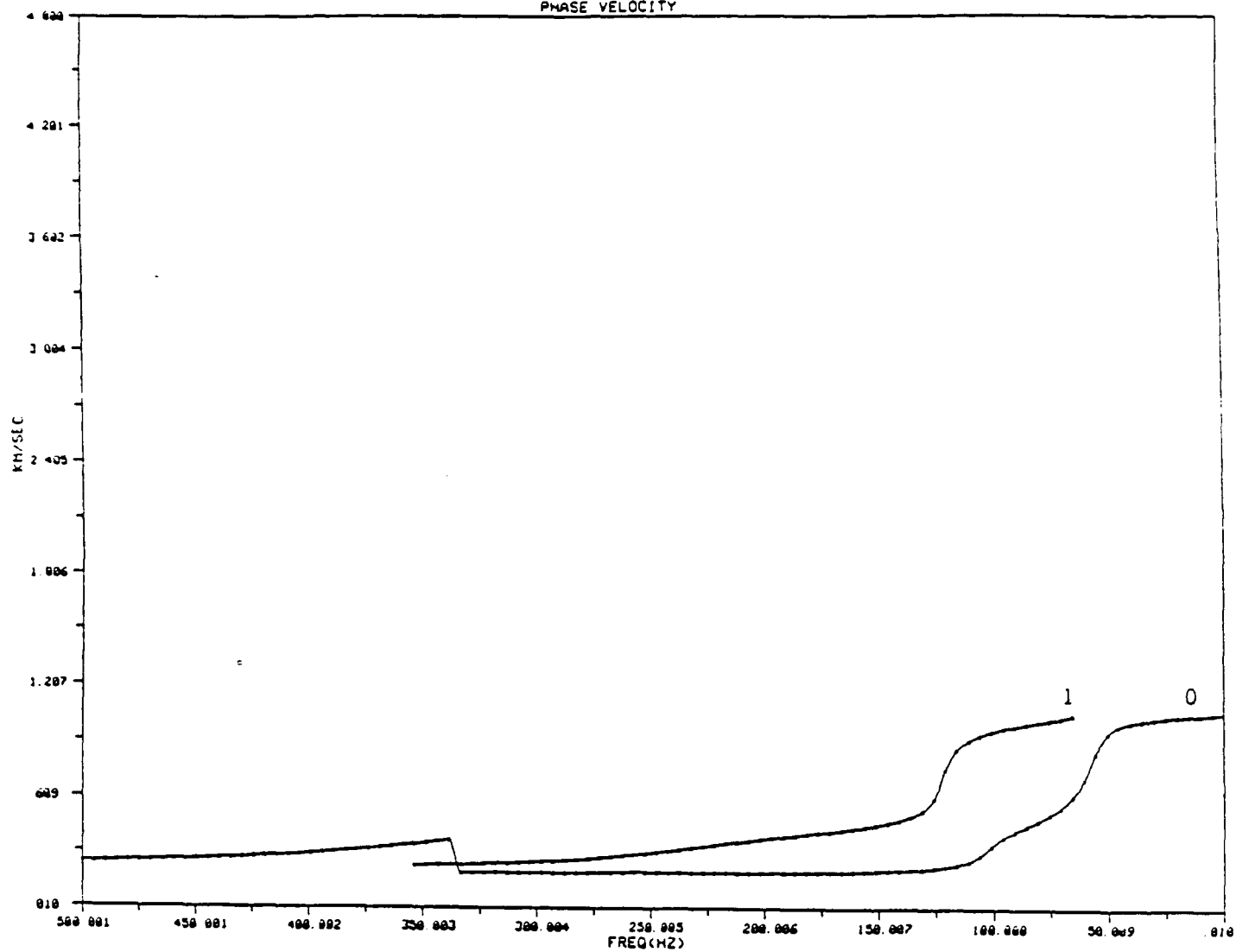


CRUST1

NO. OF LAYERS = 2

H (km)	VP (km/s)	VS (km/s)	RHO (g/cm ³)
100	.600	.210	1.500
100.000	2.000	1.155	2.530

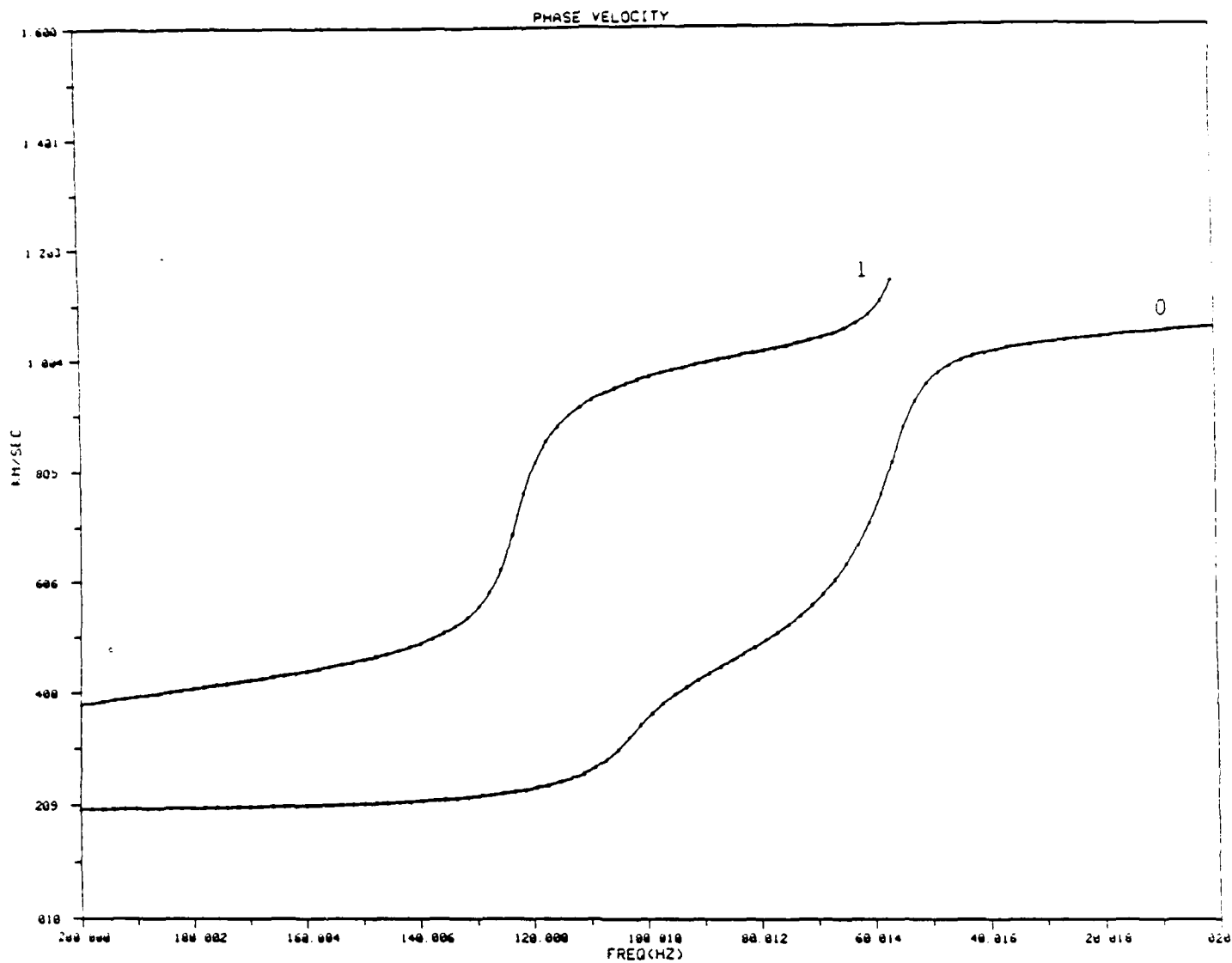
OUTMERGE.DAT
PHASE VELOCITY



CRUST1 B

NO OF LAYERS = 2

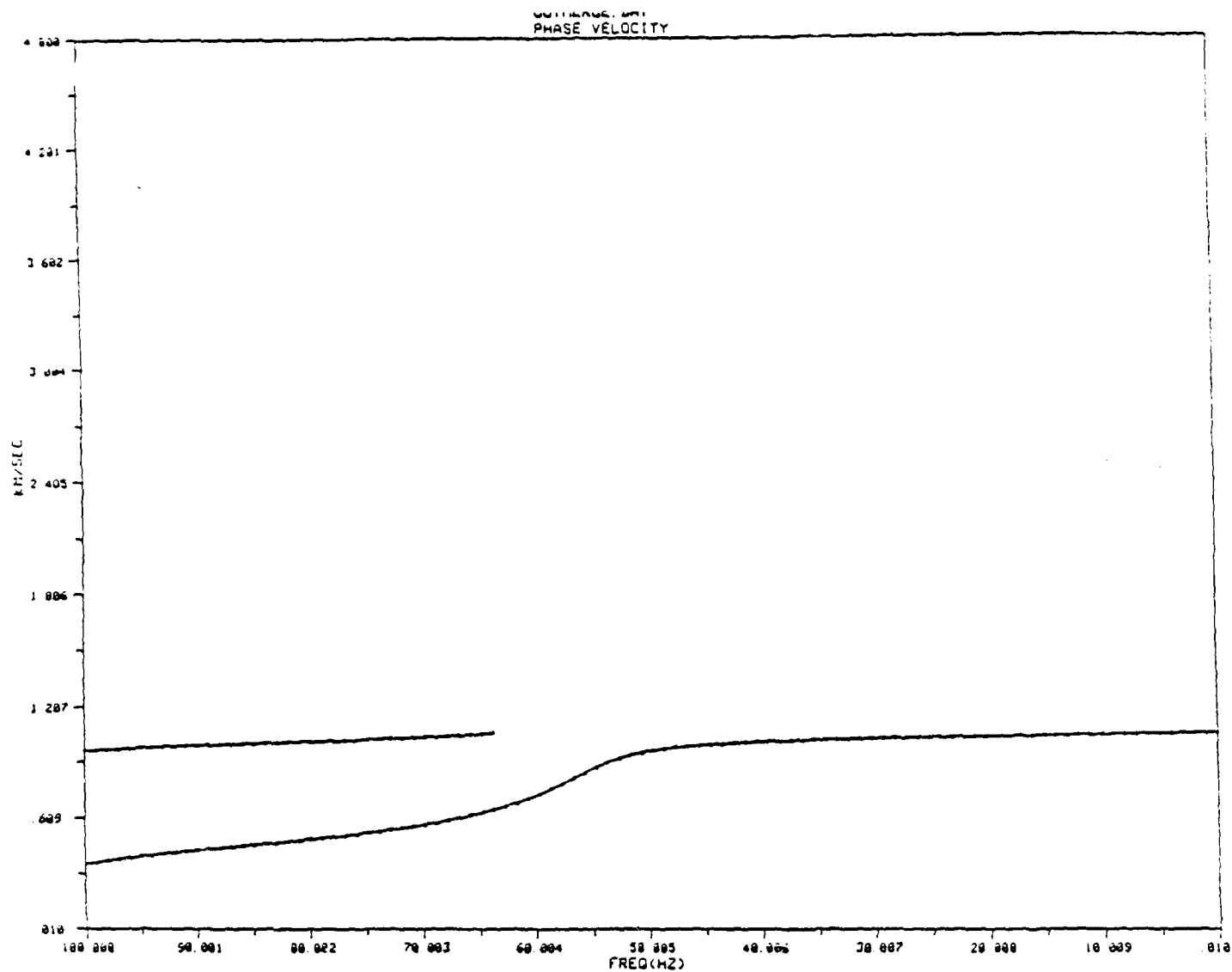
H (km)	VP (km/s)	VS (km/s)	RHO (g/cm ³)
.001	.600	.210	1.500
100.000	2.000	1.155	2.530



CRUST1B

NO. OF LAYERS = 2

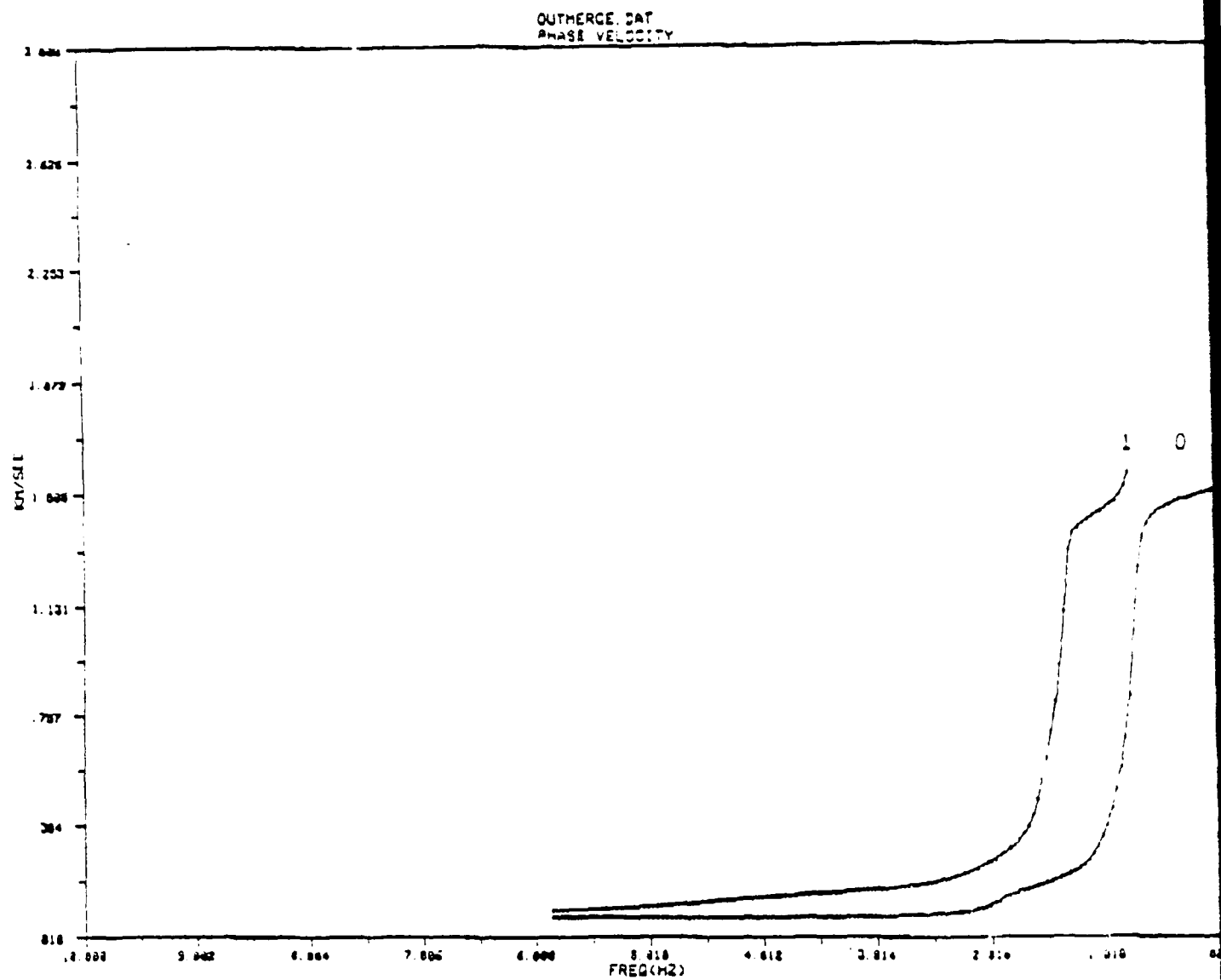
H (km)	VP (km/s)	VS (km/s)	RHO (g/cm ³)
001	600	210	1 500
100 000	2 000	1 155	2 530



CRUST1B

NO. OF LAYERS = 2

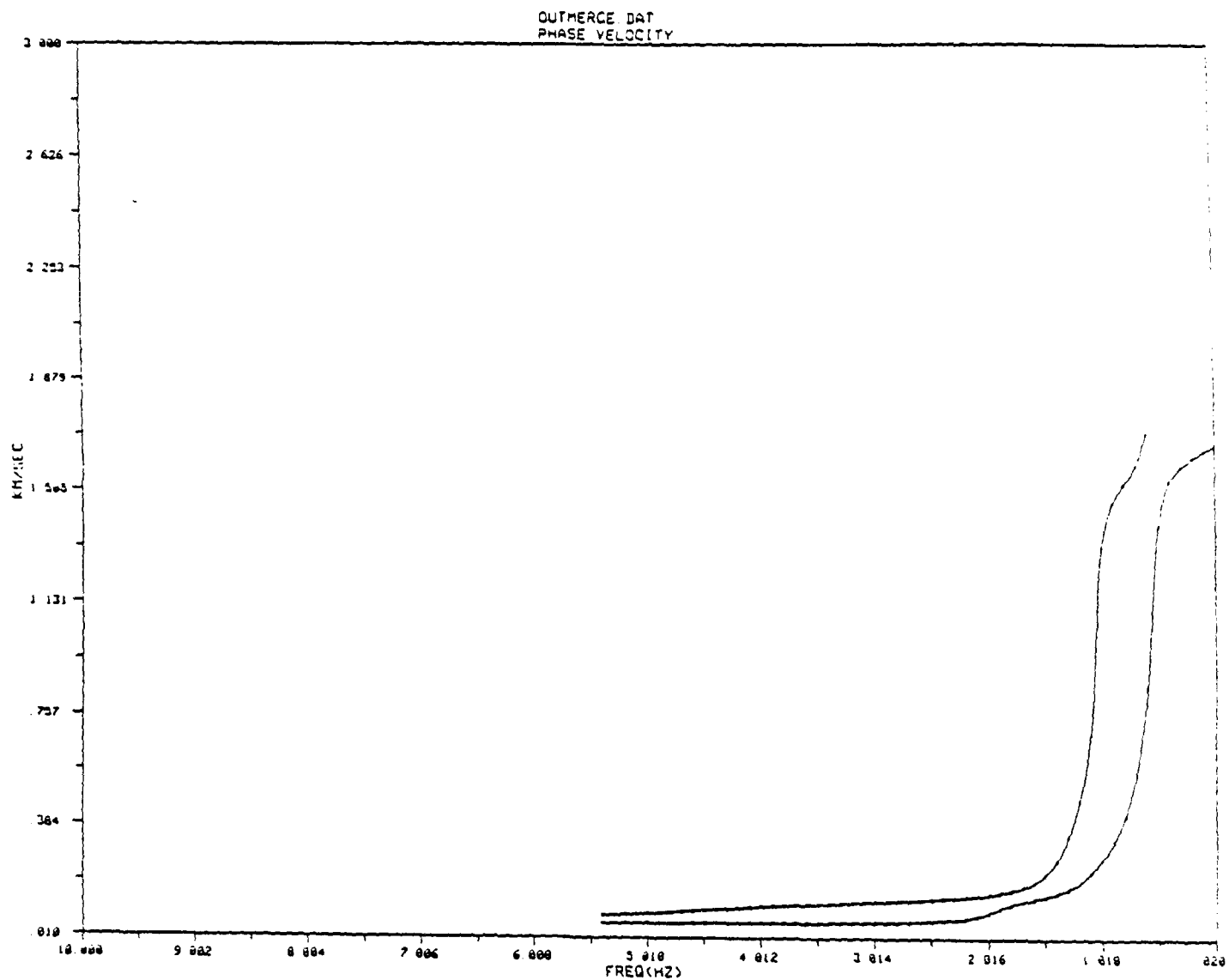
H (km)	VP (km/s)	VS (km/s)	RHO (g/cm ³)
.001	.600	.210	1.500
100.000	2.000	1.155	2.530



CRUST2

NO. OF LAYERS = 3

H (km)	VP (km/s)	VS (km/s)	RHO (g/cm3)
.020	235	.002	1.500
.075	.000	320	1.900
100.000	2.050	1.650	2.600



CRUST3

NO OF LAYERS = 4

H (km)	VP (km/s)	VS (km/s)	RHO (g/cm ³)
015	.183	.064	1.200
050	.548	.192	1.600
135	1.020	.500	1.900
100 000	3.000	1.830	2.700

Crustal Models for the Mojave Desert Region

11. Simple Crustal Model of Hadley (1978)

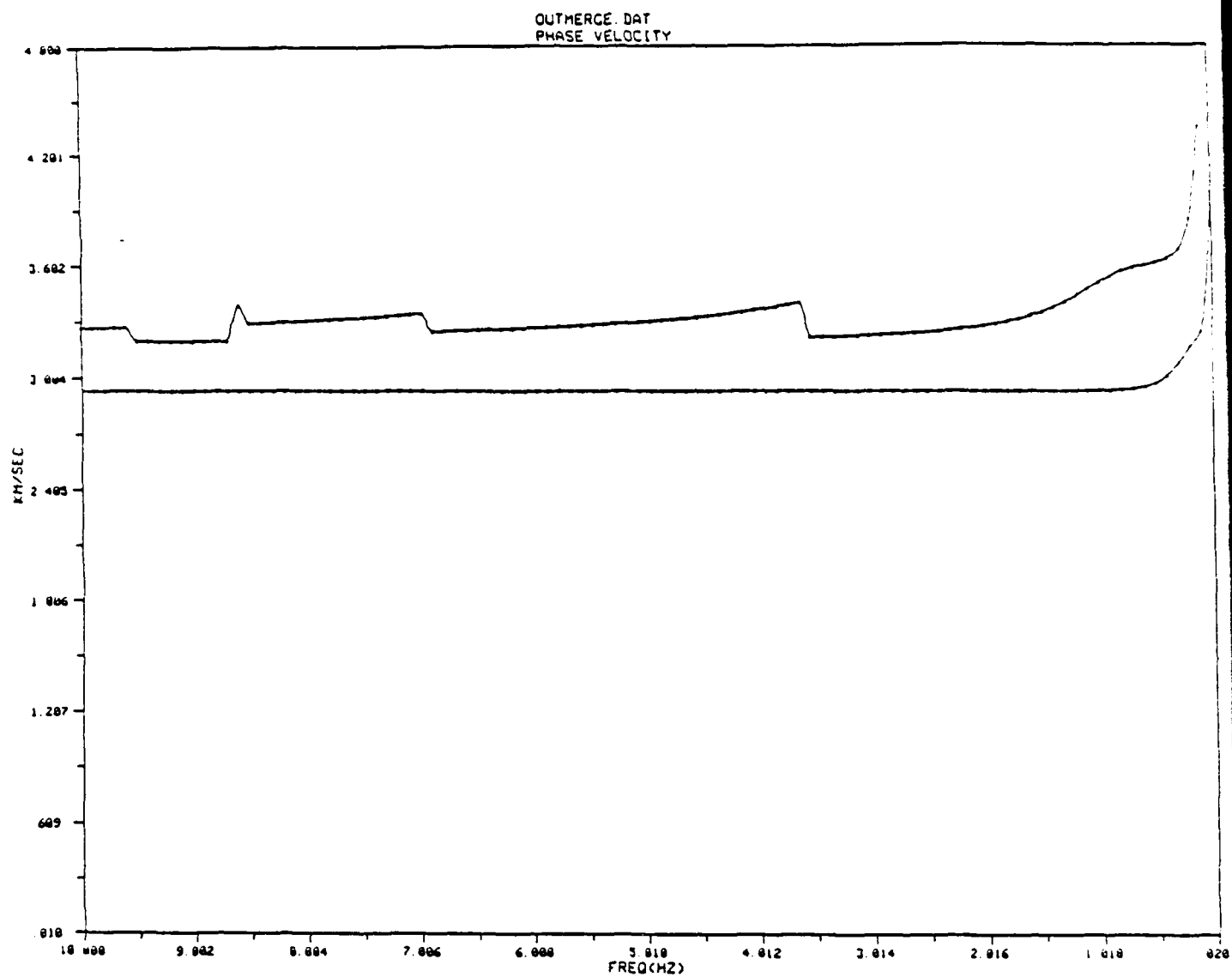
<u>H(km)</u>	<u>α(km/sec)</u>	<u>β(km/sec)</u>	<u>ρ(gm/cm³)</u>	<u>σ</u>
4.00	5.50	3.20	2.50	.24
23.4	6.30	3.60	2.65	.26
5.00	6.80	4.10	2.80	.21
--	7.80	4.50	3.30	.25

12. Crustal Model w/Sedimentary Layer

<u>H(km)</u>	<u>α(km/sec)</u>	<u>β(km/sec)</u>	<u>ρ(gm/cm³)</u>	<u>σ</u>
1.00	3.50	2.00	2.20	.26
4.00	5.50	3.20	2.50	.24
23.4	6.30	3.60	2.65	.26
5.00	6.80	4.10	2.80	.21
--	7.80	4.50	3.30	.25

13. Detailed Model w/Low Velocity Zone

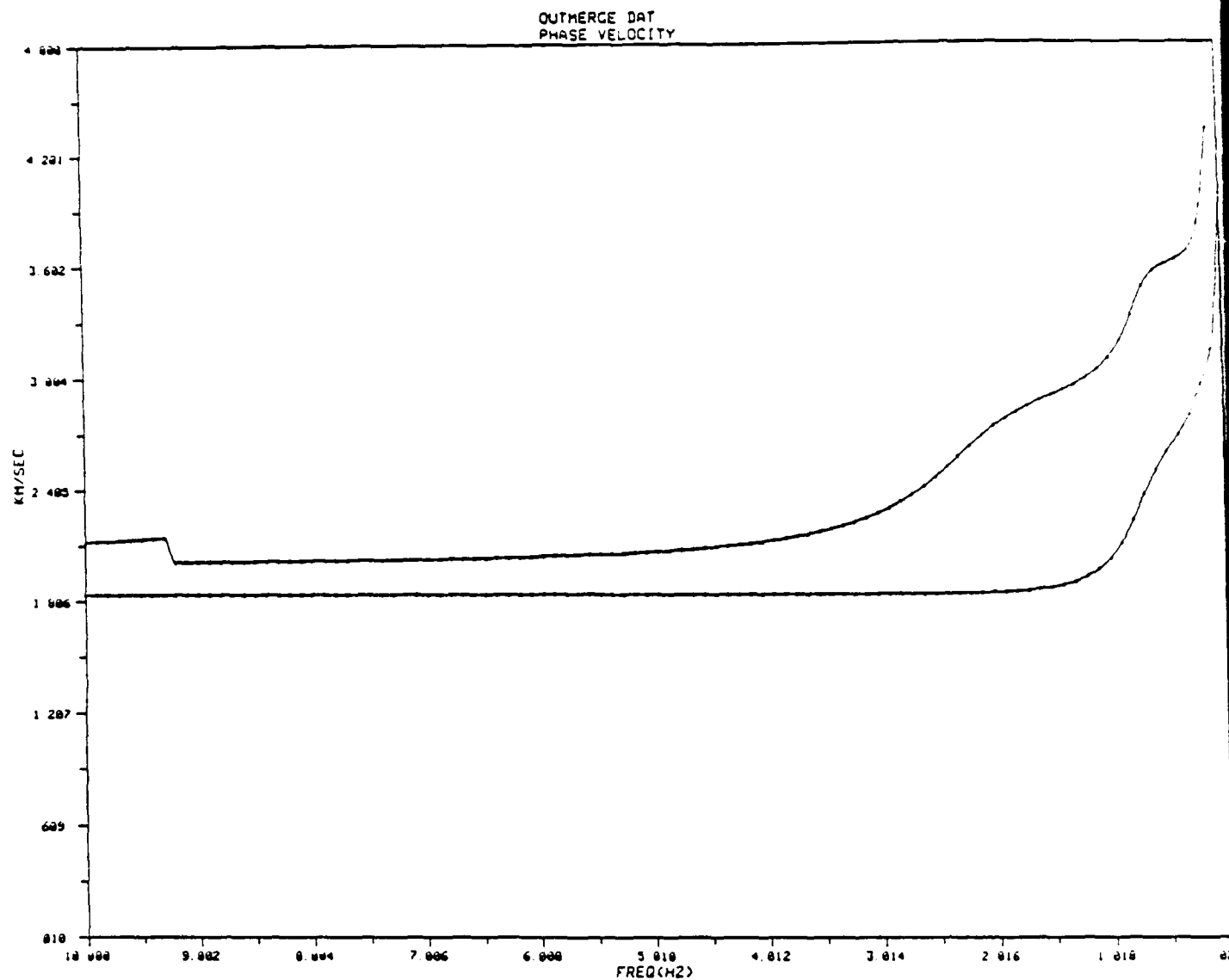
<u>H(km)</u>	<u>α(km/sec)</u>	<u>β(km/sec)</u>	<u>ρ(gm/cm³)</u>	<u>σ</u>
1.00	3.50	2.00	2.20	.26
1.00	5.32	3.10	2.50	.24
4.00	5.50	3.20	2.55	.24
5.00	6.30	3.65	2.60	.25
5.00	6.30	3.60	2.63	.26
5.00	6.30	3.55	2.65	.27
6.40	6.30	3.65	2.67	.25
5.00	6.80	4.10	2.80	.21
--	7.80	4.50	3.30	.25



CRUST11

NO. OF LAYERS = 4

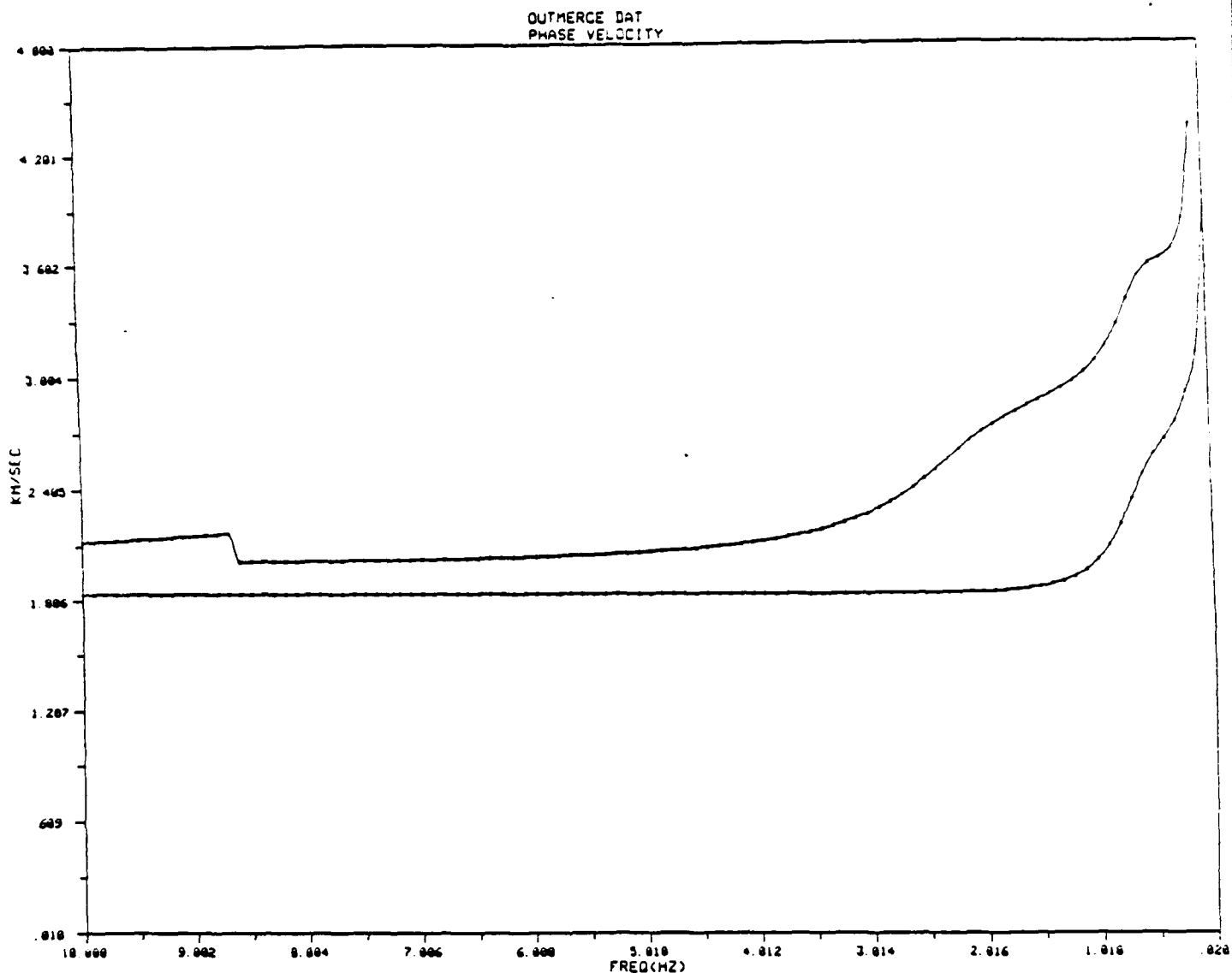
H (km)	VP (km/s)	VS (km/s)	RHO (g/cm ³)
4.000	5.500	3.200	2.500
23.400	6.300	3.600	2.650
5.000	6.800	4.100	2.800
100.000	7.800	4.500	3.300



CRUST12

NO. OF LAYERS = 5

H (km)	VP (km/s)	VS (km/s)	RHO (g/cm ³)
1.000	3.500	2.000	2.200
4.000	5.500	3.200	2.500
23.400	6.300	3.600	2.650
5.000	6.800	4.100	2.800
100.000	7.800	4.500	3.300



CRUST13

NO OF LAYERS = 9

H (km)	VP (km/s)	VS (km/s)	RHO (g/cm ³)
1.000	3.500	2.000	2.200
1.000	5.320	3.100	2.500
4.000	5.500	3.200	2.550
5.000	6.300	3.650	2.600
5.000	6.300	3.600	2.630
5.000	6.300	3.550	2.650
6.400	6.300	3.650	2.670
5.000	6.800	4.100	2.800
100.000	7.800	4.500	3.300

Crustal Models for the Mojave Desert Region

14. Detailed Model--EXP-0 Sedimentary Layer

<u>H(km)</u>	<u>α(km/sec)</u>	<u>β(km/sec)</u>	<u>ρ(gm/cm³)</u>	<u>σ</u>
0.037	0.830	0.339	1.60	.40
0.090	1.05	0.517	1.70	.34
0.113	1.60	0.788	1.80	.34
0.600	2.40	1.18	1.90	.34
1.00	3.50	2.04	2.20	.26
1.00	5.32	3.10	2.50	.24
4.00	5.50	3.20	2.55	.24
5.00	6.30	3.65	2.60	.25
5.00	6.30	3.60	2.63	.26
5.00	6.30	3.55	2.65	.27
6.40	6.30	3.65	2.67	.25
5.00	6.80	4.07	2.80	.21
--	7.80	4.50	3.30	.25

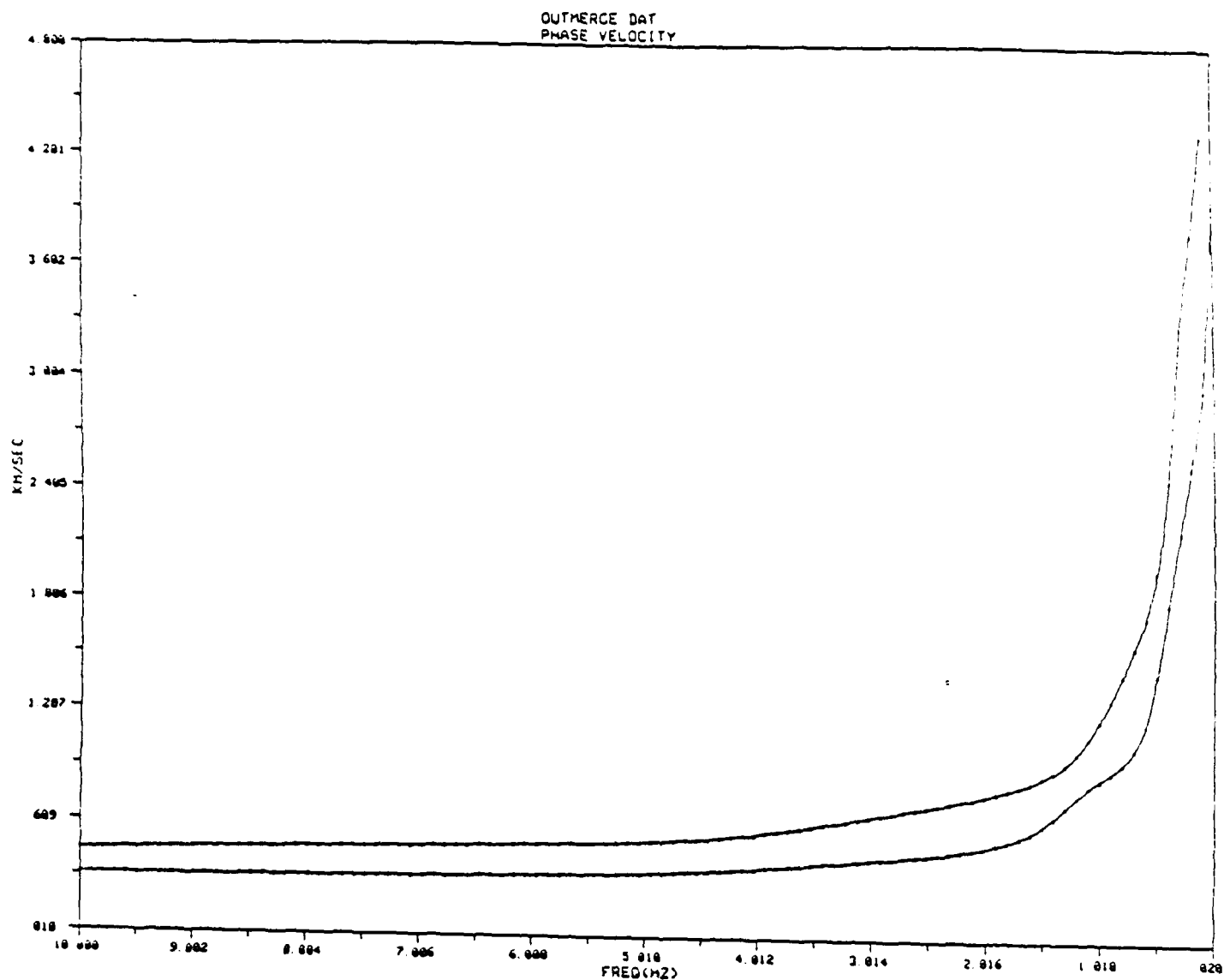
15. Baldy Mesa Sedimentary Model

<u>H(km)</u>	<u>α(km/sec)</u>	<u>β(km/sec)</u>	<u>ρ(gm/cm³)</u>	<u>σ</u>
0.083	0.770	0.314	1.60	.40
0.380	1.88	0.926	1.90	.34
0.600	5.23	3.00	2.50	.25
--	5.50	3.20	2.55	.24

16. TRASH Sedimentary Model

<u>H(km)</u>	<u>α(km/sec)</u>	<u>β(km/sec)</u>	<u>ρ(gm/cm³)</u>	<u>σ</u>
0.030	0.660	0.270	1.60	.40
0.258	2.00	0.985	1.90	.34
0.400	5.15	2.75	2.45	.30
--	5.50	3.20	2.55	.24

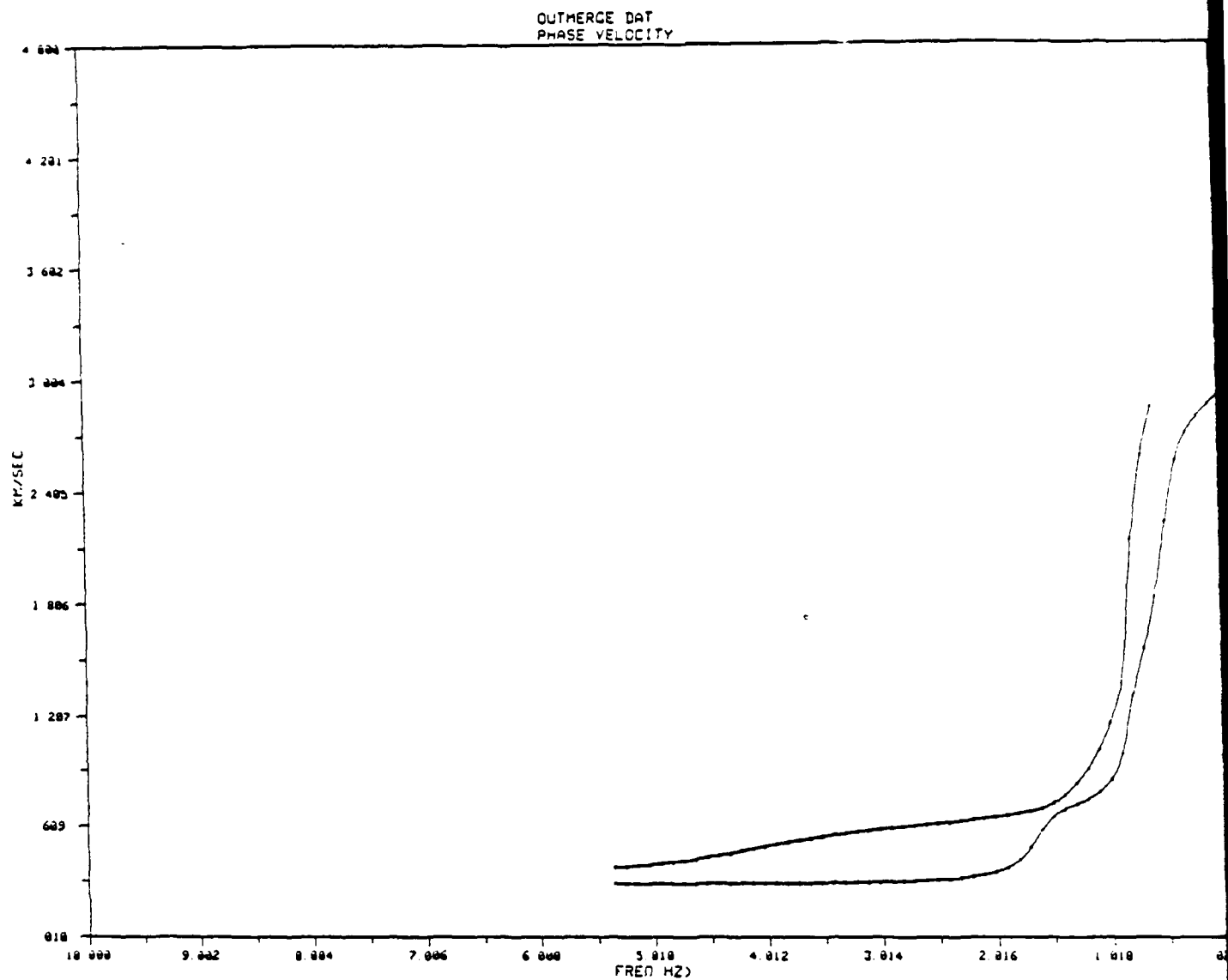
Hadley, D. M., 1978, Geophysical investigations of the structure and tectonics of southern California: Ph.D. Dissertation, California Institute of Technology, Pasadena, 167 pp.



CRUST14

NO. OF LAYERS = 13

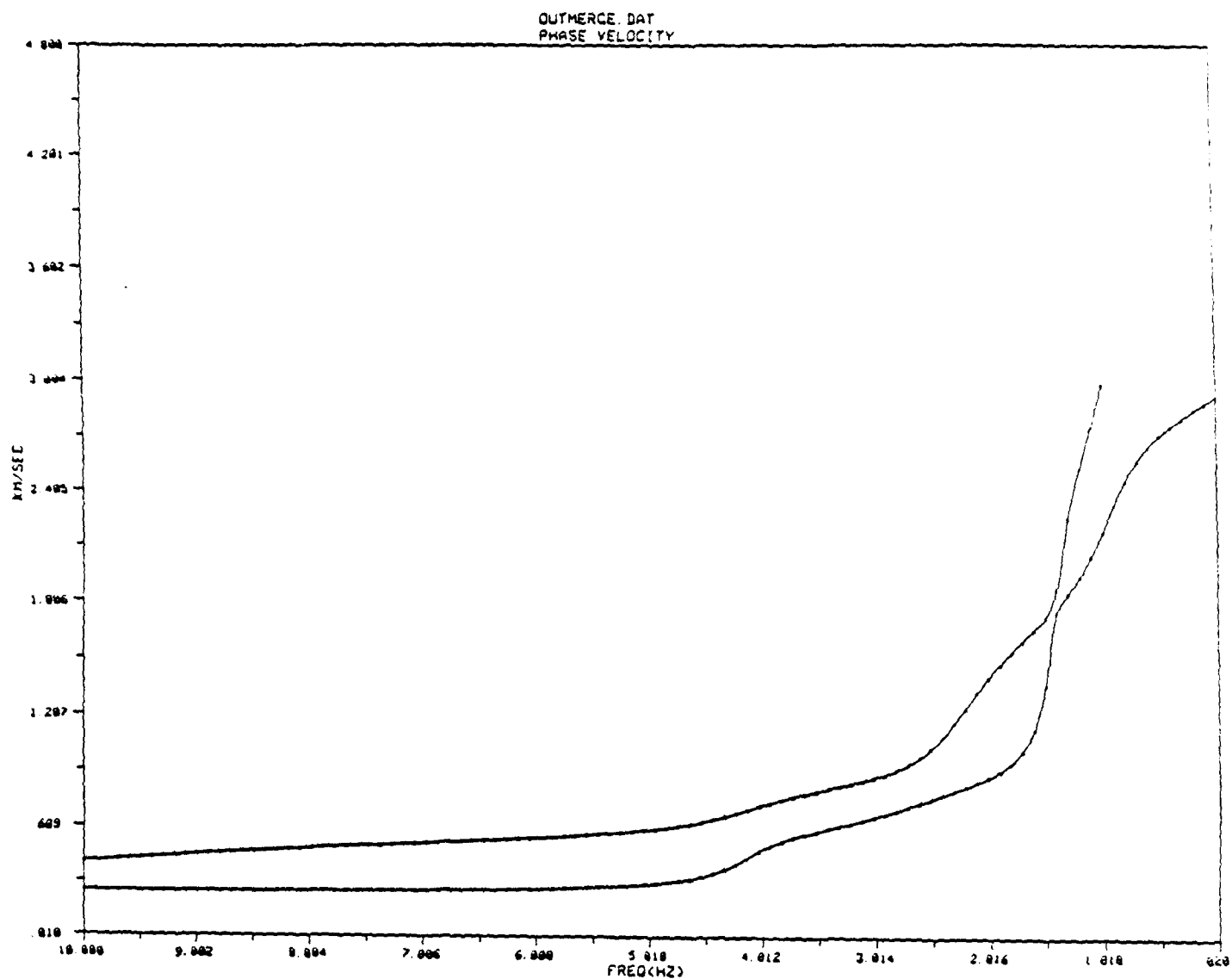
H (km)	VP (km/s)	VS (km/s)	RHO (g/cm ³)
.037	.830	.339	1.600
.090	1.050	.517	1.700
.113	1.600	.788	1.800
.600	2.400	1.180	1.900
1.000	3.500	2.000	2.200
1.000	5.320	3.100	2.500
4.000	5.500	3.200	2.550
5.000	6.300	3.650	2.600
5.000	6.300	3.600	2.630
5.000	6.300	3.550	2.650
6.400	6.300	3.650	2.670
5.000	6.800	4.100	2.800
100.000	7.800	4.500	3.300



CRUST15

NO. OF LAYERS = 4

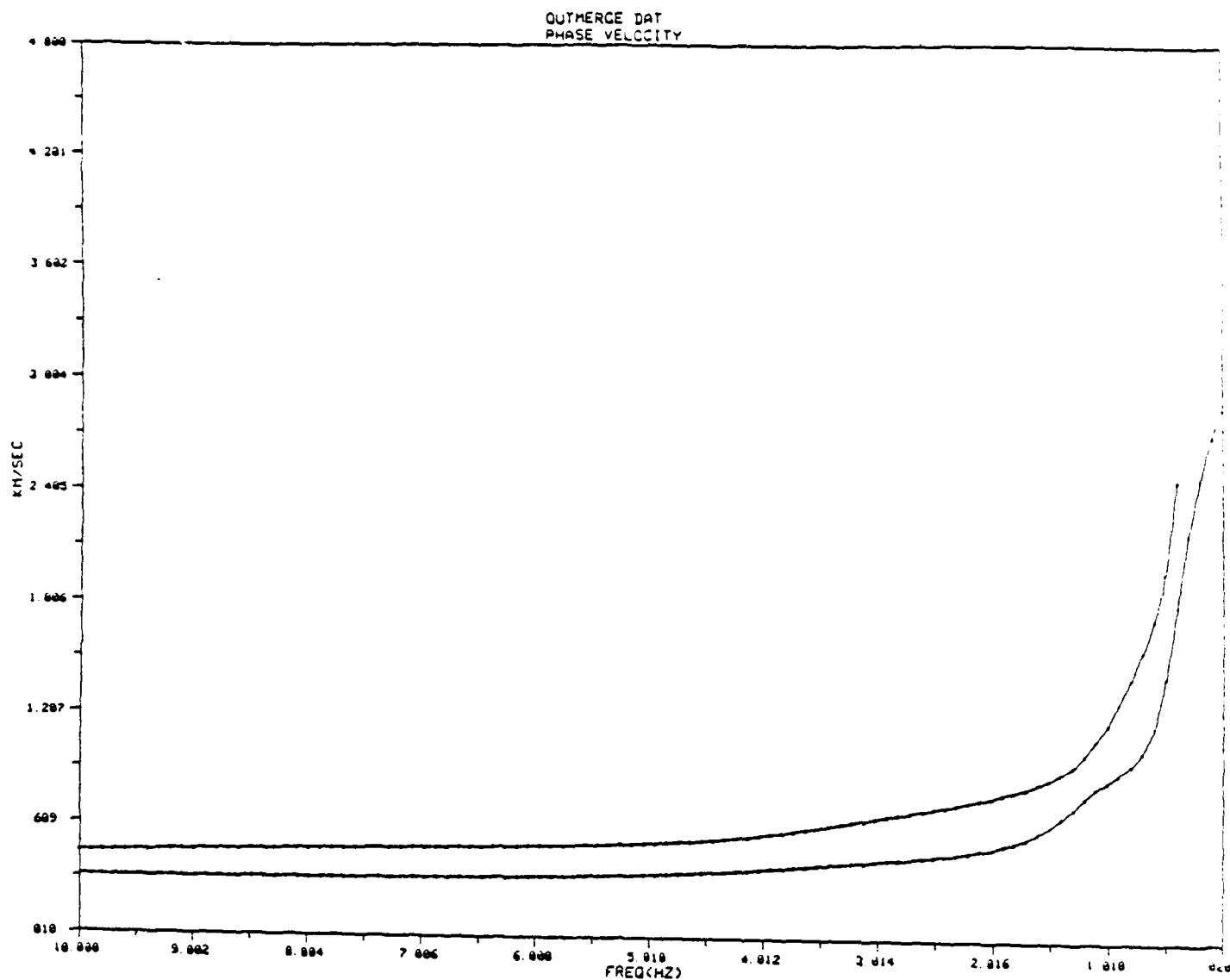
H (km)	VP (km/s)	VS (km/s)	RHO (g/cm ³)
083	770	.314	1.600
380	1.880	.926	1.900
600	5.230	3.000	2.500
100.000	5.500	3.200	2.550



CRUST16

NO. OF LAYERS = 4

H (km)	VP (km/s)	VS (km/s)	RHO (g/cm ³)
.030	.660	.270	1.600
.258	2.000	.985	1.900
.400	5.150	2.750	2.450
100.000	5.500	3.200	2.550



CRUST17

NO. OF LAYERS = 7

H (km)	VP (km/s)	VS (km/s)	RHO (g/cm3)
037	830	339	1 600
090	1 050	517	1 700
113	1 600	788	1 800
600	2 400	1 180	1 900
1 000	3 500	2 000	2 200
1 000	5 320	3 100	2 500
100 000	5 500	3 200	2 550

Cases for Colorado Plateau and Basin and Range

21. Colorado Plateau Basic Model (Langston and Helmberger, 1974)

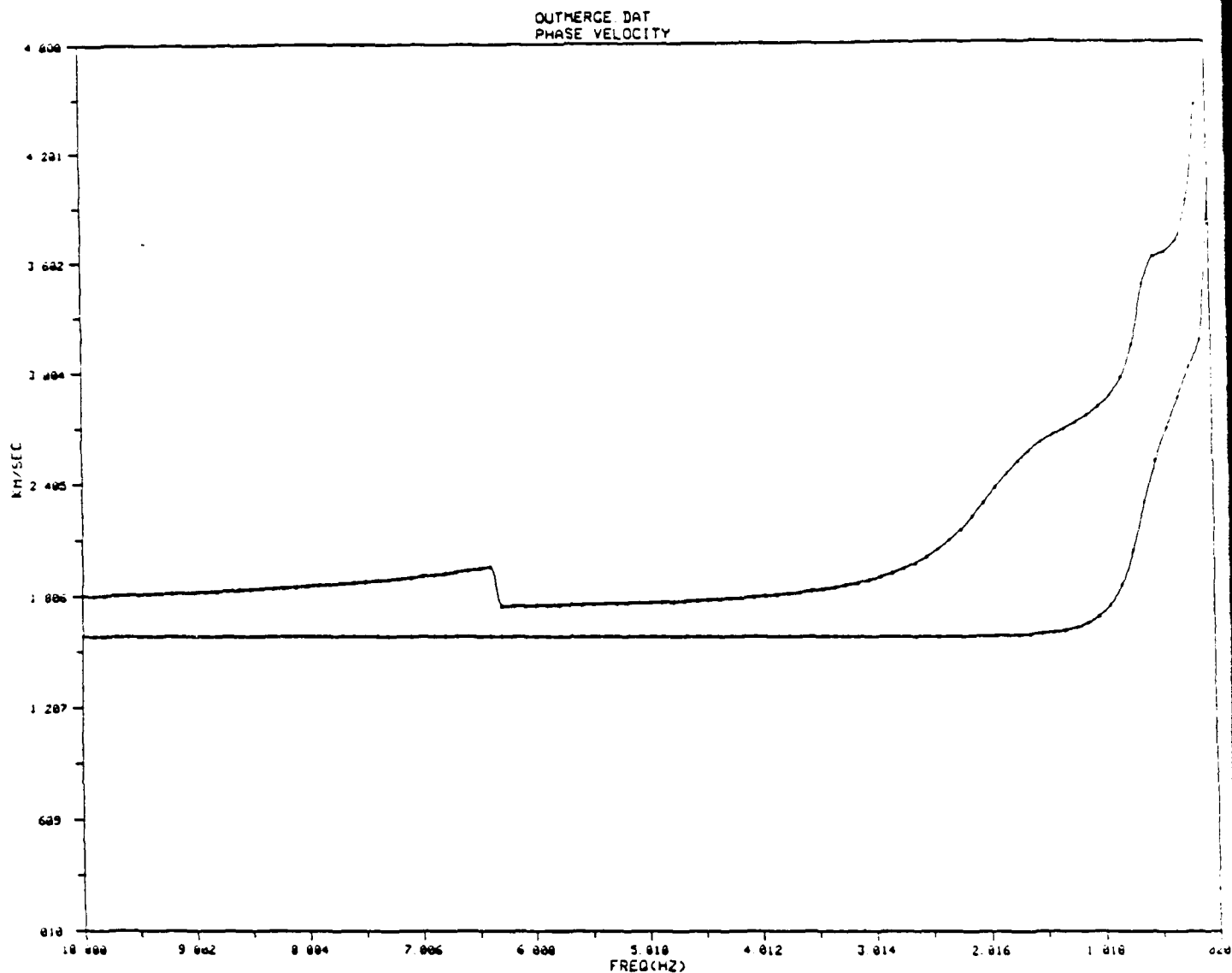
<u>H(km)</u>	<u>α(km/sec)</u>	<u>β(km/sec)</u>	<u>ρ(gm/cm³)</u>	<u>σ</u>
1.000	3.000	1.730	2.20	.25
1.000	5.500	3.300	2.50	.22
2.000	5.900	3.400	2.60	.25
22.500	6.100	3.600	2.80	.23
--	7.900	4.600	3.30	.24

22. Near Albuquerque (Sabatier et al., 1986b)

<u>H(km)</u>	<u>α(km/sec)</u>	<u>β(km/sec)</u>	<u>ρ(gm/cm³)</u>	<u>σ</u>
.0003	0.149	0.073	1.70	.34
.00274	0.451	0.283	1.70	.18
1.000	3.000	1.730	2.20	.25
1.000	5.500	3.300	2.50	.22
2.000	5.900	3.400	2.60	.25
22.500	6.100	3.600	2.80	.23
--	7.900	4.600	3.30	.24

23. Site 1 (Sabatier et al., 1986a)

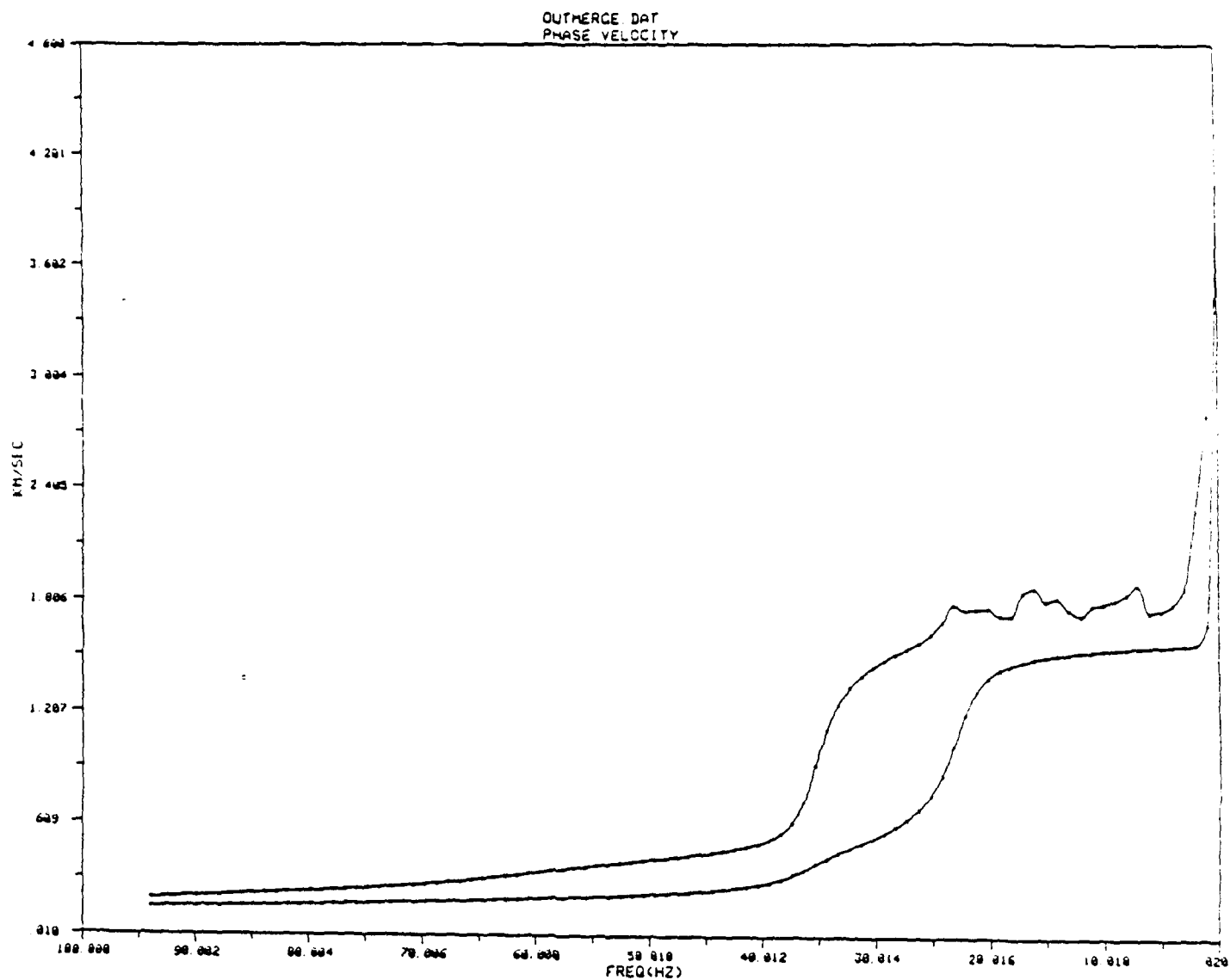
<u>H(km)</u>	<u>α(km/sec)</u>	<u>β(km/sec)</u>	<u>ρ(gm/cm³)</u>	<u>σ</u>
.00198	0.207	0.080	1.70	.41
0.200	1.590	0.116	1.90	.50
1.000	3.000	1.730	2.20	.25
1.000	5.500	3.300	2.50	.22
2.000	5.900	3.400	2.60	.25
22.500	6.100	3.600	2.80	.23
--	7.900	4.600	3.30	.24



CRUST21

NO. OF LAYERS = 5

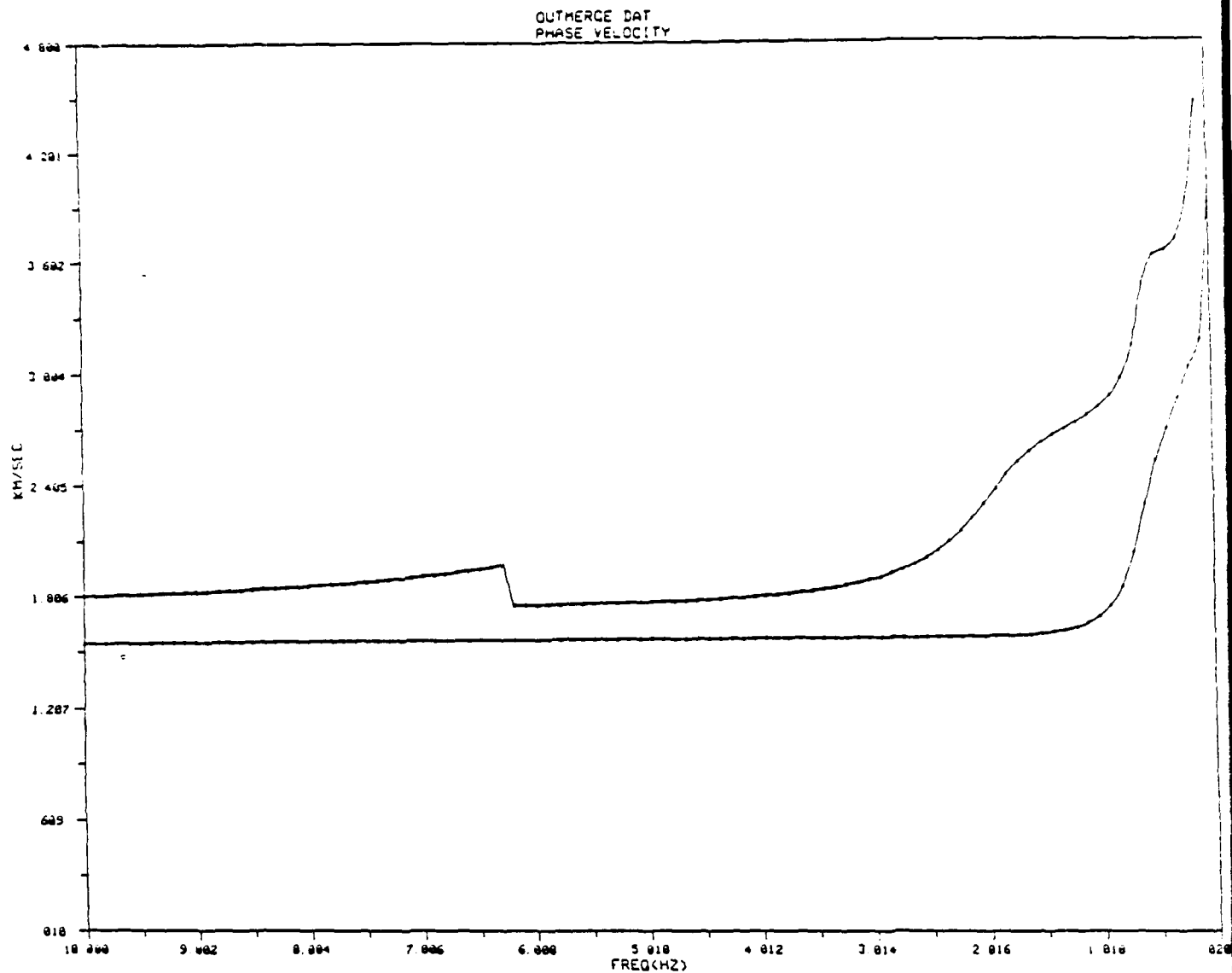
H (km)	VP (km/s)	VS (km/s)	RHO (g/cm ³)
1.000	3.000	1.730	2.200
1.000	5.500	3.300	2.500
2.000	5.900	3.400	2.600
22.500	6.100	3.600	2.800
100.000	7.900	4.600	3.300



CRUST22

NO. OF LAYERS = 7

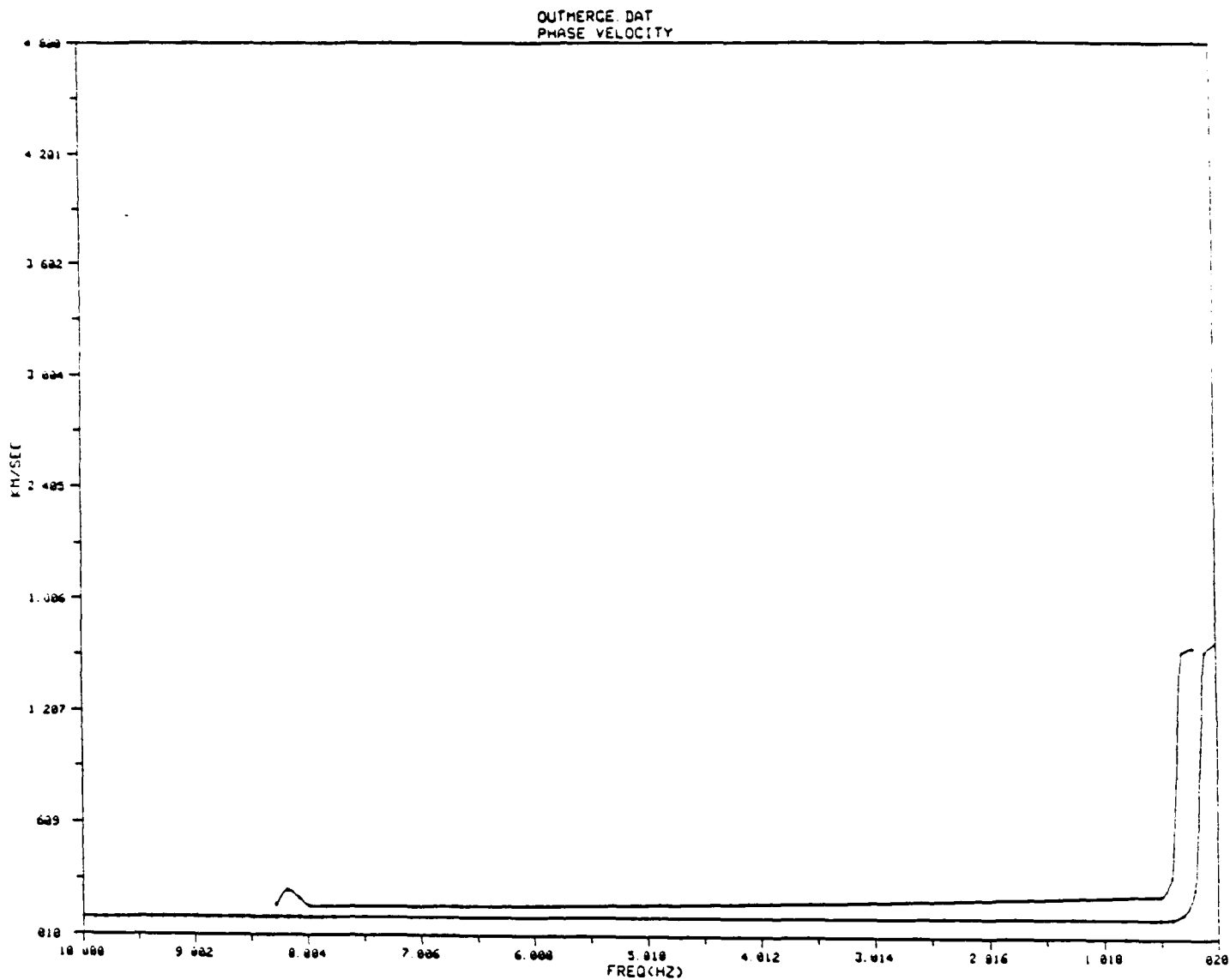
H (km)	VP (km/s)	VS (km/s)	RHO (g/cm3)
.00030	.149	.073	1.700
.00274	.451	.283	1.700
1.000	3.000	1.730	2.200
1.000	5.500	3.300	2.500
2.000	5.900	3.400	2.600
22.500	6.100	3.600	2.800
100.000	7.900	4.600	3.300



CRUST22

NO. OF LAYERS = 7

H (km)	VP (km/s)	VS (km/s)	RHO (g/cm ³)
00030	.149	.073	1.700
00274	.451	.283	1.700
1 000	3 000	1 730	2 200
1 000	5 500	3 300	2 500
2 000	5 900	3 400	2 600
22 500	6 100	3 600	2 800
100 000	7 900	4 600	3 300



CRUST23

NO. OF LAYERS = 3

H (km)	VP (km/s)	VS (km/s)	RHO (g/cm3)
00200	.20700	.08000	1.70000
.20000	1.59000	.11600	1.90000
100.00020	3.00000	1.73000	2.20000

Cases for Colorado Plateau and Basin and Range

24. Site 2 (Sabatier et al., 1986a)

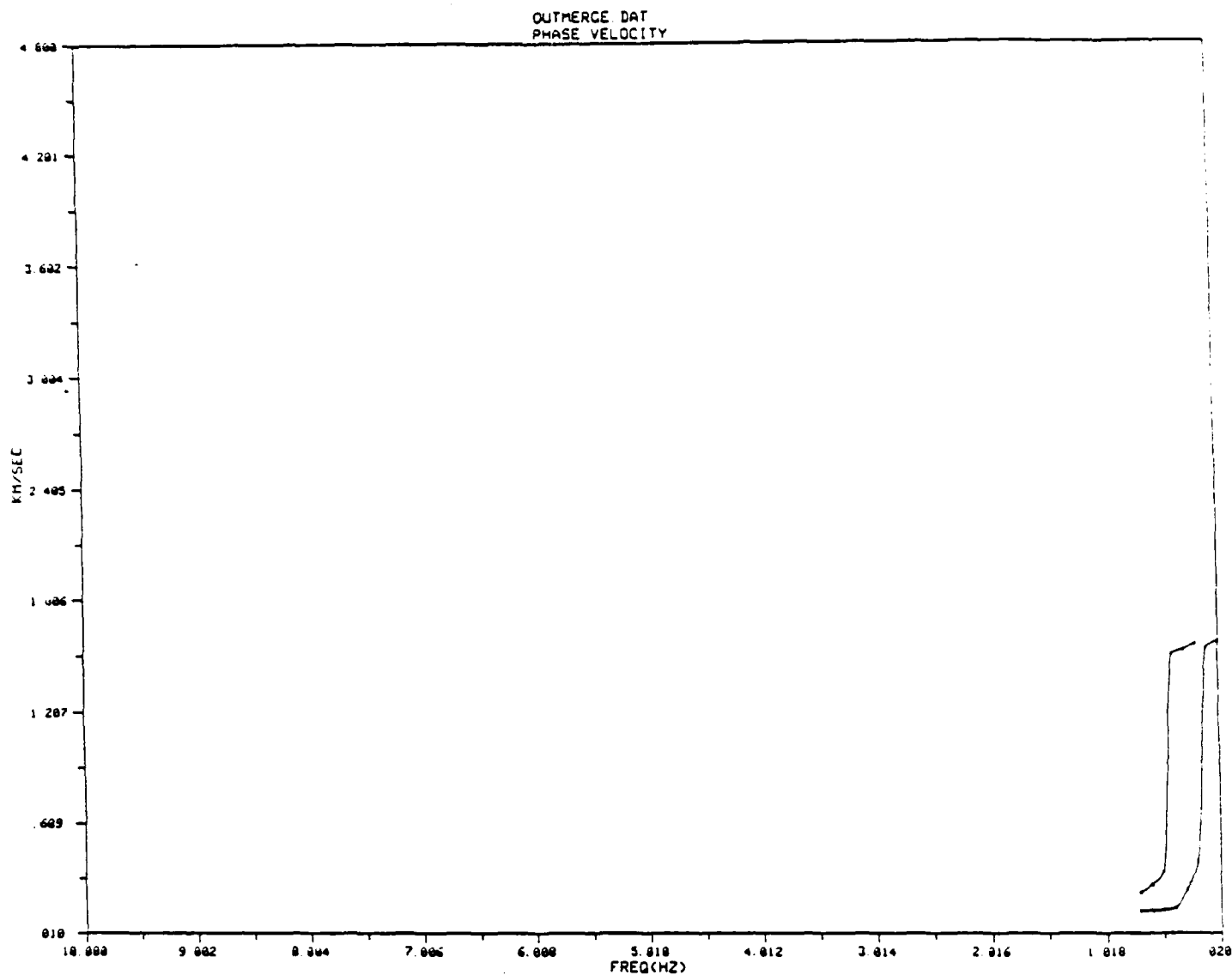
<u>H(km)</u>	<u>α(km/sec)</u>	<u>β(km/sec)</u>	<u>ρ(gm/cm³)</u>	<u>σ</u>
.00381	0.244	0.0914	1.40	.42
0.200	1.520	0.137	1.90	.50
1.000	3.000	1.730	2.20	.25
1.000	5.500	3.300	2.50	.22
2.000	5.900	3.400	2.60	.25
22.500	6.100	3.600	2.80	.23
--	7.900	4.600	3.30	.24

25. Sandy Soil (Sabatier et al., 1986a)

<u>H(km)</u>	<u>α(km/sec)</u>	<u>β(km/sec)</u>	<u>ρ(gm/cm³)</u>	<u>σ</u>
0.002	0.270	0.190	1.70	.01
0.100	0.530	0.324	1.80	.20
0.500	3.000	1.730	2.20	.25
1.000	5.500	3.300	2.50	.22
2.000	5.900	3.400	2.60	.25
22.500	6.100	3.600	2.80	.23
--	7.900	4.600	3.30	.24

26. U. Mississippi (Sabatier and Raspet, 1988)

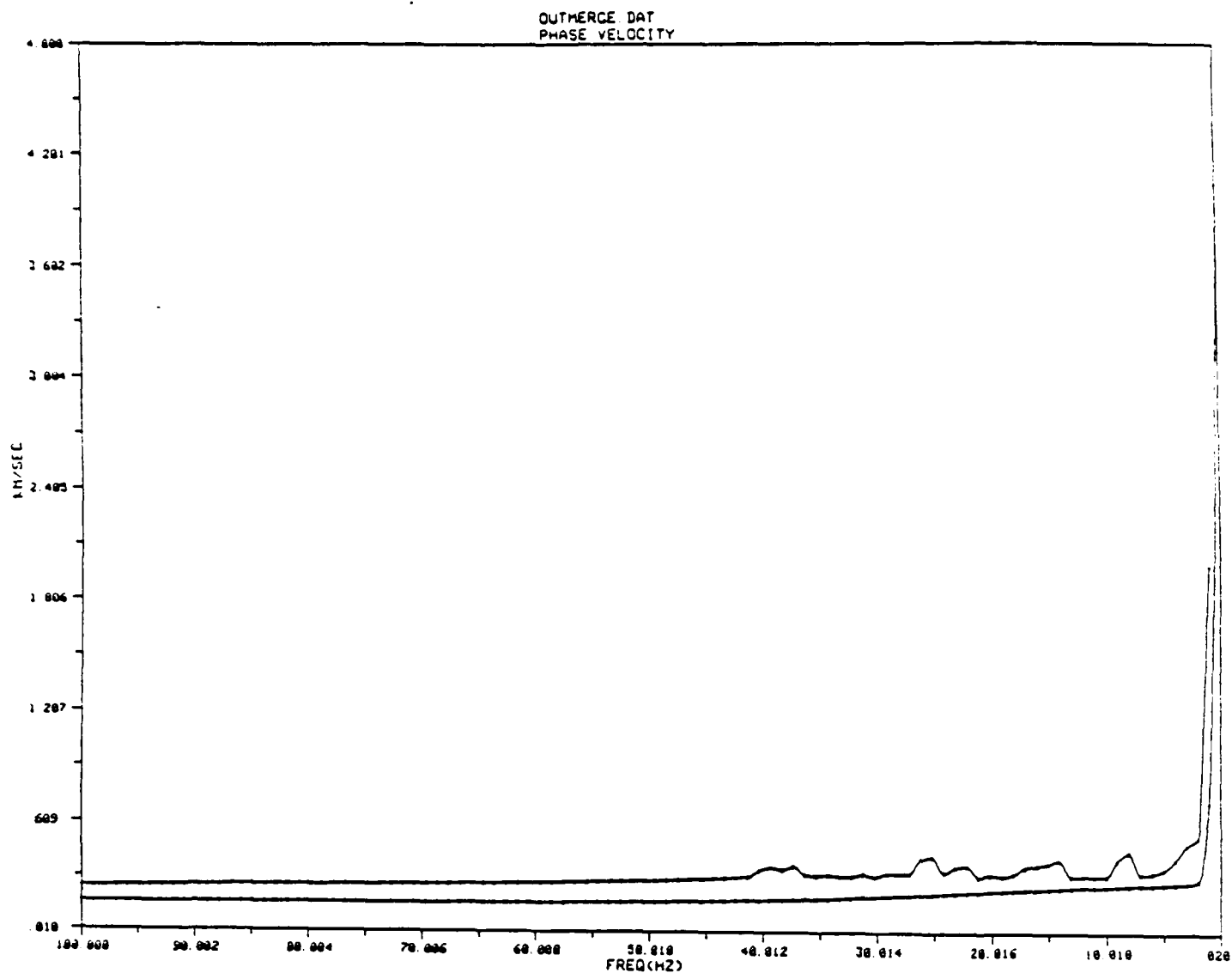
<u>H(km)</u>	<u>α(km/sec)</u>	<u>β(km/sec)</u>	<u>ρ(gm/cm³)</u>	<u>σ</u>
.0003	0.160	0.095	1.70	.23
0.100	0.320	0.190	1.80	.23
0.200	1.966	1.387	2.00	.005
0.500	3.000	1.730	2.20	.25
1.000	5.500	3.300	2.50	.22
2.000	5.900	3.400	2.60	.25
22.500	6.100	3.600	2.80	.23
--	7.900	4.600	3.30	.24



CRUST24

NO. OF LAYERS = 3

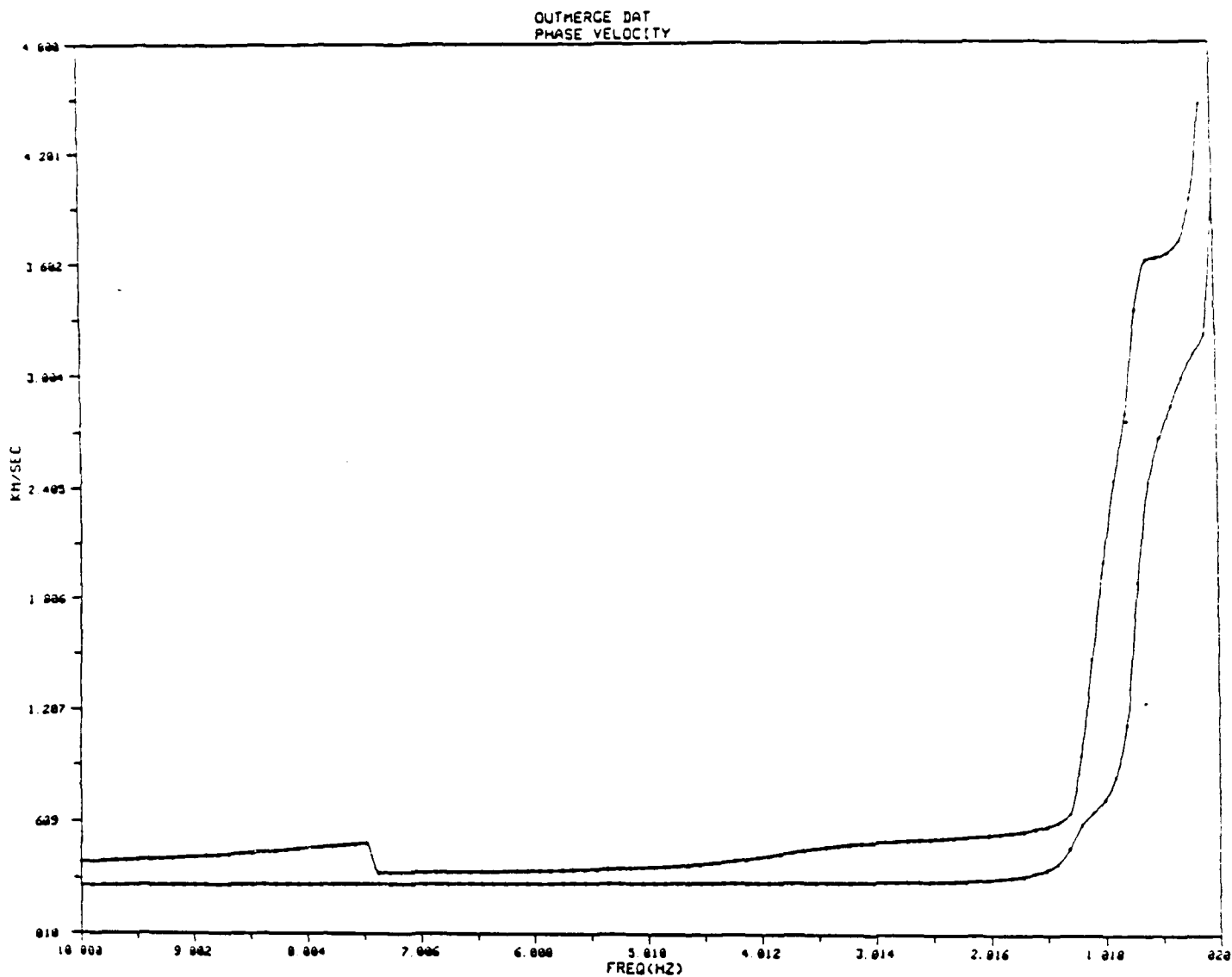
H (km)	VP (km/s)	VS (km/s)	RHO (g/cm ³)
.00380	24400	.09140	1.40000
.20000	1.52000	.13700	1.90000
100.00020	3.00000	1.73000	2.20000



CRUST25

NO. OF LAYERS = 7

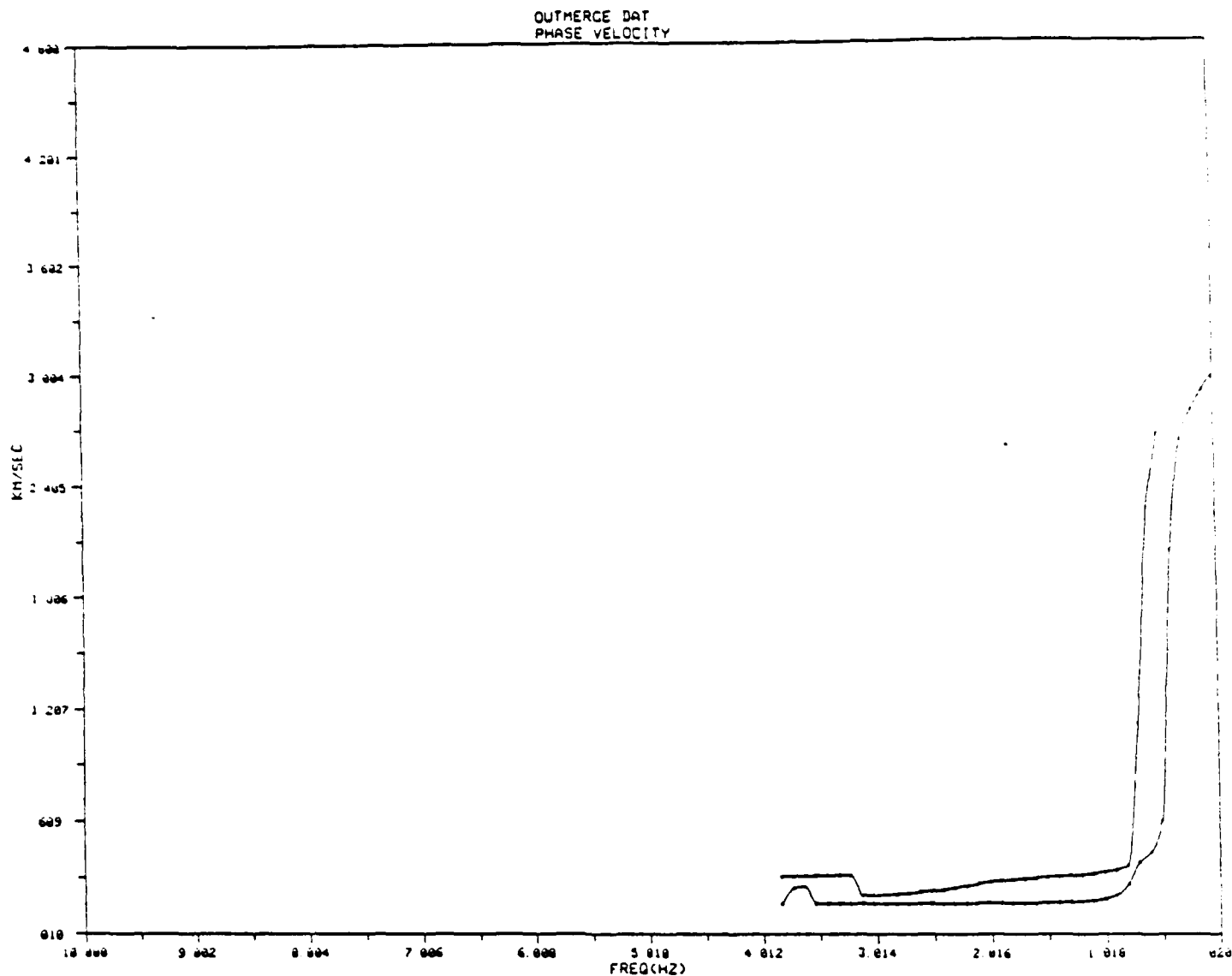
H (km)	VP (km/s)	VS (km/s)	RHO (g/cm3)
.002	270	.190	1.700
.100	.530	.324	1.800
.500	3.000	1.730	2.200
1.000	5.500	3.300	2.500
2.000	5.900	3.400	2.600
22.500	6.100	3.600	2.800
100.000	7.900	4.600	3.300



CRUST25

NO. OF LAYERS = 7

H (km)	VP (km/s)	VS (km/s)	RHO (g/cm ³)
.002	270	.190	1.700
100	530	.324	1.800
500	3.000	1.730	2.200
1.000	5.500	3.300	2.500
2.000	5.900	3.400	2.600
22.500	6.100	3.600	2.800
100.000	7.900	4.600	3.300



CRUST26

NO. OF LAYERS = 5

H (km)	VP (km/s)	VS (km/s)	RHO (g/cm ³)
00030	16000	09500	1 70000
10000	32000	19000	1 80000
20000	1 96600	1 38700	2 00000
50000	3 00000	1 73000	2 20000
100 00020	5 50001	3 30000	2 50000

Cases for Colorado Plateau and Basin and Range

27. Sites A and B (Sabatier and Raspé, 1988)

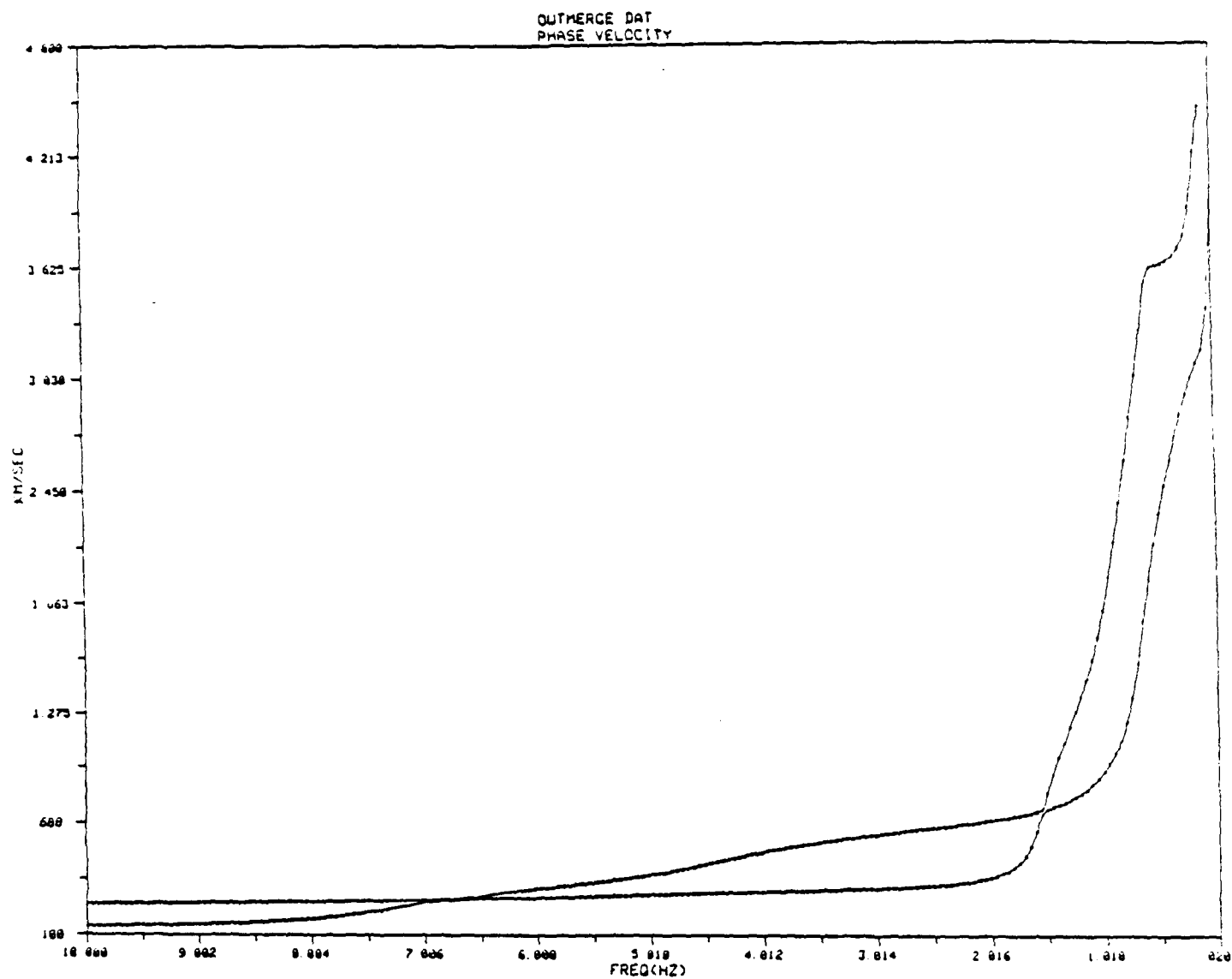
<u>H(km)</u>	<u>α(km/sec)</u>	<u>β(km/sec)</u>	<u>ρ(gm/cm³)</u>	<u>σ</u>
0.008	0.290	0.137	1.70	.36
0.100	0.800	0.400	1.90	.33
0.200	1.966	1.387	2.00	.005
0.500	3.000	1.730	2.20	.25
1.000	5.500	3.300	2.50	.22
2.000	5.900	3.400	2.60	.25
22.500	6.100	3.600	2.80	.23
--	7.900	4.600	3.30	.24

28. Pumice Layer (Sabatier et al., 1986b)

<u>H(km)</u>	<u>α(km/sec)</u>	<u>β(km/sec)</u>	<u>ρ(gm/cm³)</u>	<u>σ</u>
0.002	0.088	0.040	0.66	.37
0.005	0.149	0.073	1.70	.34
0.005	0.451	0.283	1.80	.18
0.500	1.966	1.387	2.00	.005
0.500	3.000	1.730	2.20	.25
1.000	5.500	3.300	2.50	.22
2.000	5.900	3.400	2.60	.25
22.500	6.100	3.600	2.80	.23
--	7.900	4.600	3.30	.24

29. Great Basin (Priestley and Brune, 1978) (w/near Albuquerque)

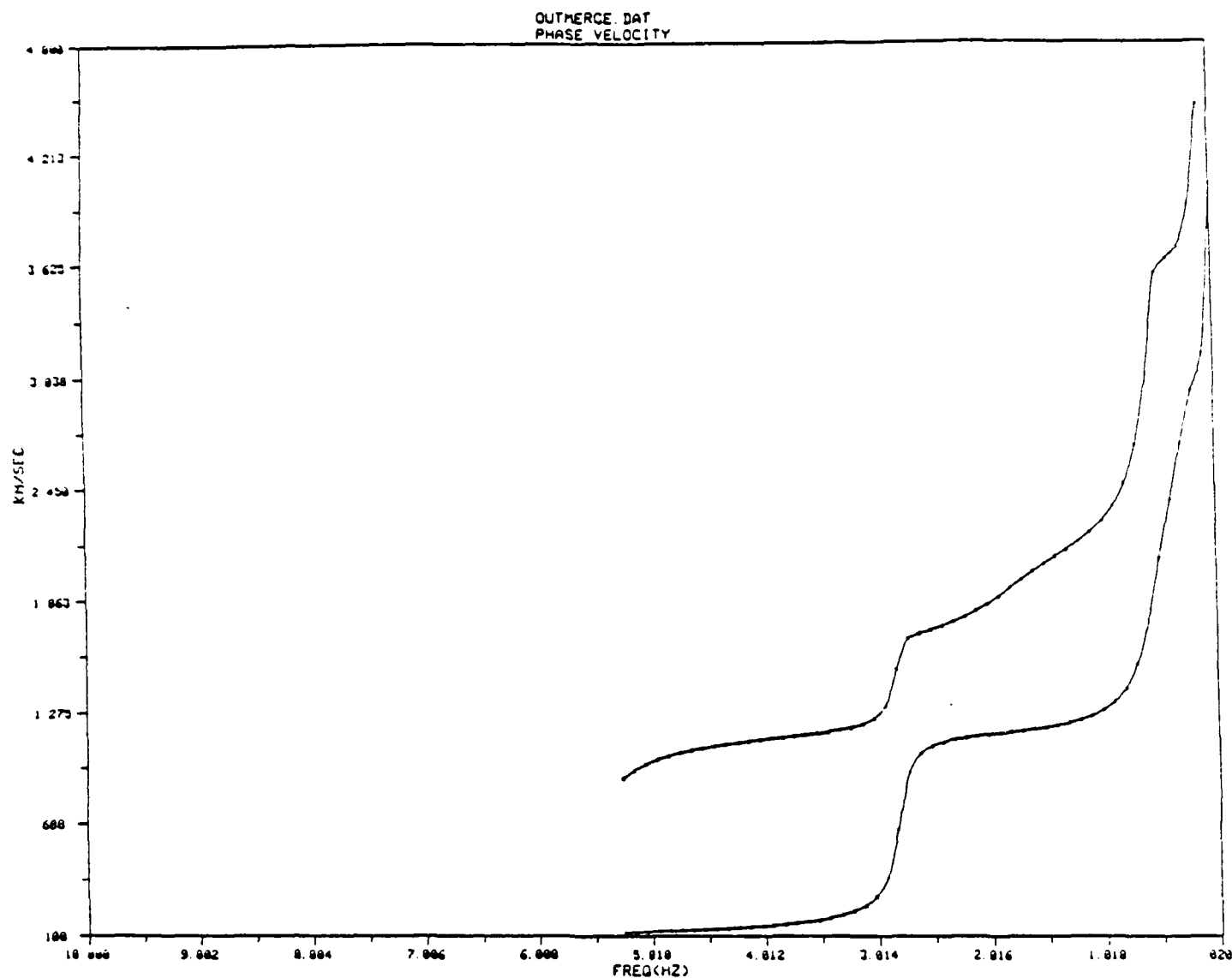
<u>H(km)</u>	<u>α(km/sec)</u>	<u>β(km/sec)</u>	<u>ρ(gm/cm³)</u>	<u>σ</u>
.0005	0.149	0.073	1.70	.34
.00274	0.451	0.283	1.70	.18
0.500	1.966	1.387	1.90	.005
2.500	3.550	2.050	2.20	.25
22.500	6.100	3.570	2.82	.24
10.000	6.600	3.850	2.84	.24
--	7.800	4.500	3.30	.25



CRUST27

NO. OF LAYERS = 8

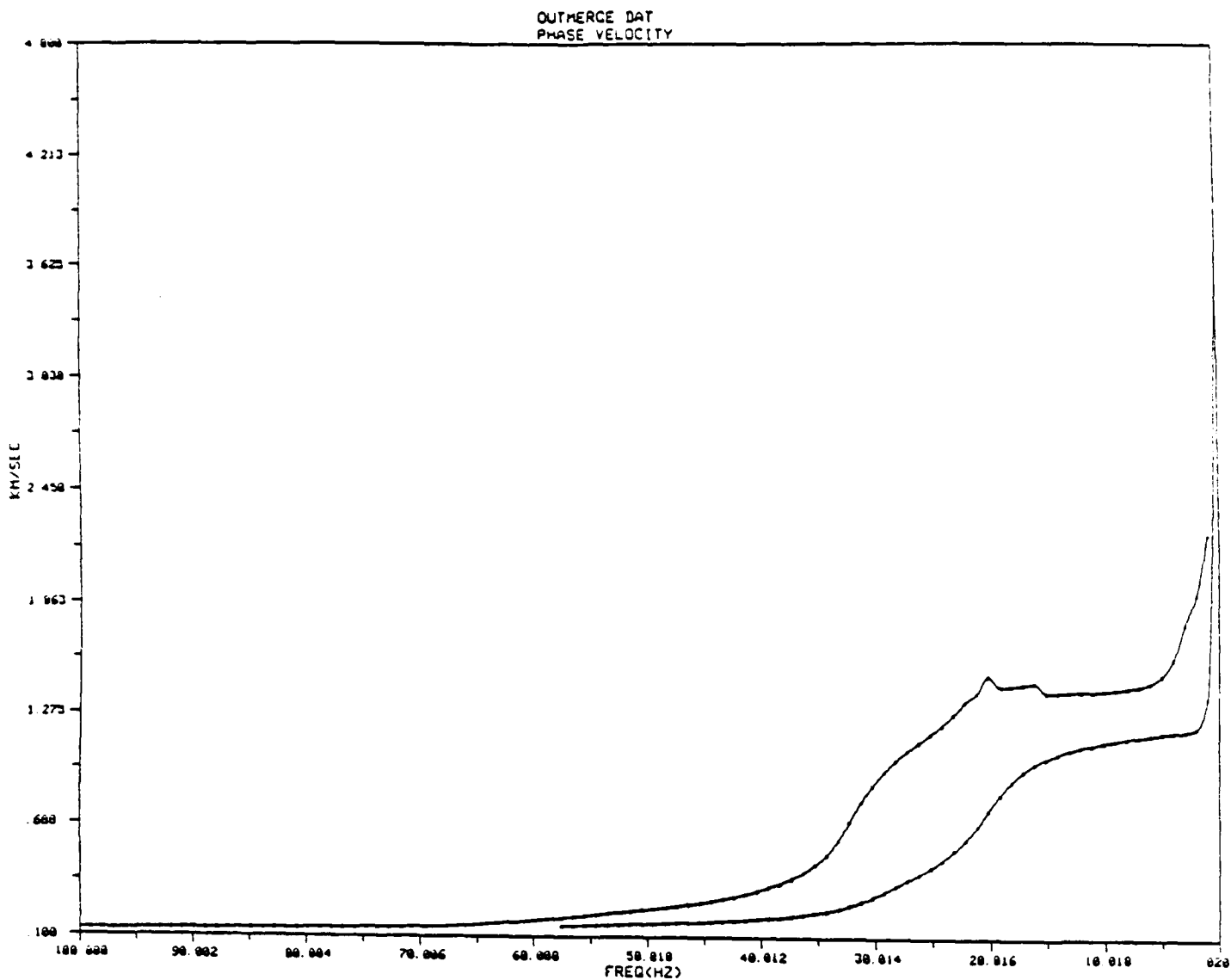
H (km)	VP (km/s)	VS (km/s)	RHO (g/cm ³)
00800	.29000	.13700	1.70000
10000	.80000	.40000	1.90000
20000	1.96600	1.38700	2.00000
50000	3.00000	1.73000	2.20000
1.00000	5.50001	3.30000	2.50000
2.00000	5.90001	3.40000	2.60000
22.50004	6.10001	3.60000	2.80000
100.00020	7.90001	4.60000	3.30000



CRUST28

NO. OF LAYERS = 9

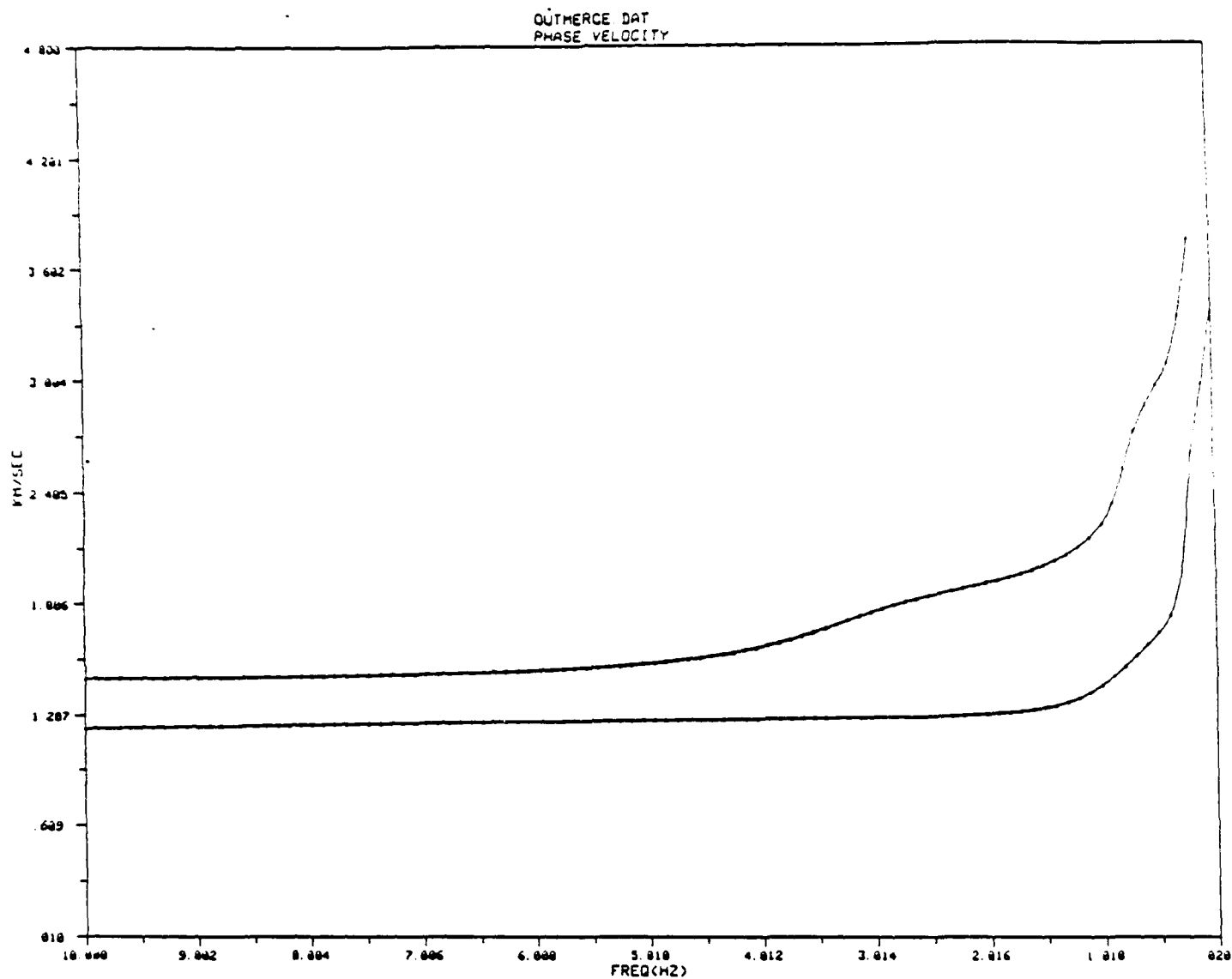
H (Km)	VP (Km/s)	VS (Km/s)	RHO (g/cm3)
002	.088	.040	.660
005	.149	.073	1.700
005	.451	.283	1.800
500	1.966	1.387	2.000
500	3.000	1.730	2.200
1 000	5.500	3.300	2.500
2.000	5.900	3.400	2.600
22.500	6.100	3.600	2.800
100.000	7.900	4.600	3.300



CRUST29

NO. OF LAYERS = 7

H (km)	VP (km/s)	VS (km/s)	RHO (g/cm3)
.00050	.149	.073	1.700
.00274	.451	.283	1.700
.500	1.966	1.387	1.900
2.500	3.550	2.050	2.200
22.500	6.100	3.570	2.820
10.000	6.600	3.850	2.840
100.000	7.800	4.500	3.300



CRUST29

NO. OF LAYERS = 7

H (km)	VP (km/s)	VS (km/s)	RHO (g/cm ³)
00050	149	.073	1.700
00274	451	.283	1.700
500	1.966	1.387	1.900
2 500	3.550	2.050	2.200
22 500	6.100	3.570	2.820
10 000	6.600	3.850	2.840
100 000	7.800	4.500	3.300

Cases for Colorado Plateau and Basin and Range

30. Great Basin #2 (Priestley and Brune, 1978)

<u>H(km)</u>	<u>α(km/sec)</u>	<u>β(km/sec)</u>	<u>ρ(gm/cm³)</u>	<u>σ</u>
0.050	0.750	0.433	1.70	.25
0.500	1.966	1.387	1.90	.005
2.500	3.550	2.050	2.20	.25
22.500	6.100	3.570	2.82	.24
10.000	6.600	3.850	2.84	.24
--	7.800	4.500	3.30	.25

31. Imperial Valley (Boore and Fletcher, 1982)

<u>H(km)</u>	<u>α(km/sec)</u>	<u>β(km/sec)</u>	<u>ρ(gm/cm³)</u>	<u>σ</u>
0.110	1.700	0.280	1.70	.49
0.090	1.700	0.530	1.75	.45
0.100	1.800	0.690	1.80	.41
0.090	1.800	0.850	1.90	.36
1.000	2.400	1.200	2.00	.33
0.900	3.000	1.500	2.10	.33
0.700	3.600	1.800	2.20	.33
2.250	4.500	2.430	2.50	.29
6.000	5.800	3.350	2.65	.25
--	7.400	4.300	3.30	.25

Boore and Fletcher, 1982, Preliminary study of selected aftershocks from digital acceleration and velocity recordings: *in* The Imperial Valley, California, Earthquake of October 15, 1979, U. S. Geological Survey Professional Paper 1254, pp. 110.

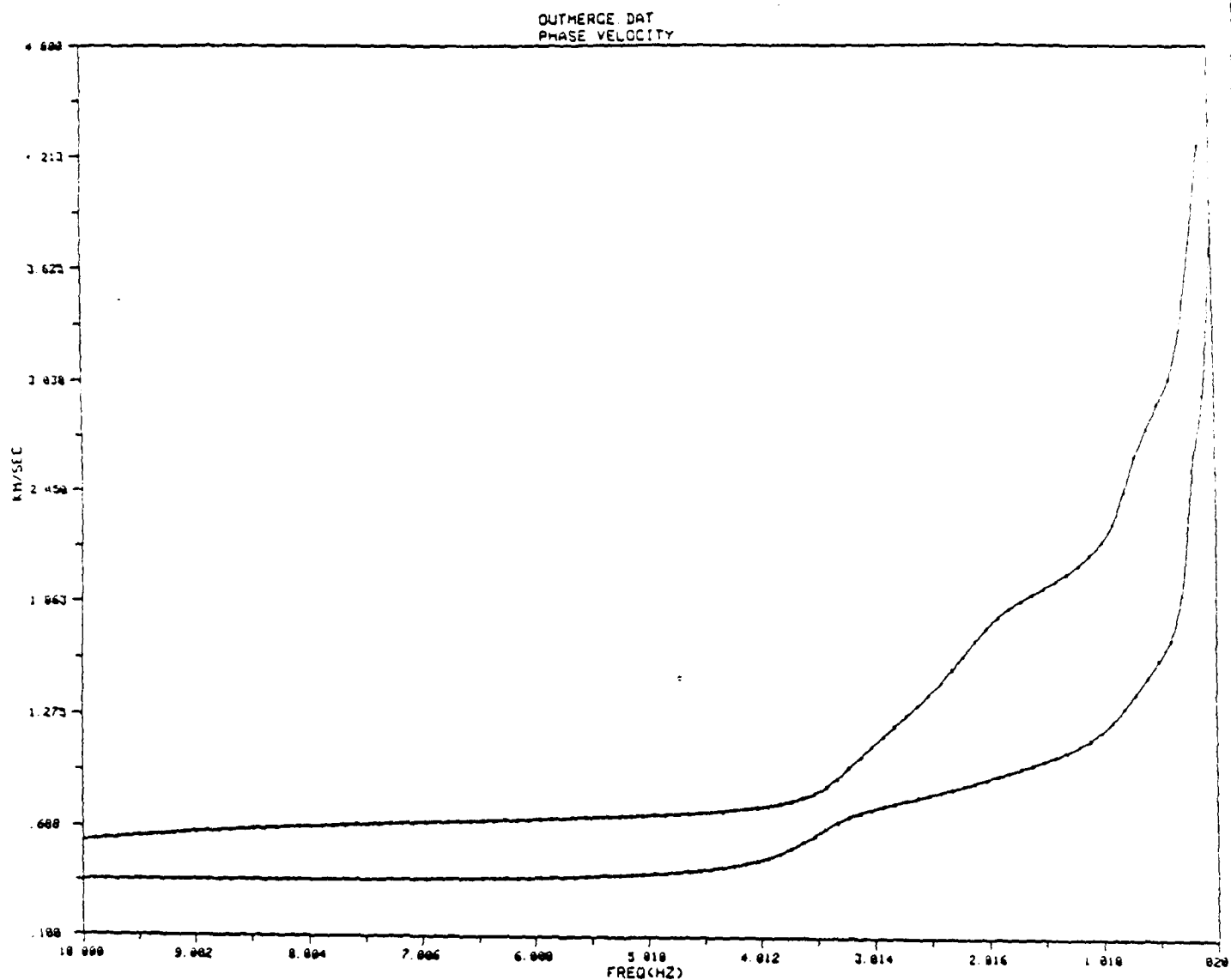
Langston and Helmberger, 1974, Interpretation of body and Rayleigh waves from NTS to Tucson: *Seismological Society of America Bulletin*, Vol. 64, pp. 1919-1929.

Priestley and Brune, 1978, Surface waves and the structure of the Great Basin of Nevada and western Utah: *Journal of Geophysical Research*, Vol. 83, pp. 2265-2272.

Sabatier, J. M., H. E. Bass, L. N. Bolen, and K. Attenborough, 1986a, Acoustically induced seismic waves: *Journal of the Acoustical Society of America*, Vol. 80, pp. 646-649.

Sabatier, J. M., H. E. Bass, and G. E. Elliott, 1986b, Acoustically induced seismic waves: *Journal of the Acoustical Society of America*, Vol. 80, pp. 1200-1202.

Sabatier, J. M., and R. Raspet, 1988, Investigation of possibility of damage from the acoustically coupled seismic waveform from blast and artillery: *Journal of the Acoustical Society of America*, Vol. 84, pp. 1478-1482.

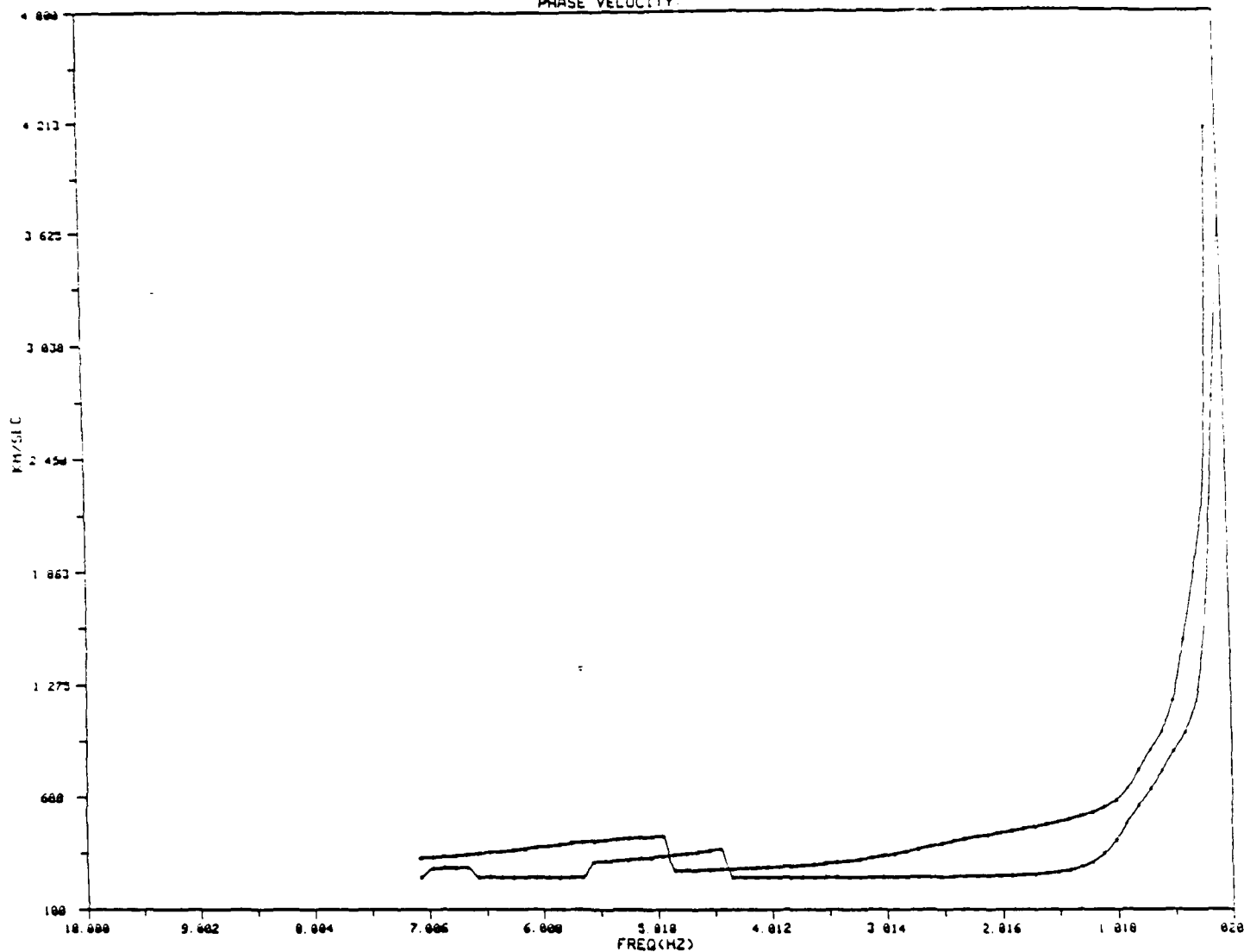


CRUST30

NO. OF LAYERS = 6

H (km)	VP (km/s)	VS (km/s)	RHO (g/cm ³)
0.50	.750	.433	1.700
.500	1.966	1.387	1.900
2.500	3.550	2.050	2.200
22.500	6.100	3.570	2.820
100.000	6.600	3.850	2.840
1000.000	7.800	4.500	3.300

OUTMERGE.DAT
PHASE VELOCITY



CRUST31

NO. OF LAYERS = 10

H (km)	VP (km/s)	VS (km/s)	RHO (g/cm3)
.110	1.700	.280	1.700
.090	1.701	.530	1.750
.100	1.800	.690	1.800
.090	1.801	.850	1.900
1.000	2.400	1.200	2.000
.900	3.000	1.500	2.100
.700	3.600	1.800	2.200
2.250	4.500	2.430	2.500
6.000	5.800	3.350	2.650
100.000	7.400	4.300	3.300

Cases for Utah (Salt Lake) and Los Angeles (Antelope Valley)

41. Salt Lake Shallow Salt Model #1 (Hays et al., 1978)

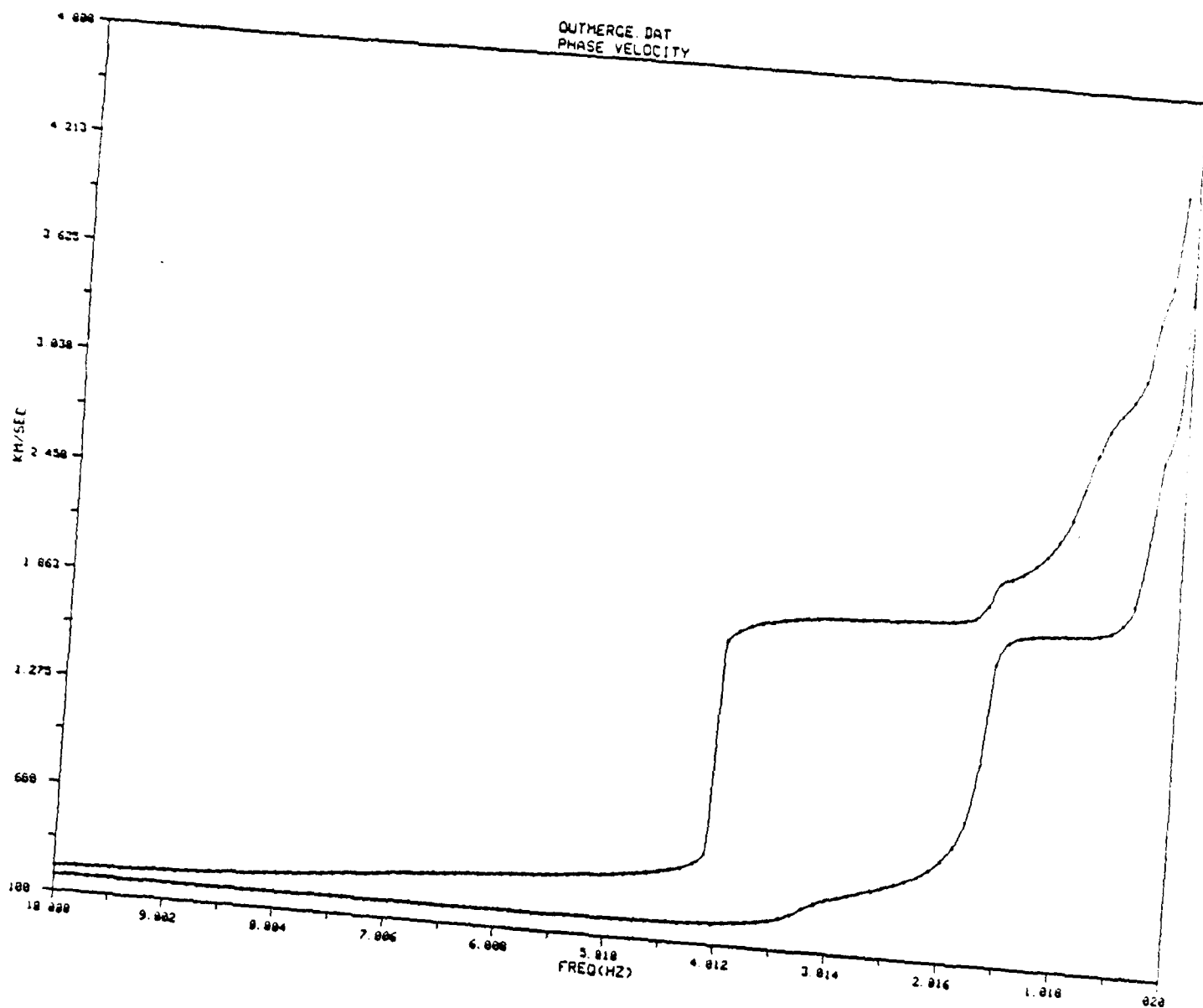
<u>H(km)</u>	<u>α(km/sec)</u>	<u>β(km/sec)</u>	<u>ρ(gm/cm³)</u>	<u>σ</u>
0.030	0.570	0.200	1.60	.43
0.100	4.600	2.650	2.15	.25
2.500	3.550	2.050	2.20	.25
22.500	6.100	3.570	2.82	.24
10.000	6.600	3.850	2.84	.24
--	7.800	4.500	3.30	.25

42. Salt Lake Shallow Salt Model #2 (Hays et al., 1978)

<u>H(km)</u>	<u>α(km/sec)</u>	<u>β(km/sec)</u>	<u>ρ(gm/cm³)</u>	<u>σ</u>
0.005	0.442	0.155	1.50	.43
0.025	0.570	0.200	1.60	.43
0.100	4.600	2.650	2.15	.25
2.500	3.550	2.050	2.20	.25
22.500	6.100	3.570	2.82	.24
10.000	6.600	3.850	2.84	.24
--	7.800	4.500	3.30	.25

43. Salt Lake Deep Salt Model (Hays et al., 1978)

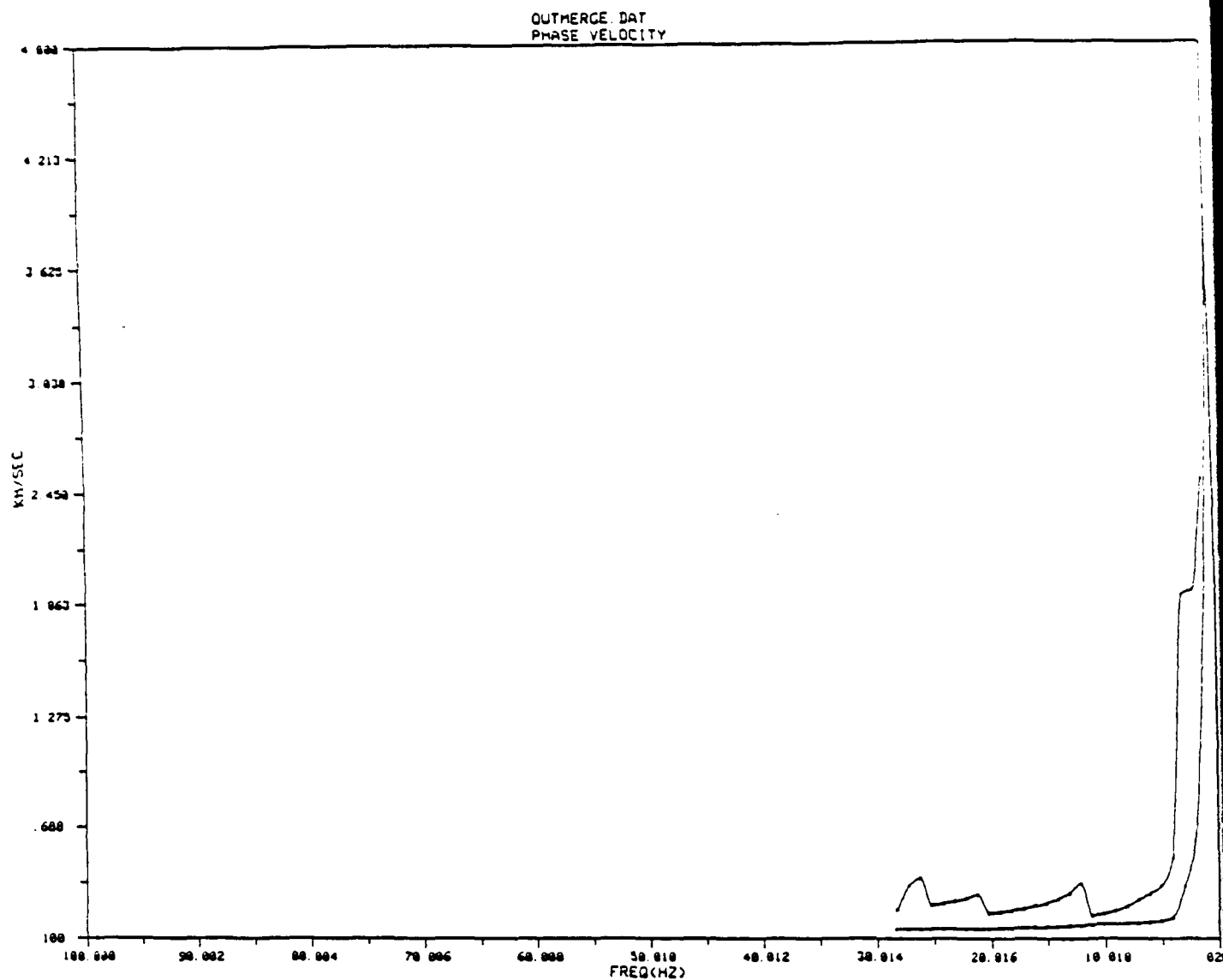
<u>H(km)</u>	<u>α(km/sec)</u>	<u>β(km/sec)</u>	<u>ρ(gm/cm³)</u>	<u>σ</u>
0.005	0.442	0.155	1.50	.43
0.025	0.570	0.200	1.60	.43
0.050	0.965	0.475	1.90	.34
0.050	1.645	0.810	2.10	.34
0.100	4.600	2.650	2.15	.25
2.500	3.550	2.050	2.20	.25
22.500	6.100	3.570	2.82	.24
10.000	6.600	3.850	2.84	.24
--	7.800	4.500	3.30	.25



CRUST41

NO. OF LAYERS = 6

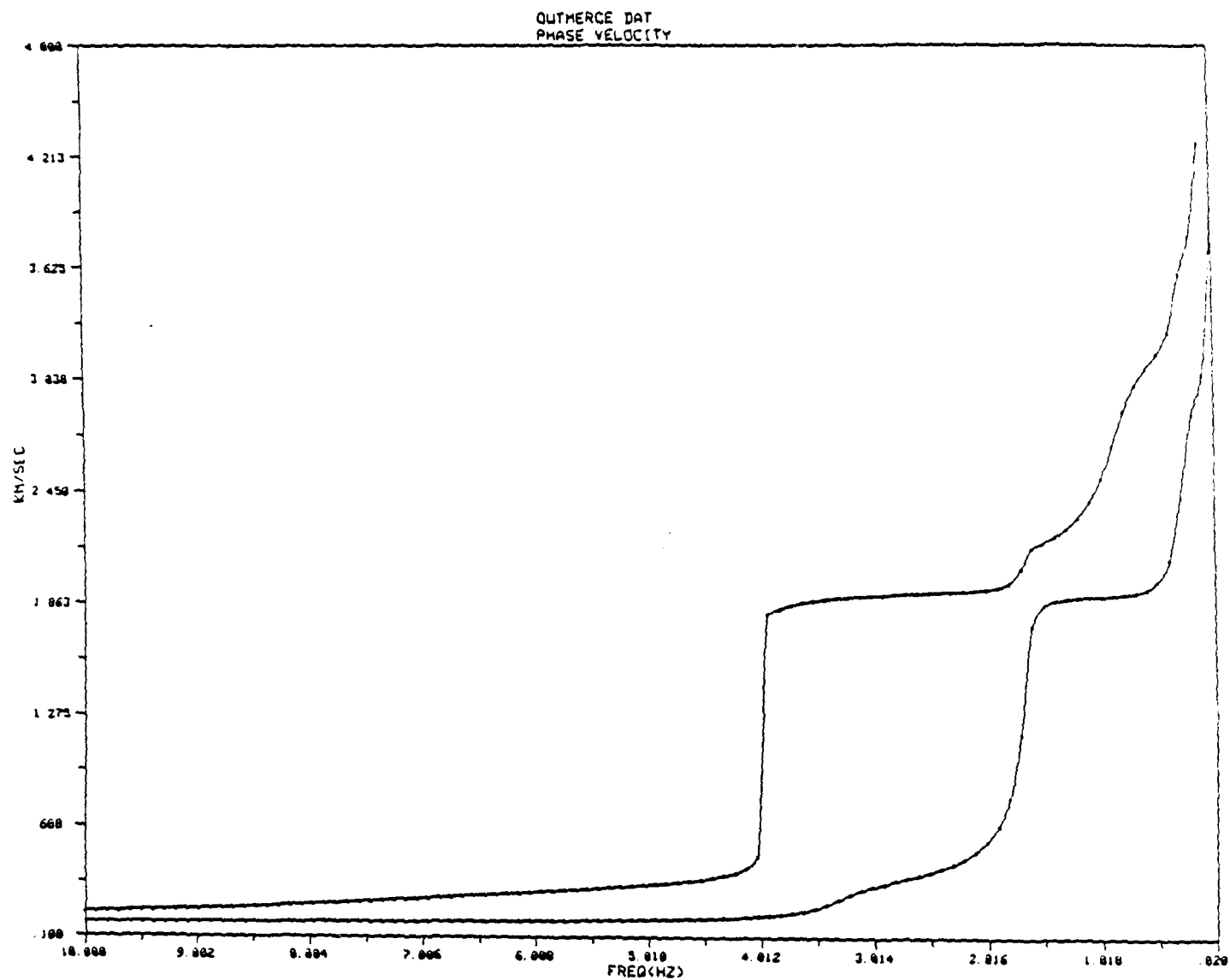
H (km)	VP (km/s)	VS (km/s)	RHO (g/cm3)
03000	.57000	.20000	1.60000
10000	4.60000	2.65000	2.15000
250000	3.55000	2.05000	2.20000
22.50004	6.10001	3.57000	2.82000
10.00002	6.60001	3.85000	2.84000
100.00020	7.80001	4.50000	3.30000



CRUST42

NO. OF LAYERS = 7

H (km)	VP (km/s)	VS (km/s)	RHO (g/cm ³)
.00500	.44200	.15500	1.50000
.02500	.57000	.20000	1.60000
10000	4.60000	2.65000	2.15000
2.50000	3.55000	2.05000	2.20000
22.50004	6.10001	3.57000	2.82000
10.00002	6.60001	3.85000	2.84000
100.00020	7.80001	4.50000	3.30000

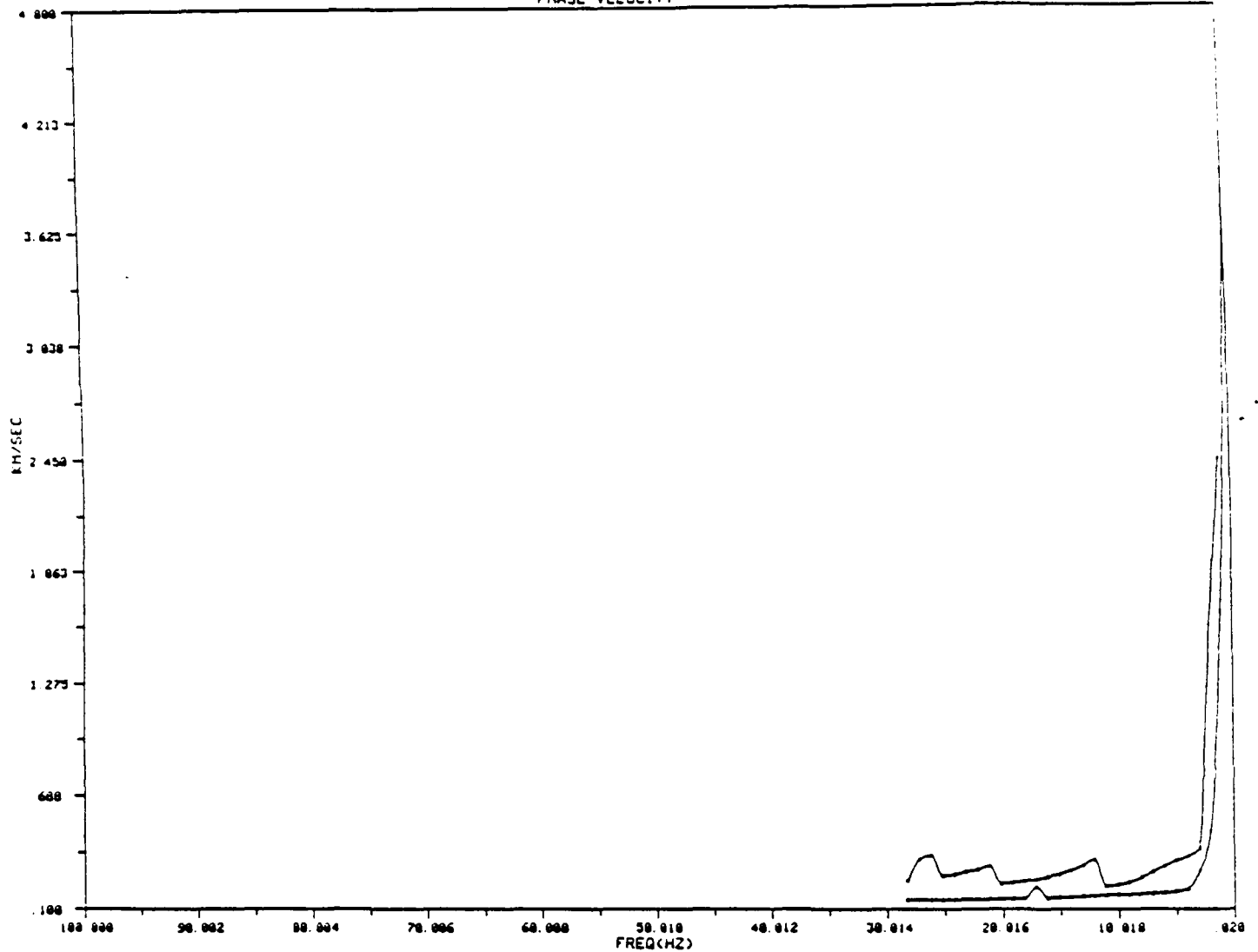


CRUST42

NO. OF LAYERS = 7

H (km)	VP (km/s)	VS (km/s)	RHO (g/cm3)
.00500	.44200	.15500	1.50000
.02500	.57000	.20000	1.60000
.10000	4.60000	2.65000	2.15000
2.50000	3.55000	2.05000	2.20000
22.50004	6.10001	3.57000	2.82000
10.00002	6.60001	3.85000	2.84000
100.00020	7.80001	4.50000	3.30000

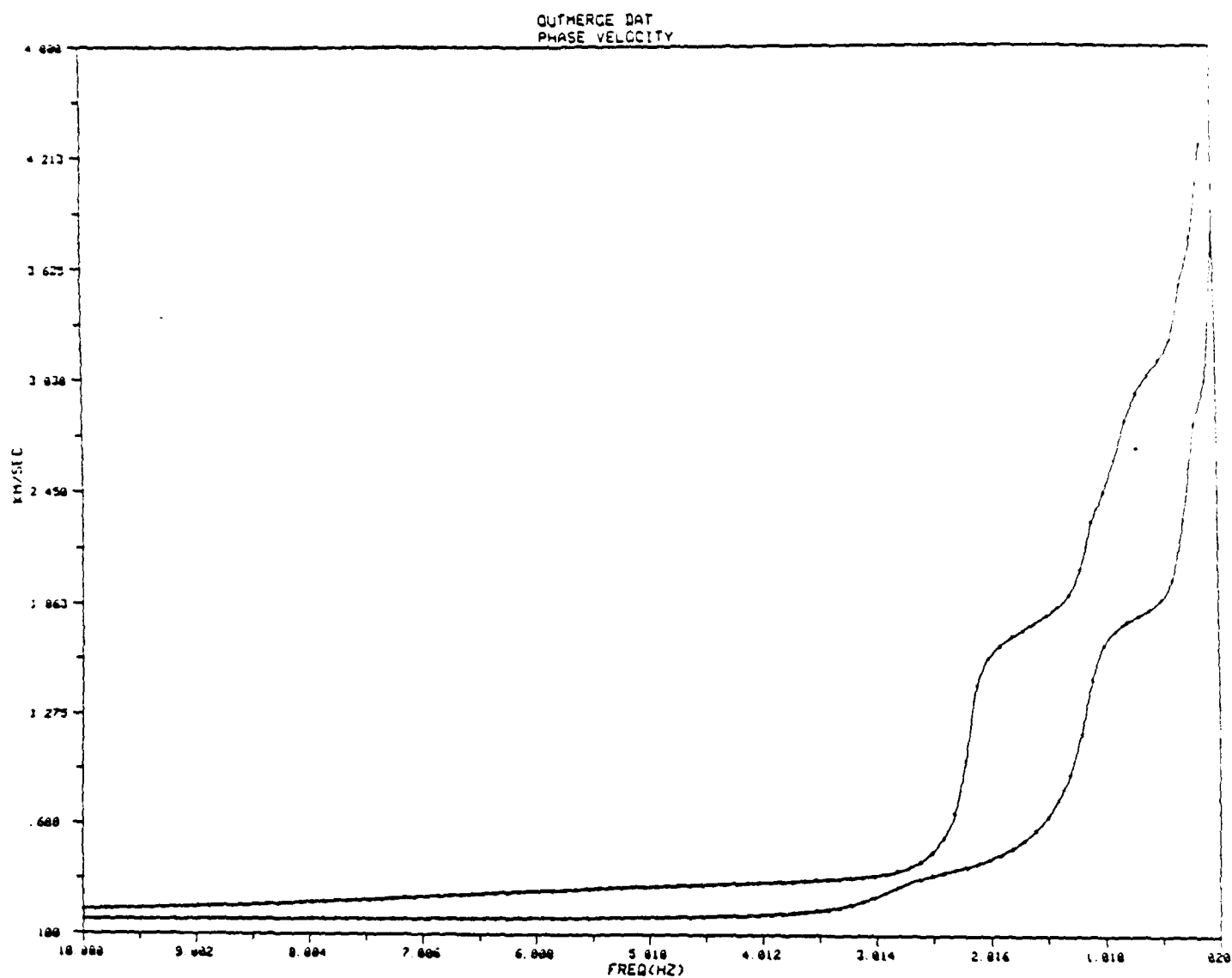
OUTMERGE DAT
PHASE VELOCITY



CRUST43

NO. OF LAYERS = 9

H (km)	VP (km/s)	VS (km/s)	RHO (g/cm ³)
00500	44200	15500	1.50000
02500	57000	20000	1.60000
05000	96500	47500	1.90000
05000	1.64500	.81000	2.10000
10000	4.60000	2.65000	2.15000
2.50000	3.55000	2.05000	2.20000
22.50004	6.10001	3.57000	2.82000
10.00002	6.60001	3.85000	2.84000
100.00020	7.80001	4.50000	3.30000



CRUST43

NO. OF LAYERS = 9

H (km)	VP (km/s)	VS (km/s)	RHO (g/cm ³)
.00500	.44200	.15500	1.50000
.02500	.57000	.20000	1.60000
.05000	.96500	.47500	1.90000
.05000	1.64500	.81000	2.10000
10000	4.60000	2.65000	2.15000
2.50000	3.55000	2.05000	2.20000
22.50004	6.10001	3.57000	2.82000
10.00002	6.60001	3.85000	2.84000
100.00020	7.80001	4.50000	3.30000

Cases for Utah (Salt Lake) and Los Angeles (Antelope Valley)

44. Los Angeles (Antelope Valley) Model #1 (Fumal and Tinsley, 1985)

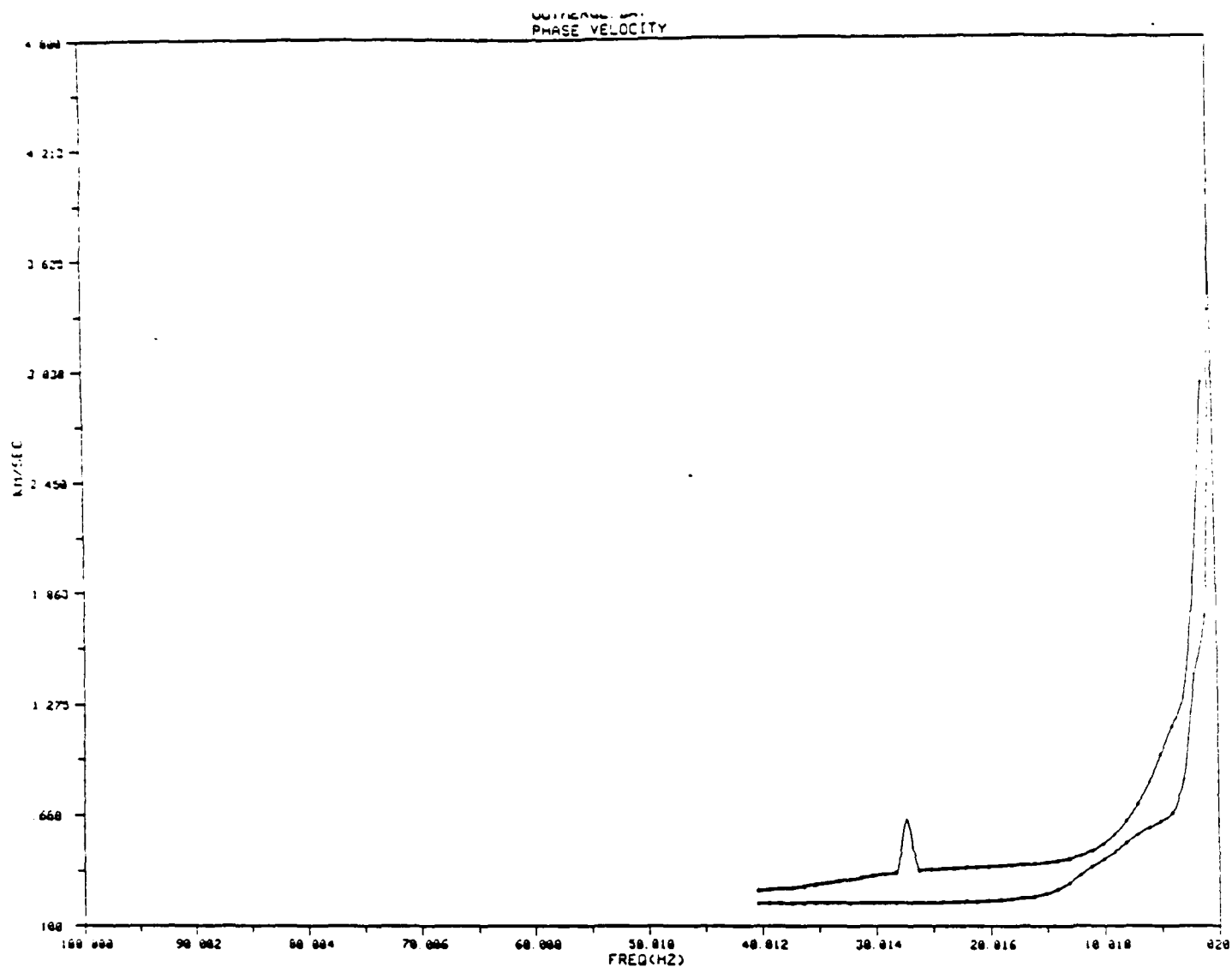
<u>H(km)</u>	<u>α(km/sec)</u>	<u>β(km/sec)</u>	<u>ρ(gm/cm³)</u>	<u>σ</u>
0.008	0.665	0.235	1.46	.43
0.017	0.965	0.475	1.90	.34
0.100	1.600	0.790	2.10	.34
1.00	3.50	2.00	2.20	.26
4.00	5.50	3.20	2.50	.24
23.4	6.30	3.60	2.65	.26
5.00	6.80	4.10	2.80	.21
--	7.80	4.50	3.30	.25

45. Los Angeles (Antelope Valley) Model #2 (Fumal and Tinsley, 1985)

<u>H(km)</u>	<u>α(km/sec)</u>	<u>β(km/sec)</u>	<u>ρ(gm/cm³)</u>	<u>σ</u>
0.005	0.830	0.330	1.50	.41
0.005	0.930	0.375	1.60	.40
0.005	0.960	0.450	1.90	.36
0.010	1.015	0.475	1.90	.36
0.100	1.645	0.810	2.10	.34
1.00	3.50	2.00	2.20	.26
4.00	5.50	3.20	2.50	.24
23.4	6.30	3.60	2.65	.26
5.00	6.80	4.10	2.80	.21
--	7.80	4.50	3.30	.25

Hays, W. W., S. T. Algermissen, R. D. Miller, and K. W. King, 1978, Preliminary ground response maps for the Salt Lake City, Utah, area: *in* Proceedings of the Second International Conference on Microzonation, San Francisco, California, pp. 497-508.

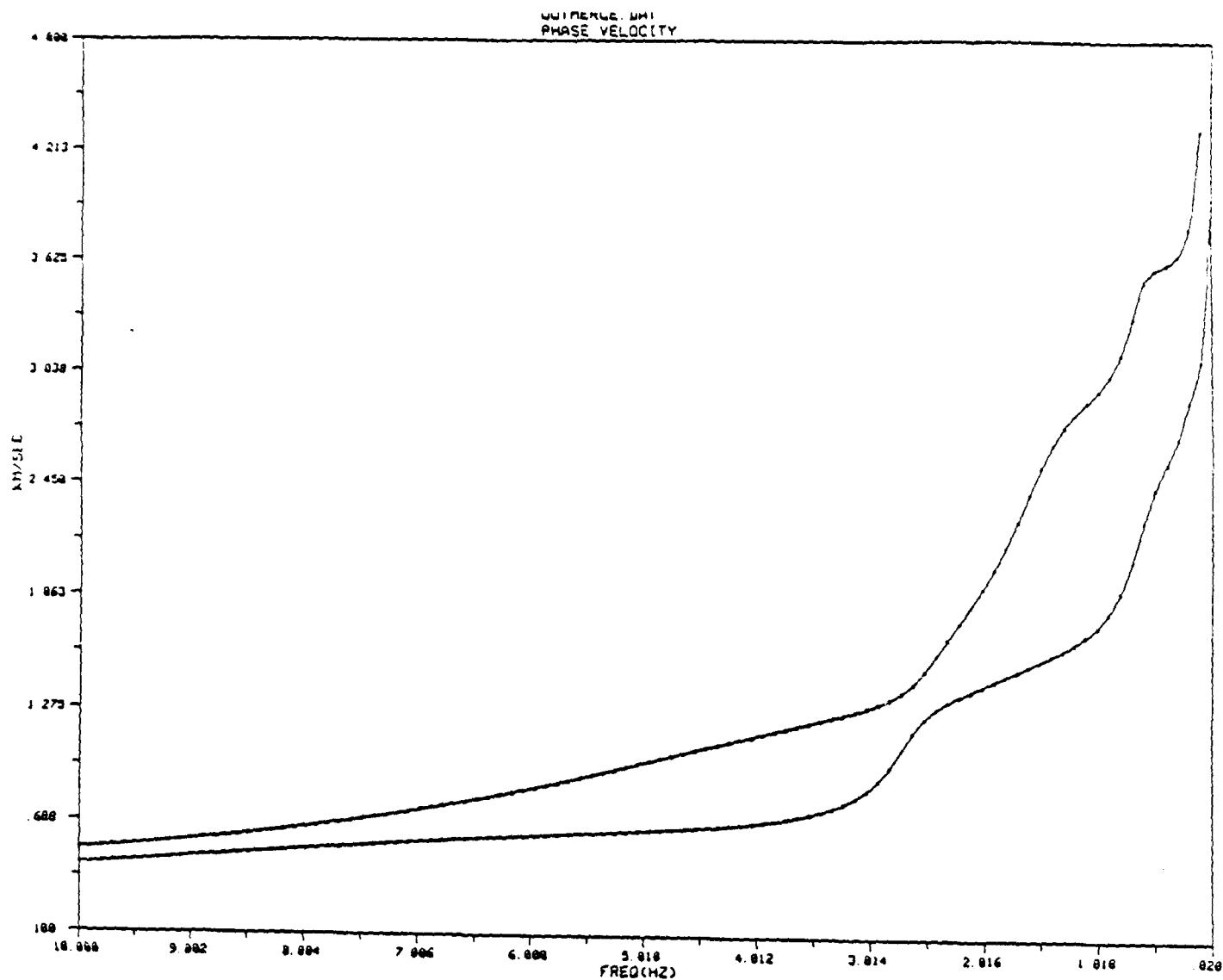
Fumal, T. E., and J. C. Tinsley, 1985, Mapping shear-wave velocities of near-surface geologic materials: *in* Ziony, J. I., editor, Evaluating Earthquake Hazards in the Los Angeles Region--An Earth-Science Perspective: U. S. Geological Survey *Professional Paper 1360*, pp. 127-150.



CRUST44

NO OF LAYERS = 8

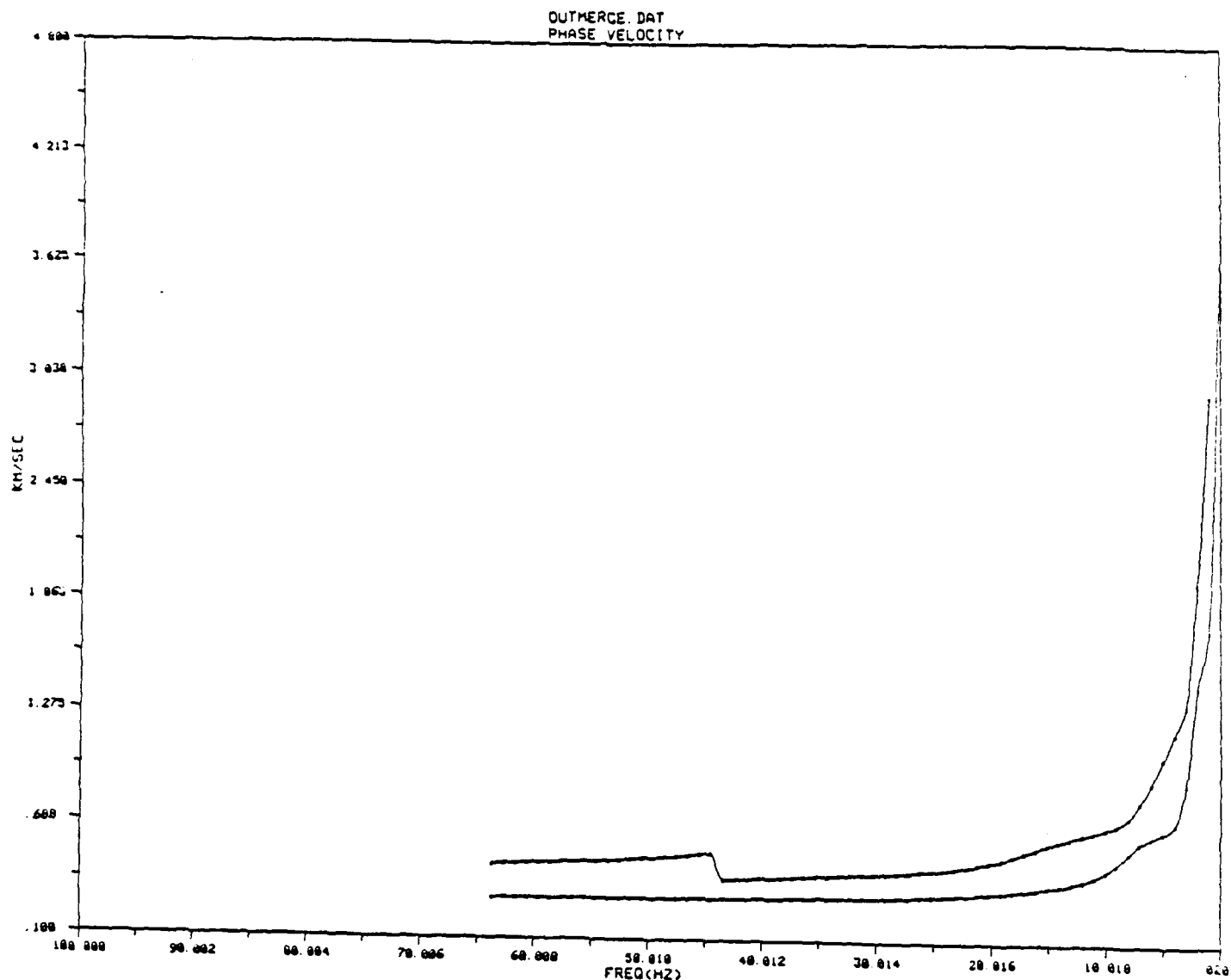
H (km)	VP (km/s)	VS (km/s)	RHO (g/cm ³)
00000	.66500	.23500	1.46000
01700	.96500	.47500	1.90000
10000	1.60000	.79000	2.10000
1.00000	3.50000	2.00000	2.20000
4.00000	5.50001	3.20000	2.50000
23.40004	6.30001	3.60000	2.65000
5.00001	6.80001	4.10000	2.80000
100.00020	7.80001	4.50000	3.30000



CRUST44

NO. OF LAYERS = 8

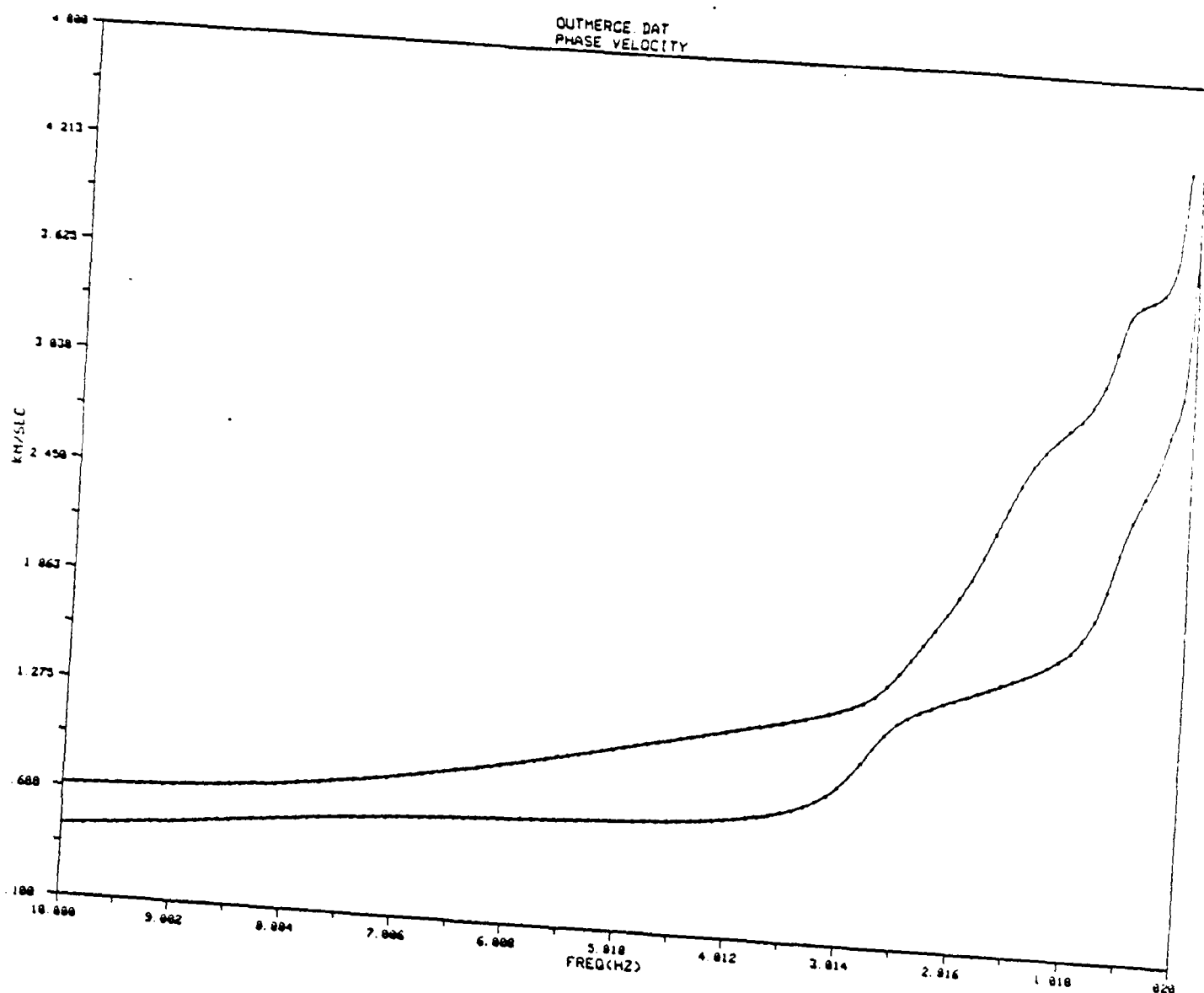
H (km)	VP (km/s)	VS (km/s)	RHO (g/cm ³)
.00800	.66500	.23500	1.46000
.01700	.96500	.47500	1.90000
.10000	1.60000	.79000	2.10000
1.00000	3.50000	2.00000	2.20000
4.00000	5.50001	3.20000	2.50000
23.40004	6.30001	3.60000	.65000
5.00001	6.80001	4.10000	2.80000
100.00020	7.80001	4.50000	3.30000



CRUST45

NO. OF LAYERS = 10

H (km)	VP (km/s)	VS (km/s)	RHO (g/cm ³)
.00500	.83000	.33000	1.50000
.00500	.93000	.37500	1.60000
.00500	.96000	.45000	1.90000
.01000	1.01500	.47500	1.90000
.10000	1.64500	.81000	2.10000
1.00000	3.50000	2.00000	2.20000
4.00000	5.50001	3.20000	2.50000
23.40004	6.30001	3.60000	2.65000
50.00001	6.80001	4.10000	2.80000
100.00020	7.80001	4.50000	3.30000



CRUST45

NO. OF LAYERS = 10

H (km)	VP (km/s)	VS (km/s)	RHO (g/cm3)
.00500	.83000	.33000	
.00500	.93000	.37500	1.50000
.00500	.96000	.45000	1.60000
.01000	1.01500	.47500	1.90000
.10000	1.64500	.81000	1.90000
1.00000	3.50000	2.00000	2.10000
4.00000	5.50001	3.20000	2.20000
23.40004	6.30001	3.60000	2.50000
5.00001	6.80001	4.10000	2.65000
100.00020	7.80001	4.50000	2.80000
			3.30000

REFERENCES

- Aki, K. & P. G. Richards, 1980, *Quantitative Seismology--Theory and Methods*: W.H. Freeman and Company, San Francisco, 932 pp.
- Amick, H., 1988, Vibrating buildings: *Development*, May-June 1988.
- Anderson, A. L. & L. O. Hampton, 1980, Acoustics of gas bearing sediments: I. Background. and II. Measurements and models: *Journal of the Acoustical Society of America*, Vol. 67, pp. 1865-1903.
- Anderson, J. G., P. Bodin, J. Brune, J. Prince, S. Singh, R. Quaas, M. Onate, & E. Mena, 1986, Strong ground motion and source mechanism of the Mexico earthquake of September 19, 1985: *Science*, Vol. 233, pp. 1043-1049.
- Ashley, C., 1976, Blasting in urban areas: *Tunnels and tunneling*, Vol. 8, No. 6, September/October 1976.
- Attenborough, K., J. M. Sabatier, H. E. Bass, & L. N. Bolen, 1986, The acoustic transfer function at the surface of a layered poroelastic soil: *Journal of the Acoustical Society of America*: Vol. 79, pp. 1353-1358.
- Bard, P.-Y., M. Campillo, F. J. Chavez-Garcia, & F. Sanchez-Sesma, 1988, The Mexico earthquake of September 19, 1985--A theoretical investigation of large- and small-scale amplification effects in the Mexico City Valley: *Earthquake Spectra*, Vol. 4, No. 3, p. 609.
- Bariola, J. & M. A. Sozen, 1990, Seismic tests of adobe walls: *Earthquake Spectra*, Vol. 6, February, 1990.
- Baron, M.L., H. H. Bleich & J. P. Wright, 1966, An investigation of ground shock effects due to Rayleigh Waves generated by sonic booms: NASA Contractor Report, CR-451, Weidlinger Consulting Engineers, New York, NY. 49 pp.
- Battis, J. C., 1983, Seismo-acoustic effects of sonic booms on archeological sites, Valentine Military Operations Area: U.S. Air Force Geophysics Laboratory, Technical Report AFGL-TR-83-0304, ERP, No. 858, Hanscomb AFB, Massachusetts, 36 pp.
- Bishop, D. E., 1988, PCBOOM Computer Program For Sonic Boom Research: BBN Report 6741, BBN Laboratories, 21120 Vanowen Street, Canoga Park, California.
- Boore, D. M. & J. B. Fletcher, 1982, Preliminary study of selected after shocks from digital acceleration and velocity recordings: in *The Imperial Valley, California, Earthquake of October 15, 1979*, U.S. Geological Survey Professional Paper 1254, p. 110.

- Bradley, J. & R. W. B. Stephens, 1973, Seismic vibrations induced by Concorde sonic booms: *Acustica*, Vol. 28, pp. 191-192.
- Brekhovskikh, L. M., 1960, *Waves in Layered Media*: Academic Press, New York.
- Carlson, H. W., R. J. Mack & O. A. Morris, 1966, Sonic Boom Pressure Field Estimation Techniques: Sonic Boom Symposium, *Journal of the Acoustical Society of America*, Vol. 39, No. 5, Part 2, pp. S1-S18.
- Celebi, M., J. Prince, C. Dietel, M. Onate, & G. Chavez, 1987, The culprit in Mexico City--Amplification of motions: *Earthquake Spectra*, Vol. 3, No. 2, pp. 315-328.
- Cook, J. C. & T. T. Goforth, 1970, Ground motion from sonic booms: *Journal of Aircraft*, Vol. 7, pp. 126-129.
- Crowley, F. A. & H. A. Ossing, 1969, On the application of air-coupled seismic waves: U.S. Air Force Cambridge Research Laboratories, *AFCRL-69-0312, Environmental Research Papers*, No. 302.
- Dobrin, M. B., 1976, *Introduction to Geophysical Prospecting*: 3rd edition, McGraw-Hill, New York, NY. 220 pp.
- Dobrin, M. B., R. F. Simon, & P. L. Lawrence, 1951, Rayleigh waves from small explosions: *Transactions of the American Geophysical Union*, Vol. 32, pp. 822-832.
- Dobrin, M. B., P. L. Lawrence, & R. Sengbush, 1954, Surface and near-surface waves in the Delaware Basin: *Geophysics*, Vol. 19, pp. 695-715.
- Donn, W. L., I. Dalins, V. McCarty, M. Ewing, & G. Kaschak, 1971, Air-coupled seismic waves at long range from Apollo launchings: *Geophysical Journal of the Royal Astronomical Society*, Vol. 26, pp. 161-171.
- Espinosa, A. F., P. J. Sierra & W. V. Mickey, 1968, Seismic waves generated by sonic booms--a geoacoustical problem: *Journal of the Acoustical Society of America*, Vol. 44, pp. 1074-1082.
- Esteves, J. M., 1978, Control of vibration caused by blasting: Laboratorio Nacional De Engenharia Civil, Lisboa, Portugal, *Memoria* 498.
- Ewing, W. M., W. S. Jardetzky & F. Press, 1957, *Elastic Waves in Layered Media*: McGraw-Hill, New York, NY. 380 pp.
- Fidell, S., R. Horonjeff, T. Schultz & S. Teffeteller, 1983, Community response to blasting: *Journal of the Acoustical Society of America*, Vol. 74, September 1983.
- Fumal, T. E. & J. C. Tinsley, 1985, Mapping shear-wave velocities of near-surface geologic materials: in Ziony, J. I., editor, *Evaluating Earthquake Hazards in the Los Angeles Region--An Earth-Science Perspective*: U.S. Geological Survey *Professional Paper* 1360, pp. 127-150.

- Galloway, W. J., 1983, Studies to Improve Environmental Assessments of Sonic Booms Produced During Air Combat Maneuvering: AFAMRL Report Number, AFAMRL-TR-83-078, Bolt Beranek and Newman, Inc., Canoga Park, California.
- Goforth, T. T. & J. A. McDonald, 1968, Seismic effects of sonic booms: NASA Report No. CR-1137, Teledyne Geotech, Garland, Texas.
- Grant, F. S. & G. F. West, 1965, *Interpretation Theory in Applied Geophysics*: McGraw-Hill, New York, NY. pp. 1-186.
- Grover, F. H., 1973, Geophysical effects of Concorde sonic boom: *Quarterly Journal of the Royal Astronomical Society*, Vol. 14, pp. 141-158.
- Haber, J., D. Nakaki, C. Taylor, G. Knipprath, V. Koppam, & M. Legg, 1989, Effects of Aircraft Noise and Sonic Booms on Structures: An Assessment of the Current State of Knowledge: U.S. Air Force Human Systems Division, Noise and Sonic Boom Impact Technology (NSBIT) Program, Technical Report HSD-TR-89-002, Wright-Patterson AFB, Ohio.
- Hadley, D. M., 1978, Geophysical investigations of the structure and tectonics of southern California: Ph.D. Dissertation, California Institute of Technology, Pasadena, 167 pp.
- Haglund, G. T. & E. J. Kane, 1971, Study Covering Calculations and Analysis of Sonic Boom During Operational Maneuvers: DOT Report Number, EQ-71-2, The Boeing Company, Renton, Washington.
- Haskell, N., 1951, A note on air-coupled surface waves: *Bulletin of the Seismological Society of America*, Vol. 41, pp. 295-300.
- Hays, W. W., S. T. Algermissen, R. D. Miller & K. W. King, 1978, Preliminary ground response maps for the Salt Lake City, Utah, area: in *Proceedings of the Second International Conference on Microzonation*, San Francisco, California, pp. 497-508.
- Hilton, D. A., Huckel, V. Huckel, R. Steiner & D. Maglieri, 1964, Sonic-Boom Exposures During FAA Community-Response Studies Over A 6-Month Period in the Oklahoma City Area: NASA Technical Note, NASA TN D-2539, NASA Langley Research Center, Hampton, Virginia.
- Kanamori, H., J. Mori, D. Anderson, T. Heaton, & L. Jones, 1989, Seismic response of the Los Angeles basin to the shock wave caused by the Space Shuttle Columbia: *Transactions of the American Geophysical Union*, Vol. 70, No. 43, pp. 1191-2.
- Kane, E. J. & T. J. Palmer, 1964, Meteorological Aspects of the Sonic Boom: FAA Report Number, FA-WA-4717, The Boeing Company, Renton, Washington.
- Lamb, H., 1932, *Hydrodynamics*: Cambridge University Press, Teddington, England, 6th edition, pp. 413-415.

- Langefors, U. & B. K. Kihlstrom, 1963, *Rock Blasting*: John Wiley and Sons, Inc., New York.
- Langston, C. A. & D. V. Helmberger, 1974, Interpretation of body and Rayleigh waves from NTS to Tucson: *Seismological Society of America Bulletin*, Vol. 64, pp. 1919-1929.
- Lansing, D. L. & D. J. Maglieri, 1965, Comparison of Measured and Calculated Sonic Boom Ground Patterns Due to Several Different Aircraft Maneuvers: NASA Technical Note, NASA TN D-2730, NASA Langley Research Center, Hampton, Virginia.
- Lee, R. A., M. Crabill, D. Mazurek, B. Palmer & D. Price, 1989, Boom Event Analyzer Recorder (BEAR): System Description: Harry G. Armstrong Aerospace Medical Research Laboratory Report Number, AAMRL-TR-89-035, Wright-Patterson Air Force Base, Ohio.
- Lermo, J., M. Rodriguez, & S. K. Singh, 1988, The Mexico earthquake of September 19, 1985-- Natural period of sites in the Valley of Mexico from microtremor measurements and strong motion data: *Earthquake Spectra*, Vol. 4, No. 4, pp. 805-834.
- Lord Rayleigh, 1885, On waves propagated along the plane surface of an elastic solid: *London Math. Soc. Proc.*, Vol. 12, pp. 4-11.
- Maglieri, D. J. & H. H. Hubbard, 1965, Atmospheric Effects on Sonic Boom Signatures: NASA Technical Report, NASA TMX 56436, NASA Langley Research Center, Hampton, Virginia.
- Maglieri, D. J., V. Huckel & T. L. Parrot, 1966, Ground Measurements of Shock Wave Pressure for Fighter Airplanes Flying at Very Low Altitudes and Comments on Associated Response Phenomena: NASA Technical Note, NASA TN D-3443, NASA Langley Research Center, Hampton, Virginia.
- McDonald, J. A. & T. T. Goforth, 1969, Seismic effects of sonic booms: Empirical results: *Journal of Geophysical Research*, Vol. 74, pp. 2637-2647.
- Medearis, K., 1976, The development of rational damage criteria for low-rise structures subjected to blasting vibrations: Kenneth Medearis Associates, Final Report to National Crushed Stone Associates, Washington, D.C.
- Miles, J. W., 1960, On the response of an elastic half-space to a moving blast wave: *Journal of Applied Mechanics*, Vol. 27, pp. 710-716.
- Oliver, J. & B. Isacks, 1962, Seismic waves coupled to sonic booms: *Geophysics*, Vol. 27, pp. 528-530.
- Pekeris, C. L., 1955, The seismic surface pulse: Proceedings of the National Academy of Sciences, U.S.A., Vol. 41, *Geophysics*, pp. 469-480.
- Plotkin, K. J., 1985, Focus Boom Footprints For Various Air Force Supersonic Operations: Wyle Research Report, WR 85-22, Wyle Research, Arlington, Virginia.

- Press, F. & W. M. Ewing, 1951a, Ground roll coupling to atmospheric compressional waves: *Geophysics*, Vol. 16, pp. 416-430.
- Press, F. & W. M. Ewing, 1951b, Theory of air-coupled flexural waves: *Journal of Applied Physics*, Vol. 22, pp. 892-899.
- Press, F. & J. Oliver, 1956, Model study of air-coupled surface waves: *Journal of the Acoustical Society of America*, Vol. 27, pp. 43-46.
- Priestley, K. & J. Brune, 1978, Surface waves and the structure of the Great Basin of Nevada and western Utah: *Journal of Geophysical Research*, Vol. 83, pp. 2265-2272.
- Raspet, R. & G. E. Baird, 1988, The acoustic surfacewave above a complex impedance ground surface: *Journal of the Acoustical Society of America*, Vol. 85, pp. 638-640.
- Romo, M. P., A. Jaime, & D. Resendiz, 1988, The Mexico earthquake of September 19, 1985--General soil conditions and clay properties in the Valley of Mexico: *Earthquake Spectra*, Vol. 4, No. 4, pp. 731-752.
- Rukos, E. A., 1988, The Mexico earthquake of September 19, 1985--Earthquake behavior of soft sites in Mexico City: *Earthquake Spectra*, Vol. 4, No. 4, pp. 771-786.
- Sabatier, J. M., H. E. Bass, L. N. Bolen & K. Attenborough, 1986a, Acoustically induced seismic waves: *Journal of the Acoustical Society of America*, Vol. 80, pp. 646-649.
- Sabatier, J. M. & H. E. Bass, 1986, On the location of frequencies of maximum acoustic-to-seismic coupling: *Journal of the Acoustical Society of America*, Vol. 80, pp. 1200-1202.
- Sabatier, J. M., H. E. Bass & G. E. Elliott, 1986b, On the location of frequencies of maximum acoustic/seismic coupling: *Journal of the Acoustical Society of America*, Vol. 80, pp. 1200-1202.
- Sabatier, J. M. & R. Raspet, 1988, Investigation of possibility of damage from the acoustically coupled seismic waveform from blast and artillery: *Journal of the Acoustical Society of America*, Vol. 84, pp. 1478-1482.
- Sanchez-Sesma, F., S. Chavez-Perez, M. Suarez, M. A. Bravo, & L. E. Perez-Rocha, 1988, The Mexico earthquake of September 19, 1985--On the seismic response of the Valley of Mexico: *Earthquake Spectra*, Vol. 4, No. 3, pp. 569-589.
- Seed, H. B., H. M. P. Romo, J. I. Sun, A. Jaime, & J. Lysmer, 1988, The Mexico earthquake of September 19, 1985--Relationships between soil conditions and earthquake ground motions: *Earthquake Spectra*, Vol. 4, No. 4, pp. 687-729.
- Sheriff, R. E. & L. P. Geldart, 1982, *Exploration Seismology*: Cambridge University Press, New York, NY.

- Singh, S. K., J. Lermo, T. Dominguez, M. Ordaz, J. M. Espinosa, E. Mena, & R. Quaas, 1988, The Mexico earthquake of September 19, 1985--A study of amplification of seismic waves in the Valley of Mexico with respect to a hill zone site: *Earthquake Spectra*, Vol. 4, No. 4, pp. 653-673.
- Siskind, D. E., M. S. Stagg, J. W. Kopp & C. H. Dowding, 1980, Structure response and damage produced by ground vibration from surface mine blasting: Bureau of Mines Report of Investigations RI 8507, United States Department of the Interior.
- Siskind, D.E., V.J. Stachura, M. S. Stagg, & J. W. Kopp, 1980, Structure response and damage produced by airblast from surface mining: U.S. Department of the Interior, Bureau of Mines *Report of Investigations RI 8485*.
- Sutherland, L. C., R. Brown & D. Goerner, 1990, Evaluation of potential damage to unconventional structures by sonic booms: Wyle Research Report Number WR 89-14, Wyle Research, El Segundo, California.
- Unger, E. E., 1985, Designing sensitive equipment and facilities: *Mechanical Engineering*, December 1985.
- Uniform Building Code, 1988, International Conference Building Officials, Whittier, California.
- Weber, G., 1972, Sonic boom exposure effects II.1: Structures and terrain: *Journal of Sound and Vibration*, Vol. 20, pp. 505-509.
- Witten, A., 1989, Vibrational impacts to archeological structures from low altitude aircraft overflights: Oak Ridge National Laboratory, Oakridge, Tennessee.
- Wyllie, M. R., A. R. Gregory & G. H. Gardner, 1958, An experimental investigation of factors affecting elastic wave velocities in porous media: *Geophysics*, Vol. 23, pp. 459-493.